INFORMATION TO USERS

INTELLIGENT TECHNIQUES APPROACH TO POWER SYSTEMS IDENTIFICATION AND CONTROL

BY

MOHAMED ALI ABIDO

A Dissertation Presented to the

FACULTY OF THE COLLEGE OF GRADUATE STUDIES

KING FAHD UNIVERSITY OF PETROLEUM & MINERALS

DHAHRAN, SAUDI ARABIA

In Partial Fulfillment of the
Requirements for the Degree of

DOCTOR OF PHILOSOPHY

In

ELECTRICAL ENGINEERING

APRIL 1997

UMI Number: 9738991
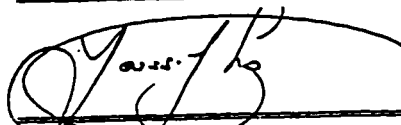
UMI

300 North Zeeb Road
Ann Arbor, MI 48103

KING FAHD UNIVERSITY OF PETROLEUM AND MINERALS
DHAHRAN, SAUDI ARABIA

COLLEGE OF GRADUATE STUDIES

This dissertation, written by *MOHAMED ALI ABIDO*
under the direction of his Dissertation Advisor and approved by his Dissertation
Committee, has been presented to and accepted by the Dean of the College of Graduate
Studies, in partial fulfillment of the requirements for the degree of *DOCTOR OF
PHILOSOPHY in ELECTRICAL ENGINEERING*
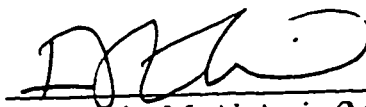
<u>Dissertation Committee</u>
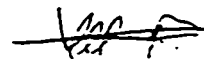
Dr. Y. L. Abdel-Magid (Chairman)
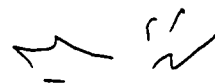
Dr. Ahmad S. Farag (Member)

Dr. Ibrahim M. Al-Amin (Member)
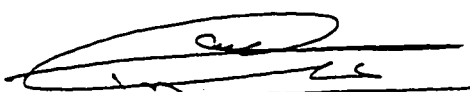
Dr. J. M. Bakhashwain (Member)

Dr. Shokri Selim (Member)

Dr. Samir Al-Baiyat
Department Chairman

Dean, College of Graduate Studies

بسم الله الرحمن الرحيم

In the Name of ALLAH, The Most Gracious, The Most Merciful

"Verily! in the creation of the heavens and the earth,

and in the alteration of night and day, there

are indeed signs for those who think"

The Holy Quran

Dedicated to

MY PARENTS, MY WIFE,
AND MY DAUGHTER *IMAN*

ACKNOWLEDGEMENTS

First of all, praise be to **ALLAH** (S.W.T.) whose help made it possible to complete this work. Acknowledgement is due to King Fahd University of Petroleum and Minerals for the support of this research.

I wish to express my indebtedness to Dr. **Youssef L. Abdel-Magid**, my Ph.D. supervisor, for his valuable guidance and support. I am thankful and will always remember his friendship and supervision. I am grateful to my other committee members Dr. **A.S. Farag**, Dr. **I. M. Al-Amin**, Dr. **J. M. Bakhashwain**, and Dr. **S. Selim** for their valuable interactions.

I am particularly grateful to the EE Dept. chairman Dr. **Samir A. Al-Baiyat** and Dean of the college of graduate studies Dr. **A. M. Al-Shehri** for their valuable support and administration.

I am also thankful to the department faculty, staff, and students who made my study a pleasant experience.

Finally, this work would not have been possible without the support and patience of my family and parents. I am particularly pleased to acknowledge their invaluable effort.

TABLE OF CONTENTS

CHAPTER 6
HYBRID NEURO-FUZZY POWER SYSTEM STABILIZERS

CHAPTER 7
GENETIC-BASED POWER SYSTEM STABILIZERS

CHAPTER 8
HYBRID GENETIC RULE-BASED PSSs

CHAPTER 9
HYBRID GENETIC-BASED FUZZY LOGIC PSSs

LIST OF TABLES

LIST OF FIGURES

ABSTRACT

Name: **Mohamed Ali Abido**

Title: **Intelligent Techniques Approach to Power Systems
Identification and Control**

Major Field: Electrical Engineering

Date: **1997**

Identification and control of power systems is one of the major problems of interest in the power system area. Conventional methods of power systems identification and control are very unattractive because they are too cumbersome for on-line applications, based on linear models of power systems, and not easy to implement. The applications of intelligent techniques to power systems identification and control are scrutinized in this dissertation.

Radial basis function networks (RBFNs) are proposed for off-line as well as on-line identification of synchronous generators. The proposed algorithms are able to capture the nonlinear dynamics of synchronous generators and produce parsimonious models with simple structures. On the control side. a strategy using RBFN to adaptively tune power system stabilizers (PSSs) parameters on-line based on real-time measurements of system operating conditions is proposed.

A hybrid neuro-fuzzy power system stabilizer using fuzzy basis function network is proposed. The proposed stabilizer combines the different strengths of neural networks and fuzzy logic systems and overcomes each other's weaknesses. Unlike the conventional PSS. the proposed stabilizer incorporates the linguistic and numerical information in a uniform fashion.

Incorporating genetic algorithms (GA) into the design of PSS is also proposed. The suggested approach uses GA to search for the optimal settings of PSS parameters. One of

the most important features of the proposed approach is the fact that minimal knowledge of the system is required. In addition, an explicit linearized mathematical model of the system is not needed to design the proposed stabilizer.

An approach to integrate the use of GA and rule-based systems to design a genetic rule-based PSS is proposed. The proposed technique is also applied to integrate the use of GA and fuzzy logic systems in order to design a genetic-based fuzzy logic PSS. The proposed approach incorporates GA to search for optimal settings of rule-based and fuzzy logic PSSs parameters and efficiently overcomes the difficulties in design of these stabilizers.

The proposed identification and control schemes introduced in this dissertation have been tested on several power systems with different complexities and under different disturbances and loading conditions. The results obtained by the proposed schemes are compared with those reported in the literature.

The major features of the proposed schemes are:

- Easy to tune because of their decentralized nature
- Easy to set up and implement using microcomputer
- Linguistic and numerical information can be easily incorporated
- Far less information than other design techniques is required
- Cooperatively work with the existing conventional schemes
- Efficiently combine strengths of different intelligent techniques
- Properly work over a wide range of operating conditions

DOCTOR OF PHILOSOPHY DEGREE
KING FAHD UNIVERSITY OF PETROLEUM AND MINERALS
DHAHRAN, SAUDI ARABIA
199⁻

خلاصة الرسالة

اسم الطالب	:	محمد علي يوسف عبيدو
عنوان الدراسة	:	استخدام الأساليب الذكية في المطابقة والتحكم في نظم القوى الكهربية
التخصص	:	الهندسة الكهربائية
تاريخ الشهادة	:	إبريل ١٩٩٧م.

تعد مشاكل المطابقة والتحكم في نظم القوى الكهربية من أهم المشاكل التي تجذب انتباه الباحثين في هذا المجال ، وتعتبر الطرق التقليدية المستخدمة لحل هذه المشاكل غير جذابة نظراً لصعوبة تطبيقها كما أنها تعتمد على النموذج الخطي لنظم القوى ، لذا تناقش هذه الرسالة استخدام الأساليب الذكية في حل هذه المشاكل .

فلقد اقترحت استراتيجية جيدة لاستخدام الشبكات العصبية (Neural Networks) من نوع دالة الأساس القطري (Radial Basis Function Network) لمطابقة الآلات المتزامنة في حالتي Off-Line وكذلك On-Line ، ولقد تبين أن هذا النوع من الشبكات العصبية له القدرة على مطابقة الخصائص الغير خطية لديناميكية الآلات المتزامنة وذلك عن طريق نماذج بسيطة وغير معقدة . وعلى جانب التحكم اقترحت أيضاً استراتيجية جديدة لاستخدام هذا النوع من الشبكات العصبية في ضبط متغيرات مثبتات نظم القوى (Power System Stabilizers) تلقائياً اعتماداً على القياسات اللحظية لظروف تشغيل نظم القوى .

كما اقترحت شبكة دالة الأساس الغير واضح (Fuzzy Basis Function Network) لضبط متغيرات مثبتات نظم القوى وتتميز الطريقة المقترحة بأنها تجمع بين مواطن القوة في نظام الشبكات العصبية ونظام المنطق غير الواضح وتتلاشى نقاط ضعف فيهما كما أنها على خلاف الطرق التقليدية يمكنها الاستفادة من المعلومات الرقمية واللفظية معاً وفي إطار و حد .

كما اقترحت استراتيجية جيدة لتصميم مثبتات نظم القوى تعتمد على استخدام الخوارزميات الجينية (Genetic Algorithms) للبحث عن القيم المثلى لمتغيرات هذه المثبتات ، وتتميز هذه الطريقة بعدم حاجتها إلى النموذج الخطي للنظام المراد التحكم فيه وقلة المعلومات المستخدمة مقارنةً بالطرق التقليدية .

كما اقترحت استراتيجية جيدة لتهجين مثبتات نظم القوى المصممة على أساس القواعد (Rule-Based PSSs) ، وكذلك المصممة على أساس المنطق غير الواضح (Fuzzy Logic PSSs) بالخوارزميات الجينية وذلك لتحسين عملية البحث عن القيم المثلى لمتغيرات هذه المثبتات والتغلب على صعوبات تصميمها .

ولقد جربت الطرق المقترحة على عدد من أنظمة القوى المتفاوتة في درجة التعقيد وكذلك تحت ظروف تحميل مختلفة وفي حدوث مشاكل متفاوتة ، كما قورنت نتائج الطرق المقترحة مع النتائج المنشورة .

ومن أهم ملامح وسمات الطرق المقترحة :

- سهولة ضبطها نظراً لطبيعتها اللامركزية .

- سهولة تطبيقها باستخدام الميكروكمبيوتر .

- يمكنها التعامل مع المعلومات اللفظية والرقمية في إطار واحد .

- تحتاج إلى معلومات أقل بكثير من الطرق الأخرى .

- يمكنها العمل بكفاءة مع النظم التقليدية الموجودة .

- تجمع بين مواطن القوى في مختلف الأساليب الذكية .

- يمكنها العمل بكفاءة على نطاق واسع من ظروف التشغيل .

درجة الدكتوراة في الفلسفة

جامعة الملك فهد للبترول والمعادن

الظهران ، المملكة العربية السعودية

إبريل ١٩٩٧

CHAPTER 1

INTRODUCTION

1.1 RESEARCH PROBLEM

When engineers are confronted with a challenging problem, it is their responsibility to conceive new and improved tools to solve the problem. On the other hand, once a new tool is available, they will use it to reexamine the problem to find still better and more economical solutions. Power system identification and control is a typical challenging engineering problem which is concerned with the behavior of the synchronous machines after they have been perturbed.

Synchronous machines are major components in electric power systems and their performance is directly related to security and stability of power system operation. A synchronous machine is a highly nonlinear, fast-acting, multi-variable system with a wide range of time constants in different loops. Interconnected in a power system, synchronous machines operate over a wide range of varying operating conditions. The dynamic

characteristics of the synchronous machines vary as conditions change, but the output has to be coordinated so as to satisfy the requirements of power system operation. As a matter of fact, identification and control of synchronous generators continues to be the subject of extensive research. The design of modern generating units, the increasing complexity in power systems, and the demands of economic and operational requirements all contribute to the need of more effective identification and control schemes.

Many synchronous machine models have been developed [1-2]. In general, simple machine models are good for analysis purposes but not accurate enough for predicting machine performance for control purposes. Unfortunately, the complicated models are too cumbersome for on-line applications. Generally, the synchronous machine is a very complex nonlinear system with dynamics and nonlinearities which cannot be modeled in precise mathematical terms.

On the other hand, nearly all the controllers described in the literature have been designed for linearized analytical models of the plant. A synchronous machine may be represented by a set of nonlinear equations. To design a controller, it is usual to reduce the order of the nonlinear model and linearize the equations by considering small deviations around a chosen steady state operating condition. The designed controller parameters remain fixed. Generally, the power systems are highly nonlinear and the operating conditions can vary over a wide range as a result of load changes, line outages, and unpredictable major disturbances such as three phase faults. Therefore, the performance is degraded whenever the operating point changes from one to another.

1.2 THESIS MOTIVATION

Recently, many intelligent techniques have been developed such as rule-based systems, neural networks, fuzzy logic systems, and genetic algorithms. The applications of these intelligent techniques to various power system problems have been demonstrated by many investigators with promising results. However, the application of these techniques is still in its infant stage and only recently has started to receive growing attention from power system researchers.

The motivations behind the interest in using the intelligent techniques approach to power system identification and control problems can be divided into two main categories: theoretical and practical reasons as follows.

1.2.1 THEORETICAL REASONS

- As a general rule, a good engineering approach should be capable of making effective use of all the available information. If the mathematical model of a system is to difficult to obtain (this is true for power systems), then the most important information comes from two sources: (1) sensors which provide numerical measurements of key variables and (2) human experts who provide linguistic description about the system and control instructions. Intelligent techniques, by design, provide a systematic and efficient way to deal with these sources of information. Moreover, they provide an efficient framework for

incorporating linguistic information from human experts. Conventional techniques, however, can not incorporate the linguistic information into their designs.

- Intelligent techniques are based on model-free approach; i.e., they do not require a mathematical model of the system under investigation. Engineers are now facing more and more complex systems, and the mathematical models of these systems are increasingly difficult to obtain. Thus, model-free approaches have taken on added importance.

- The intelligent techniques based controllers are nonlinear ones, which are well justified by the universal approximation theorem; i.e., these controllers are general enough to perform any nonlinear control actions. Therefore, by carefully choosing the parameters of controllers, it is always possible to design a controller that is suitable for the nonlinear system under control.

1.2.2 PRACTICAL REASONS

- Intelligent techniques are easy to understand. Because intelligent techniques emulate human strategy, the underlying principle can be easily understood by those who are not specialists. During the last two decades, conventional control theory has been using increasingly advanced mathematical tools. This is needed in order to solve difficult problems in a rigorous fashion. However, this also results in a diminishing number of practical engineers who can understand the theory.

Therefore, the practical engineers who are in the front line of designing consumer products tend to use approaches that are simple and easy to understand. Intelligent techniques are just such an approach.

- The recent research in optics and analog VLSI has indicated that these technologies can achieve enormous improvement in computational power relative to the current technology. To take full advantage of these new capabilities, computer programs have to be broken up into parallel calculations. But, since the vast majority of existing computer programs are loaded down with IF statements, loops, and long sequences of instructions, this would be almost impossible. The shift to the intelligent techniques is simply to develop more broad general-purpose systems which could take full advantage of the capabilities of the new hardware technologies and admit a high degree of parallel implementation.

- Intelligent techniques are inexpensive to develop. From a practical point of view, the development cost is one of the most important criteria for a successful product. Because intelligent techniques are naturally inspired models of the brain and are built to mimic its known hardware and capabilities, the time necessary to learn the approach is short: i.e., the "software cost" is low. Also, because these techniques are simple to implement, the "hardware cost" is also low. Thus, the intelligent techniques approach has a high performance cost ratio.

In the above discussion, the theoretical reasons emphasize generality and rigor of intelligent techniques, while the practical reasons emphasize applicability and implementability of these techniques.

1.3 THESIS OBJECTIVES

In this thesis, the power system identification and control problem is treated using intelligent techniques. This approach is adopted to achieve the following objectives:

1. Proposing a radial basis function neural network for the problem of off-line and on-line identification of synchronous machines.

2. Proposing a radial basis function neural network to adaptively tune the power system stabilizer parameters based on real-time measurements of machine loading conditions.

3. Proposing a hybrid neuro-fuzzy power system stabilizer. The proposed stabilizer provides a natural framework for combining numerical information in the form of input-output pairs and linguistic information in the form of IF-THEN rules in a uniform fashion.

4. Proposing genetic algorithms for searching for optimal settings of power system stabilizer parameters in order to enhance the system stability over a wide range of operating conditions.

5. Proposing a hybrid genetic rule-based power system stabilizer in which the control rules will be tuned and optimized using genetic algorithms.

6. Proposing a hybrid genetic based fuzzy logic power system stabilizer in which the parameters of fuzzy logic controller will be tuned using genetic algorithms. This incorporation of genetic learning into a fuzzy design process will add an intelligent dimension to the fuzzy controller and overcome the problems associated with fuzzy controller design.

1.4 THESIS ORGANIZATION

The thesis is organized as follows. Chapter II presents a review of the basic concepts of the intelligent techniques. In chapter III, the proposed off-line identification scheme of a synchronous machine using radial basis function networks is presented. On-line identification of a synchronous machine is presented in chapter IV. Adaptive tuning of a power system stabilizer using a radial basis function network is presented in chapter V. Chapter VI presents a hybrid neuro-fuzzy power system stabilizer which represents a natural framework to combine the numerical information and linguistic information in a uniform fashion. Chapter VII presents an approach that uses genetic algorithms to search for the optimal settings of the PSSs. Hybridizing rule-based PSSs with genetic algorithms to tune the control rules is introduced in chapter VIII. A genetic based fuzzy logic power system stabilizer is presented in chapter IX where genetic algorithms are used to optimize the fuzzy logic power system stabilizer parameters in order to overcome the design problems of fuzzy logic stabilizers. Conclusions and suggestions for future research are presented in chapter X .

CHAPTER 2

INTELLIGENT TECHNIQUES - A REVIEW

2.1 ARTIFICIAL NEURAL NETWORKS

The human information processing system consists of the biological brain. Its basic building block is the neuron, the cell that communicates information to and from the various parts of the body. Neurons are interconnected into a biological neural network. A neuron may be modeled as a processing unit that collects inputs and then processes them to produce an output. Such a processing unit is shown in Fig. 2.1. It has n input connections and a set of local parameters. These local parameters constitute its basic memory. Typically, they form a vector[1] $\mathbf{w} = (w_1, w_2, ..., w_n)^T$, where the ith component, w_i, denotes the weight associated with the ith input connection. Sometimes, there is a bias, w_0, associated with the unit. The unit receives an input $\mathbf{x} = (x_1, x_2, ..., x_n)^T$ from either the environment or the outputs of other units. Given an input $\mathbf{x}$, it uses its weight

---

[1] Throughout the thesis, vectors are denoted by small boldfaced symbols, whereas matrices are denoted by capital boldfaced symbols. Components of vectors and matrices are denoted by small symbols that are not boldfaced.

vector **w** and its possibly extra bias w_0 to compute its net input, *net*. Typical computations include:

$$net(\mathbf{x}) = \mathbf{x.w} + w_0, \tag{2.1}$$

$$= \sum_{i=0}^{n} w_i x_i \tag{2.2}$$

where $x_0 = 1$, and

$$net(\mathbf{x}) = \| \mathbf{x} - \mathbf{w} \|. \tag{2.3}$$

Equation (2.2) treats the bias w_0 as a weight associated with a connection to a fictitious input of value fixed to 1. The unit computes its net input and then passes the result through an activation (output) function f. This yields the output, o, of the unit. Typical forms of f are the linear $f(net) = net$, the logistic sigmoid $f(net) = 1/(1+\exp\{-net\})$, and, for *net* given by (2.3), the Gaussian $f(net) = \exp\{-net^2\}$.

Artificial neural networks (ANNs) are created by interconnecting many of these units. Their characteristics can be summarized as follows:

- They contain a number of processing units (neurons) operating in parallel at any given moment.

- They store information (knowledge) in the interconnection weights of the units. New information is added by adapting the weight values (learning). Networks trained to operate in a specific environment can be easily retrained to deal with minor changes in the environmental conditions. Moreover, in nonstationary environments, many networks are capable of adapting their weights in real-time.

- They usually exhibit fault-tolerant characteristics. Damage to individual units can occur without a severe degradation of the overall performance.

- They are model-free systems. They are concerned with transformations rather than traditional algorithms and procedures.

Hence, ANNs provide a completely new and unique way to look at information processing. They have already been shown to elegantly and powerfully realize solutions to problems in various fields such as identification and control of nonlinear dynamic systems, pattern recognition, prediction, and database retrieval.

In this thesis, backpropagation neural network and radial basis function network will be used. The structure and operation of these networks are discussed in what follows.

2.1.1 BACKPROPAGATION NETWORKS

A backpropagation neural network (BPNN) is a multi-layer ANN that learns an input-output mapping by using a supervised learning algorithm called "backpropagation". The backpropagation learning algorithm is a gradient descent procedure that encodes an input-output mapping by adapting the free parameters (mainly the weights) of the network so as to minimize a cost function evaluated over a training set. The name "backpropagation" stems from the fact that the error signals generated at the network output, because of differences between desired and actual output values, are propagated backwards through the network so as to make adjustments.
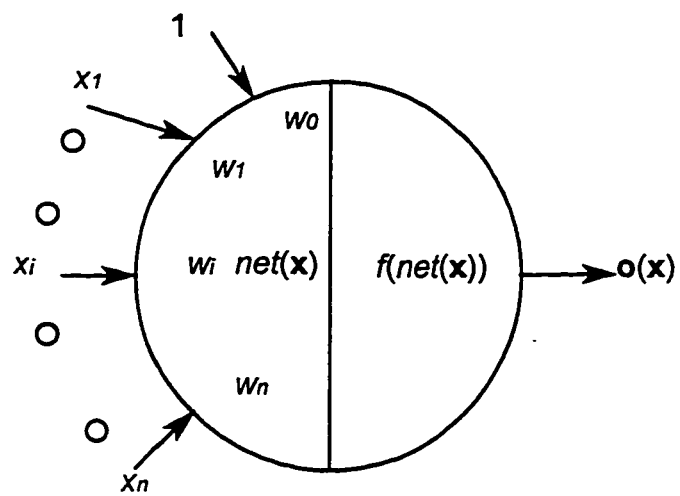
Fig. 2.1 A generic processing unit.

The basic BPNN is a multi-layer feed-forward network that contains inter-layer connections with each unit on a layer providing an input only to each and every unit on the next layer. Figure 2.2 shows a basic 3-layer BPNN. It has n input units, m hidden units, and c output units. Its operation can be described as follows:

1. An n-dimensional input vector $\mathbf{x}$ is applied to the input layer.

2. The input units have a single input and a single output. They simply pass the values on their inputs to their outputs. It is a valid remark that, here, the input layer serves no functional purpose.

3. The jth hidden unit computes its net input, net_{hj}, using

$$net_{hj}(\mathbf{x}) = \mathbf{x} \cdot \mathbf{v}_j + v_{j0}, \quad j = 1, \ldots, m, \qquad (2.4)$$

where $\mathbf{v}_j = (v_{j1}, v_{j2}, \ldots, v_{jn})^T$ and v_{j0} are the weight vector and bias of the jth hidden unit, respectively.

4. The jth hidden unit computes its activation (output), h_j, using

$$h_j(\mathbf{x}) = f_{hj}(net_{hj}(\mathbf{x})), \quad j = 1, \ldots, m, \qquad (2.5)$$

where f_{hj} is the activation function of the jth hidden unit.

5. The jth output unit computes its net input. net_{oj}, using

$$net_{oj}(\mathbf{x}) = h(\mathbf{x}) \cdot \mathbf{w}_j + w_{j0}, \quad j = 1, \ldots, c, \qquad (2.6)$$

where $\mathbf{w}_j$ and w_{j0} are the weight vector and bias of the jth output unit, respectively.

6. The jth output unit computes its activation. o_j, using

$$o_j(\mathbf{x} = f_{oj}(net_{oj}(\mathbf{x})), \quad j = 1, \ldots, c. \qquad (2.7)$$

where f_{oj} is the activation function of the jth output unit. This yields the output vector, $\mathbf{o}$, of the network and completes its operation.
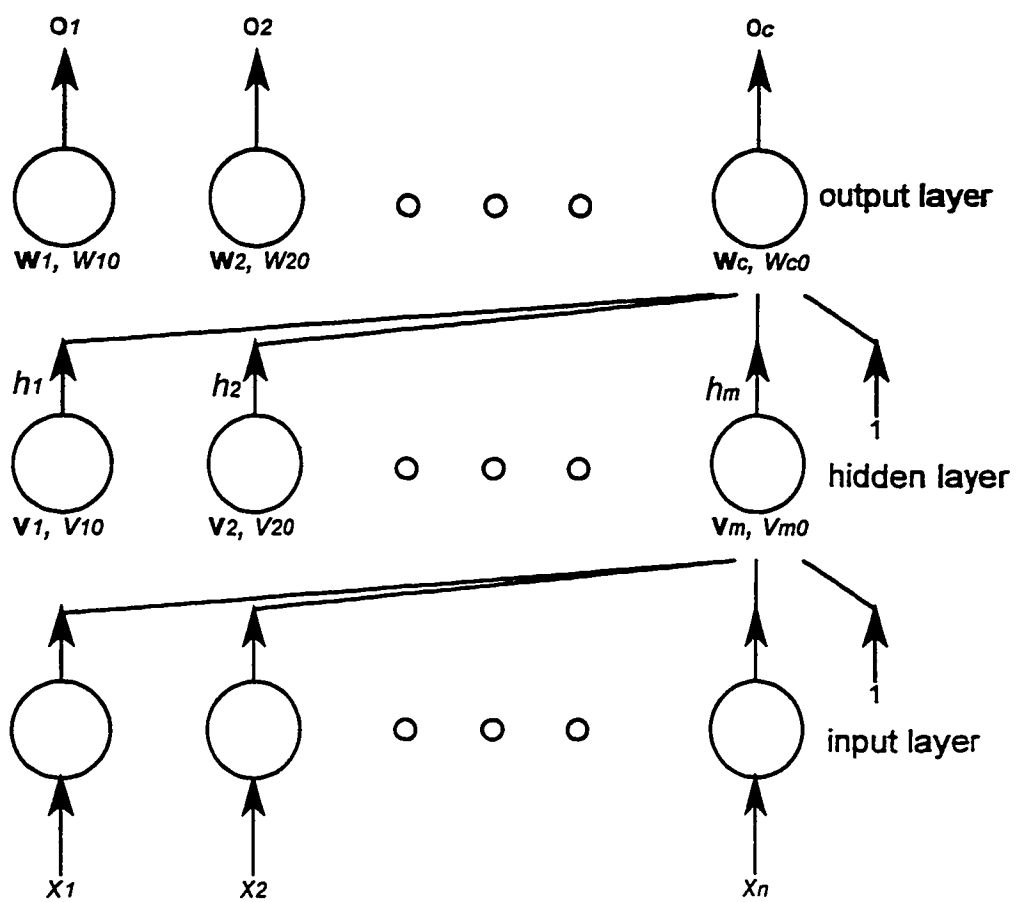
Fig. 2.2 A basic 3-layer BP network[2].

---

[2] To keep the figure clear, not all connections are shown; there is actually a connection from the output of each unit on a layer to the input of each and every unit on the next layer.

The above computations are done in parallel on a layer-by-layer basis. In brief, the jth output of the network is given by

$$o_j(\mathbf{x}) = f_{oj} \left(\sum_{i=0}^{m} w_{ji} f_{hi} \left(\sum_{k=0}^{n} v_{ik} x_k \right) \right), \quad j = 1, \ldots, c. \tag{2.8}$$

where $f_{h0}(\mathbf{x}) = x_0 = 1$. Extending the computations to a network with any number of hidden layers is straightforward. The activation functions may have identical or different forms. However, the used forms must be differentiable. The most common forms are the linear $f(net) = net$ and the logistic sigmoid $f(net) = (1 + \exp\{-net\})$, where net is the net input to the unit.

It has been proved that a 3-layer BPNN, with one hidden layer of sigmoidal units and an output layer of linear units, can approximate arbitrary continuous mappings to any required degree of accuracy[3-5].

2.1.2 RADIAL BASIS FUNCTION NETWORKS

A radial basis function network (RBFN) is a 3-layer feed-forward ANN that is based on the traditional radial basis function (RBF) approach to multi-variate interpolation. Powell [6] has reviewed the RBF interpolating approach, and Micchelli [7] has proved some important results on its solvability. Motivated by the philosophy that networks may be viewed as devices for interpolating data in multi-dimensional spaces. Broomhead and Lowe [8] have generalized some of the assumptions found in [6] and [7], and have proposed the RBFN as an alternative architecture for learning input-output mappings.

An RBFN consists of an input-hidden nonlinear mapping followed by a hidden-output linear mapping. Each hidden unit computes a nonlinear function of a measure of the distance between the network input and the unit's weight vector (usually called the "center" of the unit). Thus, the linear output of the network is expanded on a basis given by a set of radially symmetric functions. In practice, the output of the hidden unit peaks when the input is at its center and falls off monotonically as the input moves away from it. Thus, the hidden units of an RBFN may viewed as populations of neurons with response characteristics that are locally-tuned or selective for some range of the input variables.

An RBFN is a 3-layer feed-forward network with each unit on a layer providing an input only to each and every unit on the next layer. It is a linear-output network, since all output units have linear activation functions. An RBFN with n input units, m hidden units, and c output units, is depicted in Fig. 2.3. The network operation can be described as follows:

1. An n-dimensional input vector x is applied to the input layer.

2. The input units have a single input and a single output. They simply pass the values on their inputs to their outputs. It is a valid remark that, here, the input layer serves no functional purpose.

3. The jth hidden unit computes its net input, net_{hj}, using

$$net_{hj}(x) = \| x - c_j \| , \quad j = 1, \ldots, m, \qquad (2.9)$$
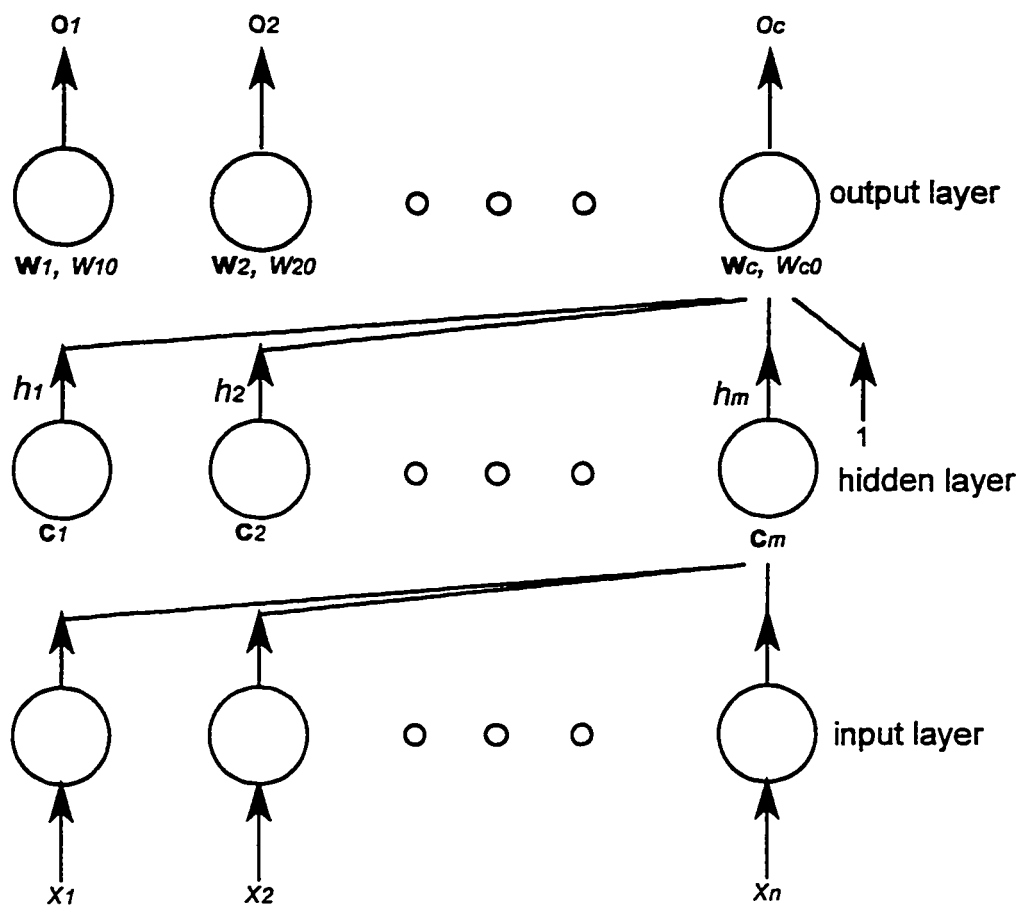
Fig. 2.3 A radial basis function network[3].

---

where $\| \ . \ \|$ is the Euclidean distance, and c_j is the weight vector (center) of the jth

hidden unit. Thus, the net input to a hidden unit equals the distance between the input

vector x and the unit center c_j.

4. The jth hidden unit computes its activation (output), h_j, using

$$h_j(x) = f_{hj}(net_{hj}(x)) \ , \quad j = 0, \ldots, m, \tag{2.10}$$

where f_{hj} is the activation function of the jth hidden unit. In (2.10) the bias term is

included by starting j at 0 and $h_0(x) = f_{h0}(x) = 1$.

5. The jth output unit computes its net input, net_{oj}, using

$$net_{oj}(x) = h(x) \cdot w_j \ , \quad j = 1, \ldots, c, \tag{2.11}$$

where w_j is the weight vector of the jth output unit.

6. The jth output unit computes its activation, o_j, using

$$o_j(x) = net_{oj}(x) \ , \quad j = 1, \ldots, c, \tag{2.12}$$

This yields the output vector, o, of the network and completes its operation.

The above computations are done in parallel on a layer-by-layer basis. In brief, the jth

output of the network is given by

$$o_j(x) = \sum_{i=0}^{m} w_{ji} f_{hi}(\| \ x - c_i \ \|) \ , \quad j = 1, \ldots, c. \tag{2.13}$$

The activation functions of all hidden units are of the same form. Typical forms

include the Gaussian

$$f_{hi}(\| \ x - c_i \ \|) = \exp \{ -0.5 \| \ x - c_i \ \|^2 / \sigma_i^2 \}, \quad i = 1, \ldots, m. \tag{2.14}$$

where the center c_i corresponds to the mean of the Gaussian function, whereas σ_i denotes

its variance or width.

Hartman, Keeler, and Kowalski [9] have proved that an RBFN employing Gaussian hidden units of the same form of (2.14) is a universal approximator for continuous real-valued mappings. Park and Sandberg [10] have proved that even with Gaussian hidden units of the same variance, RBFN is still capable of universal approximation. Other researchers have experimentally and theoretically investigated the characteristics of using Gaussian hidden units in RBFNs (see, for instance, [11] and [12]).

2.2 FUZZY LOGIC SYSTEMS

In 1965, Zadeh published the first paper on a novel way of characterizing nonprobabilistic uncertainties, which he called "fuzzy sets" [13]. This year marks the 32th anniversary of fuzzy logic and fuzzy set theory, which has now evolved into a fruitful area containing various disciplines, such as calculus of fuzzy if-then rules, fuzzy graphs, fuzzy interpolation, fuzzy topology, fuzzy reasoning, fuzzy inference systems, and fuzzy modeling. The applications, which are multi-disciplinary in nature, include automatic control, consumer electronics, signal processing, time series prediction, information retrieval, database management, computer vision, data classification. decision-making, and so on.

Fuzzy logic, which represent the logic on which fuzzy logic controller (FLC) is based. is much closer in spirit to human thinking and natural language than the traditional logical systems. It provides an effective means for capturing the approximate and inexact

nature of the real world. Generally, fuzzy control is by far the most successful application of fuzzy sets and systems theory to practical problems.

2.2.1 BASICS OF FUZZY SET THEORY

In this section, some of the basic concepts of fuzzy set theory and fuzzy logic are introduced briefly. A more detailed discussion may be found in [13-14].

2.2.1.1 FUZZY SETS

Let U be a collection of objects denoted generically by $\{u\}$. U is called the universe of discourse and u represents the generic element of U.

Definition 1: Fuzzy Set: A fuzzy set F in a universe of discourse U is characterized by a membership function μ_F which takes values in the interval [0,1], namely, μ_F: $U \rightarrow [0,1]$. A fuzzy set may be viewed as a generalization of the concept of an ordinary set whose membership function only takes two values $\{0,1\}$. Thus, a fuzzy set F in U may be represented as a set of ordered pairs of a generic element u and its grade of membership function: $F = \{(u, \mu_F(u)| u \in U\}$. The higher the value of $\mu_F(u)$, the more u belongs to F.

2.2.1.2 FUZZY SET OPERATIONS

Let A and B be two fuzzy sets in U with membership functions μ_A and μ_B, respectively. Some of the basic set operations can be defined via their membership functions as follows.

Definition 2: Union: The membership function of the union $A \cup B$ is defined as:

$$\mu_{A \cup B} = \max \{ \mu_A(u), \mu_B(u)\} \tag{2.15}$$

Definition 3: Intersection: The membership function of the intersection $A \cap B$ is defined as:

$$\mu_{A \cap B} = \min \{ \mu_A(u), \mu_B(u)\} \tag{2.16}$$

Definition 4: Complement: The membership function of the complement of a fuzzy set A is defined as:

$$\mu_{\bar{A}} = 1 - \mu_A(u) \tag{2.17}$$

Definition 5: Fuzzy Relation: If A and B are fuzzy sets in U and V, respectively, a binary fuzzy relation is a set in $U \times V$ and is defined as:

$$R = \{((u,v),\mu_R(u,v)) \mid (u,v) \in U \times V\} \tag{2.18}$$

Definition 6: Compositional Rule of Inference: Let A and B be fuzzy sets in U and V with membership functions of $\mu_A(u)$ and $\mu_B(v)$, respectively. A fuzzy relation R on $U \times V$ has a membership function of $\mu_R(u, v)$ which satisfies the compositional rule of inference as follows:

$$\mu_B(v) = \max_u (\min\{\mu_R(u,v).\mu_A(u)\}) \tag{2.19}$$

2.2.1.3 LINGUISTIC VARIABLES

A linguistic variable can be regarded as a variable whose values are defined in linguistic terms rather than numbers. For example, let u denote the name of a linguistic variable (e.g., speed). The values of u may be *negative, zero,* and *positive.* A linguistic variable is usually decomposed into a set of terms, $T(u)$, which covers its universe of discourse as follows:

$$T(speed) = \{negative, zero, positive\} \qquad (2.20)$$

2.2.1.4 FUZZY RULES

Fuzzy rules are expressed as a collection of IF-THEN statements of the form

$$\text{if } u \text{ is } A \text{ and } v \text{ is } B \text{ then } w \text{ is } C \qquad (2.21)$$

where A, B, and C are linguistic values of the linguistic variables u, v, and w, respectively. Often, "u is A and v is B" is called the *antecedent* or *premise* while "w is C" is called the *consequence* or *conclusion.*

Generally, fuzzy rules may be provided by human experts or can be extracted from numerical data.

2.2.2 FUZZY LOGIC SYSTEM STRUCTURE

In general, a fuzzy logic system that is widely used in FLCs maps crisp inputs into crisp outputs. It comprises four principal components *fuzzifier, rule base, inference engine,* and *defuzzifier*. Figure 2.4 depicts a configuration of a fuzzy logic system. The fuzzy logic system components are discussed in details in what follows.

1) *Fuzzifier* performs the following functions:

- measuring the values of input variables,

- a scale mapping, which transfers the range of values of input variables into corresponding universes of discourses,

- fuzzification, which converts the crisp input data into suitable linguistic values.

2) *Rule base* comprises a knowledge of the application domain and the control goals. It consists of a "data base" and a "fuzzy rule base" such that

- the data base provides necessary definitions of the fuzzy rules and data manipulation in an FLC,

- the rule base characterizes the control goals and control policy of the domain experts by means of a set of linguistic control rules.

3) *Inference engine* is a kernel of an FLC. It has the capability of simulating human decision-making based on fuzzy concepts and of inferring fuzzy control actions employing fuzzy rules.

4) *Defuzzifier* performs the following functions:

- a scale mapping, which converts the range of values of output variables into corresponding universes of discourses.

- defuzzification, which yields a nonfuzzy control action from an inferred fuzzy control action.

2.2.3 FLC DESIGN METHODOLOGY

The design methodology of a FLC usually follows the iterative steps shown in Fig. 2.5. These steps can be summarized as follows:

1. obtain an understanding of the plant dynamics.

2. define the boundaries of the fuzzy universe of discourse and the number of partitions within it.

3. define the membership functions of the fuzzy sets. The shapes of the membership functions used in most studies are triangular, trapezoidal, or Gaussian functions.

4. decide a fuzzification and defuzzification strategies to convert real measurements to the fuzzy domain and vice versa.

5. derive the control rules that form the expert knowledge of the controller. The traditional method of obtaining these rules is a heuristic trial-and-error approach based on analyzing process behavior. and consequent iterative modification to obtain acceptable performance.
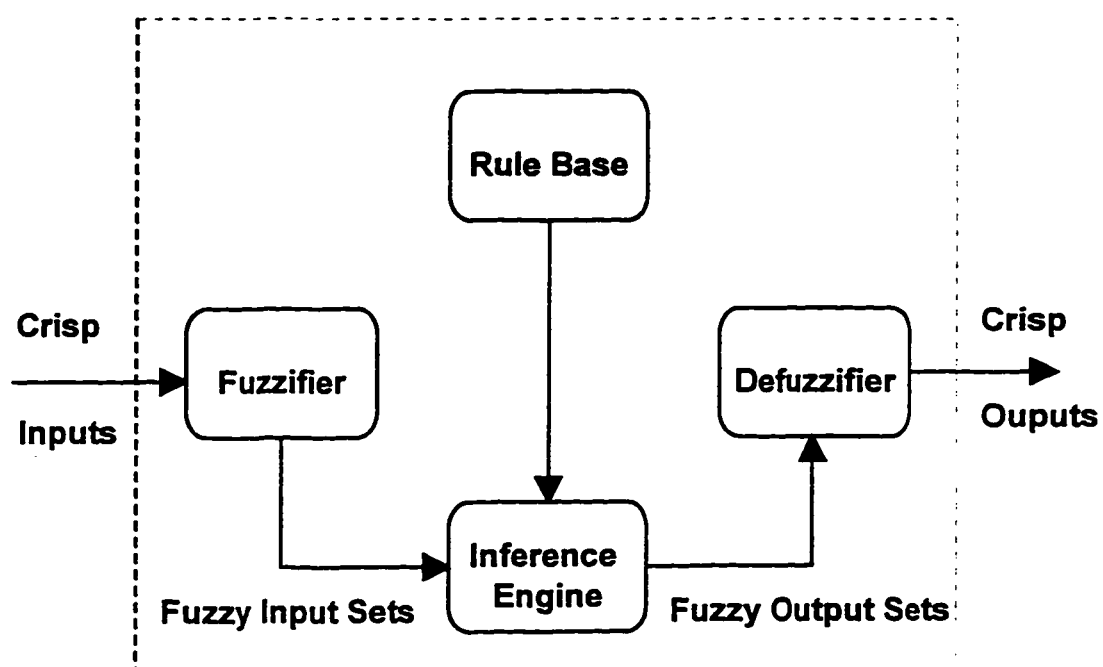
Fig. 2.4 Basic configuration of fuzzy logic systems.
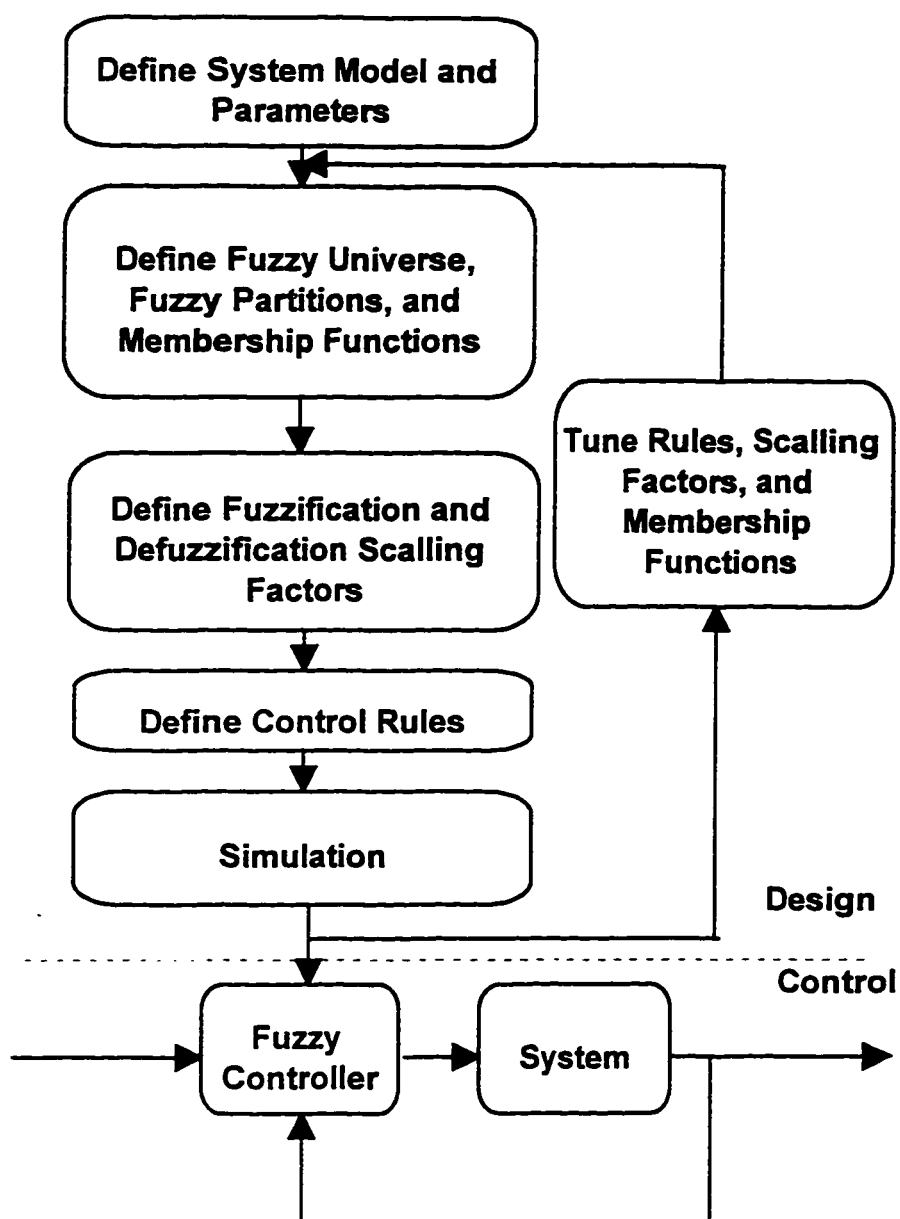
Fig. 2.5 Fuzzy design methodology.

2.2.4 FLC DESIGN PROBLEMS

Although they have been applied in many complex systems, FLCs experience a deficiency in knowledge acquisition, and rely to a great extent on empirical and heuristic knowledge which in many cases cannot be elicited objectively. Among the problems to be resolved in fuzzy design are the determination of the linguistic state space, the definition of the membership grades of each linguistic term and the derivation of control rules. At present, the fuzzy rules and membership functions are subjectively defined by studying a human-operated system or an existing controller and then testing the design for proper output. If the design fails the test, fuzzy rules and membership functions should be adjusted. Therefore, the design of the traditional fuzzy logic controller requires a lot of trial-and-error, thus making the design a laborious and time-consuming task.

2.3 GENETIC ALGORITHMS

Genetic algorithms (GA) are exploratory search and optimization procedures that were devised on the principles of natural evolution and population genetics [15-17]. GA are distinguished from other optimization techniques by the use of these principles to guide the search. Unlike other optimization techniques, GA work with a population of individuals represented by bit strings and modify the population with random search and competition. The advantages of GA over other traditional optimization techniques are:

- GA work on a coding of the parameters to be optimized, rather than the parameters themselves.

- GA search the problem space using a population of trials representing possible solutions to the problem, not a single point, i.e., GA have implicit parallelism. This property ensures GA to be less susceptible to getting trapped on local minima.

- GA use an objective function assessment to guide the search in the problem space.

- GA use probabilistic rules to make decisions.

The basic concepts of GA are given in what follows.

2.3.1 GA INITIALIZATION

At first, the optimized parameters are encoded into genes as a string of binary bits. The length of the genes and hence the length of the binary string can be calculated by prespecifying the search space, i.e., maximum and minimum values of each parameter, and the desired accuracy. The initial values of the estimated parameters are randomly assigned. Therefore, at the beginning of the optimization process, all population are generated as random binary strings. Each string can be evaluated by determining its fitness which governs the extent to which an individual can influence future generations. Therefore, a fitness function or a performance index has to be initially defined.

2.3.2 GA OPERATIONS

In general, GA include the following operations:

Reproduction is a process in which a new generation of population is formed by selecting the fittest individuals in the current population. This process results in individuals with higher fitness values obtaining one or more copies in the next generation while low fitness individuals may have none.

Crossover is the most dominant operator in GA, and is responsible for producing new children by selecting two strings among the potential parents and exchanging portions of their structures. The new children may replace the weaker individuals in the population. A simple one point crossover is shown in Fig. 2.6. The crossover point is randomly assigned by a random generator. In this way, the excellent characteristics of the parents will be inherited in the next generation. The probability of crossover is set arbitrarily and is typically greater or equal to 0.6 [16]. When a random number generated between 0 and 1 is less than the preset value of crossover probability, crossover will take place.

Mutation is a local operator which is applied with a very low probability of occurrence. Its function is to alter the value of a random position in a string. This avoids the loss of important information at a particular position in the string. Similar to crossover probability, the mutation probability is set arbitrarily and is typically 0.001 [16]. When a random number generated between 0 and 1 is less than the preset value of mutation probability, a string will be mutated. The mutation process is depicted in Fig. 2.7.

Crossover Point

Parent 1	0 0 0 0 0 0 0 0 0 0 0 0 0 0
Parent 2	1 1 1 1 1 1 1 1 1 1 1 1 1 1

Child 1	0 0 0 0 0 0 0 1 1 1 1 1 1 1
Child 2	1 1 1 1 1 1 1 0 0 0 0 0 0 0
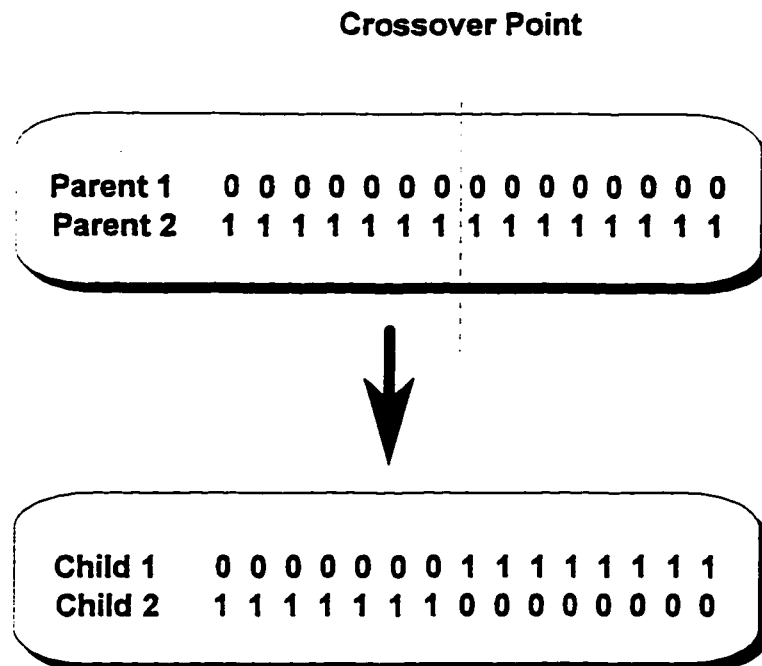
Fig. 2.6 A simple crossover

1 1 0 1 0 1 0 1 0 1 1 0 0 0 1 1

1 1 0 1 0 1 0 1 0 1 1 0 1 0 1 1
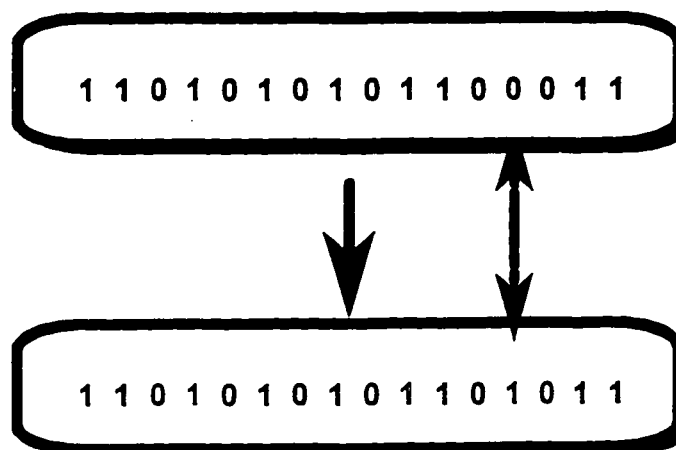
Fig. 2.7 Mutation step

Inversion is a process which inverts the order of the elements between two randomly chosen points on the string.

2.3.3 GA COMPUTATIONAL FLOW

The GA require two main stages of *generation* and *evaluation*.

Generation consists of generating an initial random population of strings representing possible solutions in the search space.

Evaluation consists of testing the probable solutions. In order to evaluate a population, a fitness function is defined. The fitness function serves as a focus towards the optimal solution and is used as a basis for selecting the parents for mating that have the greater merit. The genetic operations are systematically and repeatedly applied to the population until an acceptable solution is found or a stopping criterion is met.

The GA computational flow is shown in Fig. 2.8.

2.4 RULE-BASED SYSTEMS

A rule-based system is a computer system that encapsulates specialist knowledge about a particular domain of expertise and is capable of making intelligent decisions within that domain. Rule-based systems have been applied to different real world problems with promising results [18]. The essential components of a rule-based system are described in what follows.
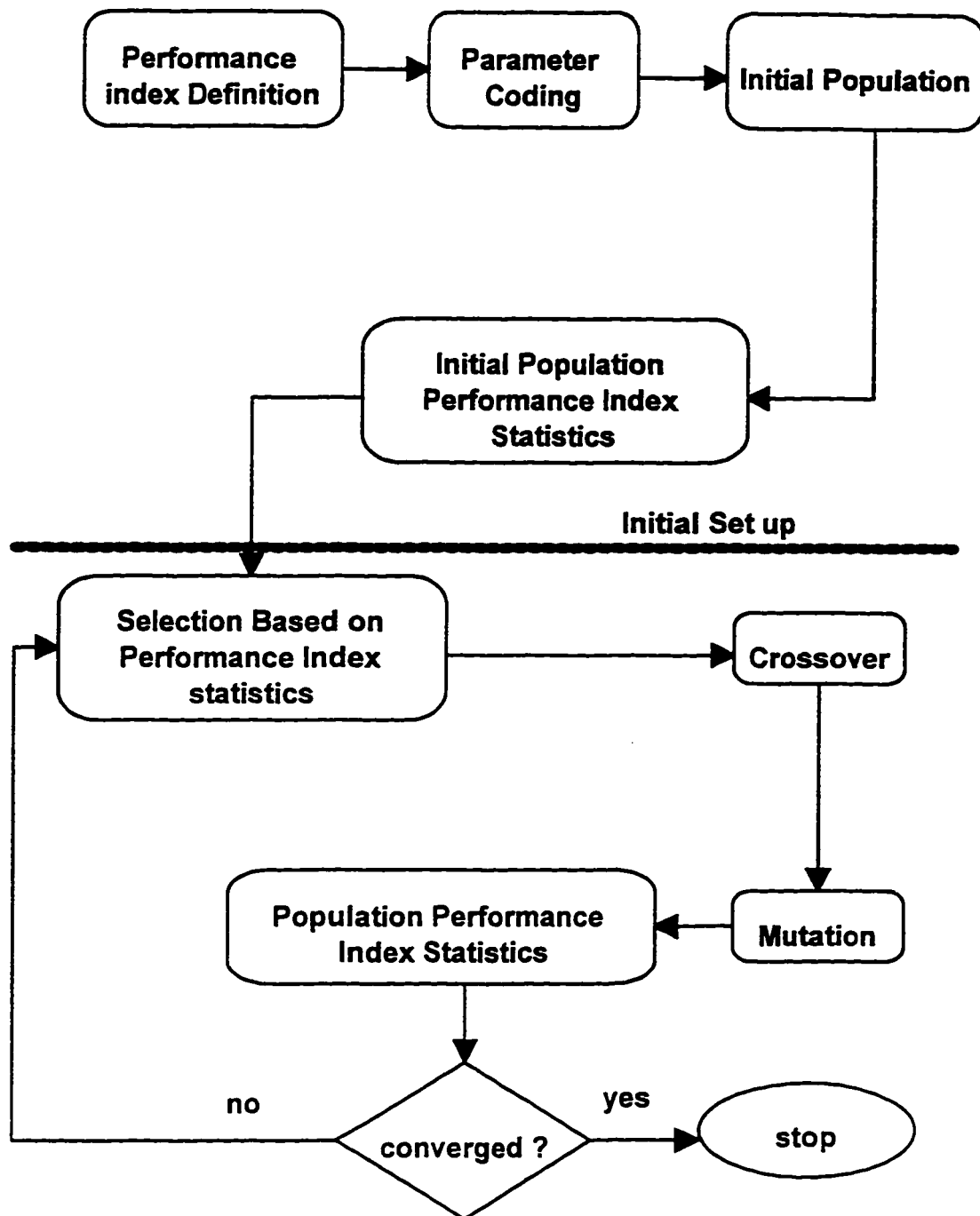
Fig. 2.8 GA computational flow chart

1) *Rule base* contains the expertise to be applied in the form of IF-THEN rules.

2) *Inference engine* models the process of a human expert's reasoning in such a way that it uses rule base to infer and take an intelligent decision.

3) *Knowledge acquisition* is a part in which the expert's knowledge can be acquired.

4) *Explanatory interface* provides an explanation to the user *why* the rule-based system is asking a question and *how* it is reaching some conclusions.

A typical rule-based system is shown in Fig. 2.9. Generally, knowledge is a scarce and costly resource. The knowledge acquisition process is the main bottleneck in the development of rule-based systems. The traditional way has been to closet a highly paid domain expert with a highly paid knowledge engineer for a long period during which they effectively negotiate a codified version of what the expert knows. This process takes time and, obviously, money.

2.5 SUMMARY

In this chapter, the intelligent techniques have been briefly introduced. The techniques used throughout this thesis are neural networks, fuzzy logic systems, genetic algorithms, and rule-based systems.

In the following two chapters, the approximation capabilities of neural networks will be exploited to approximate the nonlinear dynamics of synchronous machines. The radial basis function network will be proposed for off-line identification in chapter 3 and for on-line identification in chapter 4.
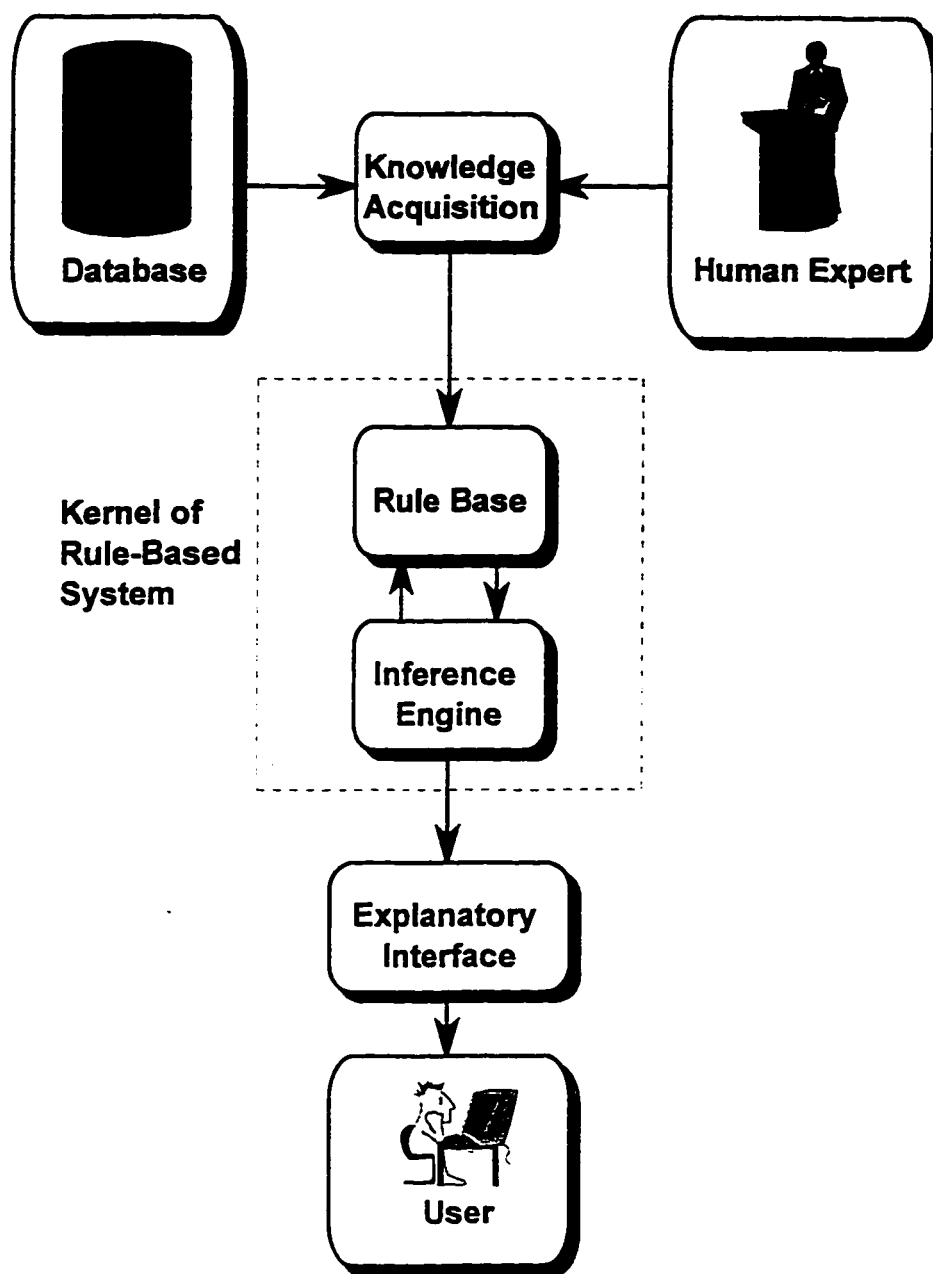
Fig. 2.9 A typical rule-based system

CHAPTER 3

OFF-LINE IDENTIFICATION OF SYNCHRONOUS

MACHINES

3.1 INTRODUCTION

System modeling and identification are fundamental problems in engineering where it

is often required to approximate a real system with an appropriate model given a set of

input-output data. The model structure needs to have sufficient representation ability to

enable the underlying characteristics to be approximated with an acceptable accuracy. For

linear time-invariant systems, model structure and identification problems have been well

studied [19-20]. Although the nonlinear autoregressive moving average with exogenous

variables (NARMAX) description [21] has been shown to provide a very useful unified

representation for a wide class of nonlinear systems. nonlinear system identification is

much more complex and difficult. In general. the problem of identifying a model

structure and its associated parameters can be related to the problem of learning a

mapping between a known input and output space. A classical framework of this problem can be found in approximation theory.

Recently, it has been shown that feedforward neural networks with one hidden layer can uniformly approximate any continuous function to a chosen degree of accuracy [3-5]. BPNNs have been applied to identification and control of dynamical systems [22]. A synchronous machine has been modeled using BPNNs [23-25]. However, BPNNs have several problems such as getting stuck in local minima and slow convergence rate [26].

On the other hand, it has recently been acknowledged that the approximation accuracy properties of RBFN are advantageous as compared to the other methods, including BPNNs [27-32]. Even more important for many applications, the RBFNs provide linear approximation in the network weights. This feature makes powerful tools of the linear system theory applicable to the RBFN identification of nonlinear systems [33]. The "linear in parameters" property of the radial basis functions guarantees the convergence of the parameters to the global minimum. Moreover, the local tunability of the radial basis functions causes only some of the nodes to be affected by any given input [27-28], and only a portion of the model parameters may need to be adjusted, thus reducing the training time and computational overhead. Furthermore, RBFNs are not as sensitive to the architecture as BPNNs [34].

3.2 PROBLEM FORMULATION

The seventh order flux linkage model of a single synchronous machine connected to an infinite bus as shown in Fig. 3.1 is used in this study. The system model and parameters are given in the Appendix A. The state and output equations of the synchronous machine are described by the following nonlinear discrete model

$$z\,((k+1)) = f(z(k),\, u(k)) \tag{3.1}$$

$$y\,(k) = g(\,z(k)) \tag{3.2}$$

where k denotes to the kth time interval. In the above model, $f(.)$ and $g(.)$ are the nonlinear state and output mapping functions respectively. The input vector $u(k)$ represents the mechanical torque T_m and the field voltage V_F that is, $u(k) = [T_m(k), V_F(k)]^T$. The vector $z(k)$ is the state vector, that is, $z(k) = [\delta,\omega,\psi_d,\psi_F,\psi_D,\psi_q,\psi_Q]^T$ and $y(k)$ is the output vector. In this study, we observe two quantities: the rotor angle, δ, and the flux linkage in the d-axis, ψ_d. Hence, the output vector $y(k) = [\delta(k),\psi_d(k)]^T$.

3.3 THE PROPOSED IDENTIFICATION SCHEME

In the dynamical system described in (3.1) and (3.2), the nonlinear mappings are assumed to be unknown. An RBFN is proposed to identify these mappings. The input vector of the RBFN identifier. $x(k)$. is comprised of the current values of $u(k)$ and $z(k)$. that is, $x(k) = [u(k),z(k)]^T$. The output vector of the RBFN identifier is the future values

of the rotor angle, $\delta(k+l)$, and d-axis flux linkage, $\psi_d(k+l)$, that is, $y_{net}(k+1) = [\delta(k+l), \psi_d(k+l)]^T$. The proposed identification scheme is depicted in Fig. 3.2.

3.4 LEARNING ALGORITHMS

The centers of RBF units, the widths of RBF units, and the weights between the hidden layer and the output layer represent the RBFN parameters that have to be determined by the learning algorithm. In order to demonstrate the potential of RBFN to identify the synchronous machine, two learning algorithms have been applied, namely, the k-means algorithm and the orthogonal least squares (OLS) algorithm.

Consider training of the RBFN shown in Fig. 1.3 to solve the approximation problem; the network is trained to learn a target mapping $t(x) : \mathcal{R}^n \rightarrow \mathcal{R}^c$. The output layer parameters are determined using supervised learning, so we must assume having a training set $\mathcal{T}_N = \{(x^1, t^1), \ldots, ((x^N, t^N)\}$. In what follows, the k-means algorithm and the OLS algorithm are discussed.

3.4.1 K-MEANS LEARNING ALGORITHM

Moody and Darken [35] have proposed a simple and efficient learning algorithm for RBFN. In this algorithm, the parameters of the RBFN are determined in three steps. First, the RBF unit centers are determined using k-means clustering algorithm by prespecifying the number of clusters which equals the number of hidden units, m.
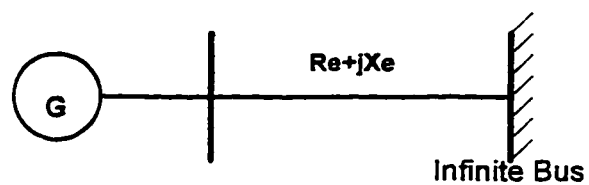
Fig. 3.1 Synchronous machine connected to an infinite bus.
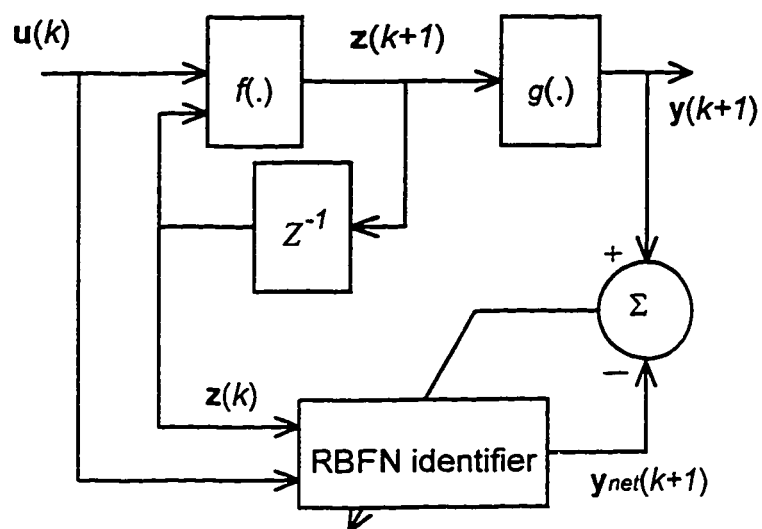
Fig. 3.2 The proposed off-line identification scheme.

Secondly, the width parameter of the ith hidden unit, σ_i, is chosen to be the root mean square distance between c_i and a number of the nearest neighboring unit centers n_n, as

$$\sigma_i = \left[\frac{1}{n_n} \sum_{j=1}^{n_n} \left(\| c_i - c_j \| \right)^2 \right]^{1/2} \qquad (3.3)$$

Finally, the weights of the output layer are determined by considering the network output to be equal the target value. Hence, rewriting (2.13) as

$$t_j(x) = \sum_{i=0}^{m} w_{ji} f_{hi}(\| x - c_i \|) , \quad j = 1, \ldots, c. \qquad (3.4)$$

Let H denote the $(m+1) \times N$ matrix whose ith column is given by h^i, the output of the hidden layer given an input x^i. In matrix form, (3.4) can be rewritten as

$$W H = T \qquad (3.5)$$

where T denotes the $c \times N$ matrix whose ith column is t^i, $W = [w_1\, w_2 \ldots w_c]^T$ denotes the $c \times (m+1)$ weight matrix of the output layer, and $w_j = (w_{j0},\, w_{j1},\, \ldots,\, w_{jm})^T$. Using the orthogonal triangularization technique [20], (3.5) can be solved for W.

In this algorithm, the number of the hidden units m and the number of the nearest neighbor centers n_n used to estimate the hidden unit width are the design parameters. These parameters are selected after several trials to yield good performance.

3.4.2 OLS LEARNING ALGORITHM

The orthogonal least squares (OLS) algorithm [36-37] is a structural identification algorithm. Unlike the k-means algorithm which requires a fixed network structure, the OLS algorithm automatically determines an adequate RBFN structure during learning. By

formulating the learning problem as a subset model selection, an OLS procedure is used

to identify appropriate RBF unit centers from the network training data, and to estimate

the network weights simultaneously. The desired property of this algorithm is that the

selection of the RBF unit centers is directly linked to the reduction in the trace of the

error covariance matrix. Although each RBF unit may have a different width, a same

width is sufficient for universal approximation [10]. Therefore, all the RBF unit widths

can be fixed to a value σ, and this can simplify the training strategy.

Initially, all the training input vectors $\{\ \mathbf{x}^i\ \}$, $i = 1, \ldots, N$, are considered as candidates

for centers. Therefore, the initial number of centers m_i is equal to N. The desired output in

(3.4) can be considered as a special case of the linear regression model

$$t_k(\mathbf{x}) = \sum_{j=0}^{N} p_j\ w_{jk} + e_k(\mathbf{x}). \quad k = 1, \ldots, c, \tag{3.6}$$

where p_js are known as regressors which are fixed functions of the input vector $\mathbf{x}$, i.e.,

$$p_j = p_j(\mathbf{x}), \quad j = 0, 1, \ldots, N \tag{3.7}$$

The bias term is represented by setting $p_0 = 1$. In (3.6), $e_k(\mathbf{x})$ is the error between the kth

desired and network outputs which is assumed to be uncorrelated with the regressors. By

defining

$$\mathbf{e}_i = [\ e_i^1, \ldots, e_i^N\ ]^T, \quad i = 1, \ldots, c, \tag{3.8}$$

$$\mathbf{t}_i = [\ t_i^1, \ldots, t_i^N\ ]^T, \quad i = 1, \ldots, c. \tag{3.9}$$

$$\mathbf{p}_j = [\ p_j^1, \ldots, p_j^N\ ]^T, \quad j = \cdots \ldots, N \tag{3.10}$$

then, (3.6) can be expressed as

$$[\mathbf{t}_l \cdots \mathbf{t}_c] = [\mathbf{p}_0 \cdots \mathbf{p}_N] \begin{bmatrix} w_{01} & \cdot & \cdot & w_{0c} \\ \cdot & & & \cdot \\ \cdot & & & \cdot \\ w_{N1} & \cdot & \cdot & w_{Nc} \end{bmatrix} + [\mathbf{e}_l \cdots \mathbf{e}_c] \qquad (3.11)$$

or, more concisely, in matrix form

$$\mathbf{T} = \mathbf{P} \, \mathbf{W} + \mathbf{E} \qquad (3.12)$$

The OLS algorithm involves the transformation of the set of $\mathbf{p}_j$ into a set of orthogonal basis vectors and uses only the significant ones to form the final RBFN. In general, the number of significant basis vectors in the final network, m, is much less than the initial number, m_i. The regression matrix P can be decomposed into

$$\mathbf{P} = \mathbf{Q} \, \mathbf{A} \qquad (3.13)$$

where A is an $m \times m$ upper triangular matrix with unity diagonal elements, that is,

$$\mathbf{A} = \begin{bmatrix} 1 & a_{12} & \cdot & a_{1m} \\ 0 & 1 & \cdot & \cdot \\ \cdot & \cdot & \cdot & a_{m-1m} \\ 0 & 0 & \cdot & 1 \end{bmatrix} \qquad (3.14)$$

and Q is an $N \times m$ matrix with orthogonal columns $\mathbf{q}_i$ such that

$$\mathbf{Q}^{\mathrm{T}} \mathbf{Q} = \mathbf{S} \qquad (3.15)$$

where S is a diagonal matrix. Using (3.13), (3.12) can be rewritten as

$$\mathbf{T} = \mathbf{Q} \, \mathbf{G} + \mathbf{E} \qquad (3.16)$$

The OLS solution for (3.16) is given by

$$\mathbf{G} = \mathbf{S}^{-1} \mathbf{Q}^{\mathrm{T}} \mathbf{T} \qquad (3.17)$$

or

$$g_{ij} = \mathbf{q}_i^{\mathrm{T}} \mathbf{t}_j / (\mathbf{q}_i^{\mathrm{T}} \mathbf{q}_i) \ , \ i = 1, \ldots, m, \quad j = 1, \ldots, c \qquad (3.18)$$

The matrices **G** and **W** satisfy the triangular system

$$\mathbf{A}\,\mathbf{W} = \mathbf{G} \tag{3.19}$$

The classical Gram-Schmidt method [38] can be used to derive (3.19) and solve for **W**. The criterion for determining the significance of candidates is the contribution of a candidate to the trace of the desired output covariance matrix. Because the error matrix **E** is orthogonal to **Q**, it can be shown that trace of the covariance of **T** is

$$\text{trace}(\mathbf{T}^{\mathsf{T}}\mathbf{T}/N) = \sum_{j=1}^{m}(\sum_{i=1}^{c} g_{ji}^{2})\mathbf{q}_{j}^{T}\mathbf{q}_{j} \,/\, N + \text{trace}(\mathbf{E}^{\mathsf{T}}\mathbf{E}/N) \tag{3.20}$$

The error reduction ratio due to $\mathbf{q}_k$ can be defined as

$$[err]_{k} = (\sum_{i=1}^{m} g_{ki}^{2})\mathbf{q}_{k}^{T}\mathbf{q}_{k}/\text{trace}(\mathbf{T}^{\mathsf{T}}\mathbf{T}) \,,\, k=1,\ldots,m \tag{3.21}$$

A candidate regressor is selected at the kth step if it produces the largest value of $[err]_k$ from among the remaining candidates. The regressor selection procedure can be summarized as follows.

* At the first step, for $i = 0, \ldots, N$ compute

$$\mathbf{q}_i^{(i)} = \mathbf{p}_i$$

$$g_{1j}^{(i)} = (\mathbf{q}_i^{(i)})^{\mathsf{T}}\mathbf{t}_j \,/\, ((\mathbf{q}_i^{(i)})^{\mathsf{T}}\mathbf{q}_i^{(i)}) \,,\, j = 1,\ldots,c$$

$$[err]_i^{(i)} = (\sum_{j=1}^{c} (g_{1j}^{(i)})^{2})(\mathbf{q}_i^{(i)})^{\mathsf{T}}\mathbf{q}_i^{(i)}/\text{trace}(\mathbf{T}^{\mathsf{T}}\mathbf{T})$$

Find

$$[err]_i^{(i1)} = max \{ [err]_i^{(i)}, i = 0,\ldots,N \}$$

and select

$$\mathbf{q}_1 = \mathbf{q}_i^{(i1)} = \mathbf{p}_{i1}$$

$$g_{1j} = g_{1j}^{(i1)} \quad , j = 1, \ldots, m$$

* At the kth step where $k = 2, \ldots, m$, for $i = 0, \ldots, N$ and $i \neq i_1, \ldots, i \neq i_{k-1}$, compute

$$a_{jk}^{(i)} = \mathbf{q}_j^T \mathbf{p}_i / (\mathbf{q}_j^T \mathbf{q}_j) \quad , j = 1, \ldots, k-1$$

$$\mathbf{q}_k^{(i)} = \mathbf{p}_i - \sum_{j=1}^{k-1} a_{jk}^{(i)} \mathbf{q}_j$$

$$g_{kj}^{(i)} = (\mathbf{q}_k^{(i)})^T \mathbf{t}_j / ((\mathbf{q}_k^{(i)})^T \mathbf{q}_k^{(i)}) \quad , j=1, \ldots, c$$

$$[err]_k^{(i)} = (\sum_{j=1}^{c} (g_{kj}^{(i)})^2)(\mathbf{q}_k^{(i)})^T \mathbf{q}_k^{(i)} / \text{trace}(\mathbf{T}^T \mathbf{T})$$

Find

$$[err]_k^{(ik)} = max\{[err]_k^{(i)}, i = 0, \ldots, N, \ i \neq i_1, \ldots, i \neq i_{k-1}, \}$$

and select

$$\mathbf{q}_k = \mathbf{q}_k^{(ik)}$$

$$g_{kj} = g_{kj}^{(ik)}, \quad j = 1, \ldots, c$$

* The procedure is terminated at the mth step when

$$1 - \sum_{j=1}^{m} [err]_j < \rho$$

where $0 < \rho < 1$ is a chosen tolerance. This gives a subset model containing m significant regressors.

3.5 ASSESSMENT OF MODEL VALIDITY

In order to assess the validity of the proposed identifier. three tests have been applied as follows.

3.5.1 CORRELATION-BASED MODEL VALIDITY TEST

The adequacy of the modeling can be tested using the correlation-based model validity tests. Define the residual vector

$$e(k) = y(k) - y_{net}(k) \qquad (3.22)$$

where $y(k)$ represents the desired output vector and $y_{net}(k)$ represents the network output vector. It can be shown [39-40] that if the identified model is operating correctly then the following correlation tests using residuals and inputs should be satisfied:

$$\Gamma_{xx} = \Gamma_{e_i e_i}(\tau) = \Gamma_{e_i e_i}(\tau) = \lambda(t), \forall \tau$$

$$\Gamma_{yx} = \Gamma_{u_j e_i}(\tau) = \Gamma_{u_j e_i}(\tau) = 0, \quad \forall \tau \qquad (3.23)$$

where e_i is the ith residual and u_j is the jth input. Γ_{xx} and Γ_{yx} are the auto-correlation and cross-correlation functions respectively while $\lambda(t)$ represents the unit impulse function. In practice, the model will be regarded as adequate if all the tests fall within the 95% confidence bands at approximately $\pm 1.96 / \sqrt{N}$ where N is the number of test patterns.

3.5.2 MEAN SQUARE ERROR TEST

The model accuracy can be tested by computing the mean square error (MSE) between the desired and network outputs. Define MSE as

$$MSE = \sum_{k=1}^{N} \sum_{i=1}^{c} [y_i(k) - y_{i\,net}(k)]^2 / (N \times c) \qquad (3.24)$$

where c is the number of outputs.

3.5.3 RELIABILITY TEST

This test measures if there is enough training data in the vicinity of the test point to reliably make a prediction. Define the maximum activation of the RBF units for a certain test pattern, x, as

$$max\text{-}act = \max \left(f_{hi}(\| \ x - c_i \ \|) \right), \quad i = 1, \ldots, m. \qquad (3.25)$$

where m is the number of RBF units.

A small value of *max-act* indicates that the test pattern is far from the training data. If the value of *max-act* is below a certain threshold, e. g. < 0.5, this indicates that the model is unreliable [12].

3.6 RESULTS AND SIMULATIONS

In order to investigate the performance of the proposed RBFN identifier, random variation signals uniformly distributed in the range of 60-140% of the initial values of the mechanical torque and field voltage have been applied. Two different sets of 1000 patterns have been generated for training and testing the proposed identifier. Due to space limitations. only the first 100 patterns will be shown in the results. Initially, the machine was operating at power of 1.0 pu with a 0.9 power factor lagging and a terminal voltage of 1.172 pu.

3.6.1 RANDOM VARIATIONS IN MECHANICAL TORQUE

A random variation in mechanical torque as shown in Fig. 3.3 has been applied. The responses of the rotor angle and d-axis flux linkage with both learning algorithms are shown in Figs. 3.4 and 3.5 respectively. It is worth pointing out that it is difficult to discern a difference between the simulated and identified responses for both learning algorithms confirming the capability of the proposed identifier to capture the nonlinear operating characteristics of the synchronous machine. The results of the model validation tests, as shown in Figs. 3.6 and 3.7, fall within the 95% confidence bands confirming the adequacy of the proposed identifier trained by either k-means algorithm or OLS algorithm. The reliability test, Fig. 3.8, shows that the maximum activation of the hidden units for all test patterns is above the threshold indicating that the model is reliable with both learning algorithms. A comparison between k-means learning algorithm and OLS learning algorithm is given in Table 3.1. It can be concluded that, with approximately the same MSE of both learning algorithms, RBFN identifier trained by OLS algorithm produces a simpler model. On the other hand, the identifier trained by k-means algorithm gives a more reliable model as shown in Fig. 3.8. This can be attributed to the large number of hidden nodes in the identified model.
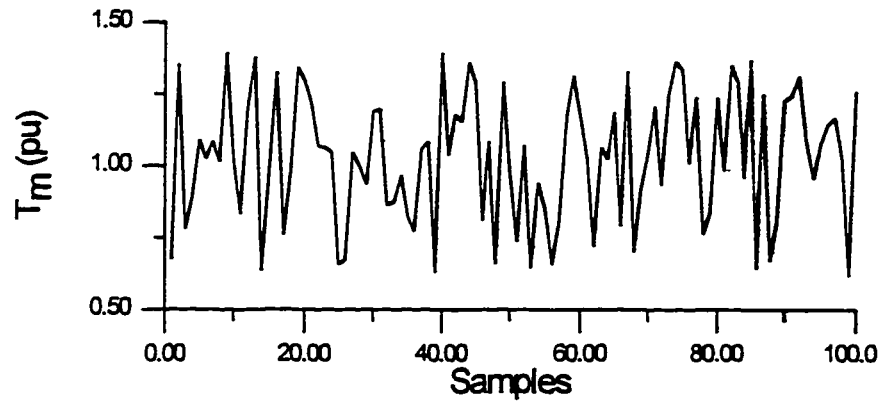
Fig. 3.3 Random variations in mechanical torque
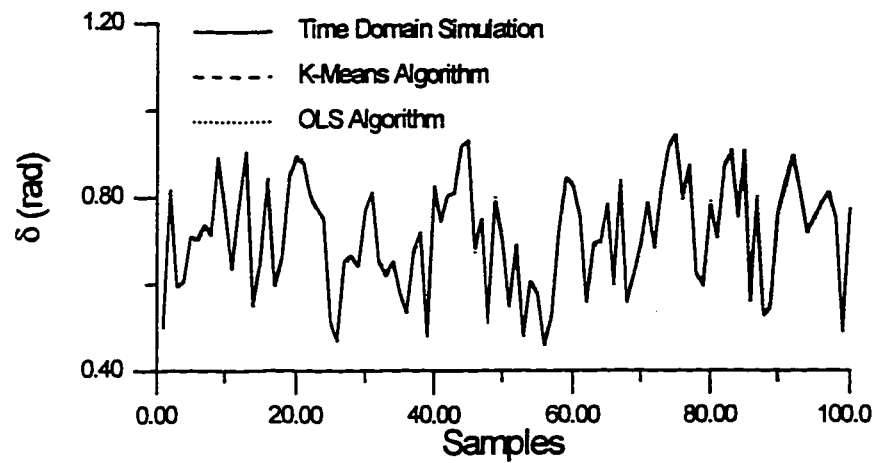
Fig. 3.4 RBFN rotor angle response due to random variations in T_m
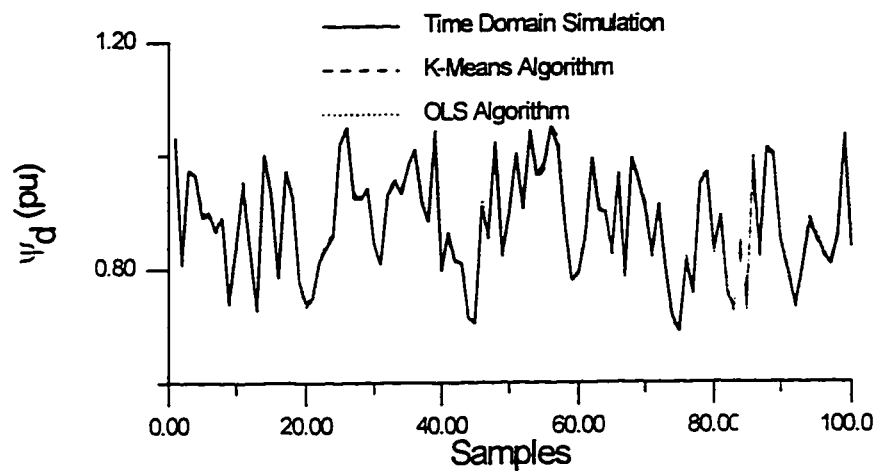
Fig. 3.5 RBFN d-axis flux linkage response due to random variations in T_m
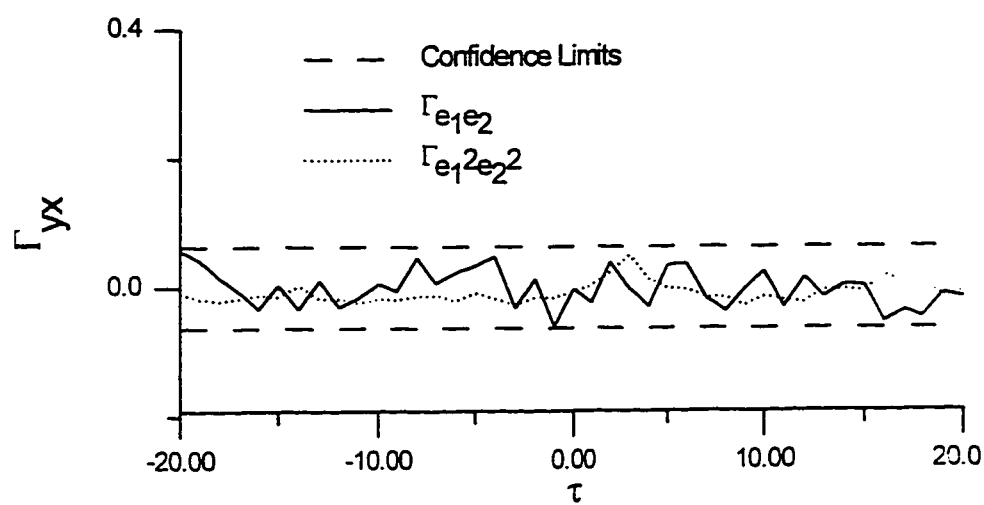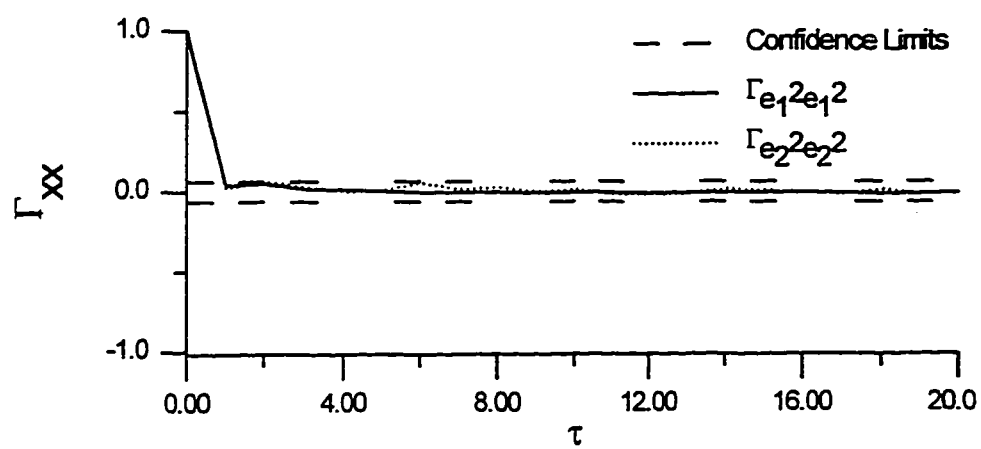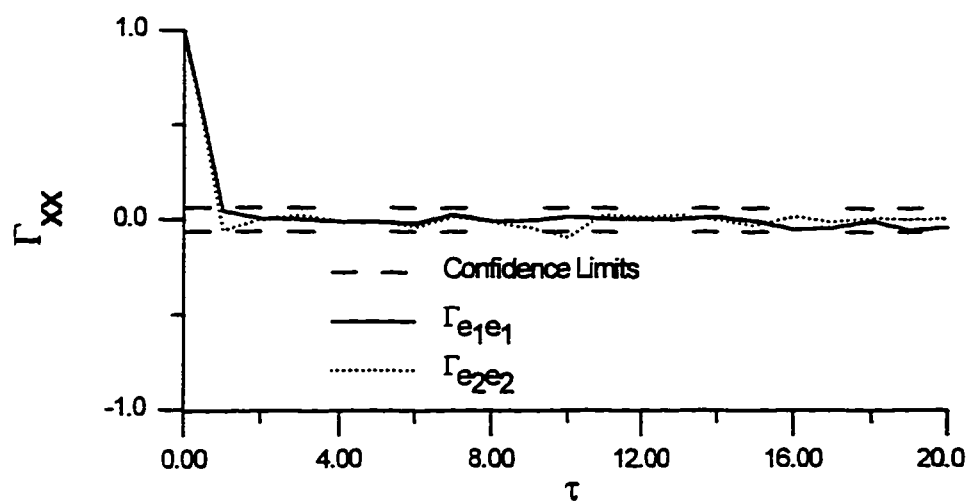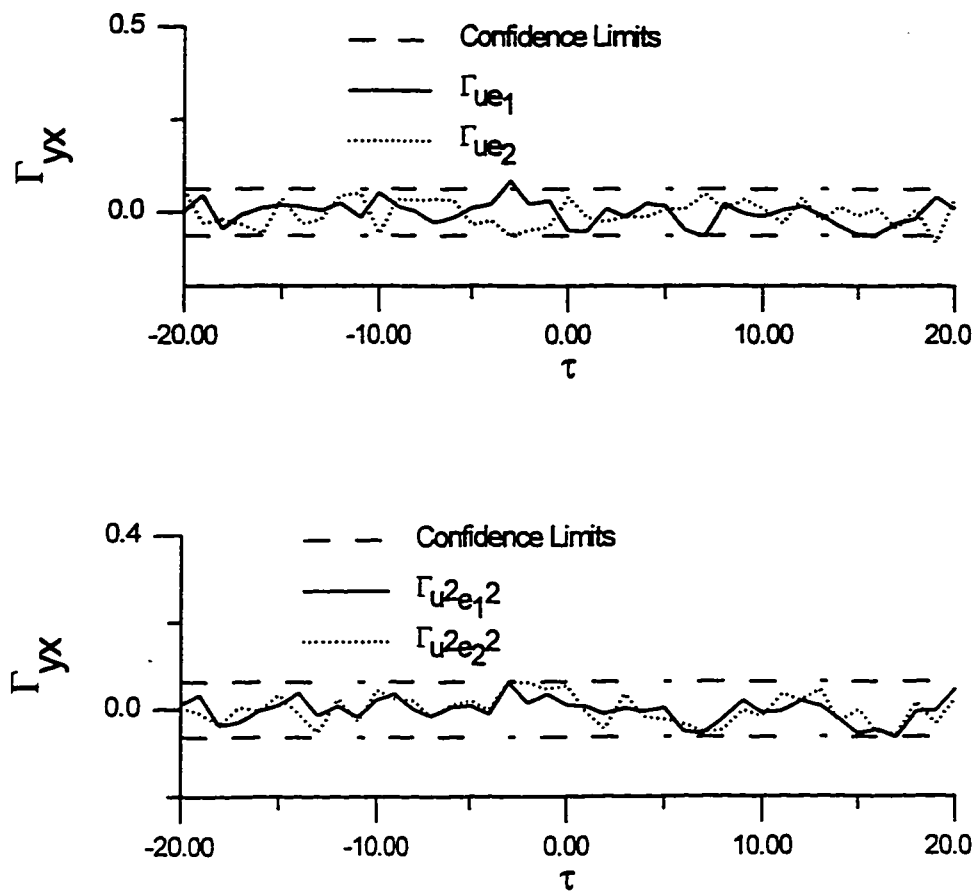
Fig. 3.6 Correlation tests using residuals and T_m with k-means training algorithm
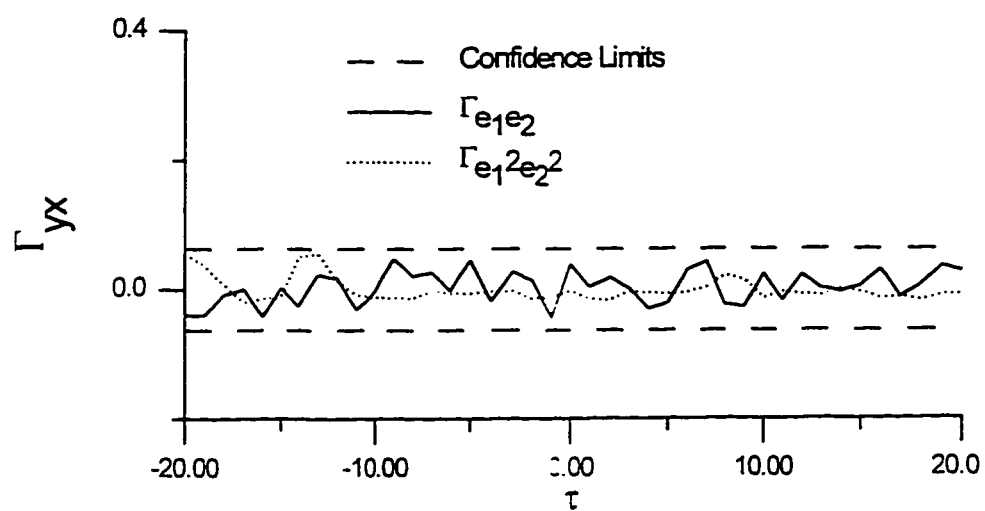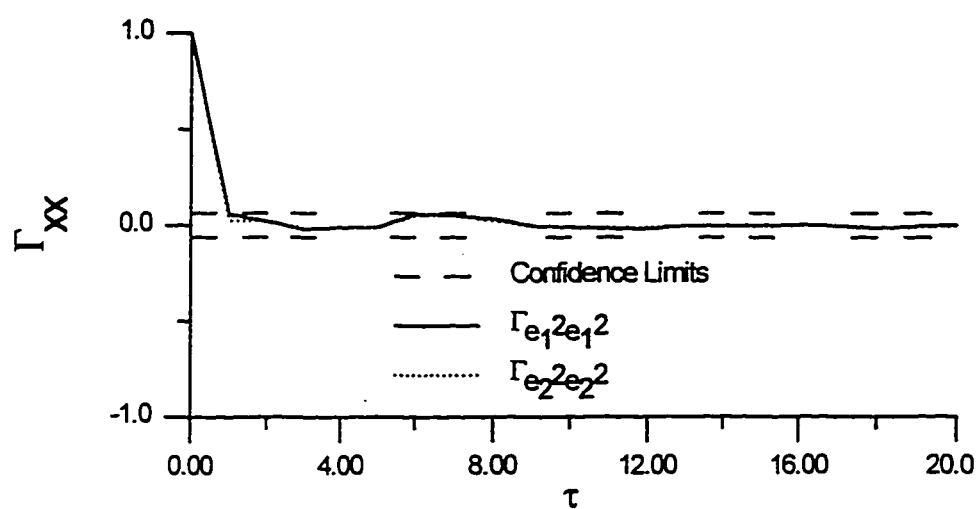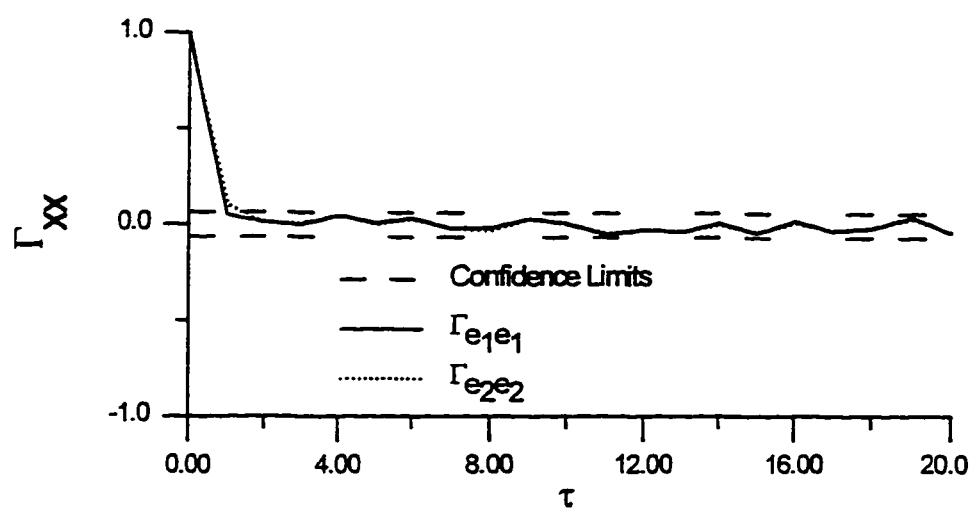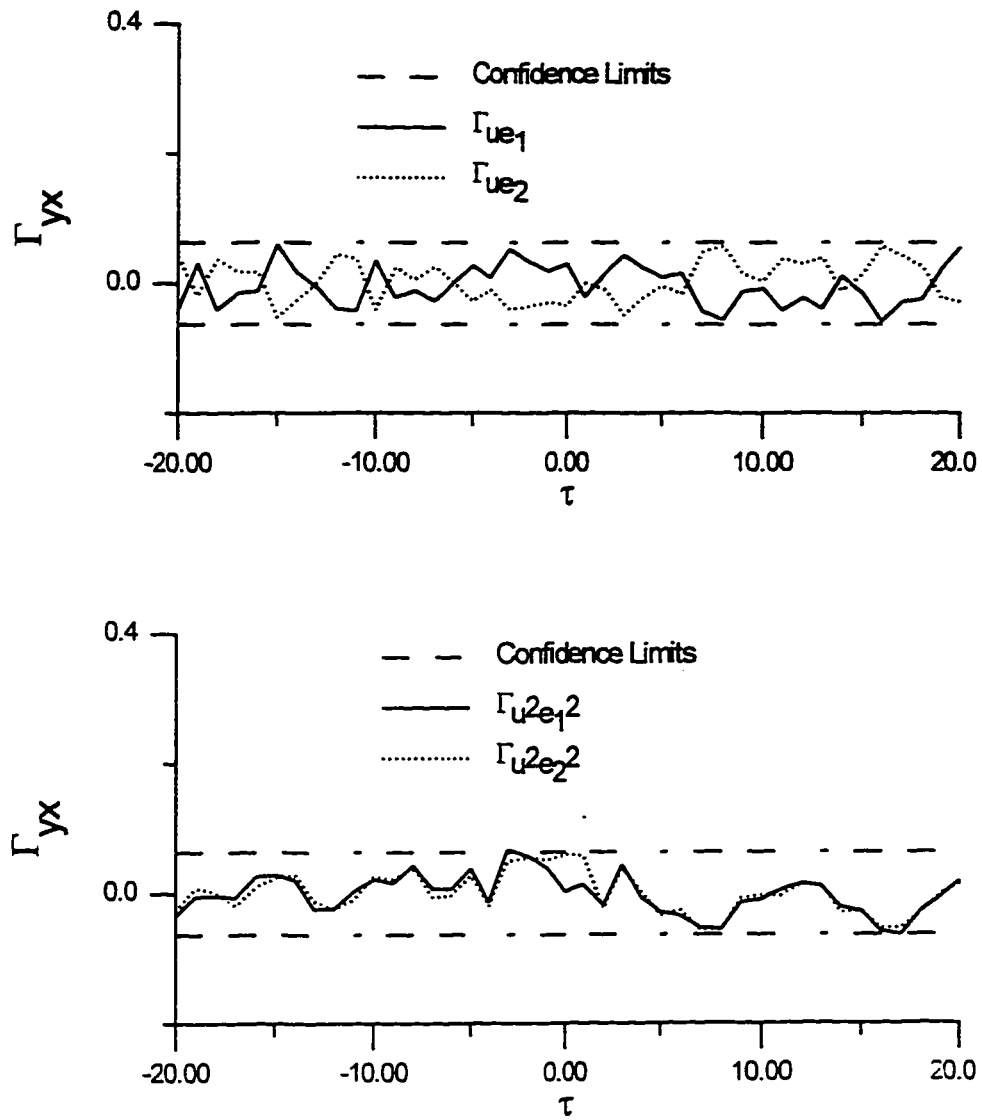
Fig. 3.7 Correlation tests using residuals and T_m with OLS training algorithm.
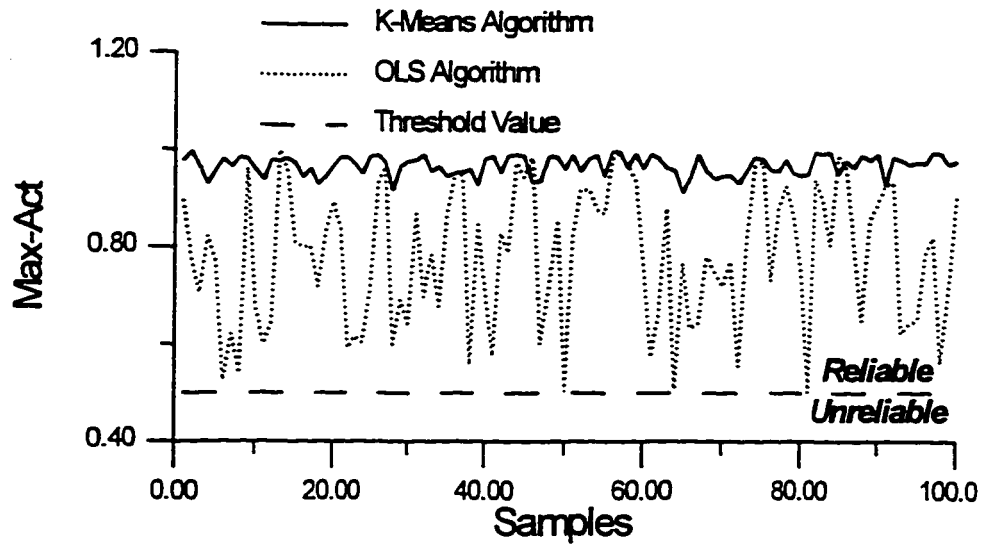
Fig. 3.8 Reliability test

TABLE 3.1 Learning algorithms with random variations in T_m

	k-means	OLS
No. of inputs	8	8
No. of hidden units	28	16
No. of outputs	2	2
MSE	5.4E-5	5.1E-5
Max. pattern error of δ	1.1E-2	1.3E-2
Max. pattern error of ψ_d	8.9E-3	1.7E-2
Min. pattern error of δ	4.0E-5	8.0E-5
Min. pattern error of ψ_d	3.0E-5	2.0E-5

3.6.2 RANDOM VARIATIONS IN FIELD VOLTAGE

The performance of the proposed identifier with random variations in field voltage shown in Fig. 3.9 was also examined. The responses of the proposed identifier are shown in Figs. 3.10 and 3.11. It can be seen that the proposed identifier responses are very close to the desired responses. This demonstrates the capability of the proposed identifier to learn the underlying characteristics of synchronous machines. The RBFN structure and MSE with both learning algorithms are given in Table 3.2. The results show the superiority of OLS algorithm in the sense that much less MSE and pattern errors can be obtained.

TABLE 3.2 Learning algorithms with random variations in V_F

	k-means	OLS
No. of inputs	8	8
No. of hidden units	28	33
No. of outputs	2	2
MSE	8.7E-5	5.9E-5
Max. pattern error of δ	4.8E-2	2.3E-2
Max. pattern error of ψ_d	3.3E-2	1.8E-2
Min. pattern error of δ	2.3E-5	6.0E-6
Min. pattern error of ψ_d	8.0E-6	2.1E-4
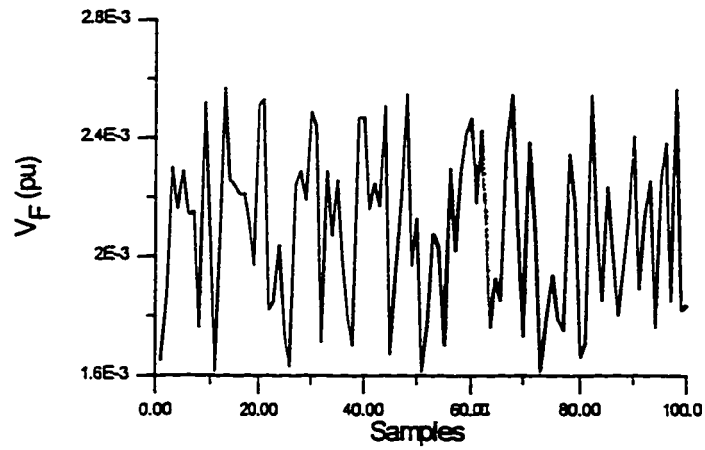
Fig. 3.9 Random variations of field voltage
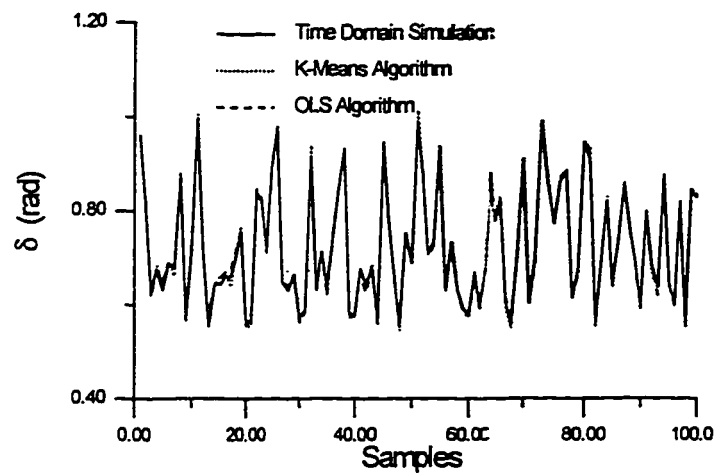
Fig. 3.10 RBFN rotor angle response due to random variations in V_F
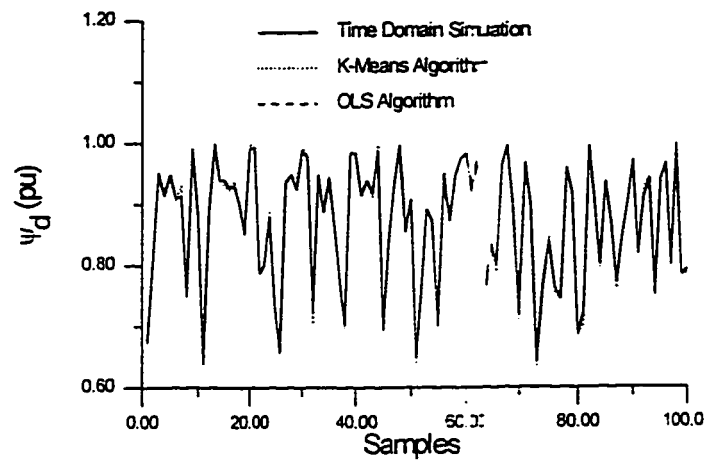
Fig. 3.11 RBFN d-axis flux linkage response due to random variations in V_F

3.7 COMPARISON BETWEEN RBFN AND BPNN

To demonstrate the superiority of the proposed RBFN identifier, a BPNN identifier has been developed and examined for random variations in the field voltage shown in Fig. 3.9. The BPNN identifier was trained using the backpropagation learning algorithm [41]. It was found after several trials that 38 hidden neurons give the minimum MSE. Fig. 3.12 shows the BPNN training error. The structure of BPNN and MSE after 3000 iterations are given in Table 3.3. It can be shown that the MSE as well as maximum and minimum pattern errors of BPNN identifier are higher than those of the proposed RBFN identifier trained with either k-means or OLS learning algorithms. This shows the potential of the proposed RBFN identifier to accurately model the synchronous machine. The BPNN identifier responses are given in Figs. 3.13 and 3.14. The residuals of δ and ψ_d for both the RBFN and BPNN identifiers are given in Figs. 3.15 and 3.16 respectively. These figures show that the residuals in the case of the proposed RBFN identifier are much less than those of the BPNN identifier confirming the capability of the proposed RBFN identifier trained with either k-means or OLS learning algorithms to capture the nonlinear characteristic of the synchronous machines.

3.8 SUMMARY

The problem of off-line identification of synchronous machines has been addressed in this chapter. Two learning algorithms were used to train the proposed RBFN identifier.

Model validation tests have been carried out. The results of the proposed RBFN identifier were compared with those of BPNN identifier in the case of random variations in machine inputs. The results reveal the potential of the proposed identifier and its capability to capture the underlying characteristics of the synchronous machines.

Due to the attractive properties of RBFN such as linearity in the parameters, local tunability, and fast learning, RBFN is a good candidate to on-line applications. In the next chapter, the problem of on-line identification of synchronous machines will be discussed using RBFN.

TABLE 3.3 BPNN with random variations in V_F

No. of inputs	8
No. of hidden units	38
No. of outputs	2
MSE	2.6E-4
Max. pattern error of δ	5.1E-2
Max. pattern error of ψ_d	6.0E-2
Min. pattern error of δ	8.0E-5
Min. pattern error of ψ_d	3.8E-4
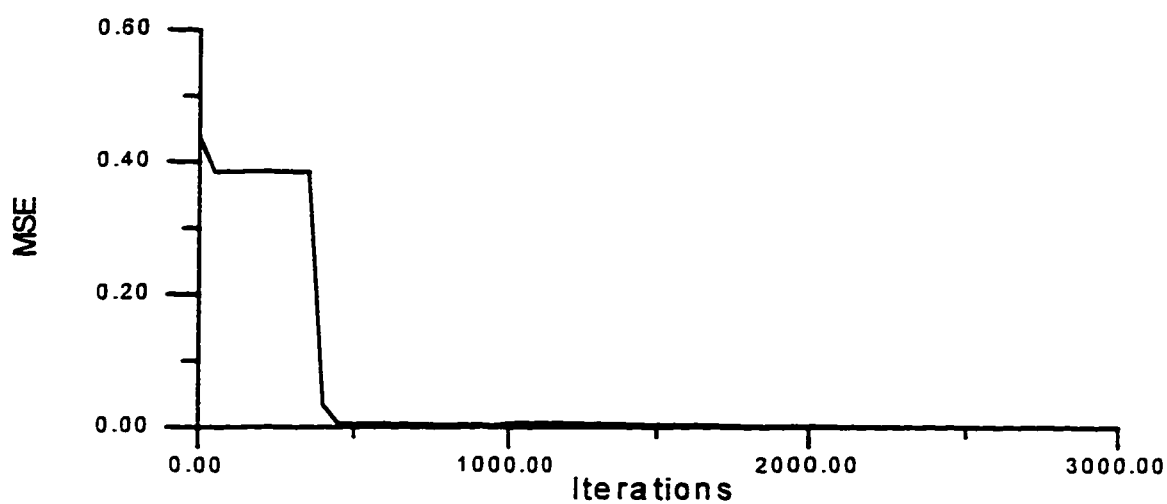
Fig. 3.12 BPNN training error
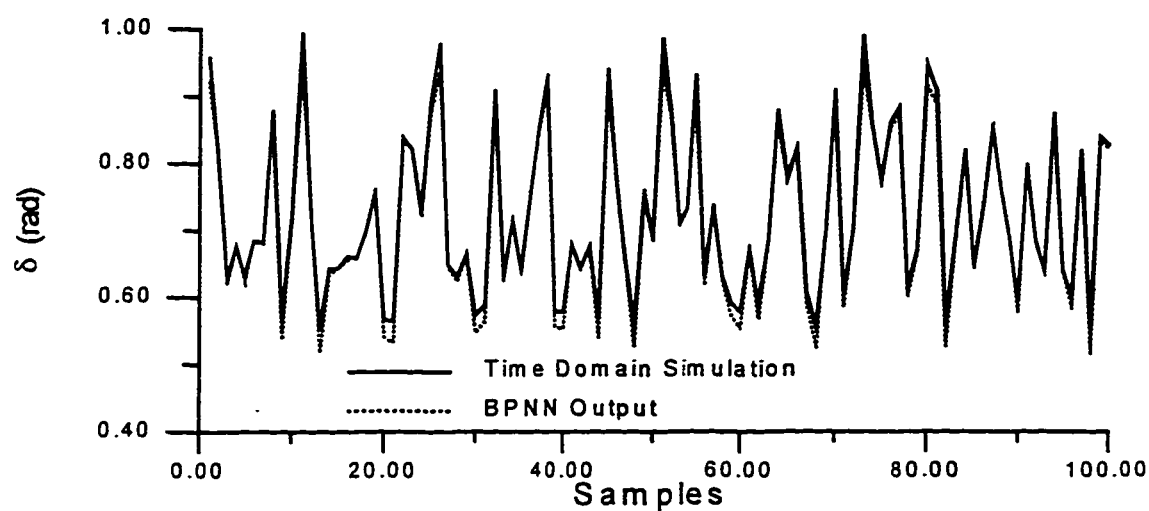
Fig. 3.13 BPNN rotor angle response due to random variations in V_F
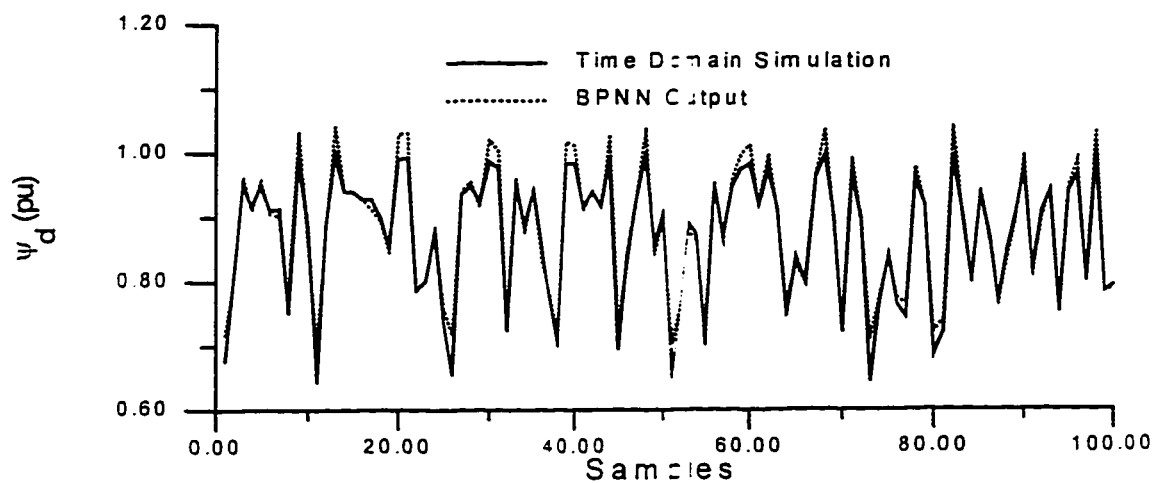
Fig. 3.14 BPNN d-axis flux linkage response due to random variations in V_F
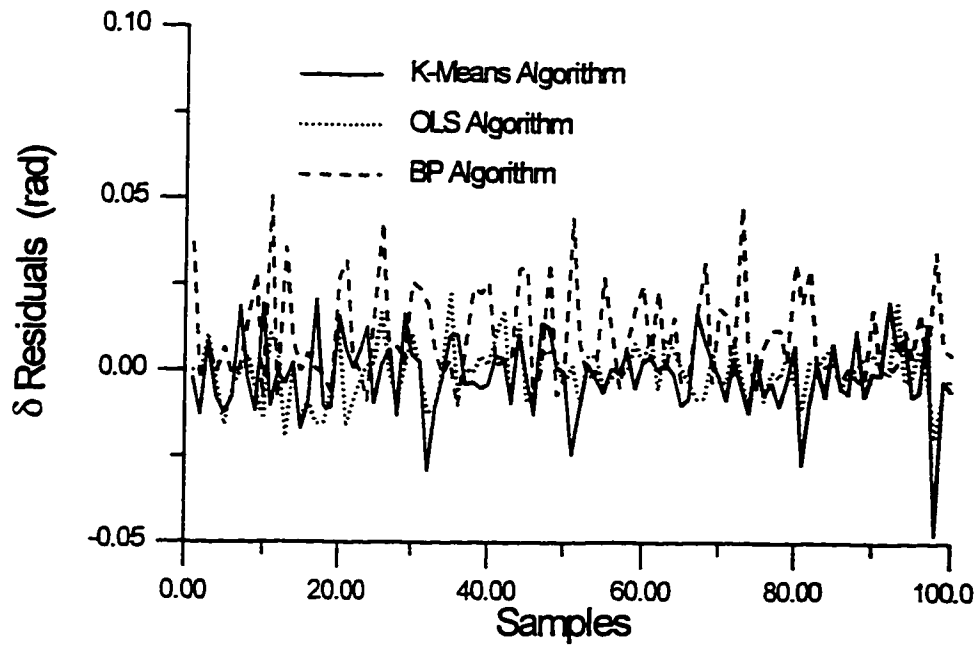
Fig. 3.15 RBFN and BPNN rotor angle residuals due to random variations in V_F
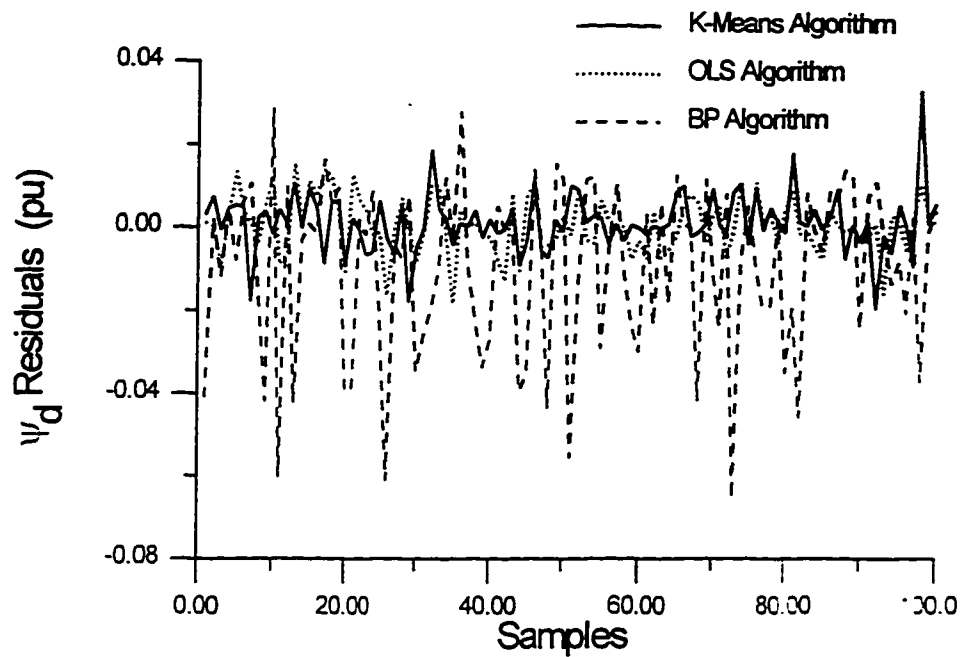
Fig. 3.16 RBFN and BPNN d-axis flux linkage residuals due to random variations in V_F

CHAPTER 4

ON-LINE IDENTIFICATION OF SYNCHRONOUS

MACHINES

4.1 INTRODUCTION

Identification of non-linear systems using RBFNs has certain attractive advantages. The general approximation capabilities of the RBFN provides the theoretical foundation of representing complex systems. Furthermore, the response of the RBFN is linear with respect to its connection weights. This property guarantees the convergence of the weights to the global minimum. Moreover, the local tunability of the RBFN reduces the training time and computational overhead and makes the RBFN a good candidate for on-line applications.

In this chapter. a novel on-line identification scheme is proposed. A recursive learning algorithm has been developed to update the network parameters. The potential of the proposed identifier is investigated using various variations in machine inputs.

Correlation-based model validity tests have been carried out to examine the validity of the proposed identifier.

4.2 THE PROPOSED IDENTIFICATION SCHEME

It has been rigorously proved that a wide class of discrete-time nonlinear systems can be represented in terms of some non-linear functional expansion of lagged inputs and outputs as given by the following difference equation model [21]

$$y(k) = f_s (y(k-1), \ldots, y(k-n_y), u(k-1), \ldots, u(k-n_u))^T \qquad (4.1)$$

where $y(k)$, and $u(k)$ are the system output and input respectively; n_y and n_u are the lags of the output and input respectively; and $f_s(.)$ is some non-linear function.

Here, the aim is to use the RBFN to capture or approximate the underlying dynamics $f_s(.)$ in (4.1). Define the input vector of the network at sample k as

$$\mathbf{v}(k) = [\mathbf{y}(k-1), \ldots, \mathbf{y}(k-n_y), \mathbf{u}(k-1), \ldots, \mathbf{u}(k-n_u)]^{T} \qquad (4.2)$$

The dimension of the input vector and consequently the dimension of the centers of the hidden nodes is given by

$$n_i = c.n_y - n.n_u \qquad (4.3)$$

where c and n are the number of outputs and inputs of the network respectively. The output vector of the RBFN identifier, $\mathbf{y}_{net}(k)$, becomes the one-step-ahead predictor of $\mathbf{y}(k)$, that is,

$$\mathbf{y}_{net}(k) = f_n(\mathbf{v}(k)) \qquad (4.4)$$

where f_n is the network approximation of f_s.

In this study, the activation functions, f_h, of all hidden units are of the Gaussian form of (2.14). Thus, the ith hidden unit activation function is given by

$$f_{hi}(\| \ \mathbf{x} - \mathbf{c}_i \ \|) = \exp \{ -0.5 \| \ \mathbf{x} - \mathbf{c}_i \ \|^2 / \sigma_i^2 \}, \quad i = 1, \ldots, m. \qquad (4.5)$$

where the center $\mathbf{c}_i$ corresponds to the mean of the Gaussian function whereas σ_i denotes the width parameter.

The proposed identification scheme is depicted in Fig. 4.1, where the output of the delay elements block is the delayed values of its input signals.

4.3 RECURSIVE LEARNING ALGORITHM

For on-line identification using RBFN, a recursive learning algorithm is required to update the network parameters. This algorithm involves a combined form of supervised and unsupervised learning. At each iteration, RBF centers and network weights are updated as follows.

4.3.1 UPDATING RBF CENTERS

Given initial centers $\{c_j(0), \ j = 1, \ldots, m\}$ which can be generated randomly in the vicinity of the input domain and an initial learning rate $\alpha(0)$, the k-means algorithm [35] computes

$$\rho_j(k) = \| \ \mathbf{v}(k) - \mathbf{c}_j(k-1) \ \|, \quad j = 1, \ldots, m \qquad (4.6)$$
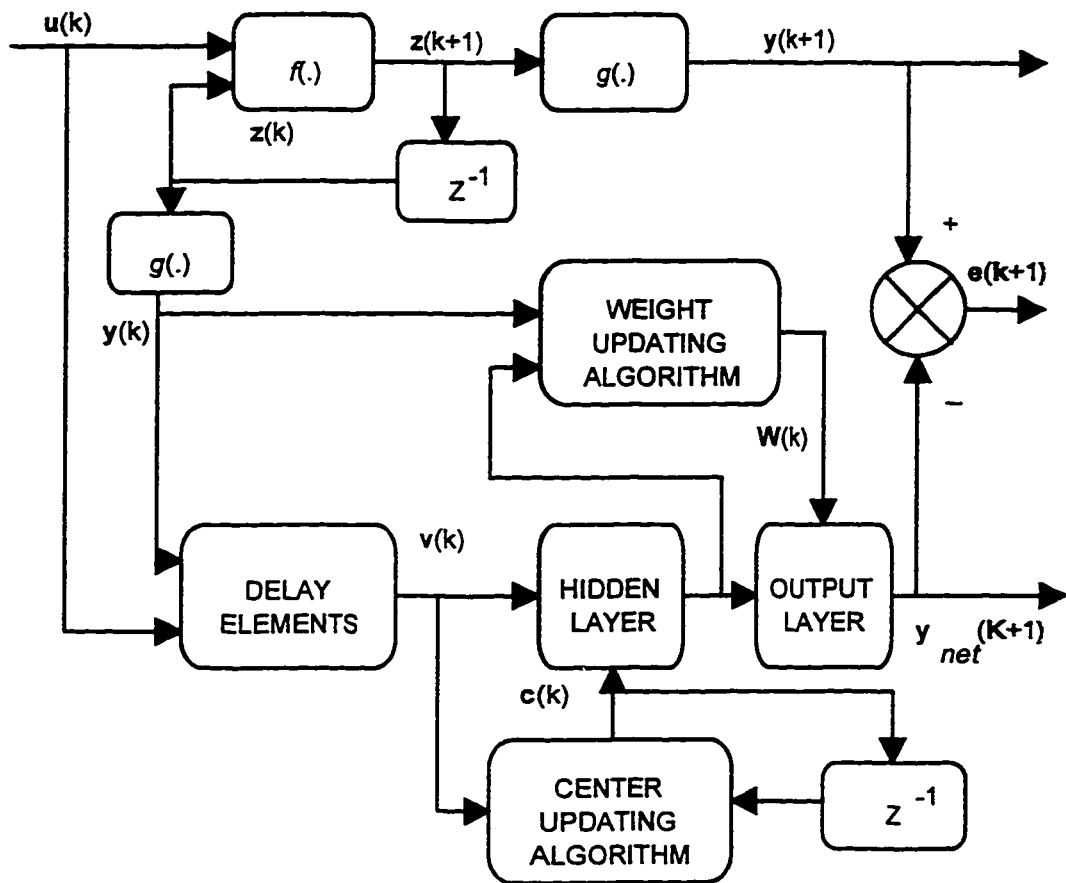
Fig. 4.1 The proposed on-line identification scheme

The updating of a center is based on how far the current input vector is away from the last updated centers. If i = argument{min($\rho_j(k)$)}, $j = 1, \ldots, m$ } then

$$c_i(k) = c_i(k\text{-}1) + \alpha(k) [v(k) - c_i(k\text{-}1)] \qquad (4.7)$$

and,

$$c_j(k) = c_j(k\text{-}1) , \forall j \neq i \qquad (4.8)$$

The learning rate $\alpha(k) \in (0,1]$ is given by

$$\alpha(k) = \alpha(k-1)/\sqrt{1 + \mathrm{int}(k / m)} \qquad (4.9)$$

where int(x) denotes the integer part of x.

4.3.2 UPDATING NETWORK WEIGHTS

Once the centers have been updated, the outputs of the hidden layer can be calculated using

$$h_j(k) = \exp \{ -0.5 \| v(k) - c_j(k) \|^2 / \sigma^2 \}, \quad j = 1, \ldots, m \qquad (4.10)$$

and the input vector to the output layer becomes

$$H(k) = [h_1(k) \ldots \ldots h_m(k)]^T \qquad (4.11)$$

Define the $m \times c$ weight matrix at sample k as

$$W(k) = [w_1(k) \ldots w_i(k) \ldots w_c(k)] \qquad (4.12)$$

and.

$$w_i(k) = [w_{1i}(k) \ldots w_{mi}(k)]^T \qquad (4.13)$$

The weighted normal equation can be written as

$$(S_k^T Q_k S_k) W(k) = S_k^T Q_k Y_k \qquad (4.14)$$

where

$$S_k = [H^T(l) \dots H^T(k)]^T \qquad (4.15)$$

$$Y_k = [y(l) \dots y(k)]^T \qquad (4.16)$$

and Q_k is an $k \times k$ diagonal matrix defined recursively by

$$Q_k = \begin{bmatrix} \mu(k)Q_{k-1} & 0 \\ 0 & 1 \end{bmatrix}, \quad Q_l = 1 \qquad (4.17)$$

$\mu(k)$ is the forgetting factor and can be computed as [42-43]

$$\mu(k) = \mu_0\, \mu(k-1) + 1 - \mu_0 \qquad (4.18)$$

μ_0 and $\mu(0)$ are chosen to be less than but close to 1.

Since the least squares problem in (4.14) may become ill-conditioned, Givens transformation method [38] has been developed to solve for $W(k)$ rather than the direct solution of the normal equation because of its numerical advantages.

4.4 RESULTS AND SIMULATIONS

In this study, the single machine infinite bus system shown in Fig. 3.1 is considered. The system model and parameters are given in Appendix A.

In order to investigate the performance of the proposed RBFN identifier, two kinds of disturbances have been applied to the machine inputs, T_m and V_F, to drive the machine and proposed identifier simultaneously. Namely, the first is a square variation in the range of 80-120% of the initial values of the inputs. The second is a random variation signal uniformly distributed in the range of 60-140% of the initial values of the inputs.

Initially, the machine is operating at power of 1.0 pu with 0.85 power factor lagging and terminal voltage of 1.0 pu. The following studies have been performed and the results of the proposed identifier and time-domain simulations were compared to demonstrate the adequacy of the proposed identifier. Moreover, some correlation-based model validity tests using residuals and inputs as given in (3.23) have been carried out to show the validity of the proposed identifier. In all cases, ten historical values of the inputs and outputs were used to construct the input vector of the network.

4.4.1 VARIATIONS IN MECHANICAL TORQUE

The behavior of the proposed identifier due to square variation in the mechanical torque is compared with the time-domain simulations in Figs. 4.2 and 4.3. Fig. 4.2 shows the response of the rotor angle while Fig. 4.3 shows the response of the d-axis flux linkage. Fig. 4.4 shows the random variations in the mechanical torque. The responses of the rotor angle and d-axis flux linkage due to random variation are shown in Figs. 4.5 and 4.6 respectively. It is worth pointing out that it is difficult to discern a difference between the simulated and identified responses confirming the capability of the proposed identifier to capture the nonlinear operating characteristics of the synchronous machine. The results of the model validation tests, as shown in Fig. 4.7, fall within the 95% confidence bands and confirming the adequacy of the proposed identifier. The training error versus time is shown in Fig. 4.8. It is clear that the training error dramatically converges almost to zero in less than 0.01 sec. This demonstrates the suitability of the proposed identifier for on-

line applications. It is found after several trials that only 10 neurons in the hidden layer are adequate which makes the structure of the identifier very simple.

4.4.2 VARIATIONS IN FIELD VOLTAGE

The random variations in the field voltage is shown in Fig. 4.9. The responses of the rotor angle and d-axis flux linkage due to random variation are shown in Figs. 4.10 and 4.11 respectively. The results demonstrate the capability of the proposed identifier to learn the underlying characteristics of the synchronous machine. In this case, 11 neurons in the hidden layer are found to be adequate.

4.5 SUMMARY

This chapter has provided a novel approach to on-line identification of synchronous machines using RBFN. A learning algorithm has been developed to update the RBFN parameters recursively. Several variations in the machine inputs have been used to test the proposed identifier. In addition, correlation based model validity tests have been carried out. The results show the adequacy of the proposed identifier and its capability to approximate the nonlinear characteristics of synchronous machines.

On the control side, the approximation capabilities of neural networks will be exploited for on-line tuning of power system stabilizers based on real-time measurements. In the following two chapters, radial basis function networks and fuzzy basis function networks will be proposed to re-tune the power system stabilizer parameters in real-time without the need of on-line parameter identification.
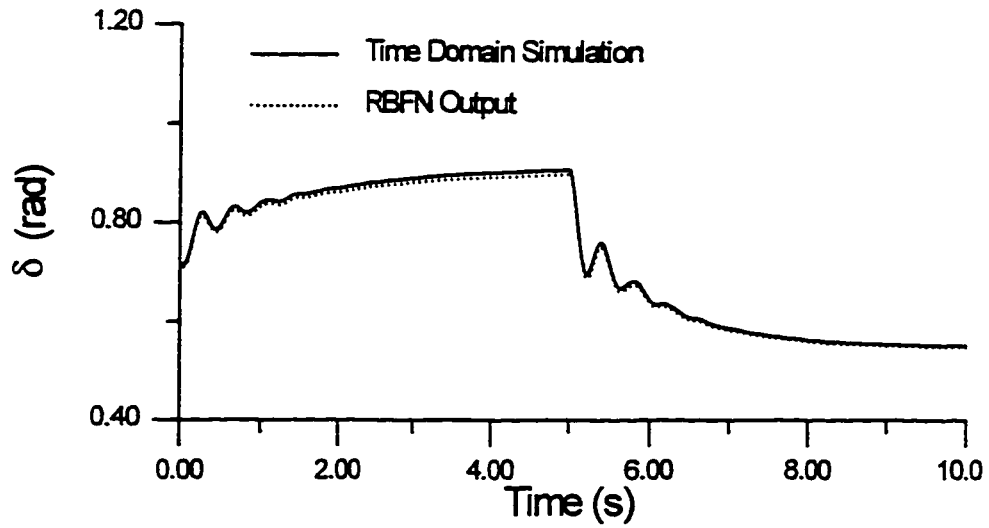
Fig. 4.2 Rotor angle response due to 80-120% square change in T_m
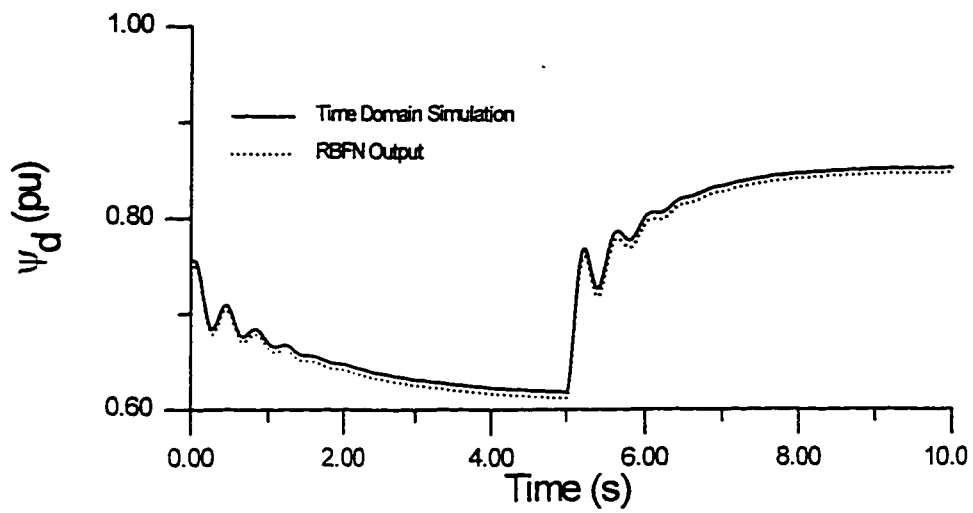
Fig. 4.3 D-axis flux linkage response due to 80-120% square change in T_m
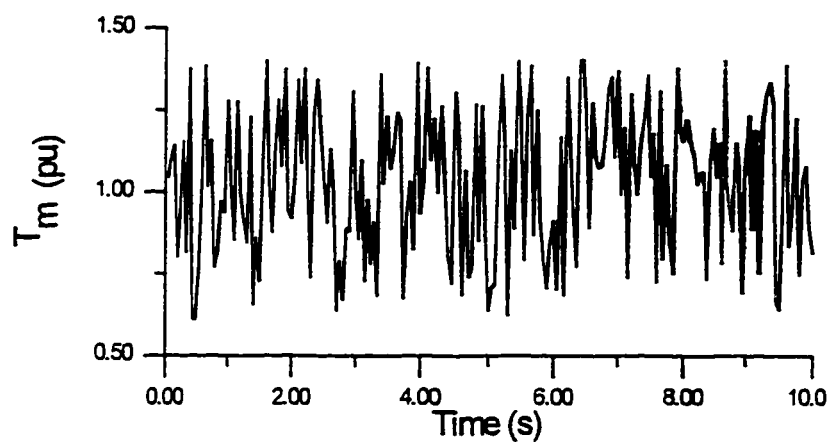
Fig. 4.4 Random variations in T_m
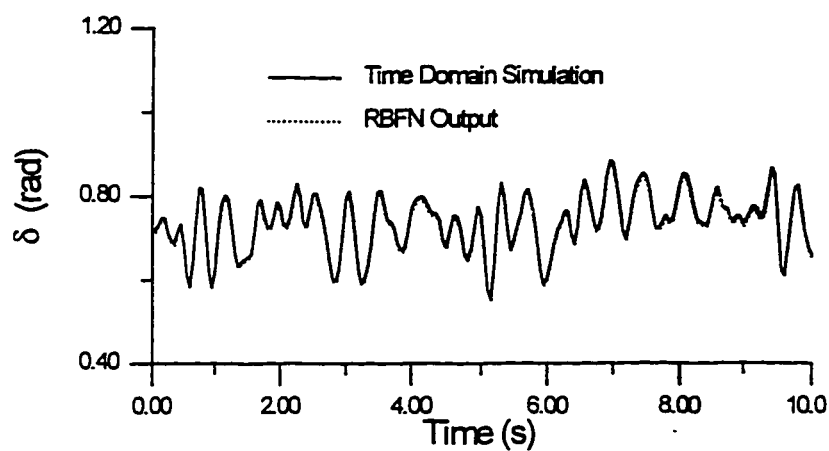
Fig. 4.5 Rotor angle response due to 60-140% random change in T_m
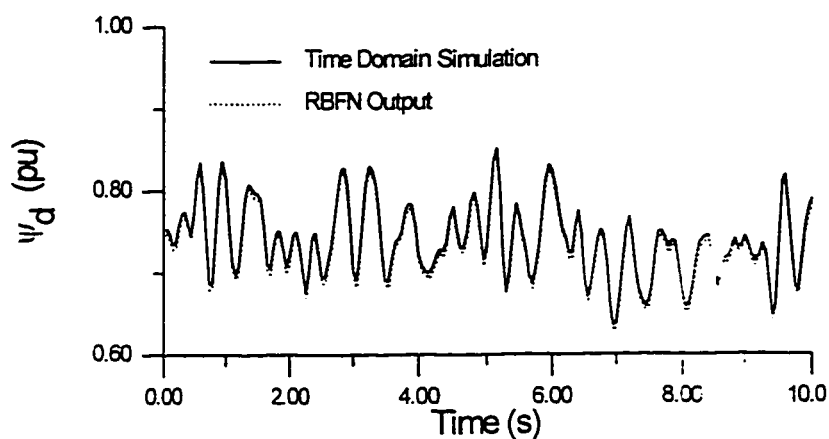
Fig. 4.6 D-axis flux linkage response due to 60-140% random variations in T_m
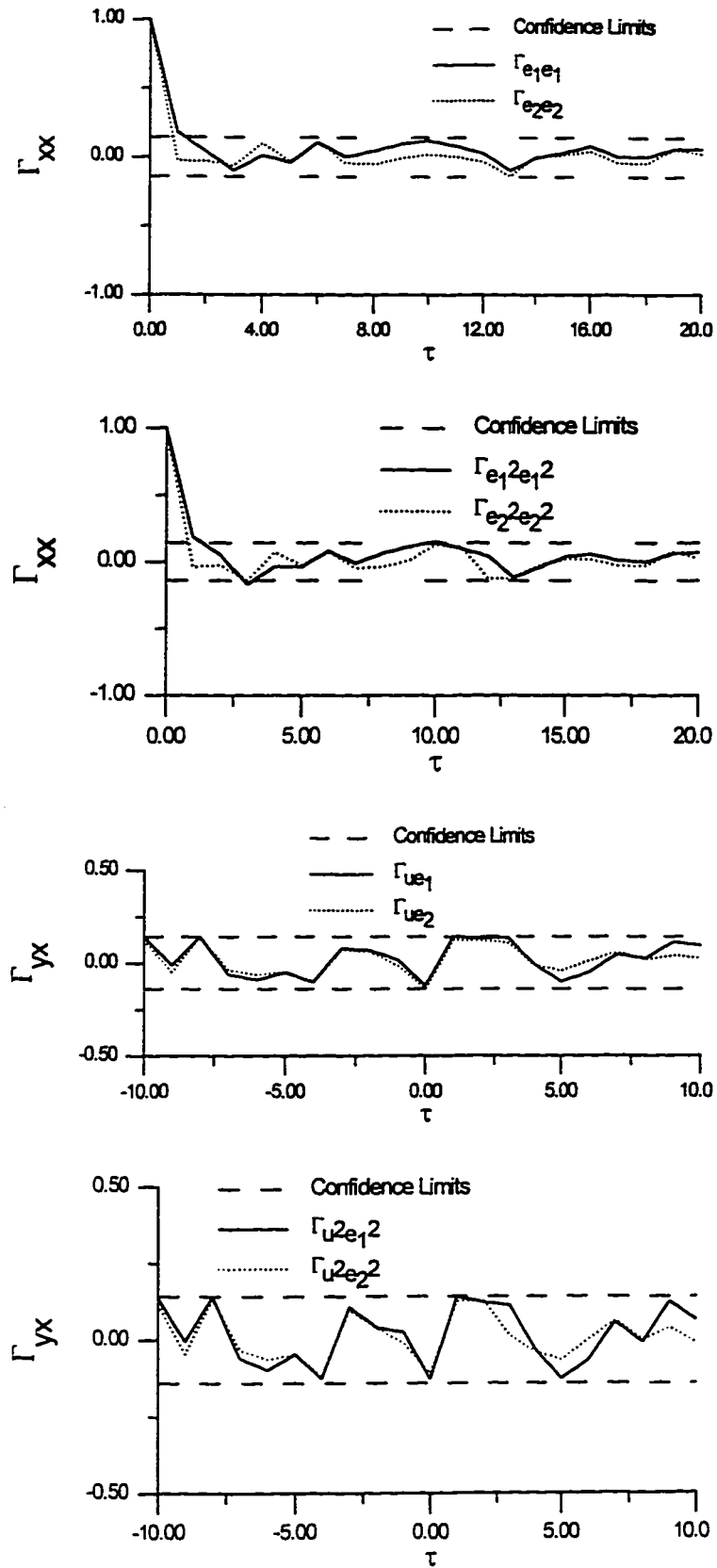
Fig. 4.7 Correlation tests using residuals and T_m
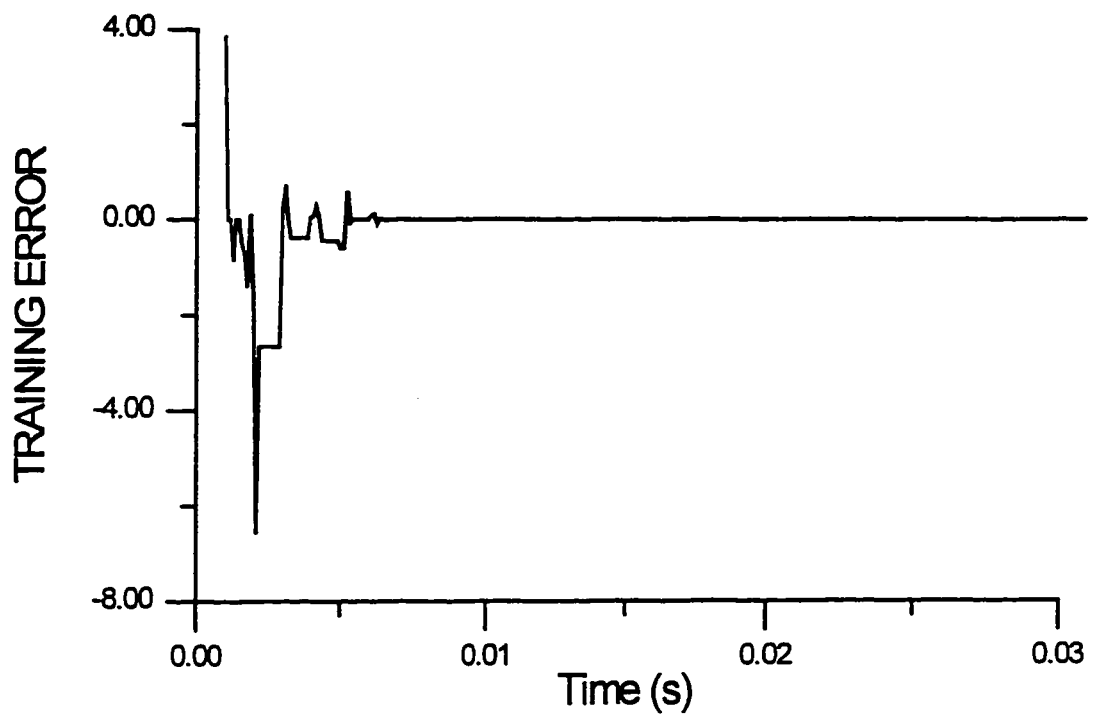
Fig. 4.8 Proposed RBFN identifier training error
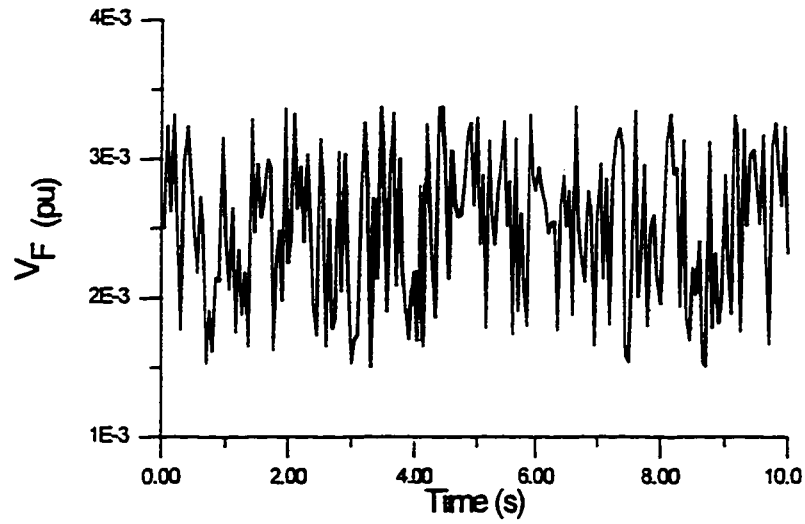
Fig. 4.9 Random variations in V_F
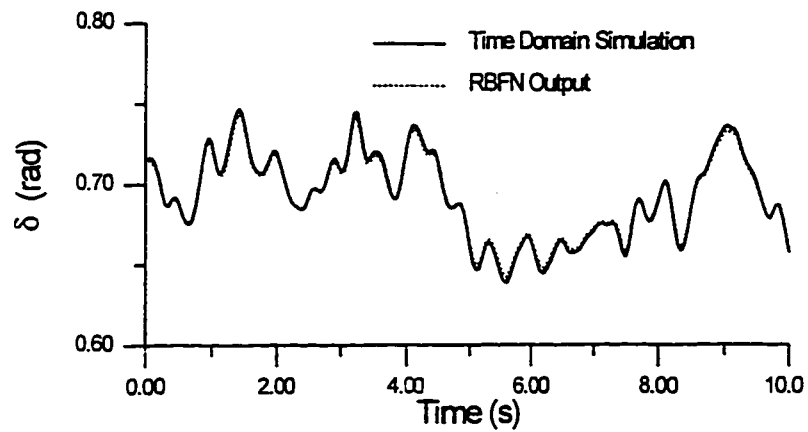
Fig. 4.10 Rotor angle response due to 60-140% random variations in V_F
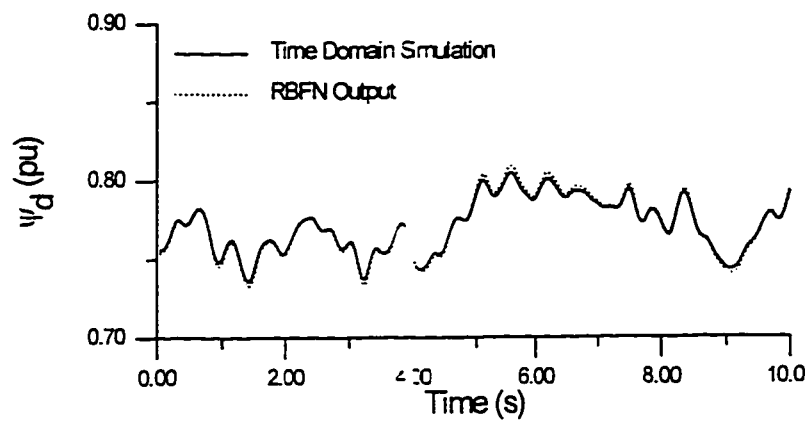
Fig. 4.11 D-axis flux linkage response due to 60-140% random variations in V_F

CHAPTER 5

ADAPTIVE TUNING OF PSSs USING RBFNs

5.1 INTRODUCTION

In the past two decades, the utilization of supplementary excitation control signals for improving the dynamic stability of power systems has received much attention [44-63]. Nowadays, the conventional lead-lag power system stabilizer (CPSS) is widely used by power system utilities [52]. Other types of PSS such as proportional-integral power system stabilizer (PI PSS) and proportional-integral-derivative power system stabilizer (PID PSS) have also been proposed [55,60]. The parameters of these stabilizers are determined based on the linearized model of the power system around a nominal operating point to provide optimal performance at this point. These parameters remain fixed. Therefore, the performance of the stabilizer is degraded whenever the operating point changes from one to another.

Alternative controllers using adaptive control algorithms have been proposed to overcome such problems [59-63]. However, most adaptive controllers are designed on the basis of a linear model which degrades practical operation of the designed controllers. Additionally, most of the adaptive controllers are designed based on the parameter identification of the system model in real-time which is a time consuming task.

Recently, ANN applications to various power system problems have received much attention [64-74]. Although ANNs trained with backpropagation algorithm are widely used, there are several problems associated with these networks such as getting stuck in local minima on the error surface giving a solution that is not optimal and with a relatively slow convergence rate, thus causing computation time for training of such networks with large number of parameters to be very long [26-27].

In power systems, RBFN has been successfully applied to modeling of the synchronous machines and short-term electric load forecasting problems [75-79]. However, applications of RBFN to the power system control have not yet been exploited.

5.2 PROBLEM FORMULATION

To enhance system damping, the generator is equipped with a PSS. A widely used conventional lead-lag power system stabilizer (CPSS) is considered in this study. The CPSS can be described as [2]

$$U = \frac{sT_w}{1 + sT_w} \frac{K_c(1 + sT_1)}{1 + sT_2} \Delta\omega \tag{5.1}$$

In the above equation, the time constants, T_w is chosen to be large enough to prevent any effect on phase shift or gain at the oscillating frequency while T_2 is chosen arbitrarily. The other parameters, K_c and T_I are determined by linearizing the nonlinear model of the system around a nominal operating point to provide optimal performance at this point. Having been determined, these parameters remain fixed. Generally, a power system is highly nonlinear and the operating conditions can vary over a wide range. Consequently, the operating point will change and these fixed-gain PSSs no longer ensure the optimal performance.

5.3 DESIGN OF THE PROPOSED STABILIZER

The proposed RBFN PSS will re-tune the stabilizer parameters based on local real-time measurements of loading conditions. The inputs to the RBFN are the real power (P) and the reactive power (Q). The performance of the proposed RBFN PSS depends on how it was trained. Generally, the input-output training patterns must cover most of the working range in order to get better performance. A set of 500 training patterns was presented to the network. The training patterns were uniformly distributed over the working range. With each operating condition, the CPSS parameters, K_c and T_I, are tuned to yield the best performance at this operating point by prespecifying the desired level of damping coefficient [2]. The CPSS parameters obtained represent the desired outputs.

The proposed RBFN was trained using the k-means algorithm developed in Chapter 3. The trained network was tested by another set of 500 input-output patterns that have

not been presented before to the network. The average percentage error (APE) is used in

order to evaluate the performance of the trained RBFN. APE can be defined as

$$APE = \frac{\sum_{i=1}^{N} | d(i) - y(i) |}{\sum_{i=1}^{N} | d(i) |} * 100 \qquad (5.2)$$

where N is the number of testing patterns and $d(i)$ and $y(i)$ are the ith desired and actual

outputs respectively.

Generally, the main features of the proposed approach can be summarized as follows:

1. The proposed RBFN PSS is one of decentralized nature since only local

   measurements are employed as the inputs to the stabilizer. This makes the proposed

   RBFN PSS easy to tune.

2. The proposed RBFN PSS can be easily implemented on a microcomputer since it

   does not require real-time model identification.

The proposed RBFN PSS control scheme is shown in Fig. 5.1.

5.4 EXAMPLE 1: SINGLE MACHINE SYSTEM

5.4.1 TEST SYSTEM

In this study. the single machine infinite bus system shown in Fig. 3.1 is considered. The

system model is given in Appendix B. For comparison , CPSS and PI PSS have been

designed based on the linearized model given in Appendix C. Several simulation studies
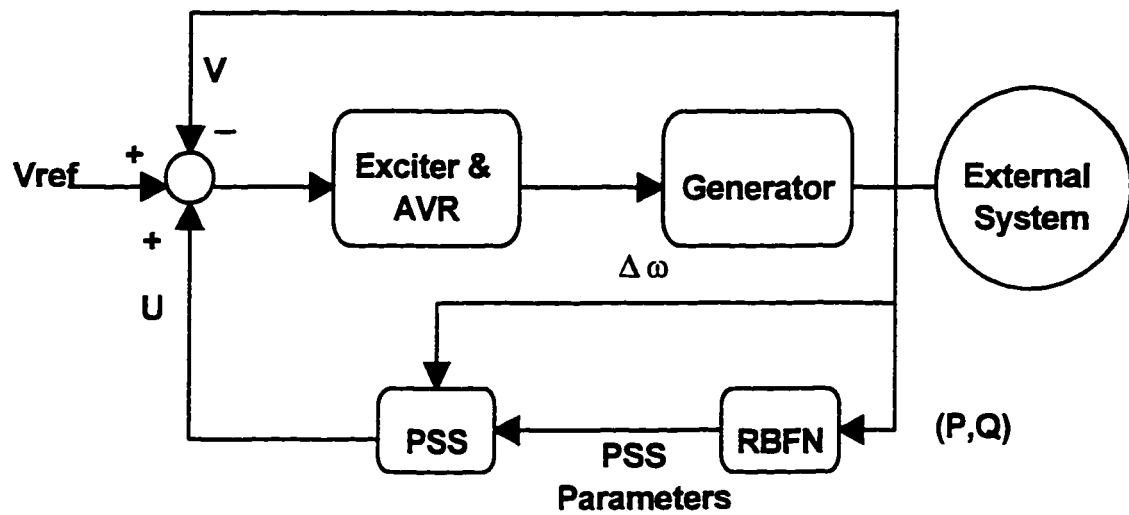
Fig. 5.1 The proposed RBFN PSS control scheme.

have been performed and the results of the proposed RBFN PSS are compared with those of the CPSS and PI PSS. It is important to indicate that all simulations are carried out using the nonlinear system model.

5.4.1.1 OPERATING CONDITIONS

In this study, four operating conditions are considered in order to test the proposed RBFN PSS over a wide loading range. These conditions are listed in Table 5.1. It is worth mentioning that these operating conditions represent a nominal, heavy, leading power factor, and light loading conditions respectively.

TABLE 5.1 Operating conditions for example 1

Operating Conditions	P (pu)	Power Factor	Designation
(P_1, Q_1)	1.0	0.85 lag.	nominal loading
(P_2, Q_2)	1.3	0.85 lag.	heavy loading
(P_3, Q_3)	0.7	0.90 lead.	leading PF loading
(P_4, Q_4)	0.3	0.85 lag.	light loading

5.4.1.2 TUNING OF CPSS AND PI PSS

The state equations of the linearized incremental model of the system [2] can be expressed as follows:

$$\dot{X} = AX + BU \qquad (5.3)$$

where $X = [\Delta\omega \quad \Delta\delta \quad \Delta E_q' \quad \Delta E_{fd}]^T$ is the state vector. Under the nominal operating conditions specified by (P_I, Q_I), the matrices A and B are given by

$$A = \begin{bmatrix} 0 & -0.227 & -0.265 & 0 \\ 377 & 0 & 0 & 0 \\ 0 & -0.290 & -0.552 & 0.169 \\ 0 & 382.1 & -3975.7 & -20 \end{bmatrix}, \quad B = \begin{bmatrix} 0 & 0 & 0 & 8000 \end{bmatrix}^T \qquad (5.4)$$

Without any PSS, the eigenvalues associated with the electromechanical mode lie in the right hand side of s-plane at $0.18 \pm j9.70$ which makes a PSS highly needed to damp out this mode. The CPSS given in (5.1) and a PI PSS given as [55]

$$U = \frac{sT_w}{1 + sT_w}(K_p + \frac{K_i}{s})\Delta\omega \qquad (5.5)$$

were designed based on the linearized model given in Appendix C. In (5.5), K_p and K_i are the proportional and integral gains of the PI PSS respectively. The tuned parameters of the CPSS and the PI PSS are given in Table 5.2. These parameters were kept the same for all simulation studies. It is observed that the eigenvalues associated with the electromechanical mode have been moved to $-2.69 \pm j8.68$ with CPSS and $-2.91 \pm j9.25$ with PI PSS.

TABLE 5.2 CPSS and PI PSS tuned parameters

PSS Type	Parameters
CPSS	$K_c = 6.543$ and $T_c = 0.190$ s
PI PSS	$K_p = 8.671$ and $K_i = -22.530$ s^{-1}

5.4.2 THE PROPOSED RBFN PSS

The proposed RBFN was trained as described above. The real power was selected from 0.1 pu to 1.5 pu and the power factor was selected from 0.9 leading to 0.8 lagging. It was found after several trials that the appropriate choices of the number of hidden units, m, and the number of nearest neighbors, n_n, are 38 and 15 respectively. In addition, APE for K_c and T_l are found to be 0.3025% and 1.0959% respectively.

5.4.3 SIMULATION RESULTS

5.4.3.1 OPERATING CONDITION (P_l, Q_l)

To verify the behavior of the proposed RBFN PSS under transient conditions, a three phase fault was applied at the infinite bus at t=1.0s for 0.1s Results of the study are shown in Fig. 5.2. It is obvious that although the CPSS and PI PSS parameters were optimized at this operating condition, the proposed RBFN PSS provides the best damping characteristics.

5.4.3.2 OPERATING CONDITION (P_2, Q_2)

A three phase fault was applied at the infinite bus at t=1.0s for 0.05s with the generator operating at heavy loading condition specified by (P_2, Q_2). The simulation results of this test are shown in Fig. 5.3. The results here demonstrate the superiority of the proposed RBFN PSS to the CPSS and PI PSS. It can be concluded that the system with the proposed RBFN PSS returns to its previous operating point faster than the conventional stabilizers. This is very helpful in the improvement of the disturbance tolerance ability of the system.

5.4.3.3 Operating Condition (P_3, Q_3)

With the leading power factor, the stability margin is reduced and it becomes very important to test the PSS under this difficult situation. A 0.1 pu step in mechanical torque was applied at t=1.0s while the generator was operating at (P_3, Q_3). The simulation results are shown in Fig. 5.4. Another test has been conducted with the generator operating at this condition, that is, a three phase fault was applied at the infinite bus at t=1.0s. The fault duration was 0.1s. The simulation results are shown in Fig. 5.5. It can be concluded that the performance of the proposed RBFN PSS is much better than those of the CPSS and PI PSS and the oscillations are damped out much quicker.

5.4.3.4 Operating Condition (P_4, Q_4)

At light loading condition (P_4, Q_4), a local load of admittance of $0.3 - j0.2$ pu has been switched on at t=1.0s. The simulation results are shown in Fig. 5.6. It is seen that the proposed RBFN PSS provides better damping characteristics.
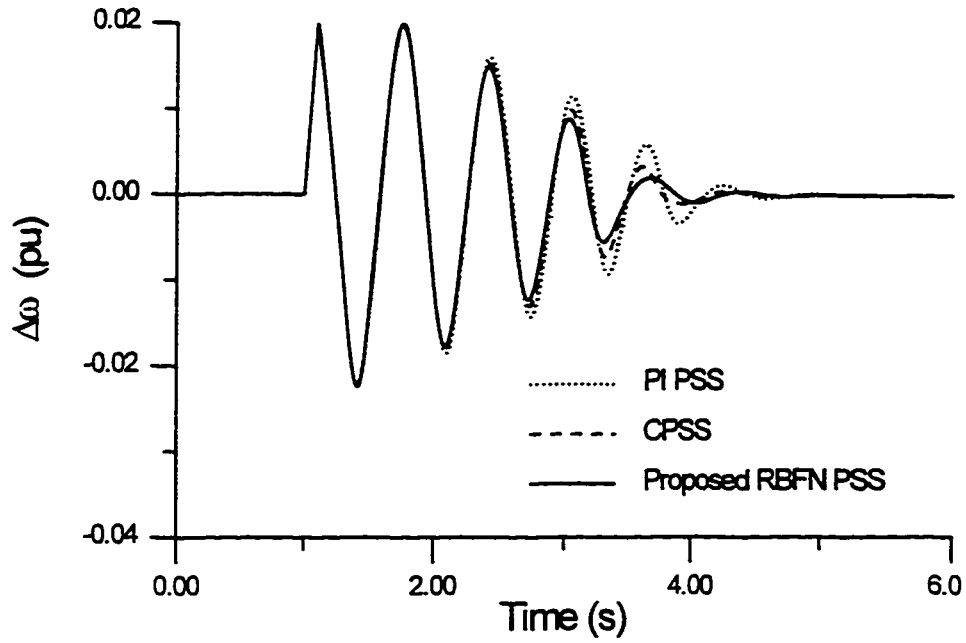
Fig. 5.2 Response to a 0.1s three phase fault with loading of (P_1, Q_1)
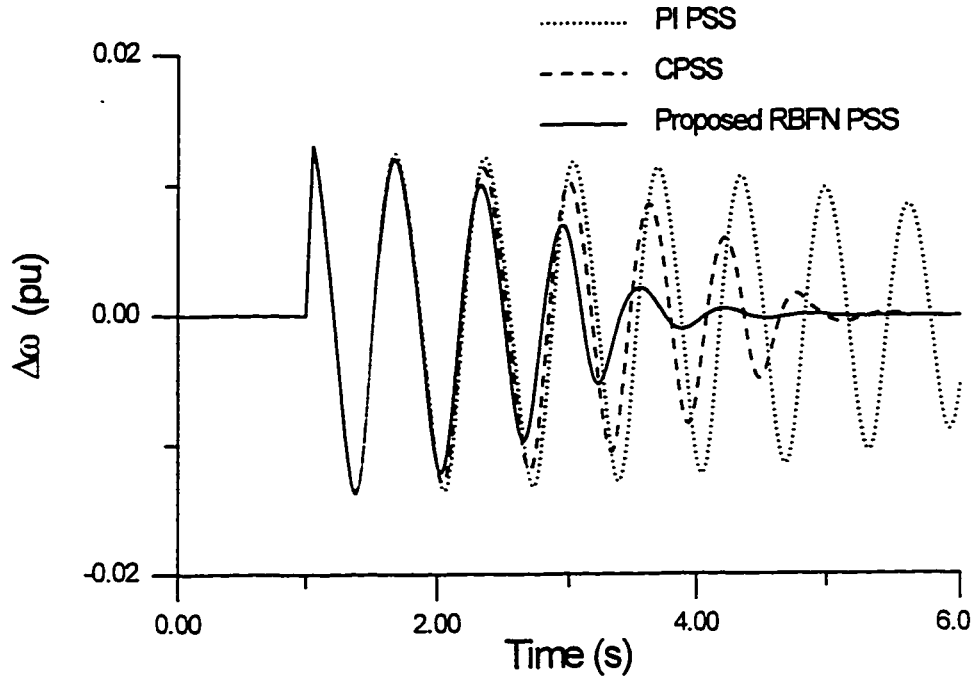
Fig. 5.3 Response to a 0.05s three phase fault with loading of (P_2, Q_2)
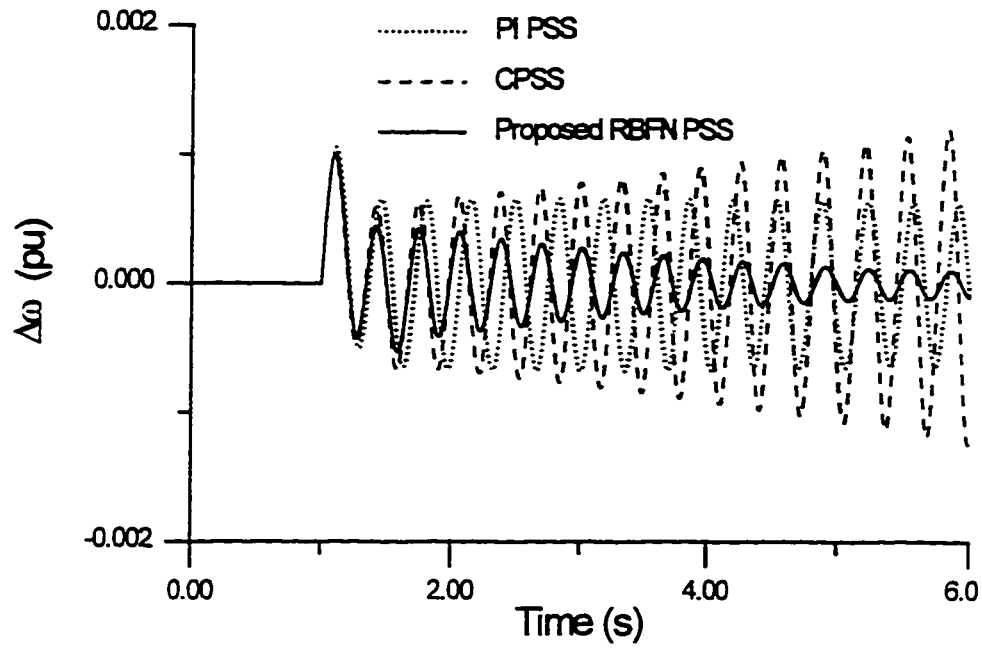
Fig. 5.4 Response to a 10% step in mechanical torque with loading of (P_3, Q_3)
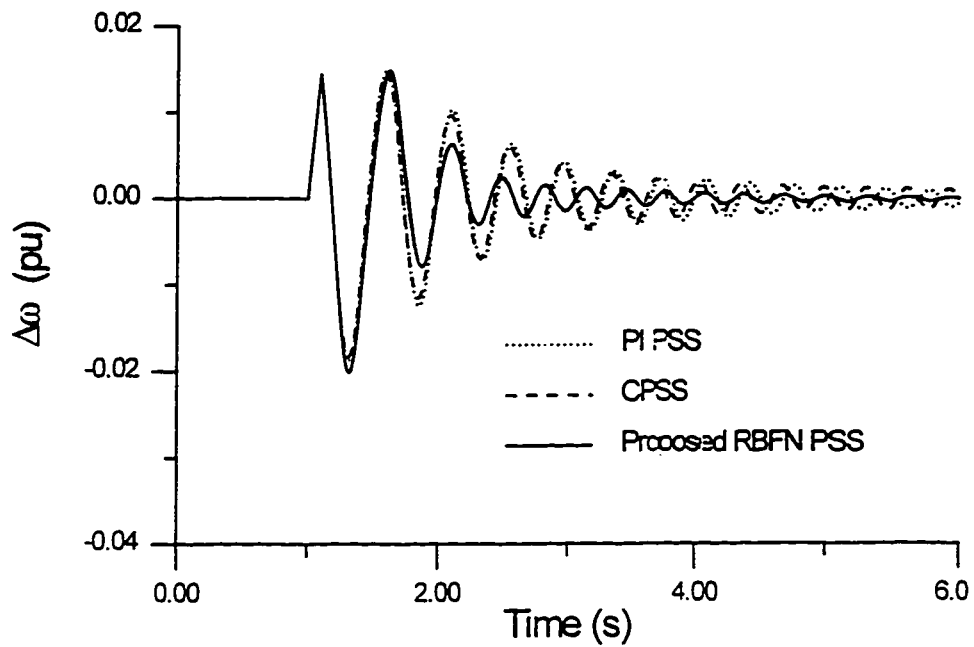
Fig. 5.5 Response to a 0.1s three phase fault with loading of (P_3, Q_3)
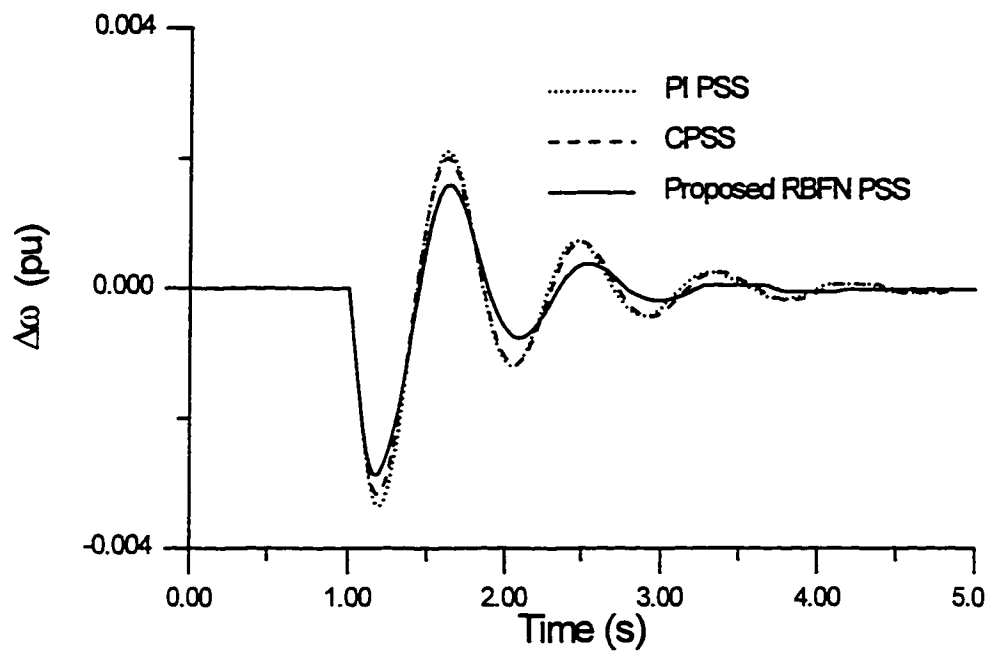
Fig. 5.6 Response to switching on a local load with loading of (P_4, Q_4)

5.5 EXAMPLE 2: MULTIMACHINE POWER SYSTEM

5.5.1 TEST SYSTEM AND OPTIMUM PSS LOCATIONS

To evaluate the effectiveness of the proposed RBFN PSS, the nine-bus three-machine power system shown in Fig. 5.7 was considered [1]. Details of the system model and parameters are given in Appendix D. Without PSSs, the system response curves due to a 6-cycle three phase fault at bus 7 at the end of line 5-7 are shown in Fig. 5.8. It is observed from Fig. 5.8 that the system damping is poor and the system is highly oscillatory. Therefore, it is necessary to install stabilizers in order to have good dynamic performance. To identify the optimum locations of PSSs, the participation factor method [80] and the sensitivity of PSS effect (SPE) method [81] were used. The results of both methods indicate that the generators G2 and G3 are the optimum locations for installing PSSs to damp out the electromechanical modes of oscillations. Therefore, the generators G2 and G3 were equipped with two of the proposed RBFN PSS. The performance of the proposed stabilizers was compared to that of CPSSs installed on G2 and G3 with the transfer function [1]

$$G(s) = \frac{10s}{1 + 10s} \frac{(1 + 0.568s)^2}{(1 + 0.0227s)^2} \qquad (5.6)$$

To demonstrate the capability of the proposed RBFN PSS to enhance the system damping over a wide range of operating conditions, three different loading conditions

were considered as given in Table. 5.3. Load admittances in each case are given in Table 5.4.

TABLE 5.3 Operating conditions for example 2

Generator	Nominal		Heavy		Light	
	P (pu)	Q (pu)	P (pu)	Q (pu)	P (pu)	Q (pu)
G1	0.713	0.275	2.207	1.092	0.362	0.166
G2	1.63	0.068	1.920	0.565	0.800	-0.107
G3	0.852	-0.108	1.280	0.360	0.450	-0.203

TABLE 5.4 Load admittances for example 2

Load	Nominal	Heavy	Light
A	1.261-j0.504	2.314-j0.925	0.640-j0.542
B	0.878-j0.293	2.032-j0.677	0.431-j0.335
C	0.969-j0.339	1.584-j0.634	0.472-j0.236
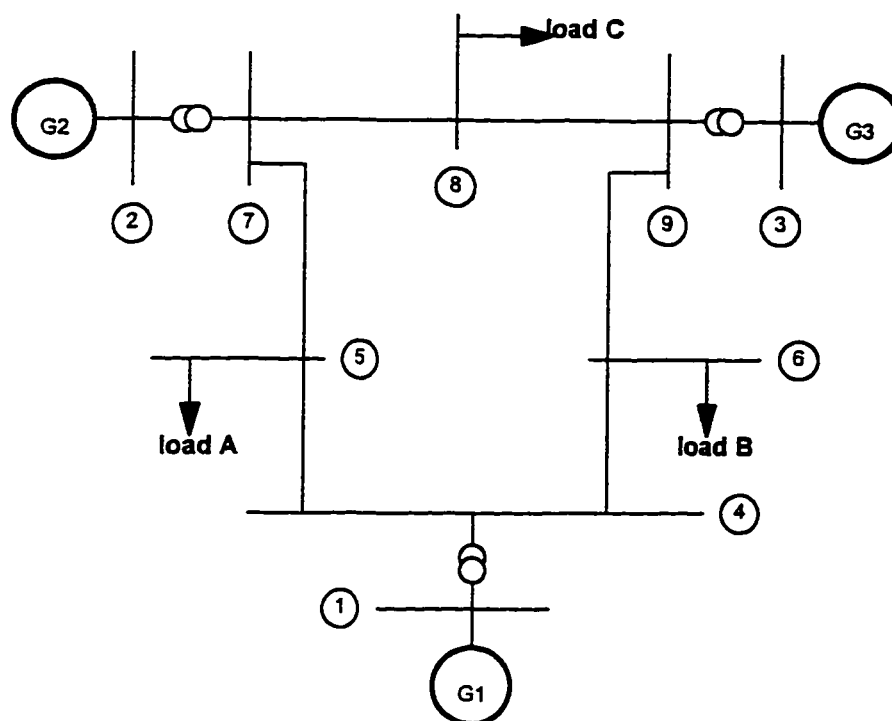
Fig. 5.7 Three-machine nine-bus power system [1]
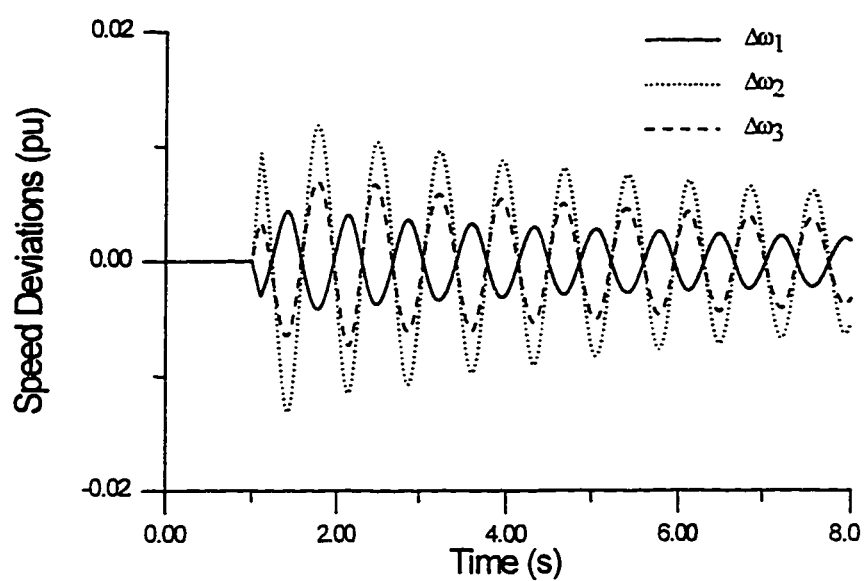
Fig. 5.8 Response to a three phase fault without PSSs

5.5.2 THE PROPOSED RBFN PSSs

Two RBFNs are proposed to re-tune the stabilizers installed on G2 and G3. The proposed networks were trained using k-means algorithm. The purpose of the training in this paper is to make the proposed RBFN able to update the values of K_{ci} and T_{li} parameters based on real-time measurements of the ith machine loading conditions. To generate the training patterns, the load admittances have been randomly varied in the range of 0.5 to 2.0 of their nominal values. With each variation, the load flow solution of the system is obtained and the CPSS is designed by linearizing the system model around the current operating point. Therefore, each training pattern consists of the real power P_i and the reactive power Q_i as the network inputs and the parameters K_{ci} and T_{li} as the desired outputs. A computational flow chart of the training and testing procedure is shown in Fig. 5.9.

Each RBFN was trained using a set of 500 input-output patterns. The trained networks were tested by another set of 500 input-output patterns. The errors APE and the structure of the networks are given in Table 5.5.

TABLE 5.5 APE and RBFN structures

Generator	APE		RBFN Structure	
	K_c	T_l	m	n_n
G2	0.020	0.026	25	6
G3	0.031	0.028	25	6
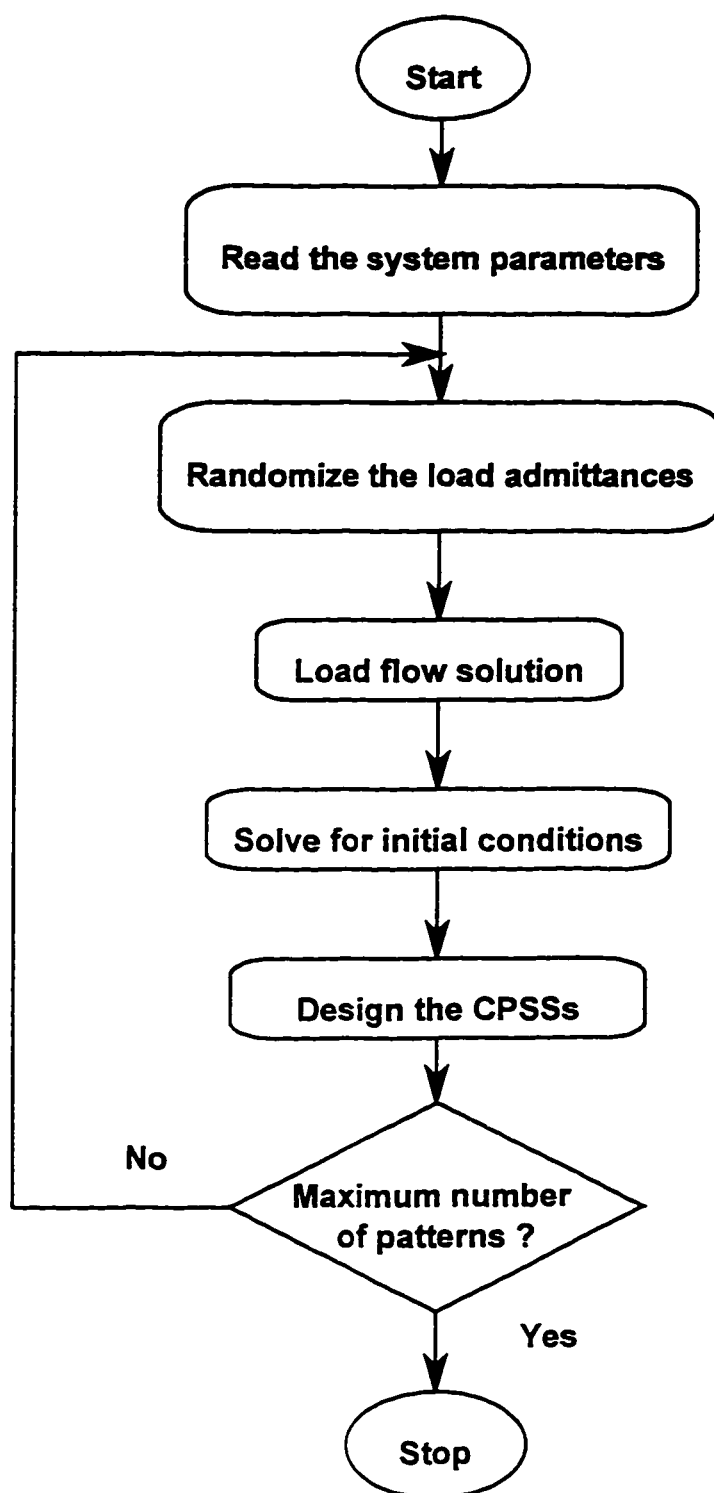
Fig. 5.9 Training and testing patterns preparation

5.5.3 RESULTS AND SIMULATIONS

With each loading condition described above, a three phase fault at bus 7 was applied. The fault duration was 6 cycles. It is worth pointing out that all time simulations have been carried out using the nonlinear model of the system. The simulation results are shown as follows.

5.5.3.1 NOMINAL LOADING CONDITION

The system response is shown in Fig. 5.10. It is obvious that with the proposed RBFN PSSs, the system returns to its previous operating point faster than the CPSSs. This is very helpful in the improvement of the disturbance tolerance ability of the system.

5.5.3.2 HEAVY LOADING CONDITION

It may become necessary to operate the power system with heavy loading conditions. Accordingly, it becomes very important to test the PSS under this difficult situation. The simulation results are shown in Fig. 5.11. The results here show the superiority of the proposed RBFN PSSs to the CPSSs. It can be concluded that the proposed RBFN PSS provides very good damping over a wide range of operating conditions.

5.5.3.3 LIGHT LOADING CONDITION

The simulation results are shown in Fig. 5.12. It can be seen that the proposed RBFN PSSs produce much better results and the oscillations are damped out much quicker as compared to CPSSs.

5.6 SUMMARY

This chapter presents a novel technique for on-line tuning of PSSs. The proposed technique overcomes the major problem of the adaptive stabilizers which is the necessity of on-line parameter identification. The proposed RBFN PSS was trained over a wide range of operating conditions. The proposed strategy has been applied to a single machine infinite bus system and to a multimachine system. The results show that the system performance with the proposed stabilizer is greatly improved and the oscillations are damped out much faster than conventional stabilizers. The major features of the proposed stabilizer are the fact that it is easy to tune and to implement.

To overcome the weaknesses of neural networks and fuzzy logic systems and to combine their strengths, fuzzy basis function network based power system stabilizer will be proposed in the next chapter.
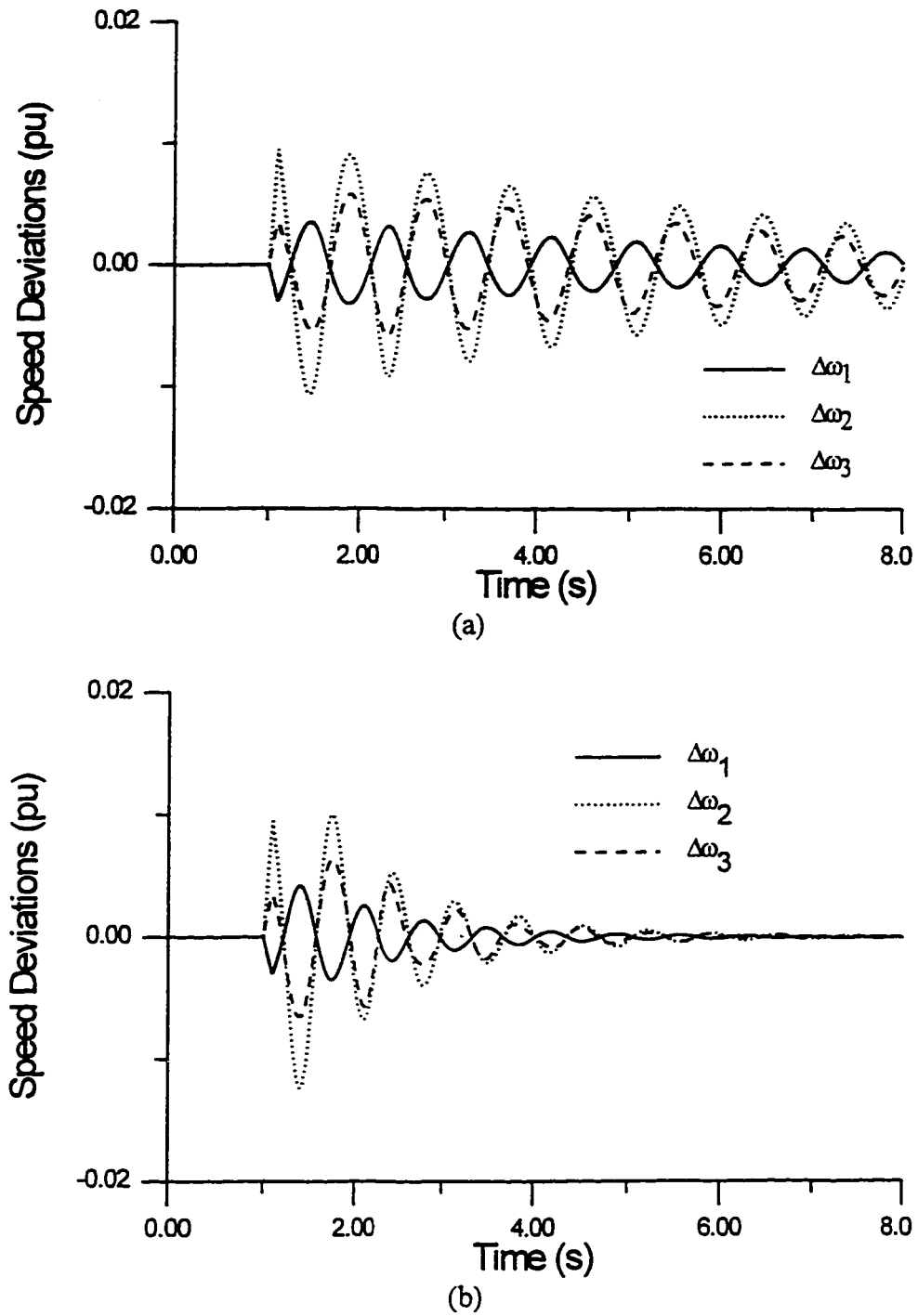
Fig. 5.10 Response to a three phase fault disturbance at nominal loading condition

(a) CPSS
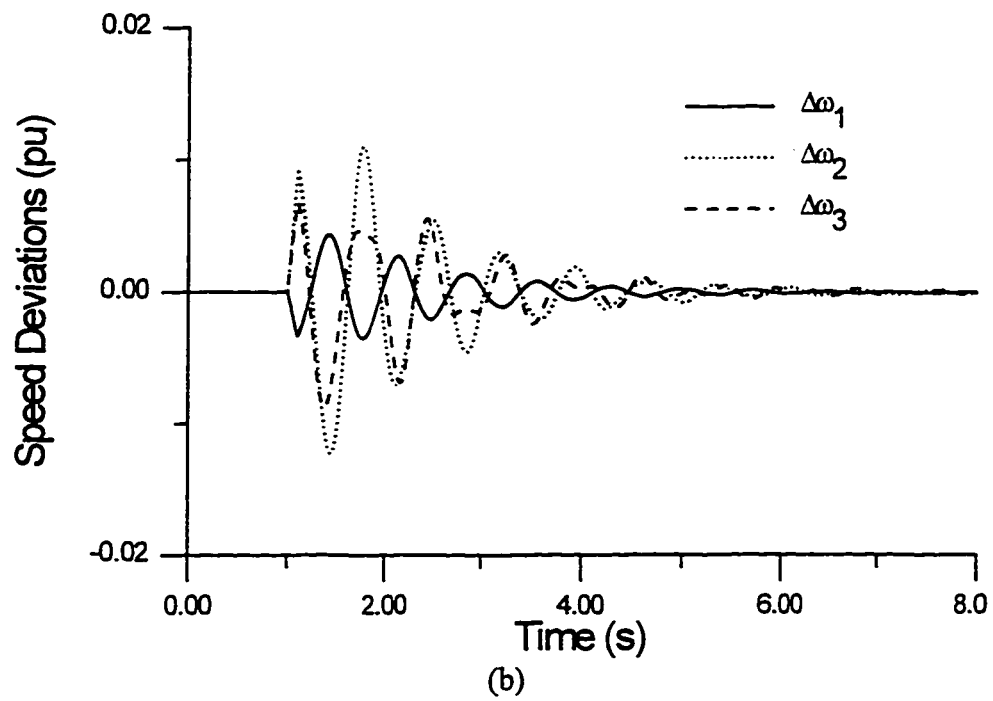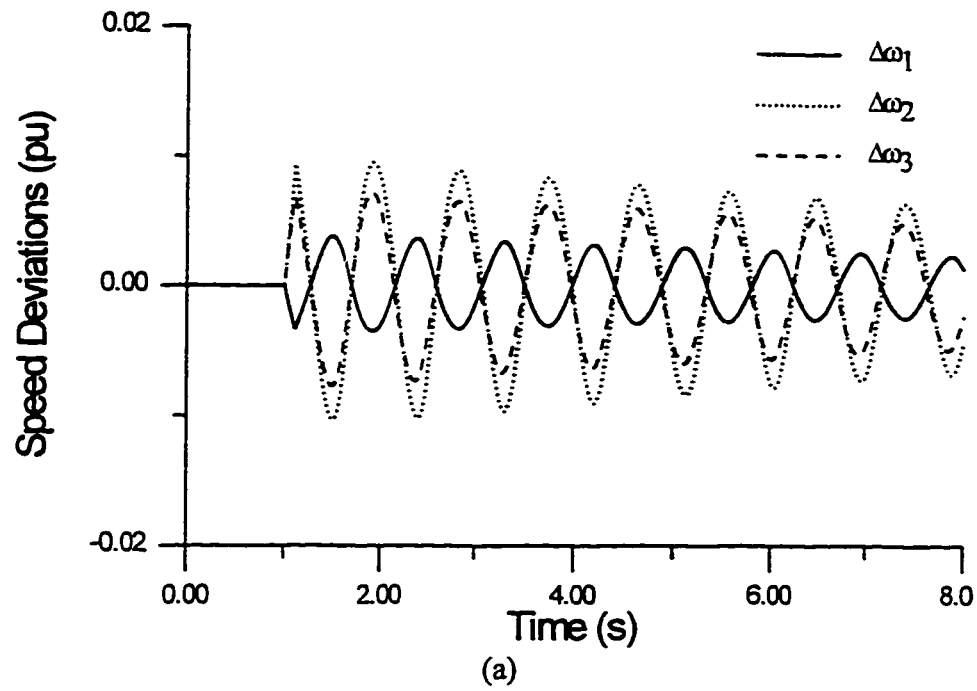
(b) Proposed RBFN PSS

Fig. 5.11 Response to a three phase fault disturbance at heavy loading condition

(a) CPSS
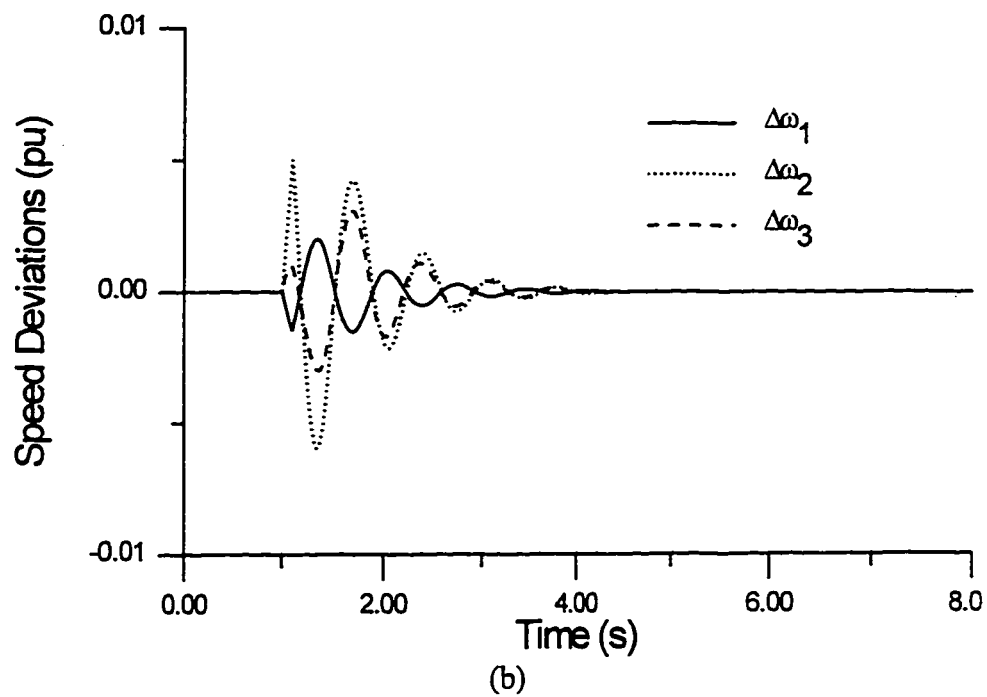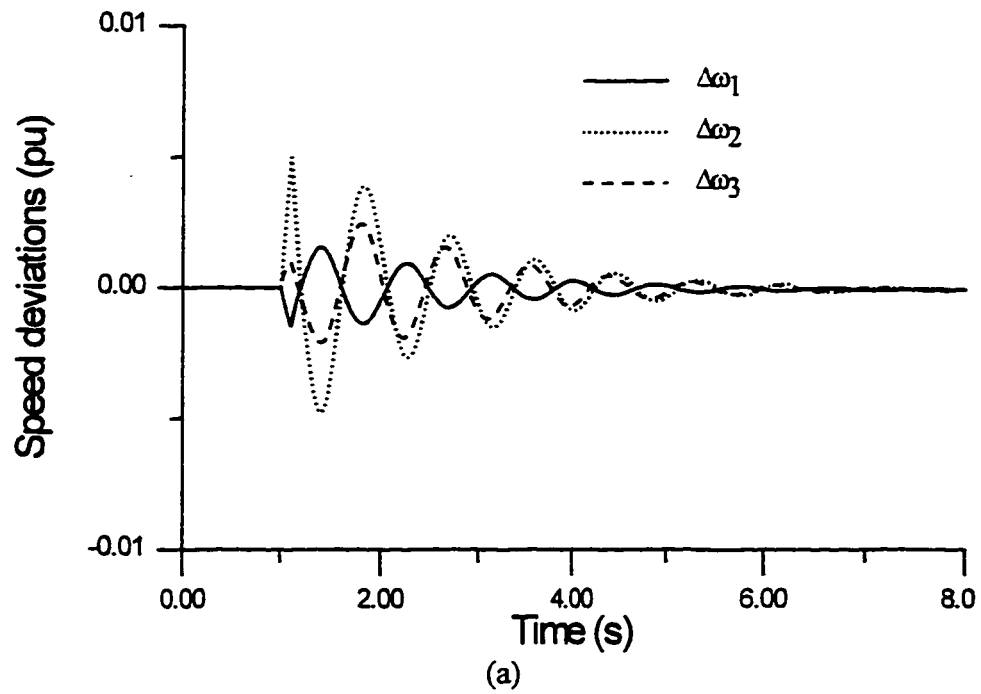
(b) Proposed RBFN PSS

Fig. 5.12 Response to three phase fault disturbance at light loading condition.

(a) CPSS

(b) Proposed RBFN PSS

CHAPTER 6

HYBRID NEURO-FUZZY POWER SYSTEM STABILIZERS

6.1 INTRODUCTION

Recently, many intelligent system techniques have been developed and introduced such as neural networks (NN) and fuzzy logic systems (FLS). Unlike the most conventional methods, an explicit mathematical model of the system dynamics is not required to design a controller using NN and/or FLS. NN and FLS have been successfully applied to various power system control problems with promising results. A neural network that mimic the function of the brain has a large number of massively interconnected processing elements (nodes) that demonstrate the ability to learn and generalize from training examples. Distributed representation and learning capabilities are the major features of NN. Since the NN are nonlinear in the parameters [64-68], the backpropagation training algorithm is commonly used to estimate the network

parameters. However, there are several problems associated with these networks such as getting stuck in local minima and slow convergence rate.

On the other hand, FLS base their decisions on inputs in the form of linguistic variables derived from membership functions which are used to determine the fuzzy set to which a crisp value of the input belongs and the degree of membership in that set. The variables are then matched with the preconditions of linguistic IF-THEN rules and the response of each rule is obtained through fuzzy implication. The response of each rule is weighted according to the degree of membership of its inputs. Finally, the centroid of responses is calculated to generate the appropriate output. Although fuzzy logic controllers showed promising results [82-95], they are subjective and somewhat heuristic. In addition, the determination of fuzzy rules and the choice of membership functions depend on trial-and-error which, in turn, makes the design of fuzzy logic controller a time-consuming task.

In power systems, because of the nature of various problems, different types of solutions may be required. The recent direction to deal with these problems is to integrate the use of NN and FLS in order to combine their different strengths and overcome each other's weaknesses [96-101]. In this chapter, we propose a fuzzy basis function network based power system stabilizer (FBFN PSS) which brings the learning capabilities of NN to FLS. The proposed RBFN is trained to adapt the parameters of PSS based on real-time measurements.

The main features of the proposed FBFN PSS can be summarized as follows:

1. The proposed FBFN PSS is of a decentralized output feedback form since only local measurements are employed as the inputs to each stabilizer. This makes the proposed FBFN PSS easy to tune.

2. The proposed FBFN PSS can be easily implemented on a microcomputer since it does not require real-time model identification.

3. The proposed FBFN PSS incorporates the linguistic and numerical information in a uniform fashion and combines the strengths of NN and FLS.

6.2 FUZZY BASIS FUNCTION NETWORK

The problem that can be raised in the training of neural networks is that the test inputs used to generate the input-output pairs may not be rich enough to excite all modes of the system [97]. In this case, using neural networks only to design the stabilizer may be neither sufficient nor effective.

On the other hand, the major difficulty in the design of a traditional fuzzy logic controller is the determination of the fuzzy rules and the associated input/output membership functions. At present, the fuzzy rules and membership functions are subjectively defined by studying a human-operated system or an existing controller and then testing the design for proper output. If the design fails the test, fuzzy rules and membership functions should be adjusted. Therefore, the design of the traditional fuzzy logic controller requires a lot of trial-and-error, thus making the design a time-consuming task. However, the linguistic rules are very important and often contain information

which is not contained in the input-output pairs used to train neural networks. The proposed FBFN combines the strengths of both FLS and NN.

Like the feedforward networks, the proposed FBFN has four layers as shown in Fig. 6.1. It is worth noting that Fig. 6.1 shows the initial network structure where the number of fuzzy rules, M, is equal to the number of training patterns, N, whereas the final structure is much simpler. In what follows, we will denote the output of the ith node in the kth layer by O_i^k. The proposed network structure with n inputs and m outputs can be described as follows:

Layer 1: For the ith input, every node in this layer computes the degree of membership of the input. Every node j has a function of

$$O_j^l = \mu_{ij}(x_i) , \quad j=1,2,\ldots,M \tag{6.1}$$

where $\mu_{ij}(x_i)$ is a Gaussian membership function associated with the ith input and jth rule. It can be expressed as

$$\mu_{ij}(x_i) = \exp(-\frac{1}{2}(\frac{x_i - c_{ij}}{\sigma_{ij}})^2) \tag{6.2}$$

where c_{ij} and σ_{ij} are the mean and the variance of the jth function.

Layer 2: Every node in this layer multiplies the incoming signals and sends the product out, i.e.,

$$O_j^2 = \prod_{i=1}^{n} \mu_{ij}(x_i) \quad , j=1,2,\ldots,M \tag{6.3}$$

Basically, each node output represents the firing strength of a fuzzy rule.
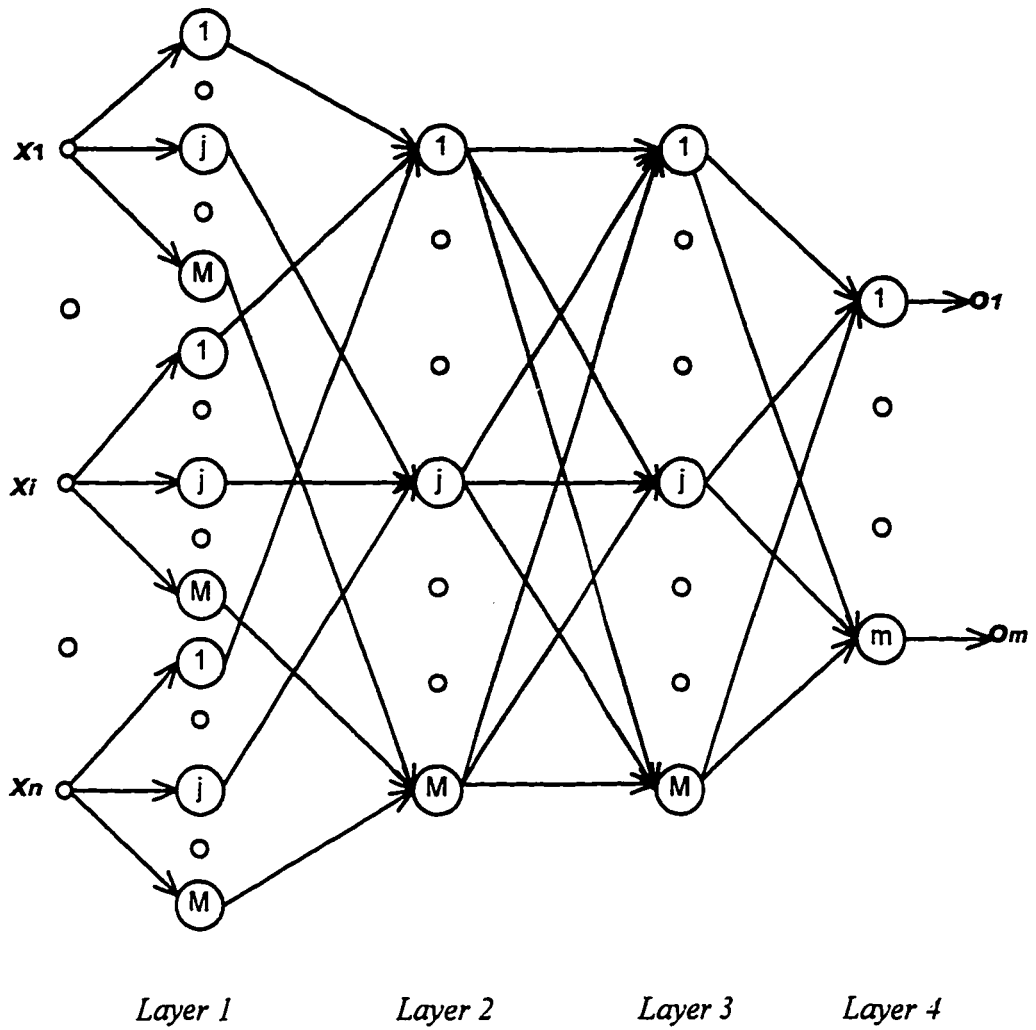
Fig. 6.1 A schematic diagram of the proposed FBFN

Layer 3: Every node in this layer calculates the ratio of the jth rule's firing strength to the sum of all rules' firing strengths, i.e.,

$$O_j^3 = \frac{\prod_{i=1}^{n} \mu_{ij}(x_i)}{\sum_{j=1}^{M} \prod_{i=1}^{n} \mu_{ij}(x_i)} \qquad ,j=1,2,\ldots,M \qquad (6.4)$$

In other words, nodes in this layer compute the normalized firing strength of each rule. In fact, the output of each node in this layer represents a fuzzy basis function, $p_j(x)$, that is,

$$p_j(x) = O_j^3 \qquad ,j=1,2,\ldots,M \qquad (6.5)$$

where $x = [x_1,\ldots,x_n]^T$ is the input vector.

Layer 4: In this layer each node represents an output and linearly combines the fuzzy basis functions as

$$O_k^4 = \sum_{j=1}^{M} p_j(x)\theta_{jk} \qquad ,k=1,2,\ldots,m \qquad (6.6)$$

where θ_{jk} is the weight between the jth node in layer 3 and the kth node in layer 4.

6.3 THE PROPOSED FBFN TRAINING

The objectives of the training are to construct an adequate and parsimonious model of the network, to select a set of appropriate means, c_{ij}s, of the membership functions, and to estimate the weights, θ_{jk}s, between layer 3 and layer 4. Although each membership function may have a different variance, σ_{ij}, a same variance is sufficient for universal

approximation [37,97]. All the variances in the network can therefore be fixed to a value σ, and this can simplify the training strategy. Initially, all the training patterns are considered as candidates for centers. Therefore, the initial number of centers M is equal to the number of training patterns N.

Since FBFN is linear in the parameters, the OLS learning algorithm developed in Chapter 3 is used to determine a set of significant fuzzy basis functions and the network parameters. The OLS learning algorithm requires only one pass of the training examples, therefore, it is much faster than backpropagation algorithm. Moreover, the OLS algorithm is a linear optimization technique, hence, it guarantees the convergence of the network parameters to the global minimum. While most of the learning algorithms require a prespecified network structure, the OLS algorithm provides a systematic approach to the selection of FBFN structure in an intelligent way in the sense that an adequate and parsimonious structure is self-organized.

6.4 DESIGN OF THE PROPOSED FBFN PSS

The proposed FBFN PSS is used to re-tune the parameters of the CPSS described in (5.1) based on local real-time measurements of loading conditions. The inputs to the FBFN are the real power (P) and the reactive power (Q). A set of 500 training patterns was presented to the network. The training patterns were uniformly distributed over the specified range. For each operating condition, the CPSS parameters, K_c and T_l, are tuned

to yield the best performance at this operating point by prespecifying the damping coefficient [2]. The CPSS parameters obtained represent the desired outputs.

The trained network was tested by another set of 500 input-output patterns that have not been presented before to the network. The average percentage error (APE) described in (5.2) is used in order to evaluate the performance of the trained FBFN.

The proposed FBFN PSS control scheme is shown in Fig. 6.2.

6.5 EXAMPLE 1: SINGLE MACHINE SYSTEM

6.5.1 TEST SYSTEM

In this study, the single machine infinite bus system shown in Fig. 3.1 is considered. The system model and parameters are given in the Appendix B. In order to investigate the performance of the proposed FBFN PSS, CPSS and PI PSS have been designed as described in Chapter 5. A number of studies have been performed and the results of time domain simulations of the proposed FBFN PSS are compared with those of the CPSS and PI PSS. All time domain simulations are carried out using the nonlinear model of the system.

In this study, the same operating conditions given in Table 5.1 are considered in order to test the proposed FBFN PSS over a wide loading range.
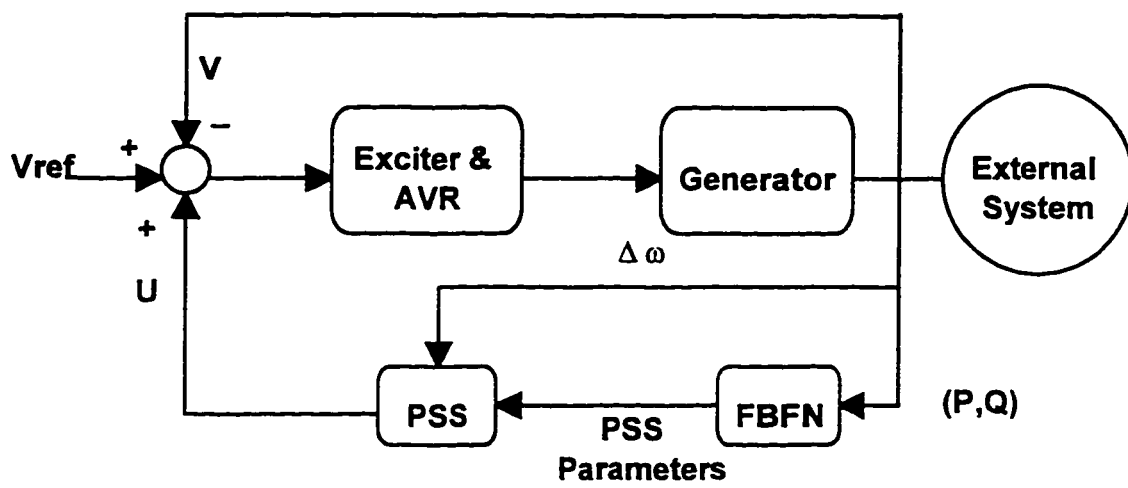
Fig. 6.2 The proposed FBFN PSS control scheme

6.5.2 THE PROPOSED FBFN PSS

The proposed FBFN was trained as described above. To cover a wide range of loading conditions, P is ranging from 0.1 pu to 1.5 pu and the power factor is ranging from 0.9 leading to 0.8 lagging. Out of the training patterns presented to the network, a set of 41 patterns was selected by the OLS algorithm to represent the significant fuzzy basis functions. In addition, APE for K_c and T_I are found to be 0.3546% and 0.9290% respectively.

6.5.3 SIMULATION RESULTS

6.5.3.1 OPERATING CONDITION (P_I, Q_I)

A three phase fault was applied at t=1.0s at the infinite bus for a duration of 0.1s. Results of the study are shown in Fig. 6.3. It is obvious that although the CPSS and PI PSS parameters were optimized at this operating condition, the proposed FBFN PSS provides the best damping characteristics.

6.5.3.2 OPERATING CONDITION (P_2, Q_2)

A three phase fault was applied at the infinite bus for 0.05s with the generator operating at the heavy loading condition specified by (P_2, Q_2). The simulation results of

this test are shown in Fig. 6.4. It can be concluded that the system with the proposed FBFN PSS returns to its previous operating point faster than the conventional and proportional-integral stabilizers. This improves the disturbance tolerance ability of the system.

6.5.3.3 OPERATING CONDITION (P_3, Q_3)

A 10% step in mechanical torque was applied at t=1.0s while the generator is operating at (P_3, Q_3). The simulation results are shown in Fig. 6.5. Another test has also been conducted with the generator operating at this condition, that is, a three phase fault was applied at t=1.0s at the infinite bus for a duration of 0.1s. The simulation results are shown in Fig. 6.6. It is clear that the performance of the proposed FBFN PSS is superior to those of the CPSS and PI PSS and the oscillations are damped out much quicker.

6.5.3.4 OPERATING CONDITION (P_4, Q_4)

At the light loading condition (P_4, Q_4), a local load of admittance of $0.3 - j0.2$ pu has been switched on at t=1.0s. The simulation results are shown in Fig. 6.7. It is seen that the proposed FBFN PSS provides better damping characteristics.
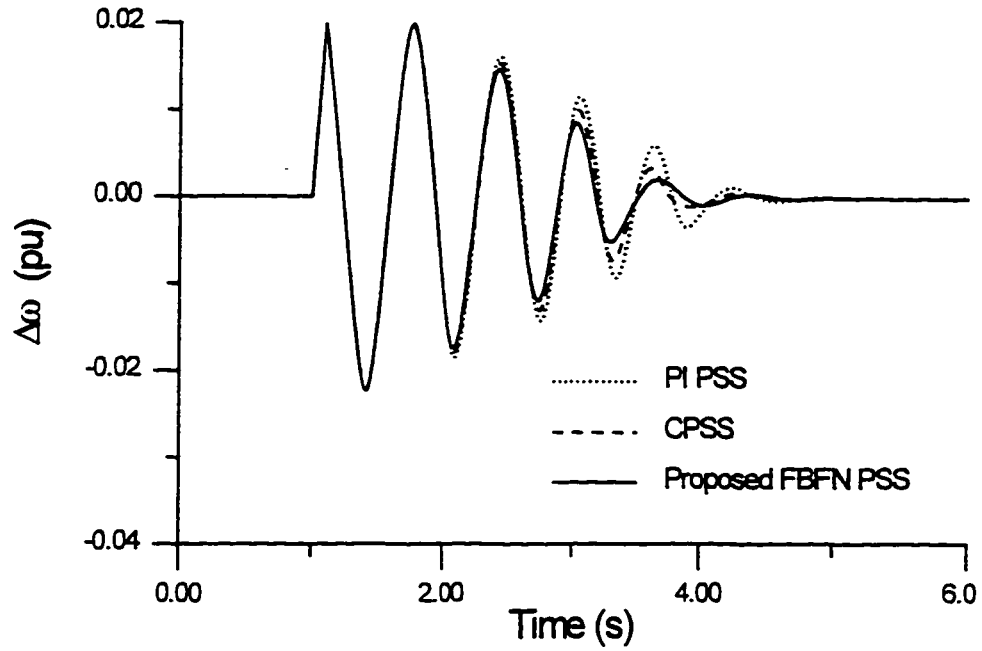
Fig. 6.3 Response to a 0.1s three phase fault with loading of (P_1, Q_1)
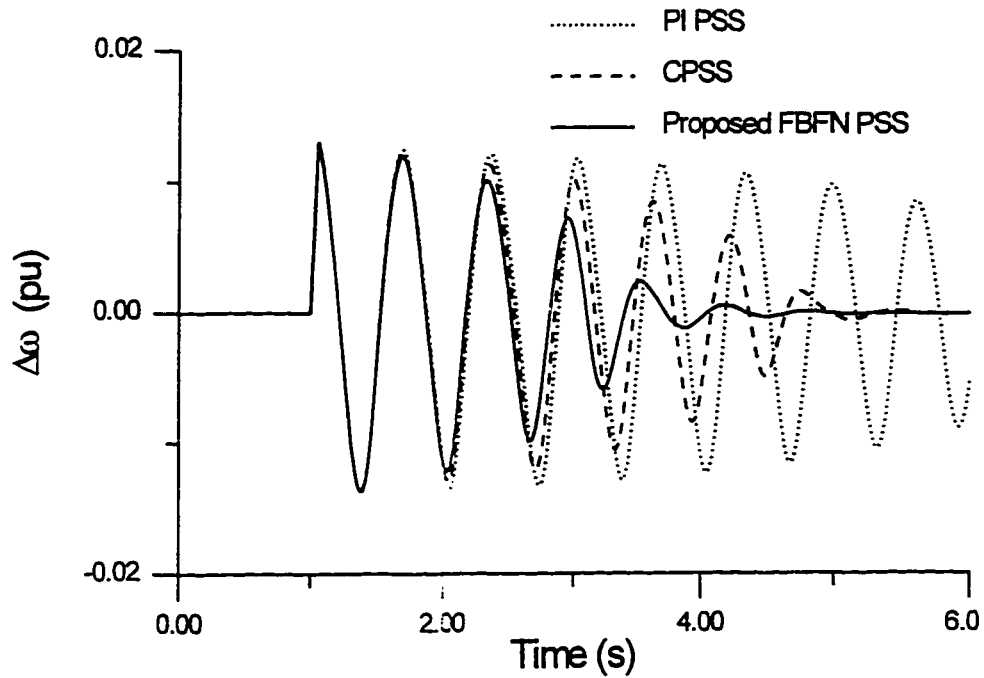
Fig. 6.4 Response to a 0.05s three phase fault with loading of (P_2, Q_2)
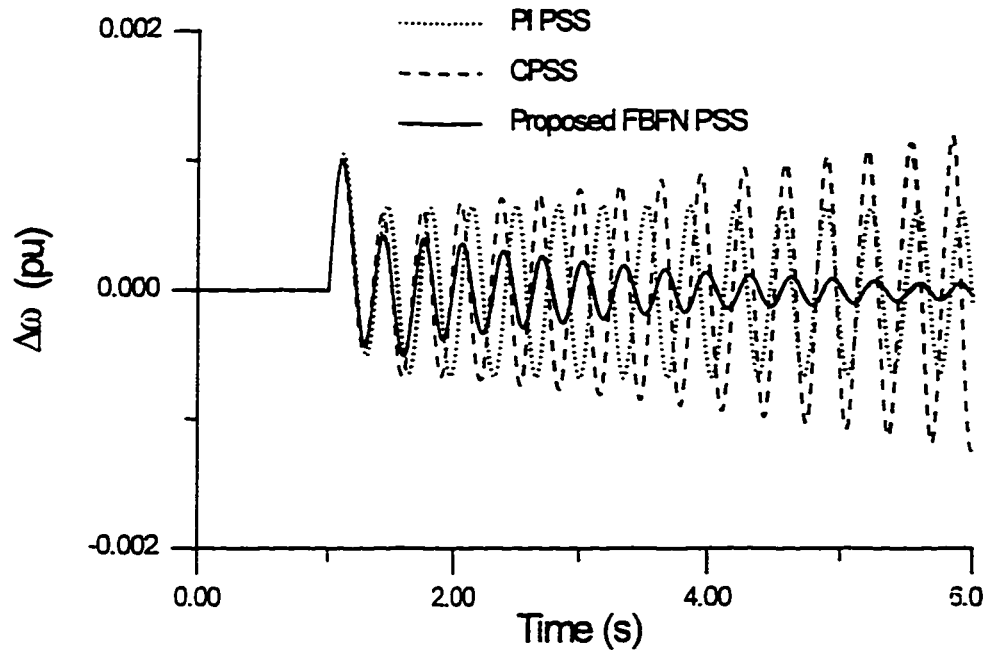
Fig. 6.5 Response to a 10% step in mechanical torque with loading of (P_3, Q_3)
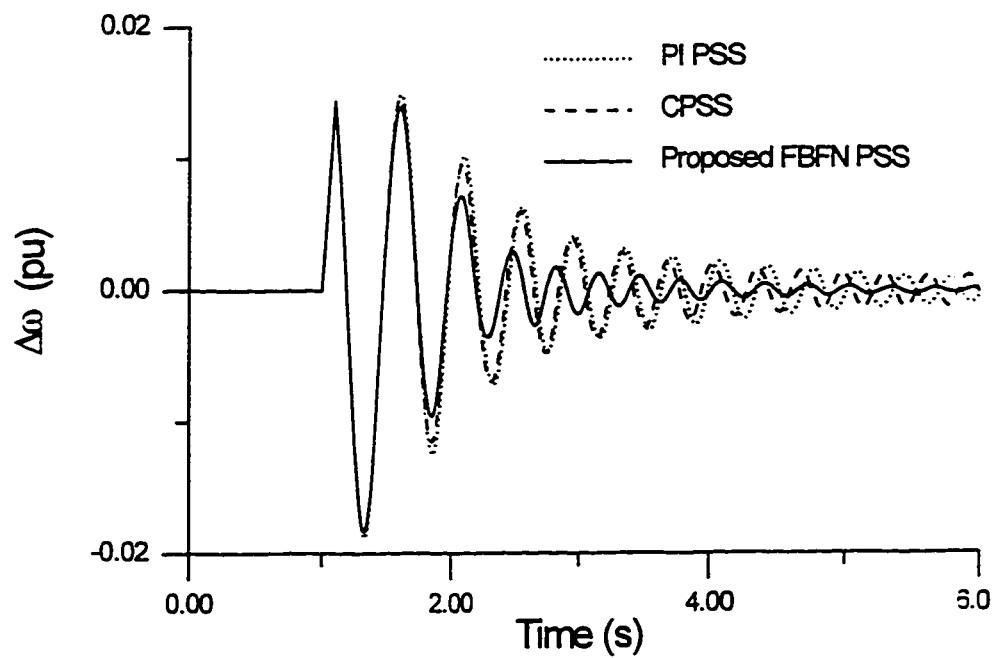
Fig. 6.6 Response to a 0.1s three phase fault with loading of (P_3, Q_3)
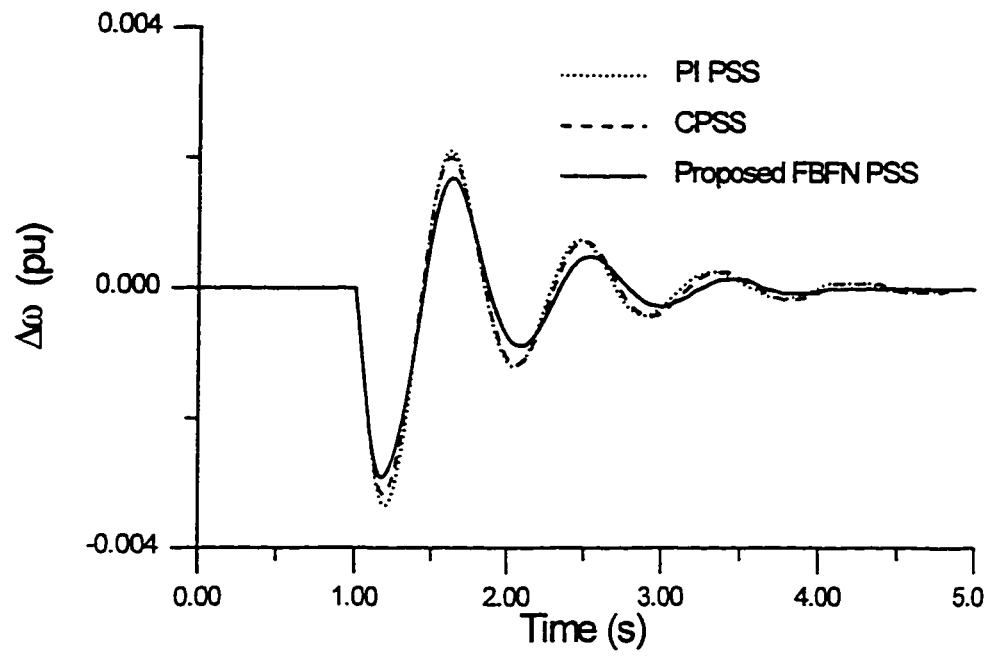
Fig. 6.7 Response to switching on a local load with loading of (P_+, Q_+)

6.6 EXAMPLE 2: MULTIMACHINE SYSTEM

6.6.1 TEST SYSTEM

The nine-bus three-machine power system shown in Fig. 5.7 is considered. Details of

the system model and parameters are given in Appendix D. Without PSSs, the system

response curves due to a 6-cycle three phase fault at bus 7 at the end of line 5-7 are shown

in Fig. 5.8. As described in Chapter 5, the system damping is poor and the system is

highly oscillatory. Therefore, it is necessary to install stabilizers in order to have good

dynamic performance. It was mentioned in Chapter 5 that the generators G2 and G3 are

the optimum locations for installing PSSs to damp out the electromechanical modes of

oscillations. Therefore, the generators G2 and G3 are equipped with two of the proposed

FBFN PSS. The performance of the proposed stabilizers was compared to that of CPSSs

installed on G2 and G3 with the transfer function given by (5.6)

To demonstrate the capability of the proposed FBFN PSS to enhance system damping

over a wide range of operating conditions, the same loading conditions and load

admittances given in Tables 5.3 and 5.4 were considered respectively.

6.6.2 THE PROPOSED FBFN PSSs

Two FBFNs are proposed to re-tune the stabilizers installed on G2 and G3. The

proposed networks were trained using OLS algorithm. The training patterns were

generated as shown in Fig. 5.9. Each training pattern consists of the real power P_i and the reactive power Q_i to represent the network inputs and the values of K_{ci} and T_{li} to represent the desired outputs.

Each FBFN was trained using a set of 500 input-output patterns. The trained networks were tested by another set of 500 input-output patterns. The errors APE and the number of significant fuzzy basis functions selected by OLS algorithm are given in Table 6.1.

6.6.3 RESULTS AND SIMULATIONS

With each loading condition, a three phase fault disturbance at bus 7 was applied. The fault duration was 6 cycles. The simulation results are shown as follows.

6.6.3.1 NOMINAL LOADING CONDITION

The dynamic response of the system is shown in Fig. 6.8. It is obvious that the proposed FBFN PSSs provide good damping characteristics since the speed deviations with the proposed stabilizers show smaller settling times than those of CPSSs.

6.6.3.2 HEAVY LOADING CONDITION

The simulation results are shown in Fig. 6.9. The results here show the superiority of the proposed FBFN PSSs to the CPSSs in the sense that the speed deviations of all units

are significantly reduced. It can be concluded that the proposed FBFN PSS provides very good damping over a wide range of operating conditions.

6.6.3.3 LIGHT LOADING CONDITION

The simulation results are shown in Fig. 6.10. It can be seen that the system performance with the proposed FBFN PSSs is much better and the oscillations are damped out much quicker as compared to CPSSs.

TABLE 6.1 APE and FBFN structures

Generator	APE		Significant FBF
	K_c	T_I	
G2	0.027	0.017	33
G3	0.030	0.016	20
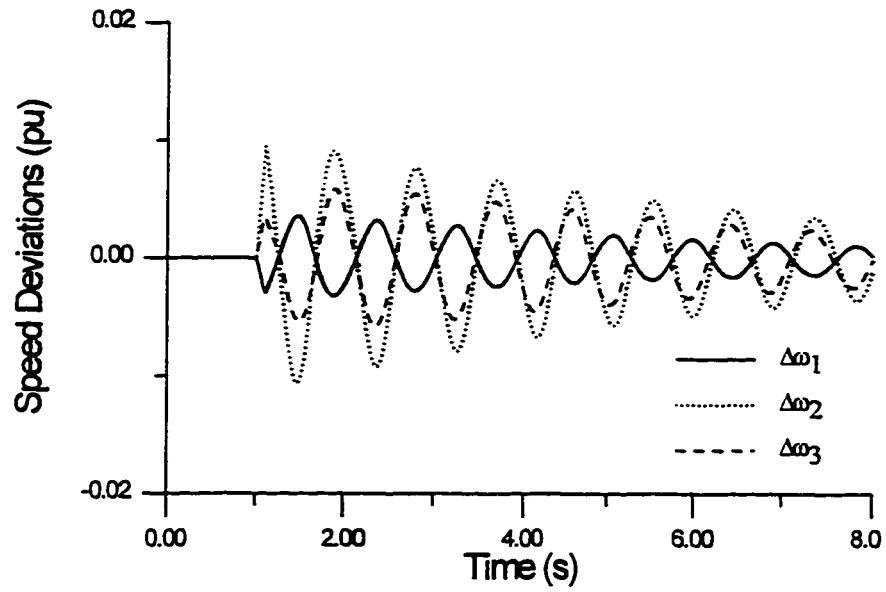
(a)
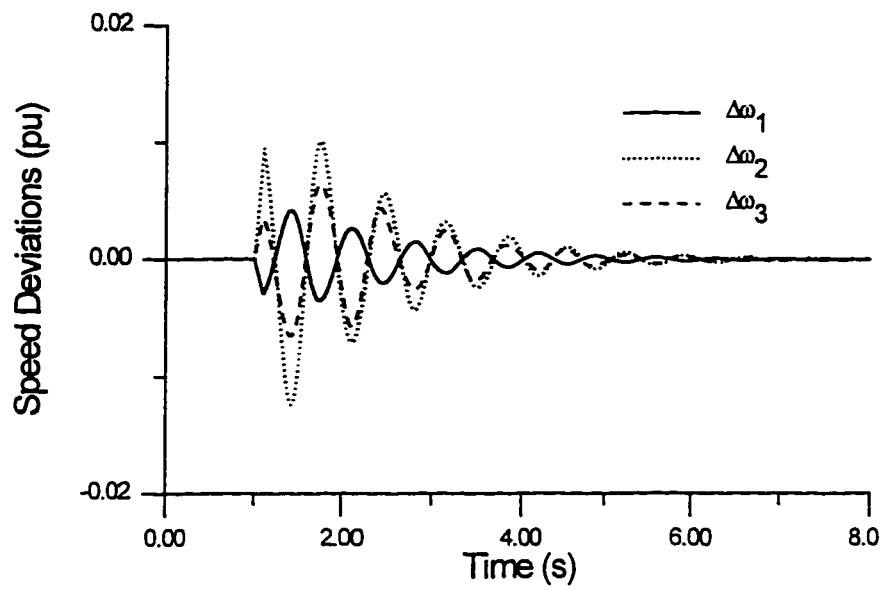
(b)

Fig. 6.8 Response to a three phase fault disturbance at nominal loading condition

(a) CPSS
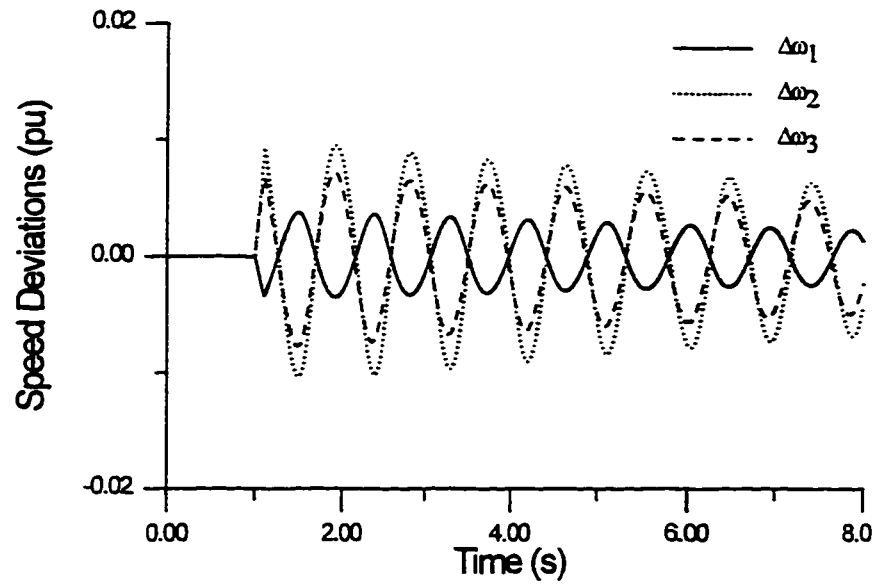
(b) Proposed FBFN PSS

(a)
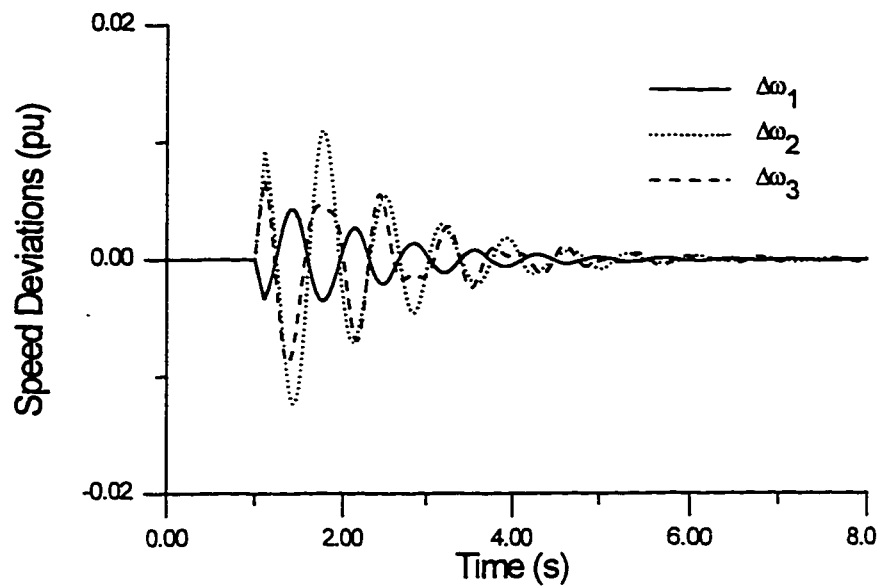
(b)

Fig. 6.9 Response to a three phase fault disturbance at heavy loading condition

(a) CPSS
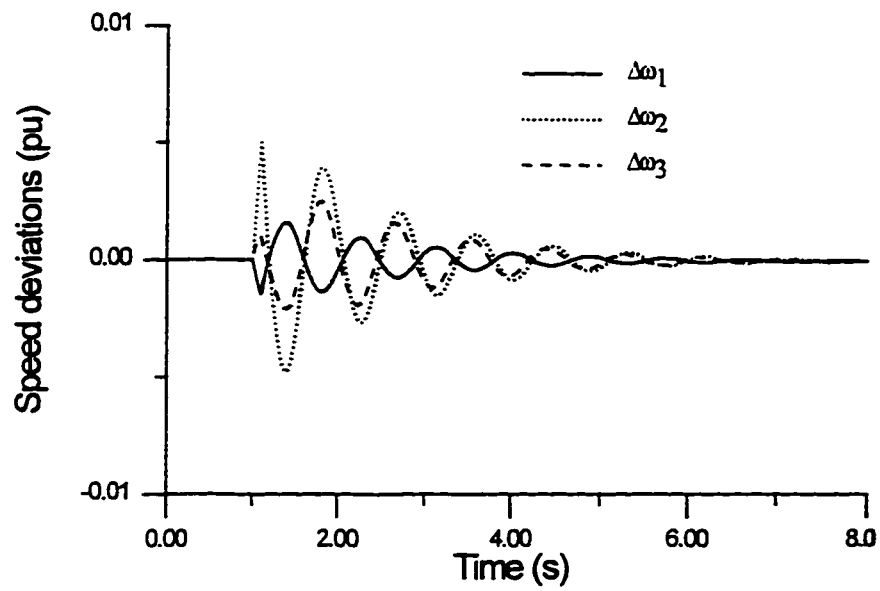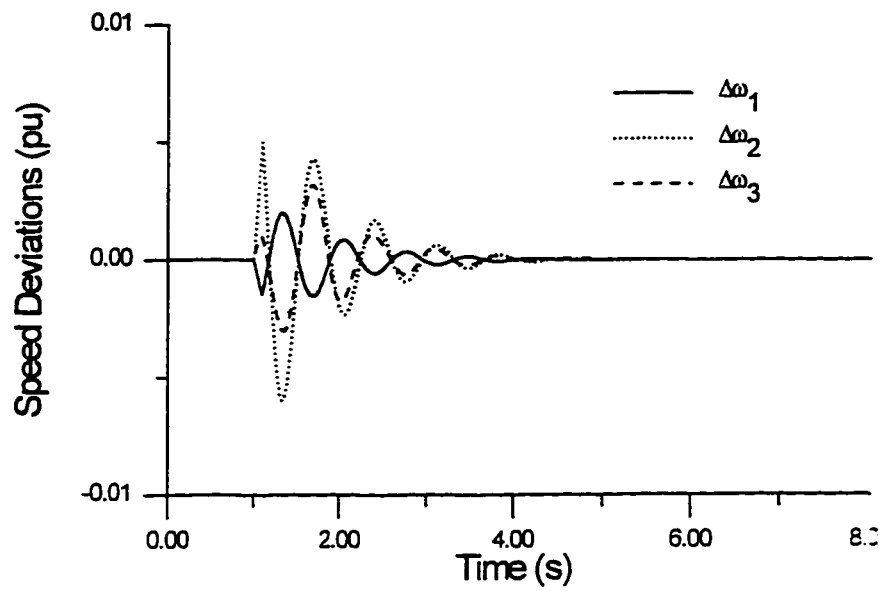
(b) Proposed FBFN PSS

Fig. 6.10 Response to three phase fault disturbance at light loading condition

(a) CPSS

(b) Proposed FBFN PSS

6.7 A COMPARISON BETWEEN FBFN AND RBFN

The RBFN proposed in Chapter 5 and the FBFN proposed in Chapter 6 were trained by a set of 500 training patterns uniformly distributed over the input space. The simulation results using RBFN and FBFN emphasize the fact that given a sufficient number of training patterns, both networks can successfully tune the PSS parameters based on real-time measurements of loading conditions.

In this section, the performance of each network is reexamined in the case of insufficient number of training patterns. Therefore, each network is retrained using a set of 50 training patterns only. In addition, OLS algorithm is used to train both networks. The number of hidden units selected by OLS algorithm for both systems considered in examples 1 and 2 are given in Table 6.2.

For the sake of comparison, two performance indices are considered, namely, the integral of squared time multiplied by square error which can be defined as

$$J_1 = \int_0^\infty t^2 \Delta\omega^2(t)\, dt \qquad (6.7)$$

and the integral of the square of the error which can be defined as

$$J_2 = \int_0^\infty \Delta\omega^2(t)\, dt \qquad (6.8)$$

The trained networks have been used to tune the PSS parameters for the same operating conditions described in examples 1 and 2. The simulation results for 0.1s three phase fault with the nominal operating condition of examples 1 are shown in Fig. 6.11.

Fig. 6.12 shows the simulation results of a 6-cycle three phase fault at bus 7 with the nominal operating condition of example 2. It can be seen that the system performance with FBFN is much better and the oscillations are damped out in both cases of single machine and multimachine systems. The values of J_1 and J_2 for different loading conditions of systems considered in examples 1 and 2 are given in Tables 6.3 and 6.4 respectively. It is obvious that the values of performance indices J_1 and J_2 with FBFN are much less. It can be concluded that the control performance of the FBFN PSS is much better than that of RBFN PSS in the case of 50 training patterns which represent an insufficient number of the training patterns. This can be attributed to the robustness of the fuzzy logic concepts embedded in FBFN structure.

6.8 SUMMARY

In this chapter, an FBFN PSS has been proposed. The proposed stabilizer overcomes the problems that can be raised in neural network training and fuzzy logic controller design. In addition, the proposed stabilizer incorporates the fuzzy logic concepts with a radial basis function network structure in a uniform fashion. The proposed stabilizer has been tested in a single machine infinite bus system and in a multimachine power system environments. The results show the superiority of the proposed stabilizer over conventional stabilizers. A comparison between RBFN and FBFN in case of insufficient number of training patterns reveals the robustness property of the proposed FBFN.

In the remaining chapters, genetic algorithms will be incorporated in the design of conventional PSSs in chapter 7, rule-based PSSs in chapter 8, and fuzzy logic PSSs in chapter 9. Incorporating GA in the design process will add an intelligent dimension to these stabilizers and reduce significantly the time consumed to search for optimal settings of the stabilizer parameters.

TABLE 6.2 Hidden units for reduced number of training patterns

Network Type	Example 1	Example 2	
		G2	G3
FBFN	20	20	18
RBFN	20	17	15
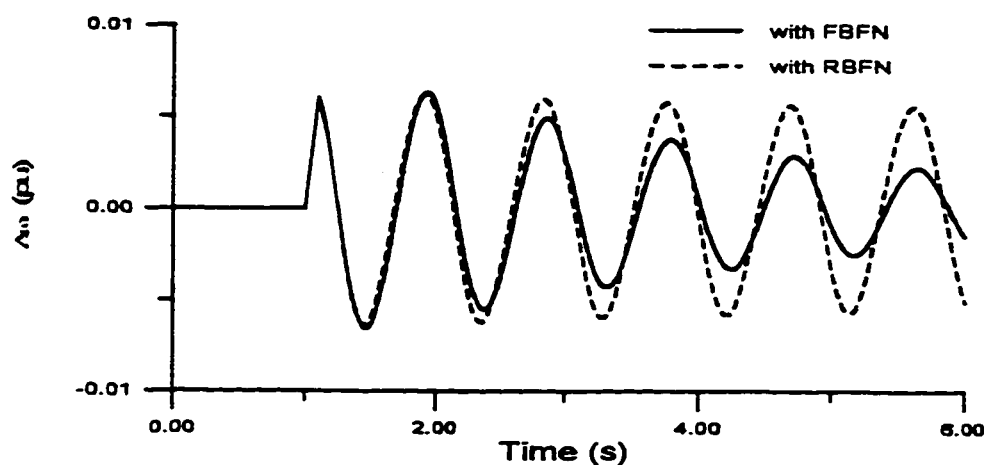
Fig. 6.11 Response to a 0.1s three phase fault with nominal loading of example 1

(a)

(b)
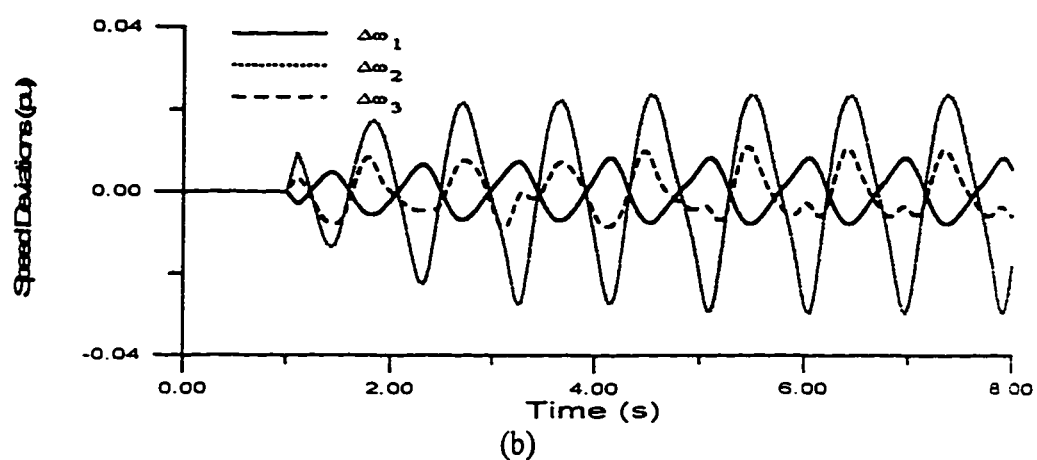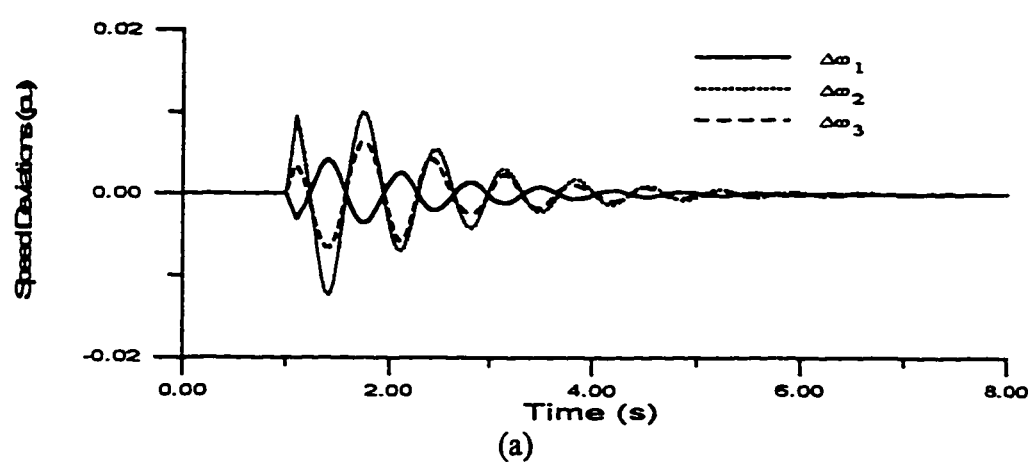
Fig. 6.12 Response to a 6-cycle three phase fault with nominal loading of example 2

(a) FBFN PSSs

(b) RBFN PSSs

TABLE 6.3 Comparison between FBFN and RBFN for example 1

Loading condition	Fault Time (ms)	J_1		J_2	
		FBFN	RBFN	FBFN	RBFN
P_1, Q_1	100	2.0010	6.6041	0.4955	0.8529
P_2, Q_2	50	0.5135	4.6413	0.1278	0.4925
P_3, Q_3	120	3.1397	6.7476	0.7533	0.9106
P_4, Q_4	150	5.8131	6.9937	1.3090	1.4752

TABLE 6.4 Comparison between FBFN and RBFN for example 2

Loading Condition	Fault Time (ms)	J_1		J_2	
		FBFN	RBFN	FBFN	RBFN
Nominal	100	1.1622	397.42	1.0733	21.462
Heavy	100	1.2543	437.72	1.1969	22.536
Light	100	0.0830	189.70	0.1806	9.5615

CHAPTER 7

GENETIC-BASED POWER SYSTEM STABILIZERS

7.1 INTRODUCTION

Genetic algorithms (GA) are search algorithms based on the mechanics of natural selection and survival-of-the-fittest. One of the most important features of the GA as a method of control system design is the fact that minimal knowledge of the plant under investigation is required. Since the GA optimize a performance index based on input/output relationships only, far less information than other design techniques is needed. Further, because the GA search is directed towards increasing a specified performance, the net result is a controller which ultimately meets the performance criteria. In addition, because derivative information is not needed in the execution of the algorithm, many pitfalls that gradient search methods suffer can be overcome. Finally, because the GA do not need an explicit mathematical relationship between the performance of the system and the search update, the GA offer a more general

optimization methodology than conventional analytical techniques. Recently, GA have been successfully applied to various power system problems [102-107].

This chapter introduces the application of GA to the design of power system stabilizers. At first the design problem is transformed into an optimization problem which is then solved using GA. This approach is successfully applied to search for the optimal settings of PSS parameters. The simulation results show that the proposed genetic-based power system stabilizer (GPSS) can improve the dynamic performance of power systems over a wide range of operating conditions and system parameter variations.

7.2 PROBLEM FORMULATION

Before the GA are employed for design purposes, it is necessary to carry out coding, selecting an initial population, and adopting a performance index. In this study, the PSS parameters are coded in a binary string and the initial population is randomly generated. A simple performance index that promotes small steady state errors and small overshoots and oscillations is given by

$$J = \sum_{i=1}^{NM} \int_{t=0}^{\infty} (t\,\Delta\omega_i(t))^2 dt \qquad (7.1)$$

where $\Delta\omega_i$ represents the ith machine speed deviation and NM represents the total number of machines.

The commonly used lead-lag type of PSS with speed deviation as its input is chosen in this study. Let the transfer function of each local stabilizer be

$$\frac{U_i}{\Delta\omega_i} = K_{ci}[\ \frac{1+sT_{1i}}{1+sT_{2i}} \ ]^{p_i} \tag{7.2}$$

where U_i and $\Delta\omega_i$ are the output and input of the ith stabilizer. The order of each PSS

and its lag time, i.e., p_i and T_{2i} are usually prespecified [53]. In this study, p_i and T_{2i} are

assumed to be 1 and 0.1s respectively. Thus, K_{ci} and T_{1i} are the parameters which remain

to be determined. The proposed approach is to use GA to select these parameters so as to

minimize the performance index J in (7.1).

The particular choices of population size, number of generations, crossover

probability, and mutation probability are generally problem dependent. However, GA

perform better with relatively high crossover probability, small mutation probability, and

moderate population size [17].

Applying GA to the problem of PSS design involves repetitively performing the

following two basic steps:

1. The performance index value must be calculated for each of the strings in the current

   population. To do this, the PSS parameters must be decoded from each string in the

   population and the system simulated to obtain the performance index value.

2. GA operations are applied to produce the next generation of the strings.

These two steps are repeated from generation to generation until the population has

converged. The computational flow of the problem can be shown in Fig. 7.1.
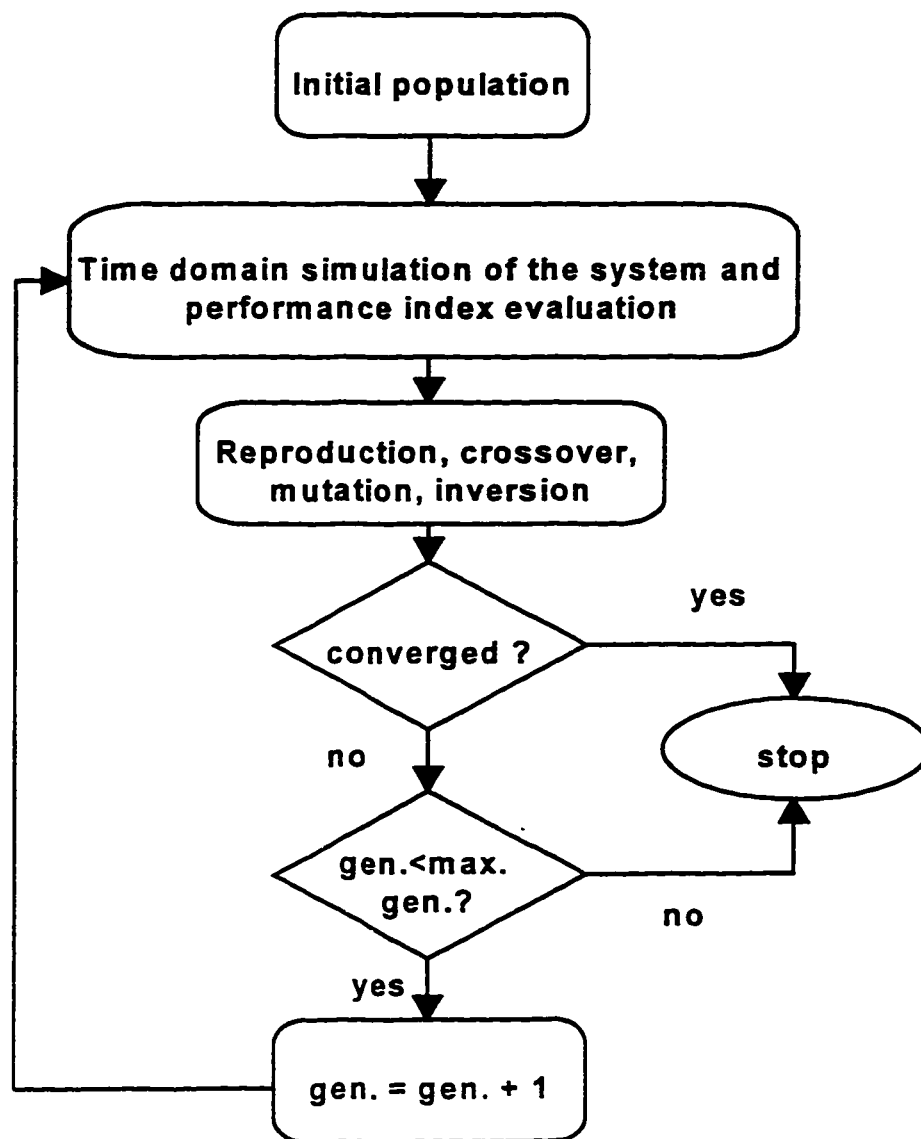
Fig. 7.1 Computational flow chart

7.3 EXAMPLE 1: SINGLE MACHINE SYSTEM

7.3.1 TEST SYSTEM

In this study, the single machine infinite bus system shown in Fig. 3.1 is considered. The system model and parameters are given in Appendix B. In order to investigate the performance of the proposed GPSS, a CPSS has been designed as described in Chapter 5 and a number of studies have been performed. All time domain simulations are carried out using the nonlinear model of the system.

7.3.2 THE PROPOSED GPSS

To design the proposed GPSS, K_c and T_l are coded in a binary string with a length of 14 bits. The first 7 bits represent K_c while the remaining bits represent T_l. GA are applied to find the optimal values of these parameters to minimize the performance index in (7.1). The initial population is generated randomly. Population size, maximum number of generations, and crossover and mutation probabilities are selected after many trials to be 50, 50, 0.75, and 0.001 respectively. It is found that the optimal values of K_c and T_l are 11.24989 and 0.14094 respectively. Fig. 7.2 shows the variations of the performance index with the number of generations.
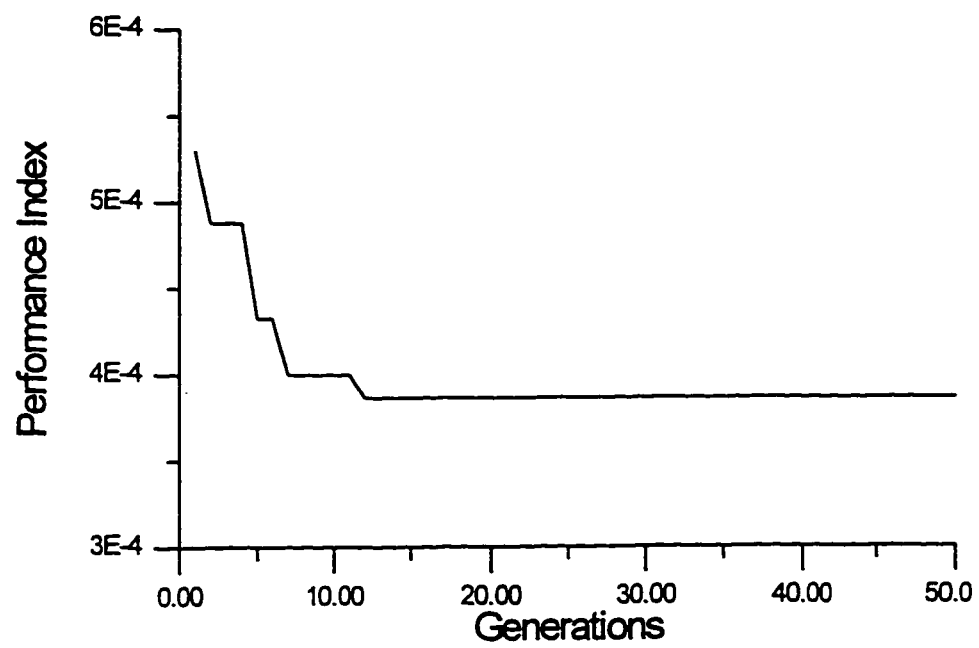
Fig. 7.2 Performance index variations for example 1

7.3.3 SIMULATION RESULTS

To investigate the performance of the proposed GPSS, the following simulation studies have been carried out using the nonlinear model of the system.

7.3.3.1 NOMINAL LOAD TEST

Under the nominal operating conditions specified by P=1.0 pu with 0.85 power factor lagging, a 0.1 pu step increase in mechanical torque was applied at time 1.0 s. The results of this study are shown in Fig. 7.3. It can be seen that GPSS damps out the low frequency oscillations very quickly. The first swing in the torque angle is significantly suppressed which means increasing of stability margin.

Next, a 10% reduction of reference voltage was applied at t=1.0s and removed at t=3.0s. The simulation results are shown in Fig. 7.4. It is clear that the oscillations with GPSS are damped out very quickly .

7.3.3.2 LIGHT LOAD TEST

In this case, the generator operates at a light load condition specified by a power of 0.3 pu with a 0.85 lagging. A 0.4 pu step increase in mechanical torque was applied at t=1.0 s. The results are shown in Fig. 7.5. It can be seen that the GPSS produces much better results and the oscillations are damped out much quicker compared with the CPSS.

This means that the GPSS can provide very good damping over a wide range of operating conditions.

Next, a three phase fault at the generator terminals was applied at t=1.0 s for 130 ms. Fig. 7.6 shows the simulation results of this study. It can be seen that the proposed GPSS minimizes the deviations and improves the system settling time. This is very helpful in the improvement of the disturbance tolerance ability of the system.

7.3.3.3 LEADING POWER FACTOR OPERATION TEST

A 0.4 pu step increase in mechanical torque was applied at t=1.0s while the generator operating at a power of 0.4 pu with a 0.95 power factor leading. The simulation results are shown in Fig. 7.7. It can be concluded that the performance of the GPSS is much better and the oscillations are damped out much quicker.

Another test has been conducted with the generator operating at this condition. That is a local load of admittance of $0.2 - j0.1$ pu has been switched on at t=1.0s. The simulation results are shown in Fig. 7.8. It is seen that the proposed GPSS provides better damping characteristics than CPSS.
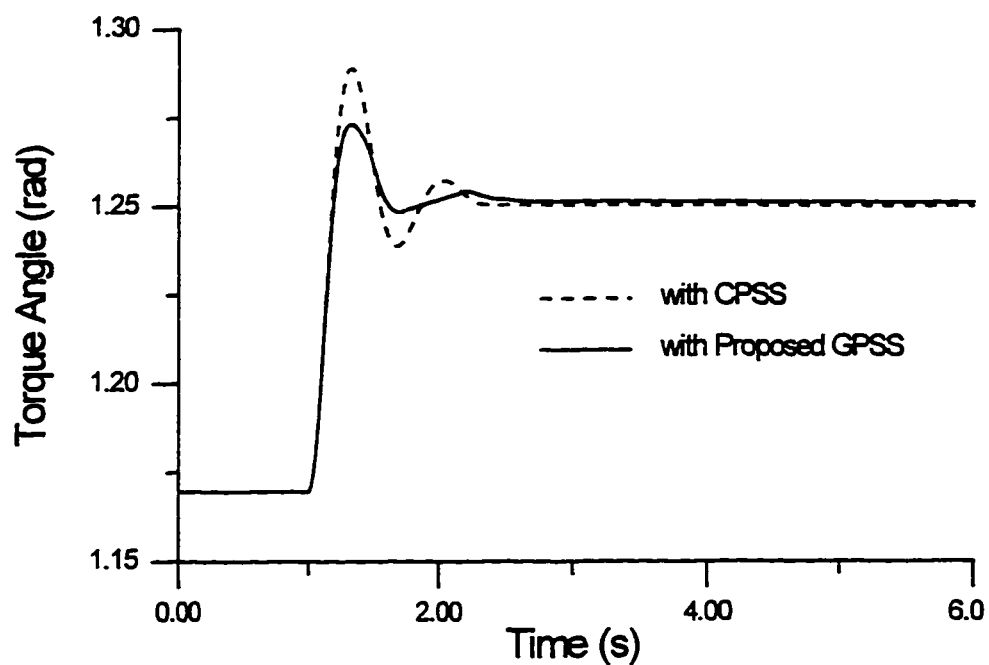
Fig. 7.3 Response to 10% step in torque at nominal operating condition
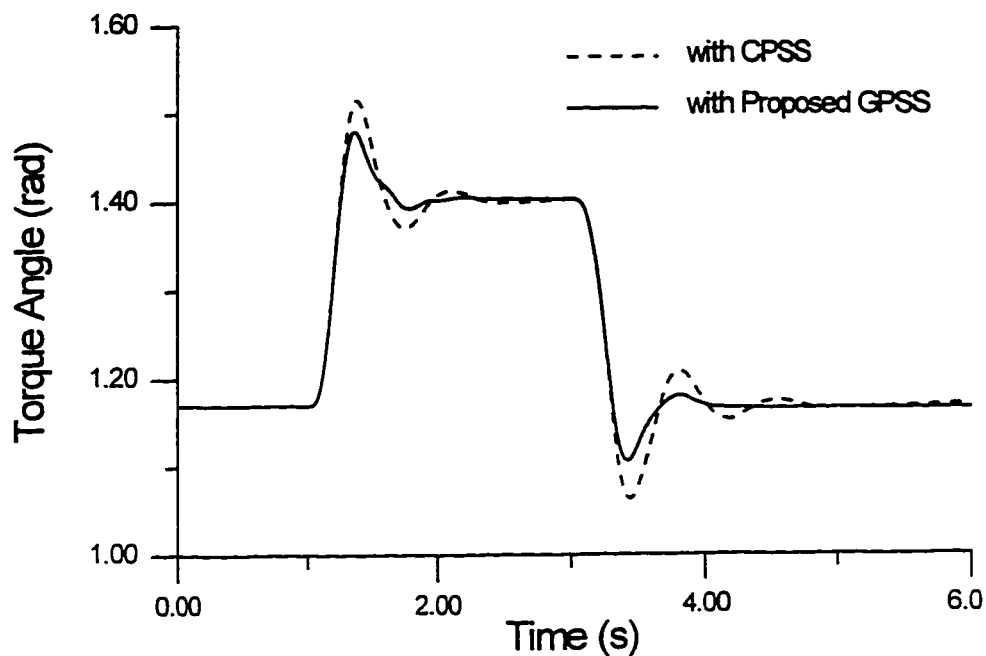
Fig. 7.4 Response to 10% pulse in reference voltage at nominal operating conditions
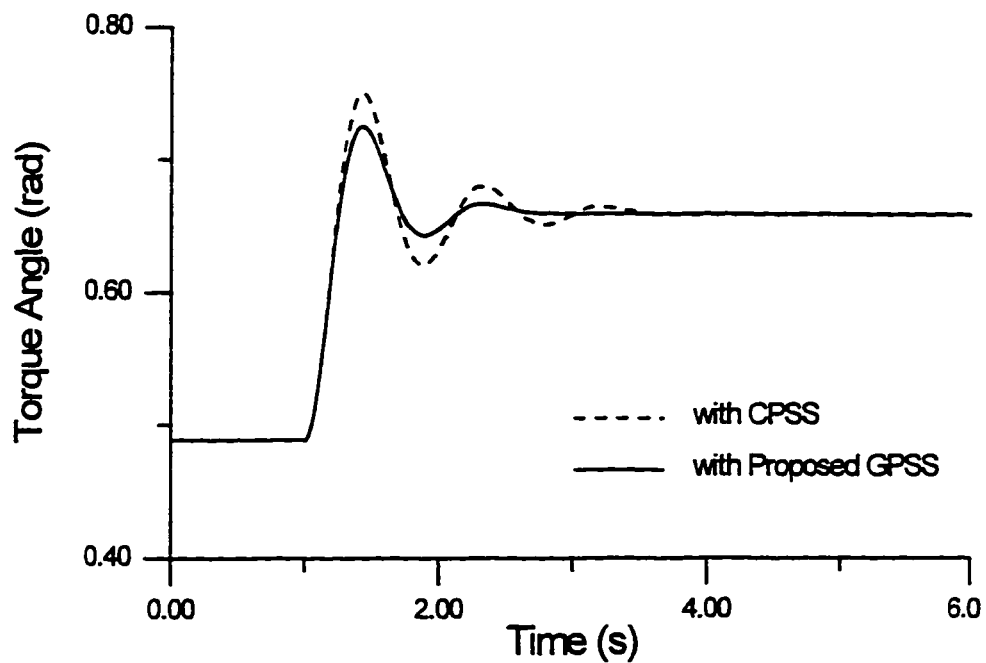
Fig. 7.5 Response to 40% step disturbance in torque at light loading conditions
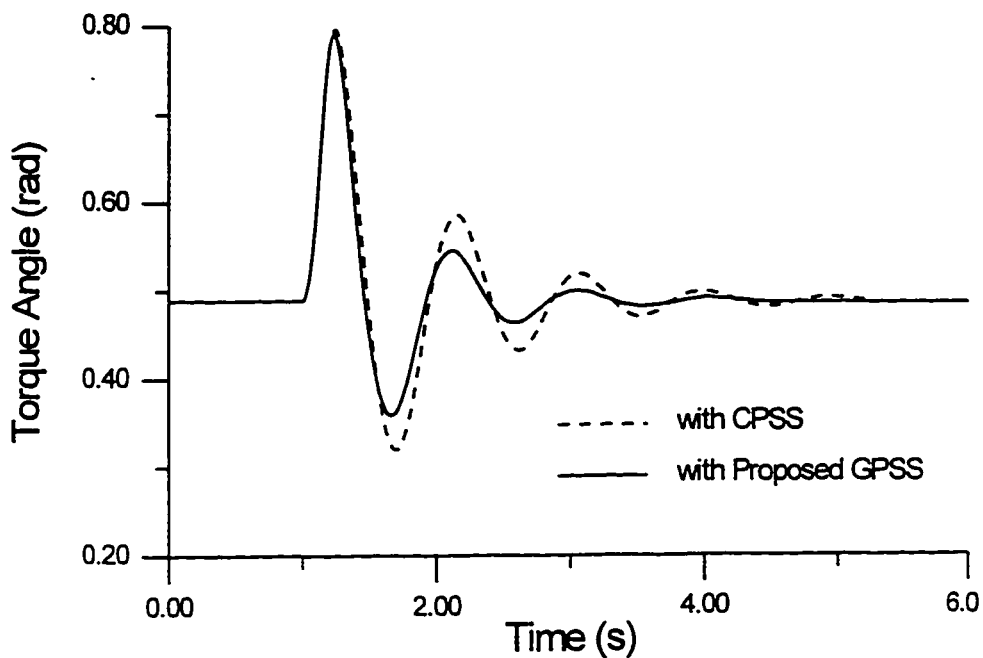
Fig. 7.6 Response to three phase fault disturbance at light loading conditions
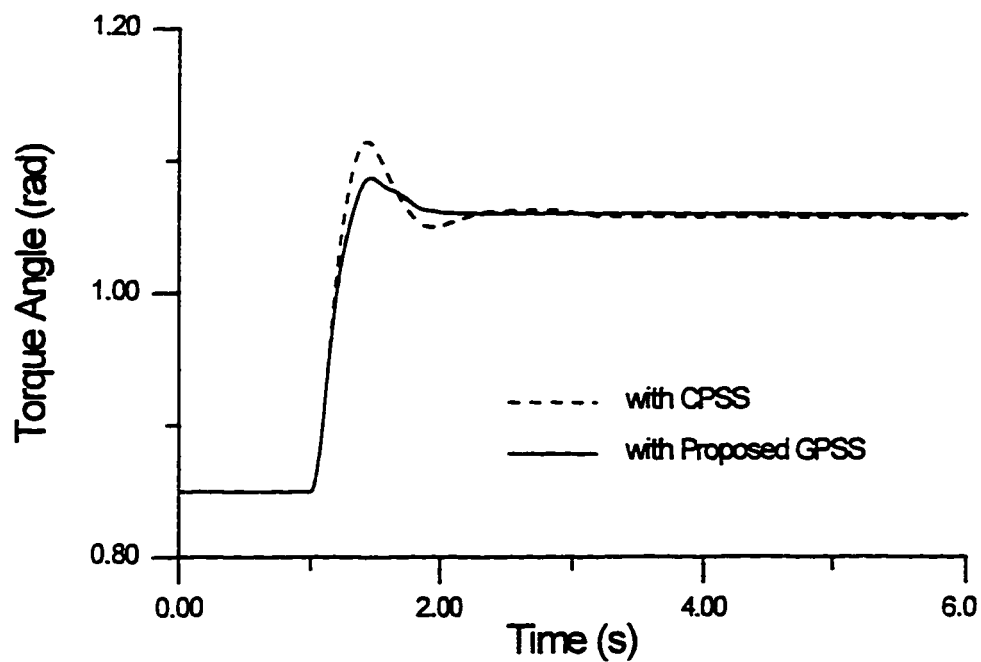
Fig. 7.7 Response to 40% step in torque with leading power factor condition
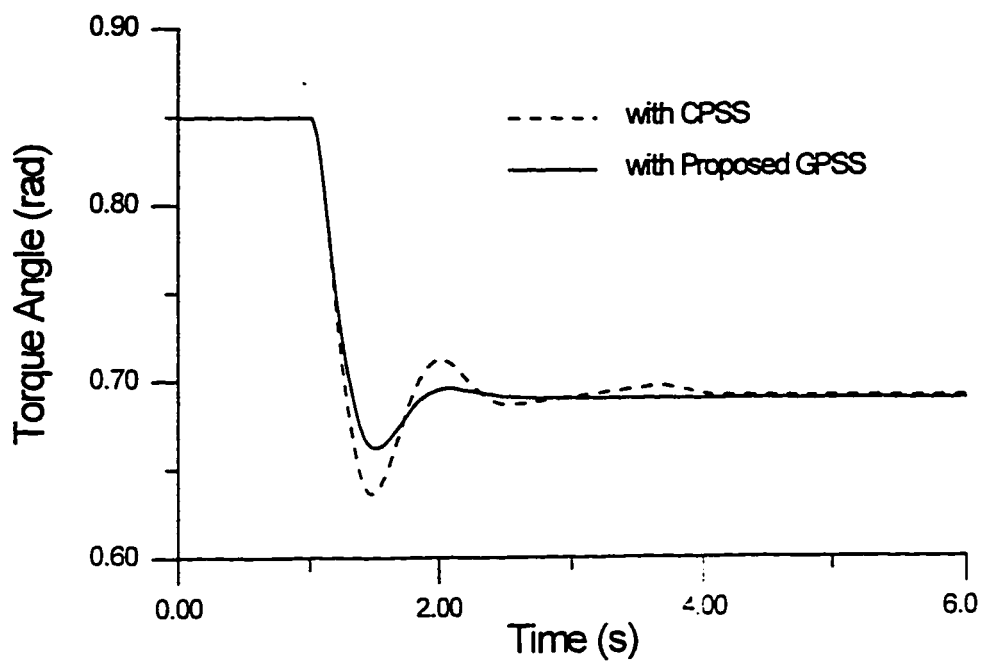
Fig. 7.8 Response to switching on a local load with leading power factor condition

7.4 EXAMPLE 2: MULTIMACHINE SYSTEM

7.4.1 TEST SYSTEM

The nine-bus three-machine power system shown in Fig. 5.7 is considered. Details of the system model and parameters are given in Appendix D. It was found earlier in Chapter 5 that the generators G2 and G3 are the optimum locations for installing PSSs to damp out the electromechanical modes of oscillations. Therefore, the generators G2 and G3 are equipped with two of the proposed GPSS. The performance of the proposed stabilizers was compared to that of CPSSs installed on G2 and G3 with the transfer function given by (5.6)

To demonstrate the capability of the proposed GPSS to enhance system damping over a wide range of operating conditions, the same loading conditions and load admittances given in Tables 5.3 and 5.4 were considered respectively.

7.4.2 THE PROPOSED GPSSs

Two GPSSs are installed on G2 and G3. There are four parameters to be optimized, K_{ci} and T_{Ii}, $i=2,3$. These parameters are coded in a binary string with length of 28 bits, 7 bits for each. GA are applied to find the optimal values of these parameters to minimize the performance index in (7.1). The initial population is generated randomly. Population size, maximum number of generations. and crossover and mutation probabilities are

selected after several trials to be 40, 50, 0.75, and 0.001 respectively. The optimal values of K_{ai} and T_{li} are given in Table 7.1. Fig. 7.9 shows the variations of performance index.

7.4.3 RESULTS AND SIMULATIONS

With each loading condition described in Table 5.3, a three phase fault disturbance at bus 7 was applied. The fault duration was 6 cycles. The simulation results are as follows.

7.4.3.1 NOMINAL LOADING CONDITION

The system response is shown in Fig. 7.10. It is obvious that with the proposed GPSSs, the system returns to its previous operating point much faster than the CPSSs.

7.4.3.2 HEAVY LOADING CONDITION

The simulation results are shown in Fig. 7.11. The results show that the proposed GPSS provides very good damping characteristics over a wide range of operating conditions.

7.4.3.3 LIGHT LOADING CONDITION

The simulation results are shown in Fig. 7.12. It can be seen that the proposed GPSSs produce much better results and the oscillations are damped out much quicker as compared to CPSSs.

TABLE 7.1 The proposed GPSS parameters for example 2

Generator	GPSS Parameters	
	K_c	T_I
G2	5.9491	0.4540
G3	3.7182	0.3444
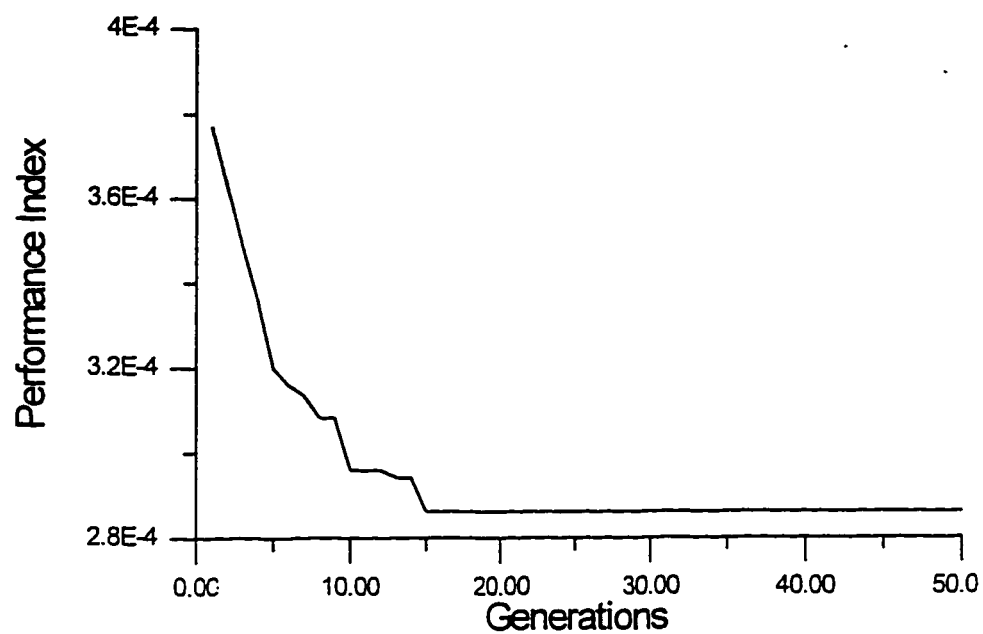
Fig. 7.9 Performance index variations for example 2
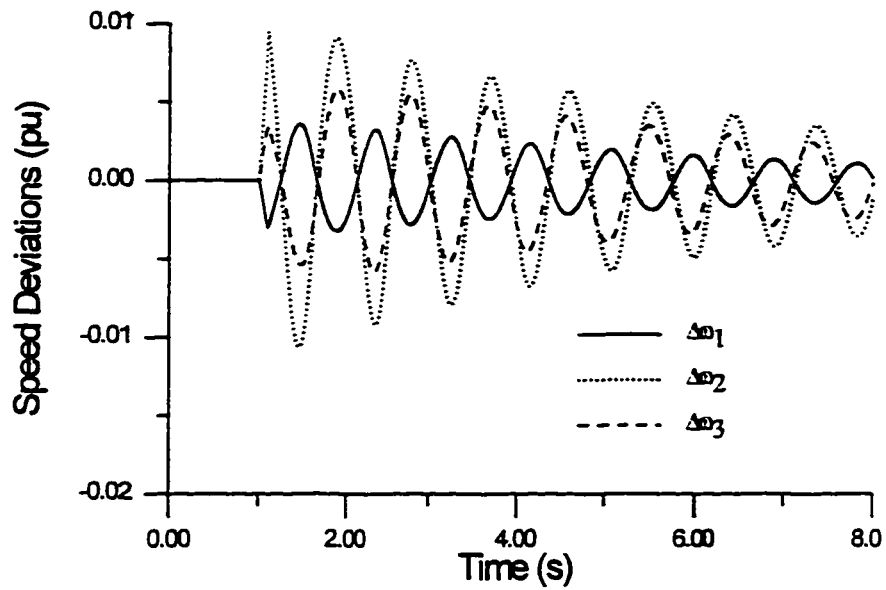
(a)
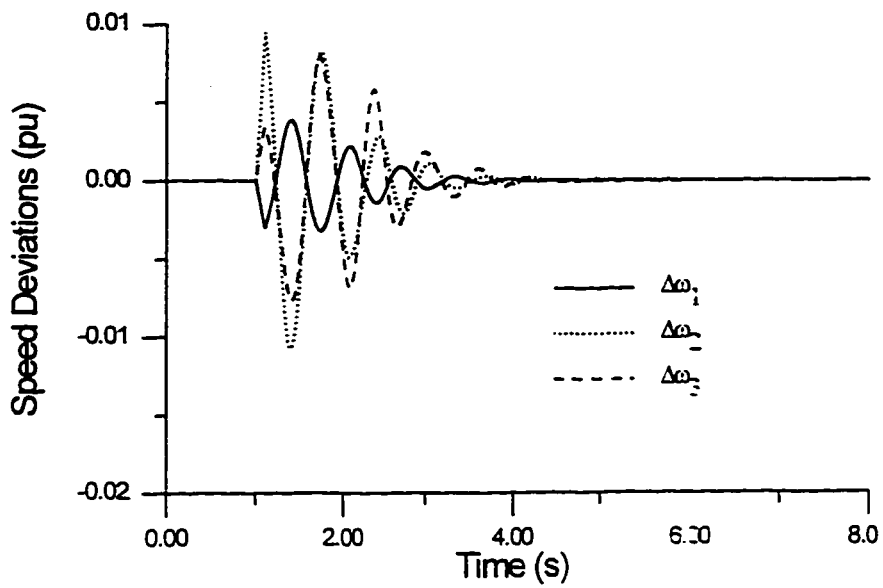
(b)

Fig. 7.10 Response to a three phase fault disturbance at nor̄mal loading condition.

(a) CPSS
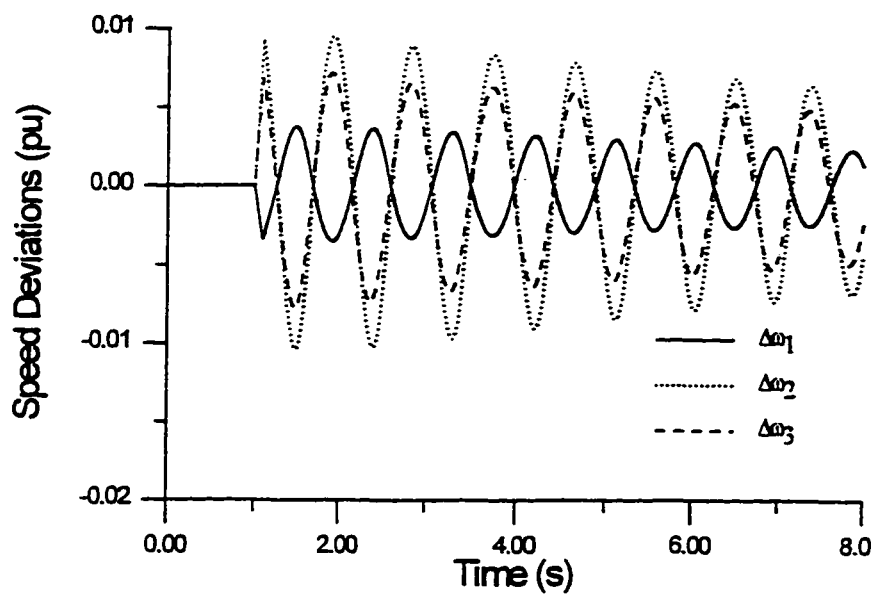
(b) Proposed GPSS

(a)
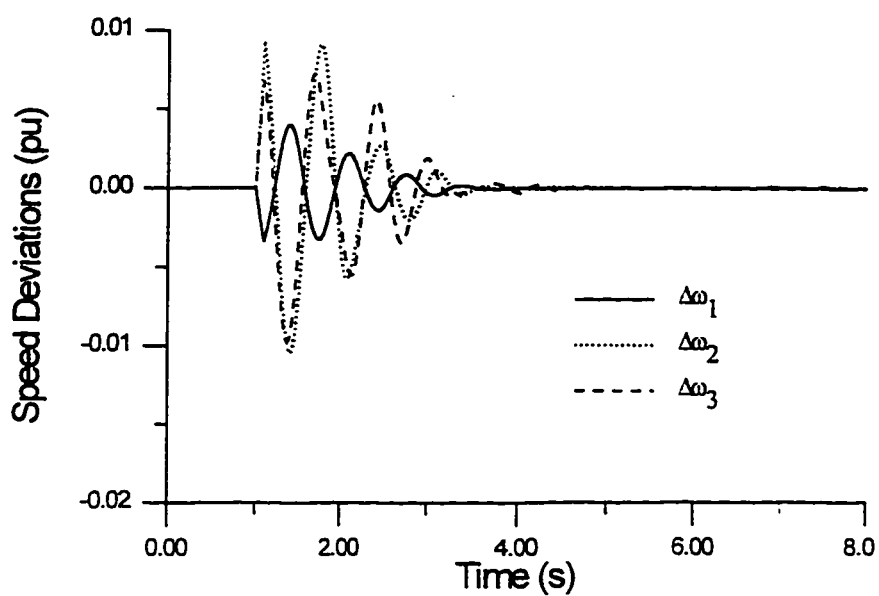
(b)

Fig. 7.11 Response to a three phase fault disturbance at heavy loading condition.
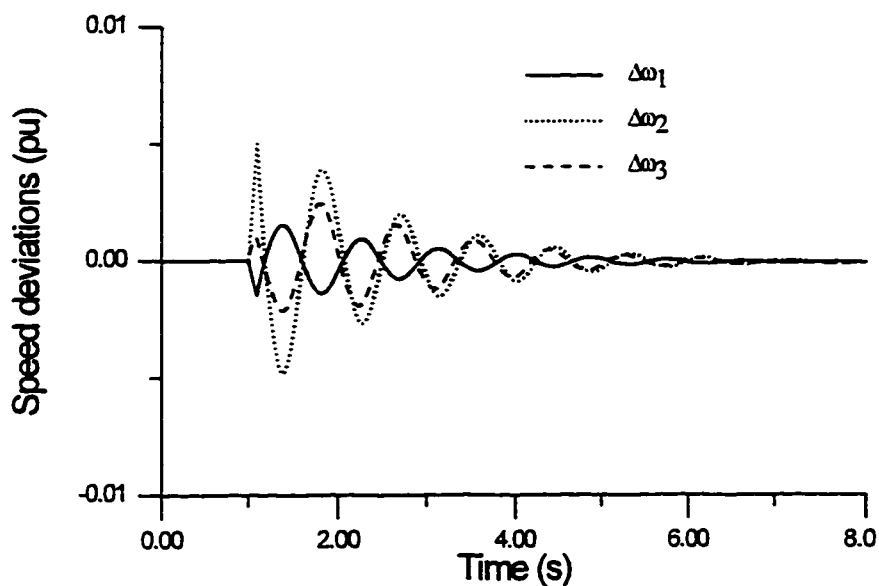
(a) CPSS
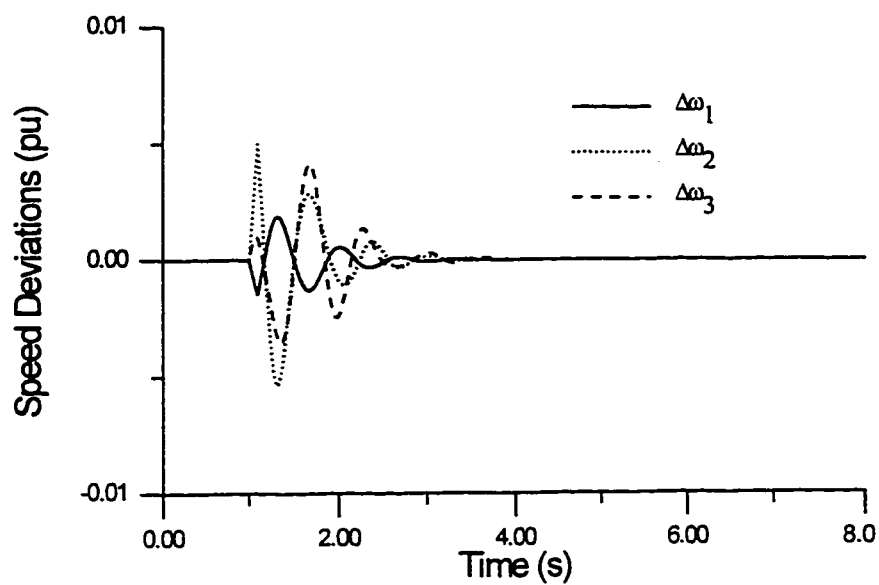
(b) Proposed GPSS

Fig. 7.12 Response to a three phase fault disturbance at light loading condition.

(a) CPSS

(b) Proposed GPSS

7.5 COORDINATION BETWEEN GPSS AND CPSS

In most situations, the newly PSSs may replace a part of the existing stabilizers. In this case, the newly installed GPSSs will have to work together with CPSSs which already exist in a power system. In this section, system response with the proposed GPSSs and CPSSs working together has been also investigated. For the three-machine nine-bus system considered in example 2, the proposed GPSS was installed on G2 with a CPSS set on G3. The system response to a 6-cycle three phase fault at bus 7 for different loading conditions is shown in Fig. 7.13. It can be seen that the two types of PSSs can work cooperatively. The response with the proposed GPSS and CPSS combination is better than the response with only CPSSs on G2 and G3 in the corresponding Figs. 7.10-a, 7.11-a, and 7.12-a.

7.6 SUMMARY

In this chapter, GA has been used to search for optimal parameter settings of conventional lead-lag PSSs. The proposed approach avoids the linearization process required to design such stabilizers. The proposed GPSS has been tested in a single machine and in a multimachine power system environments. The coordination of the proposed GPSS with the existing CPSS has been also discussed. The results show that the system performance with the proposed GPSS is greatly improved and the low frequency oscillations are damped out much quicker than CPSSs. In addition, the proposed GPSS can operate cooperatively with the existing conventional control schemes.

It has been acknowledged that the damping characteristics of rule-based PSSs are much better than those of fixed-parameter stabilizers. However, the design process of these stabilizers is a time-consuming task since their parameters are optimized iteratively. To alleviate such problems of the traditional rule-based stabilizers design, GA will be incorporated in the design process of these stabilizers in the next chapter.
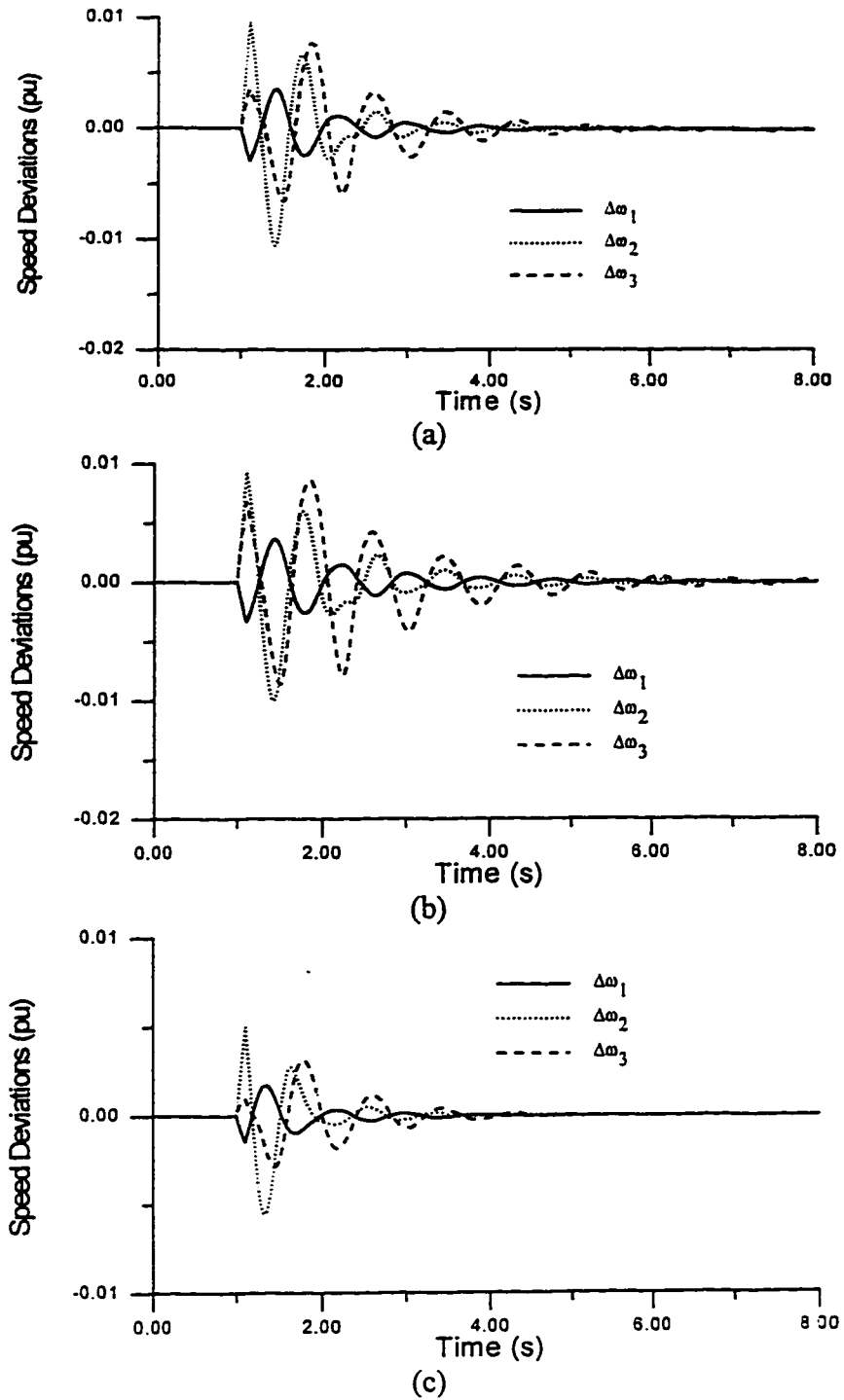
Fig. 7.13 System response with the proposed GPSS on G2 and CPSS on G3

(a) Nominal loading condition

(b) Heavy loading condition

(c) Light loading condition

CHAPTER 8

HYBRID GENETIC RULE-BASED PSSs

8.1 INTRODUCTION

Recently, rule-based power system stabilizers (RBPSSs) have been proposed and investigated [108-109]. RBPSSs appear to be suitable stabilizers due to their lower computation burden and robustness. Unlike the most conventional methods, an explicit mathematical model of the system dynamics is not required to design a good RBPSS which makes it more suitable for on-line computer control. In addition, RBPSSs can be easily set up and implemented using a microcomputer with A/D and D/A converters [108-109].

Although RBPSSs showed promising results, they are subjective and somewhat heuristic. In addition, their parameter settings are done either iteratively, by trial-and-error, or by human experts. That makes the design of such stabilizers a laborious and time-consuming task.

In this chapter, we propose an approach to integrate the use of GA and rule-based systems in order to combine their different strengths, overcome the difficulties in RBPSSs design, and efficiently tune the control rules. The proposed genetic based RBPSS (GRBPSS) show that the performance of the RBPSS can be improved significantly by incorporating a genetic-based optimizing mechanism.

8.2 DESIGN OF RULE-BASED STABILIZERS

The supplementary stabilizing signal u is added to the excitation loop as shown in Fig. 8.1. At time t, the stabilizing signal $u(t)$ is given by

$$u(t) = U(k) \qquad , kT < t < (k+1)T \qquad (8.1)$$

where k is an integer and T is the sampling period. The value of $U(k)$ is determined at each sampling time based on the operating state. At time kT, the operating state is specified by speed deviation $\Delta\omega(k)$ and acceleration $A(k)$ where

$$A(k) = [\ \Delta\omega(k) - \Delta\omega(k-1)\ ] / T \qquad (8.2)$$

The operating state is given by the point $z(k)$ in the phase plane as shown in Fig. 8.2, where

$$z(k) = (\Delta\omega(k)\ , A(k)\ ) \qquad (8.3)$$

Define $R(k)$ and $\alpha(k)$ as

$$R(k\ =\ z(k)\ | \qquad (8.4)$$
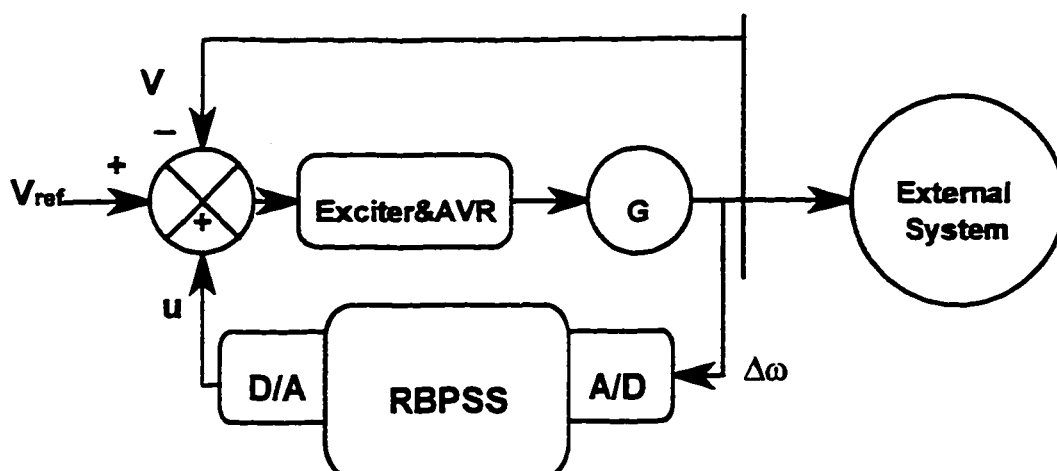
Fig. 8.1 Study system configuration
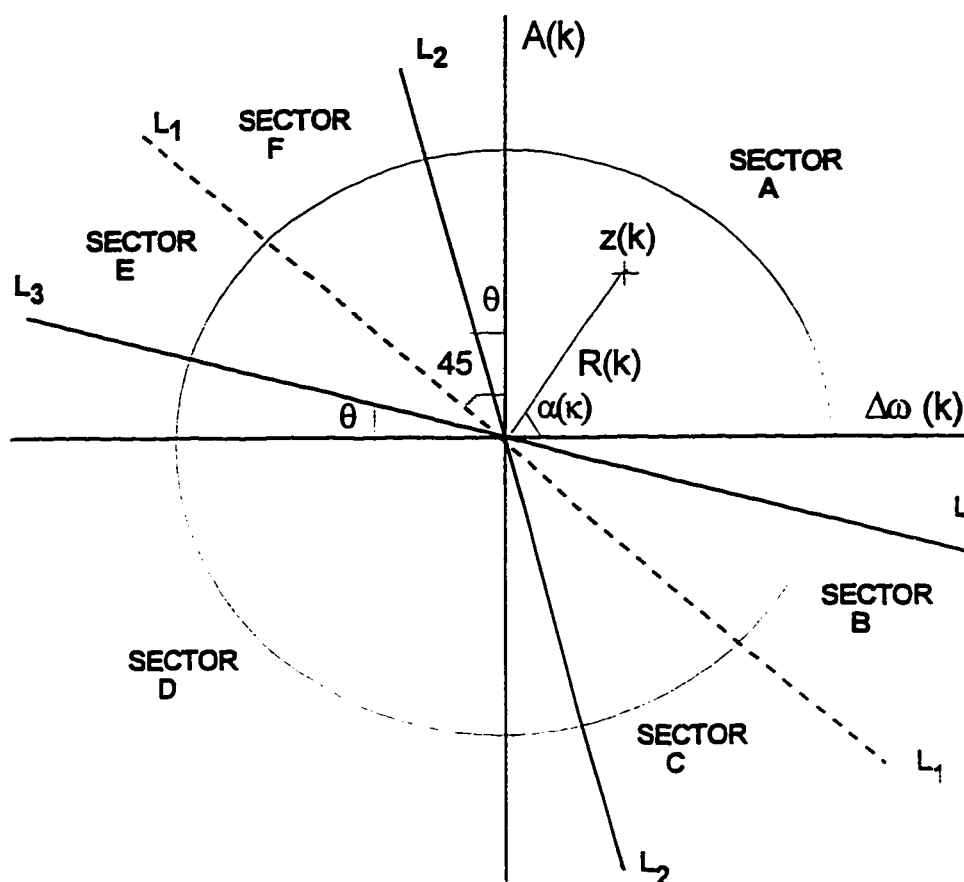
Fig. 8.2 Operating state in the phase plane

and,

$$\alpha(k) = \tan^{-1}(A(k) / \Delta\omega(k))$$

(8.5)

The phase plane is divided into six sectors by three switching lines L_1, L_2, and L_3 as shown in Fig. 8.2. Each sector has its own control rule as follows [108]:

Rule 1: If $z(k) \in$ sector A, then $U(k) = G(k)U_{max}$

(8.6)

Rule 2: If $z(k) \in$ sector B, then $U(k) = G(k)U_{min}$

(8.7)

Rule 3: If $z(k) \in$ sector C, then $U(k) = -G(k)U_{min}$

(8.8)

Rule 4: If $z(k) \in$ sector D, then $U(k) = -G(k)U_{max}$

(8.9)

Rule 5: If $z(k) \in$ sector E, then $U(k) = -G(k)U_{min}$

(8.10)

Rule 6: If $z(k) \in$ sector F, then $U(k) = G(k)U_{min}$

(8.11)

where U_{max} and U_{min} are the maximum and minimum values of the control signal respectively. $G(k)$ is the gain factor which is given by a nonlinear function as follows:

$$G(k) = \begin{cases} R(k)/D_r, & \forall R(k) \le D_r \\ 1.0 & \forall R(k) > D_r \end{cases}$$

(8.12)

where D_r is an adjustable real value. The switching line L_1 is assumed to be fixed while L_2 and L_3 are located θ degrees apart from vertical and horizontal axes respectively. The maximum value of control signal U_{max} depends on the generating unit and assumed to be known [109]. Therefore, the adjustable parameters are θ, D_r, and U_{min}. For the optimal settings of these parameters, a quadratic performance index J is considered:

$$J = \sum_{j=1}^{NM} \sum_{k=1}^{N} [kT \Delta\omega_j(k)]^2$$

(8.13)

where NM is the number of machines and N is the total data number. In the above index, the speed deviation of jth machine $\Delta\omega_j(k)$ is weighted by the respective time kT. The tuning parameters are adjusted so as to minimize the performance index J.

8.3 DESIGN OF THE PROPOSED STABILIZER

The RBPSS adjustable parameters are usually optimized to minimize the performance index in (8.13) one at a time [108-109]. Therefore, the optimization process becomes a laborious, tedious, and time consuming task. Moreover, the interaction between parameters has not been taken into consideration. The proposed approach employs GA for optimum settings of the adjustable parameters. At first, the adjustable parameters are coded in a binary string and the initial population is generated randomly. The design steps of the proposed GRBPSS can be summarized in the flow chart shown in Fig. 8.3.

8.4. EXAMPLE 1: SINGLE MACHINE SYSTEM

8.4.1 TEST SYSTEM AND OPERATING CONDITIONS

In this study, the single machine infinite bus system shown in Fig. 8.1 is considered. The system model and parameters are given in Appendix E. Three different operating conditions are used in simulations to cover a wide range of operating conditions. These operating conditions are given in Table 8.1.
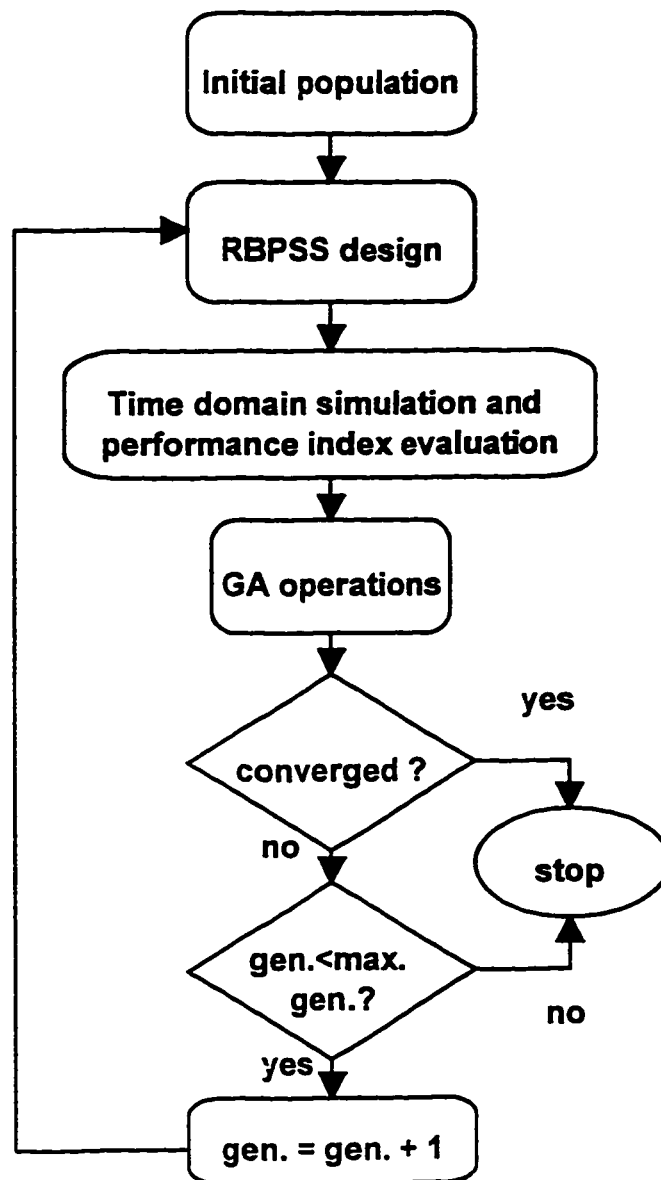
Fig. 8.3 The proposed GRBPSS computational flow chart

TABLE 8.1 Operating conditions for example 1

Operating Conditions	P (pu)	Q (pu)
(P_1, Q_1)	1.1	0.4
(P_2, Q_2)	0.4	0.2
(P_3, Q_3)	0.7	-0.2

8.4.2 PARAMETER SETTINGS

The proposed approach has been applied to search for optimal settings of the tuning parameters θ, D_r, and U_{min}. Population size, maximum number of generations, and crossover and mutation probabilities are selected after several trials to be 30, 100, 0.75, and 0.001 respectively. The final values of the tuning parameters are given in Table 8.2. Fig. 8.4 shows the convergence rate of the performance index J with the number of generations.

TABLE 8.2 The proposed GRBPSS parameter settings for example 1

θ (rad)	D_r	U_{min} (pu)
0.1242	10.1	0.0945
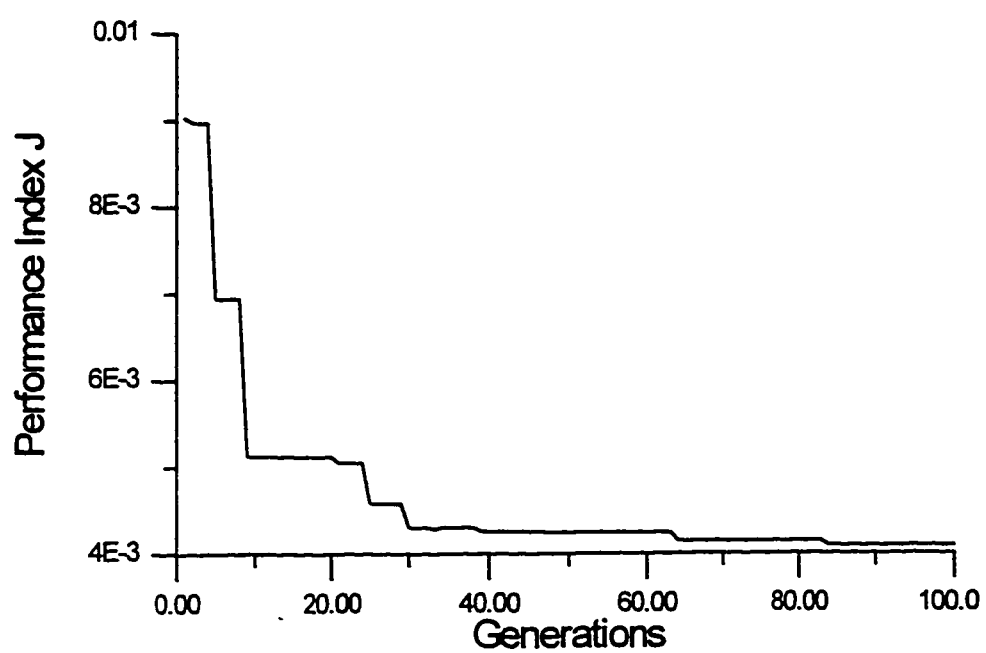
Fig. 8.4 Variations of performance index J for example 1

8.4.3 SIMULATION RESULTS

A number of studies have been performed with the proposed GRBPSS. The performance of the proposed GRBPSS is compared to those of the RBPSS [108] and the CPSS [94] with a transfer function given by

$$u = 7.091(\frac{3s}{1+3s})(\frac{1+0.685s}{1+0.1s}) \Delta\omega \qquad (8.14)$$

8.4.3.1 OPERATING CONDITION (P_1, Q_1)

The system performance with a 10% step increase in input torque is shown in Fig. 8.5. Fig. 8.6 shows the simulation results with a three phase fault disturbances at the infinite bus for 0.1s. The results with a 10% pulse in reference voltage for 2s are shown in Fig. 8.7. It is obvious that, the system performance with the proposed GRBPSS is the best in the sense that the first swing in the torque angle is significantly suppressed. This is very helpful in the improvement of the disturbance tolerance ability of the system.

8.4.3.2 OPERATING CONDITION (P_2, Q_2)

A 40% step increase in input torque and a 0.1s three phase fault at infinite bus disturbances were applied. The simulation results are shown in Figs. 8.8 and 8.9

respectively. The results show the capability of the proposed GRBPSS to damp out the oscillations and work properly over a wide range of operating conditions.

8.4.3.3 OPERATING CONDITION (P_3, Q_3)

A 30% step increase in input torque and a 0.1s three phase fault at infinite bus disturbances were applied. The simulation results are shown in Figs. 8.10 and 8.11 respectively. It can be concluded that the proposed GRBPSS provides good damping characteristics to system oscillations.
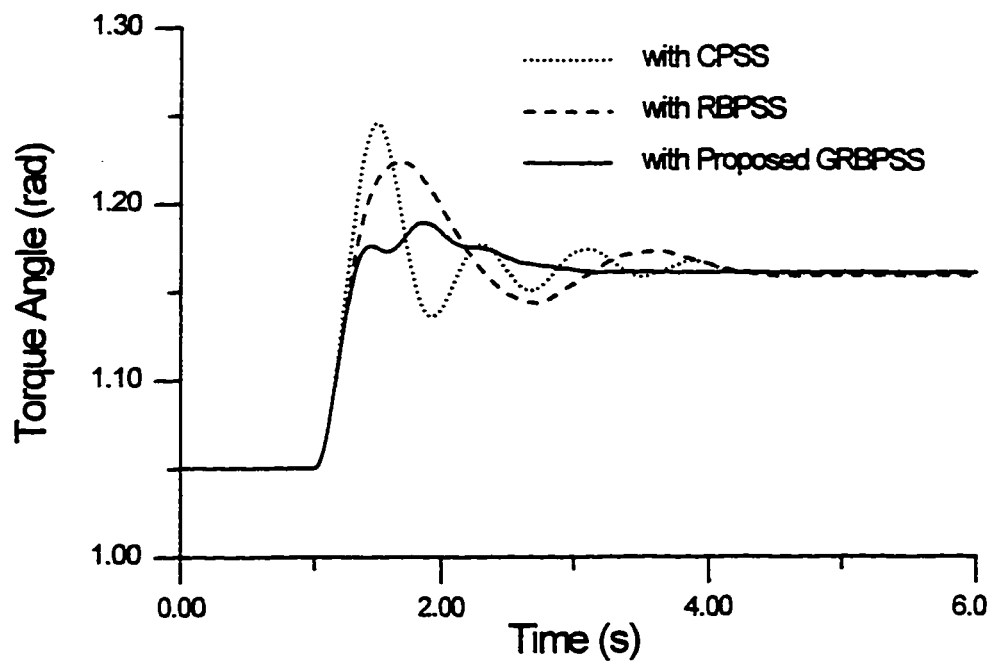
Fig. 8.5 Response to 10% step in torque for operating condition (P_1, Q_1)
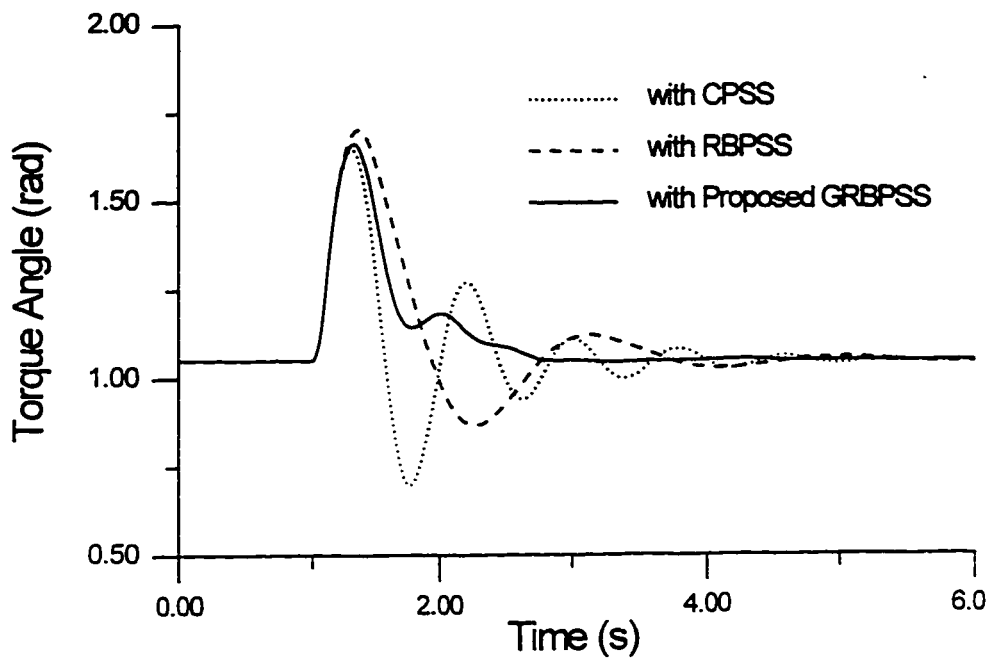
Fig. 8.6 Response to three phase fault for operating condition (P_1, Q_1)
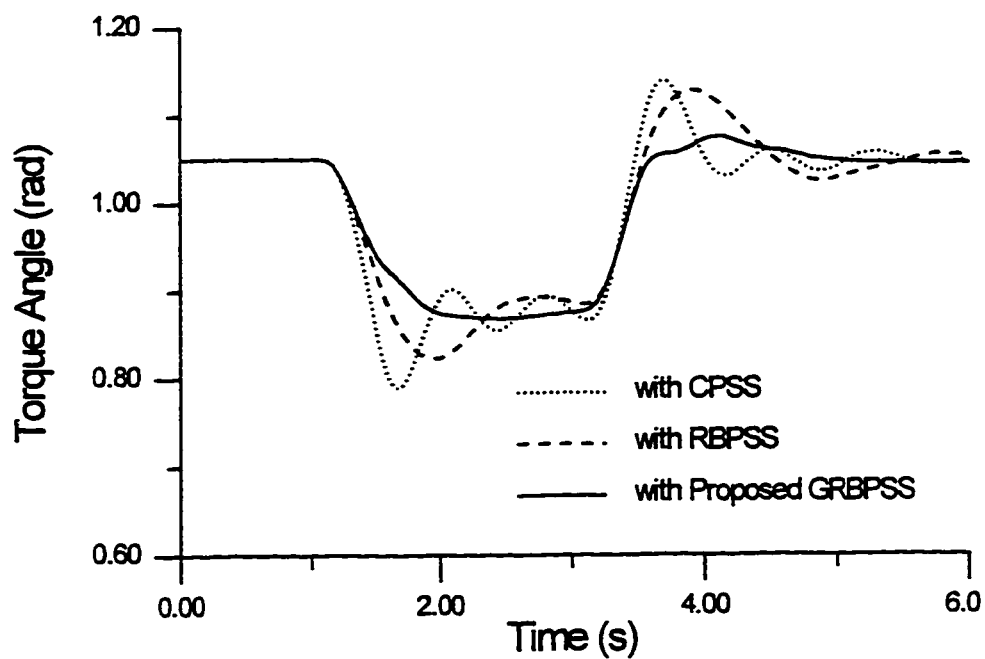
Fig. 8.7 Response to 10% pulse in reference voltage for operating condition (P_1, Q_1)
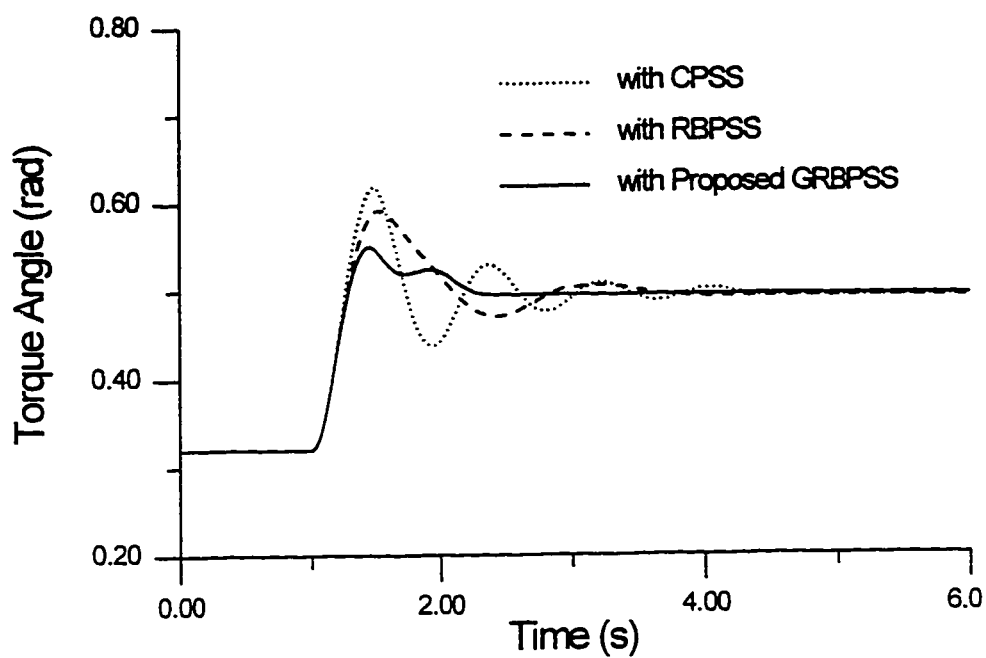
Fig. 8.8 Response to 40% pulse in torque for operating condition (P_2, Q_2)
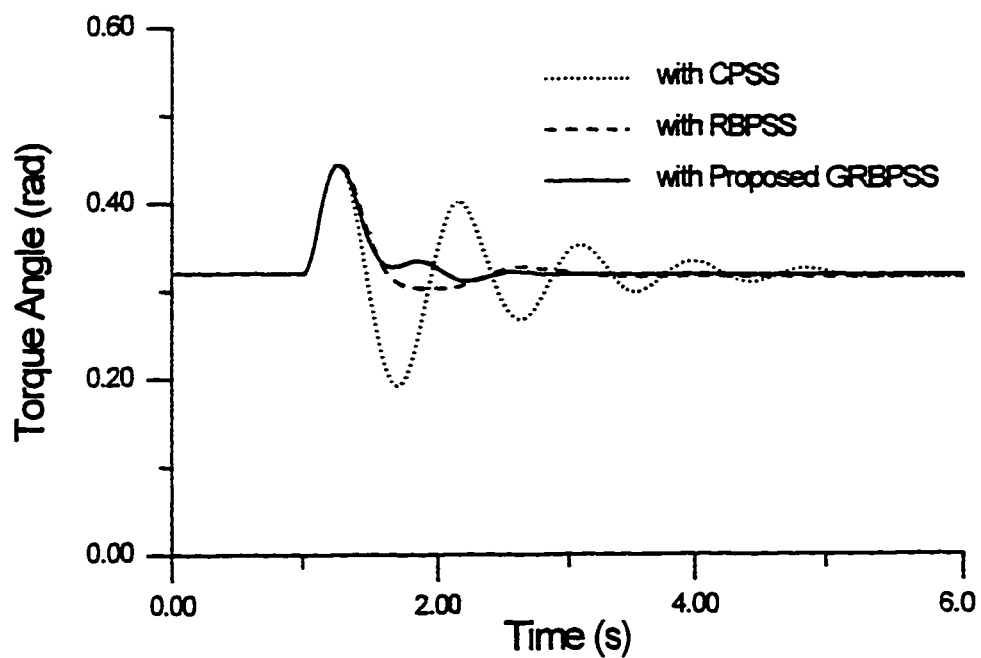
Fig. 8.9 Response to three phase fault for operating condition (P_2, Q_2)
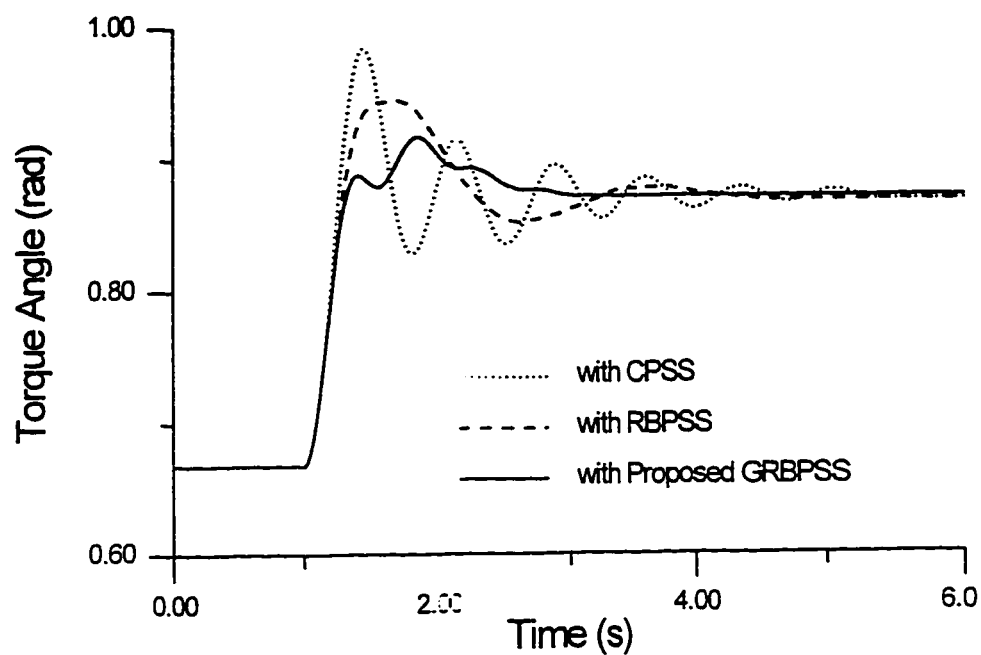
Fig. 8.10 Response to 30% step in torque for operating condition (P_3, Q_3)
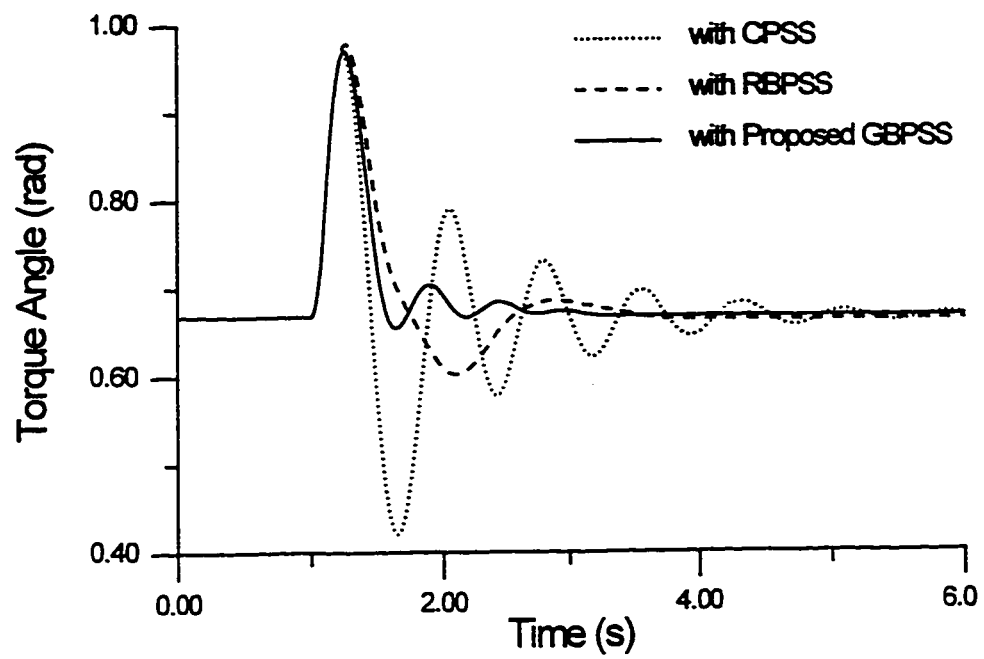
Fig. 8.11 Response to three phase fault for operating condition (P_3, Q_3)

8.5 EXAMPLE 2: 3-MACHINE 9-BUS SYSTEM

8.5.1 PARAMETER SETTINGS

In this study, the nine-bus three-machine power system shown in Fig. 5.7 was considered. It was shown in Chapter 5 that two stabilizers are enough to damp out the electromechanical modes of oscillations. Therefore, we proposed two GRBPSSs installed on G2 and G3. However, for the sake of comparison with the RBPSSs developed in [109], the case of three installed stabilizers was also considered. GA have been applied to search for optimal settings of the proposed GRBPSS parameters. Population size, maximum number of generations, and crossover and mutation probabilities are selected to be 40, 60, 0.75, and 0.001 respectively. The final values of the tuning parameters in both cases of two and three installed stabilizers are given in Table 8.3. Fig. 8.12 shows the convergence rate of the performance index J with the number of generations.

8.5.2 SIMULATION RESULTS

To demonstrate the capability of the proposed GRBPSS to enhance system damping over a wide range of operating conditions, various loading conditions, as given in Table 5.3, were considered. The system performances with two GRBPSSs and three GRBPSSs are compared with that of RBPSS [109]. A 6-cycle three phase fault at bus 7 was applied as follows.
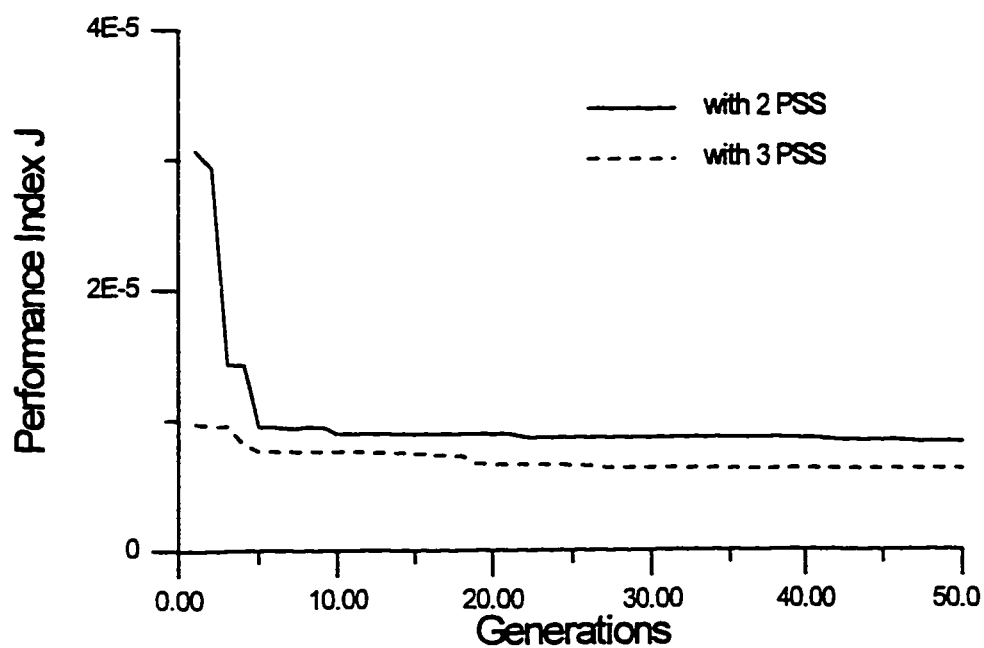
Fig. 8.12 Variations of performance index J for example 2

TABLE 8.3 The proposed GRBPSS parameter settings for example 2

No. of GRBPSSs	Location	θ (rad)	D_r	U_{min} (pu)
Two	G2	-0.1213	7.5597	0.0283
	G3	0.0110	20.000	0.1197
	G1	0.0079	10.079	0.1984
Three	G2	-0.0110	17.795	0.0173
	G3	0.0551	18.853	0.0110

8.5.2.1 NOMINAL LOADING CONDITION

The dynamic response of the system is shown in Fig. 8.13. It is obvious that the system performance with two of the proposed GRBPSSs is much better than its performance with three of RBPSSs and the oscillations are damped out much quicker. However, the system performance is further improved using three of the proposed GRBPSSs and the system returns to its initial state much faster.

8.5.2.2 HEAVY LOADING CONDITION

Fig. 8.14 shows the simulation results in this case. The results here show that the settling times of the speed deviations of all units are much reduced confirming the superiority of the proposed GRBPSS to RBPSS.

8.5.2.3 LIGHT LOADING CONDITION

The simulation results are shown in Fig. 8.15. The results show clearly that the proposed GRBPSS provides very good damping characteristics over a wide range of operating conditions.
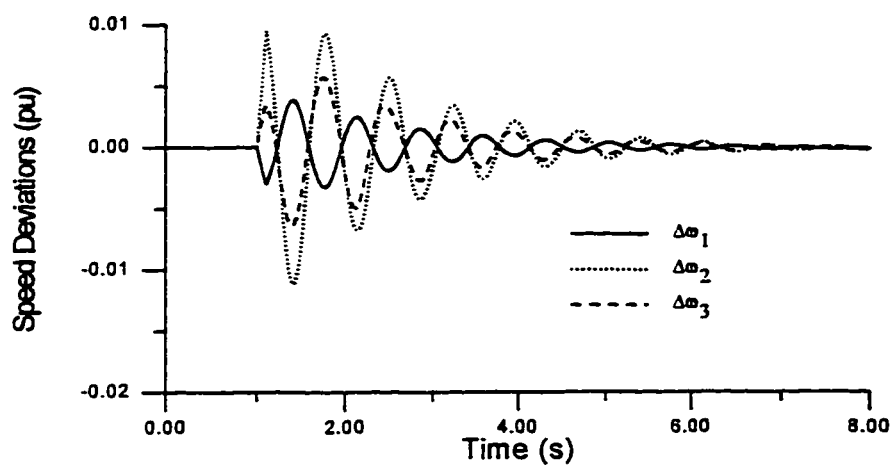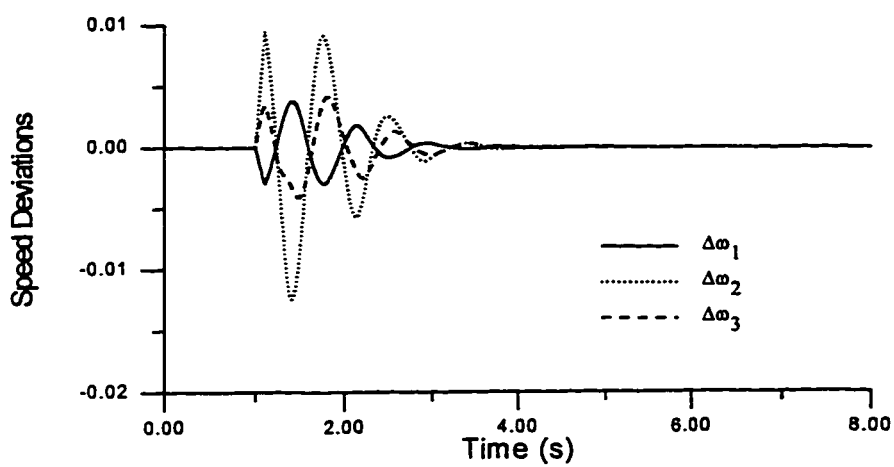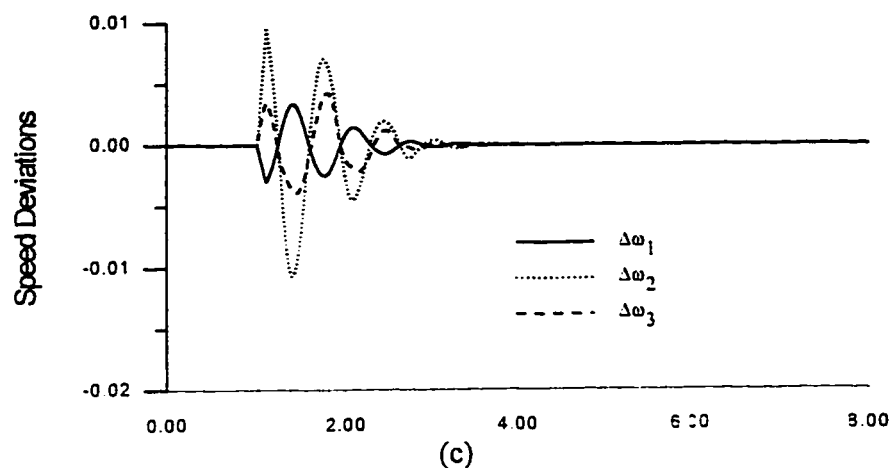
Fig. 8.13 System response with nominal operating condition

(a) with RBPSSs

(b) with two of the proposed GRBPSSs

(c) with three of the proposed GRBPSSs
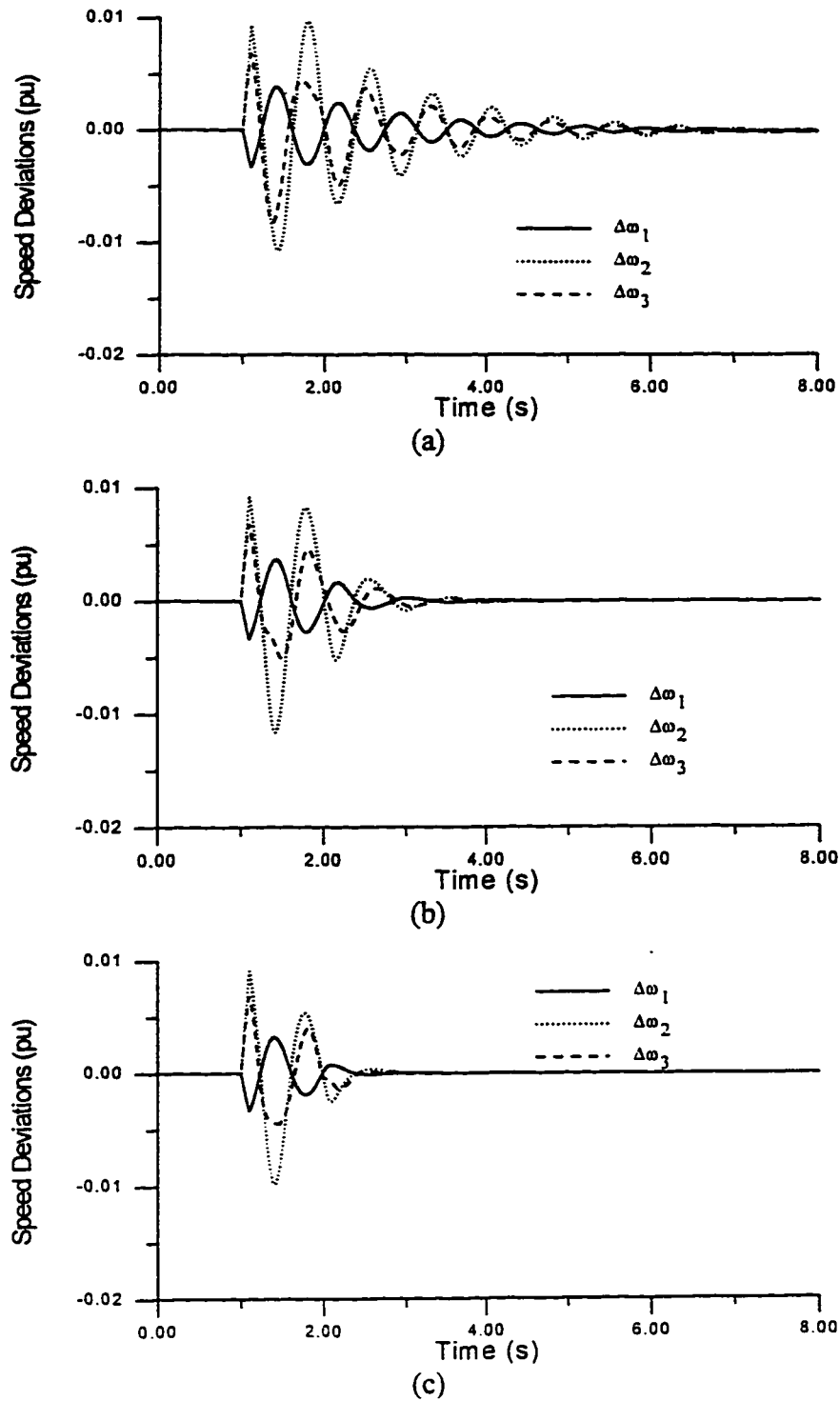
Fig. 8.14 System response with heavy loading condition

(a) with RBPSSs

(b) with two of the proposed GRBPSSs

(c) with three of the proposed GRBPSSs
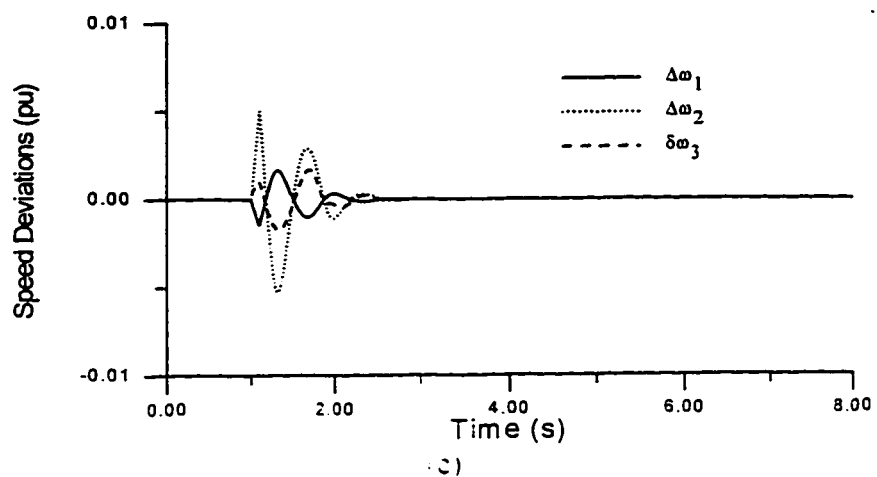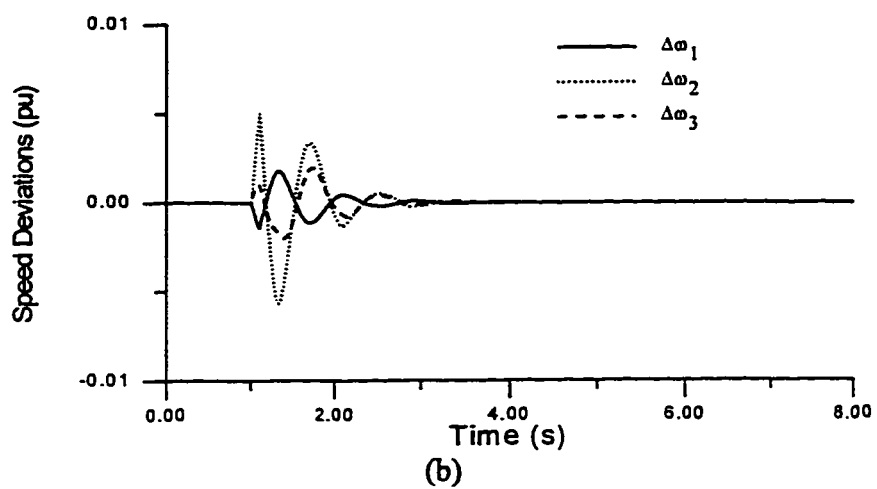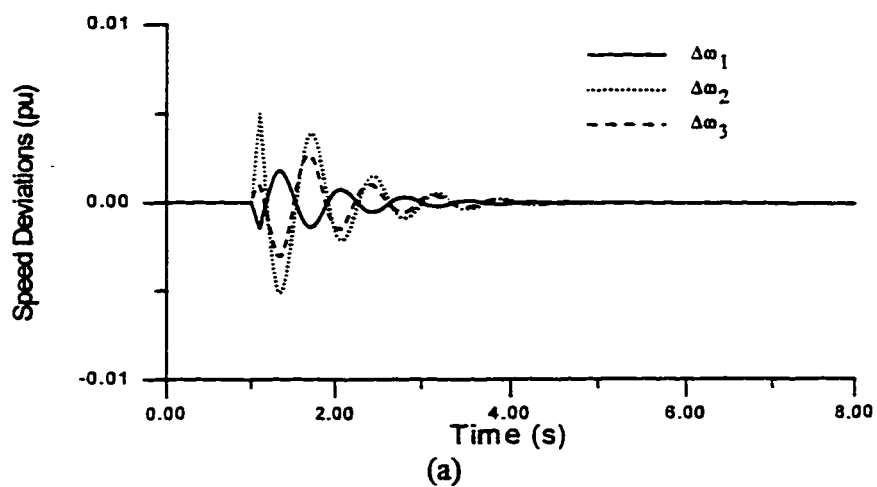
Fig. 8.15 System response with light loading condition

(a) with RBPSSs

(b) with two of the proposed GRBPSSs

(c) with three of the proposed GRBPSSs

8.6 EXAMPLE 3: NEW ENGLAND SYSTEM

8.6.1 SYSTEM DESCRIPTION

In this study, the 10-machine 39-bus New England power system shown in Fig. 8.16 was considered [80,85]. Each machine has been represented by a fourth order two-axis nonlinear model. Generator G1 is an equivalent power source representing parts of the U.S.-Canadian interconnection system. Details of the system data are given in Appendix F. In this study, the following disturbances are considered for the simulations:

(a) Three phase fault for 0.10s at bus 29 at the end of line 26-29.

(b) Three phase fault for 0.15s at bus 15 at the end of line 14-15.

Without PSSs, the system responses due to the above disturbances are shown in Figs. 8.17 and 8.18 respectively. It is observed that the system damping is very poor and the system is highly oscillatory. Therefore, it is necessary to install stabilizers in order to have good dynamic performance. To identify the optimum locations of PSSs, the participation factor method [80] and the sensitivity of PSS effect (SPE) method [81] were used. The results of both methods indicate that the generators G5, G7, and G9 are the optimum locations for installing PSSs to damp out the electromechanical modes of oscillations. Therefore, these generators are equipped with three of the proposed GRBPSSs.
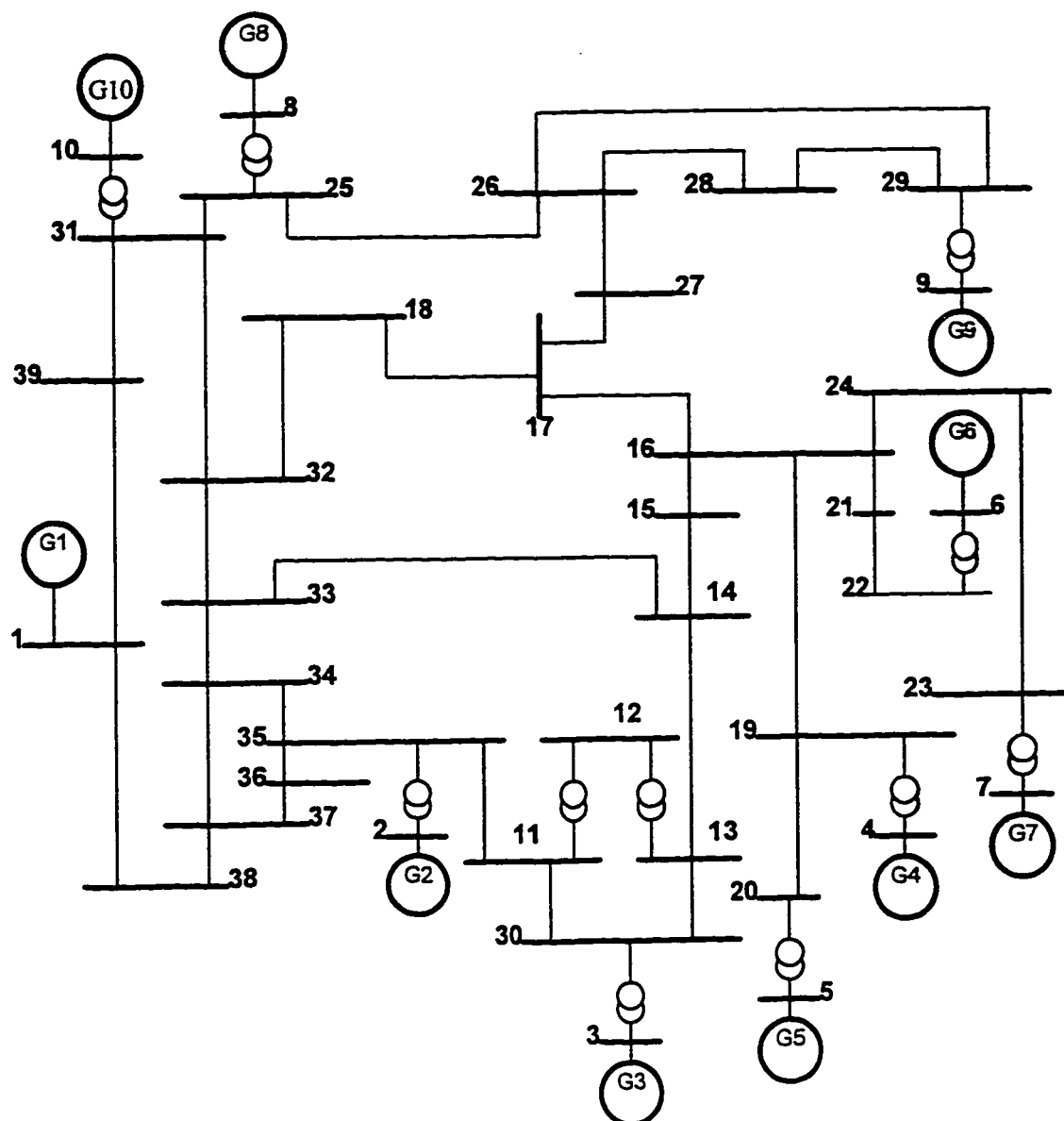
Fig. 8.16 Single line diagram of the New England system [85]
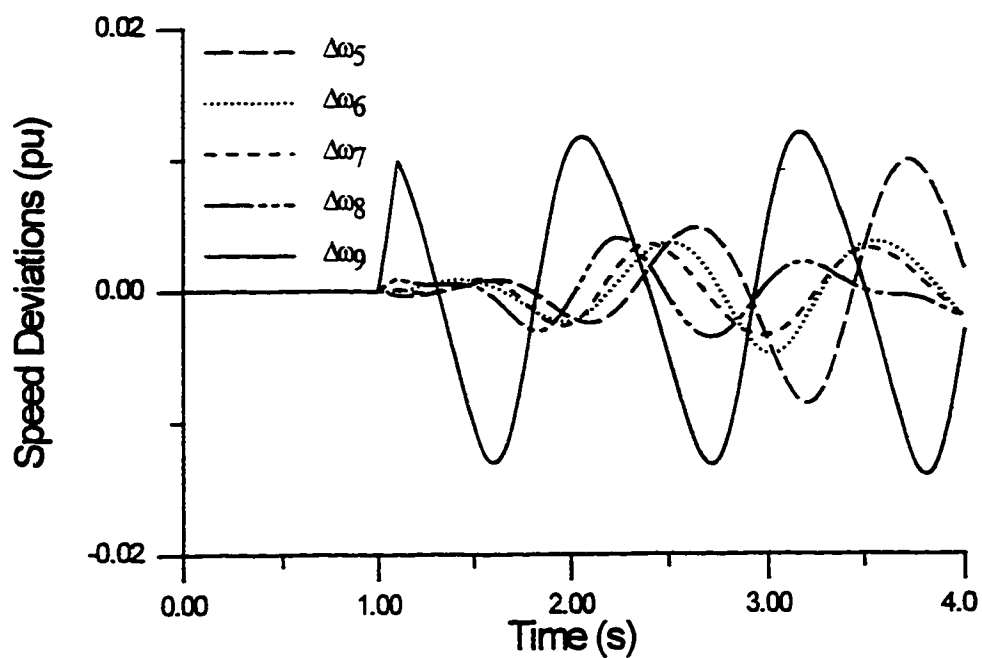
Fig 8.17 System response without PSSs for disturbance (a)
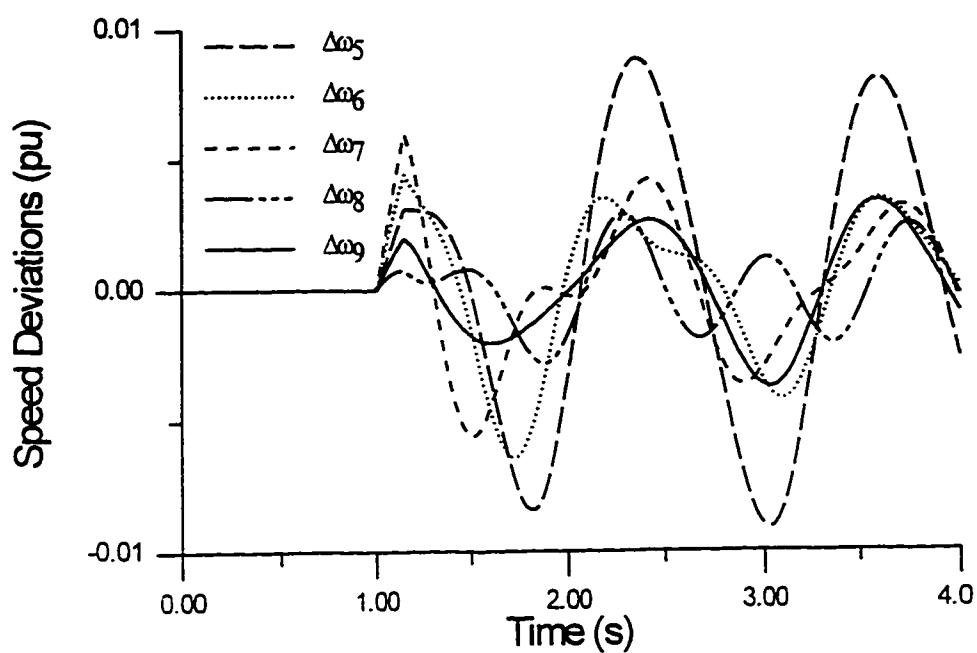
Fig 8.18 System response without PSSs for disturbance (b)

8.6.2 PARAMETER SETTINGS

The proposed approach has been applied to search for optimal settings of the proposed GRBPSSs parameters. Population size, maximum number of generations, and crossover and mutation probabilities are selected after several trials to be 30, 50, 0.75, and 0.005 respectively. The final values of the tuning parameters are given in Table 8.4. Fig. 8.19 shows the convergence rate of the performance index J with the number of generations.

8.6.3 SIMULATION RESULTS

To demonstrate the capability of the proposed GRBPSSs to damp out the electromechanical modes of oscillations, the system performance with the proposed GRBPSSs is compared to that with CPSSs [85]. The simulation results for the disturbances (a) and (b) described above are shown in Figs. 8.20 and 8.21. It can be seen that the dynamic behavior of the system is highly improved by applying the proposed GRBPSSs in the sense that the oscillations are damped out very quickly. However, for accurate and meaningful assessment, the speed deviations of the generators G5 through G9 for disturbance (a) and for disturbance (b) are given in Figs. 8.22 and 8.23 respectively. These results show the capability of the proposed GRBPSS to damp out local modes and interarea modes of oscillations.
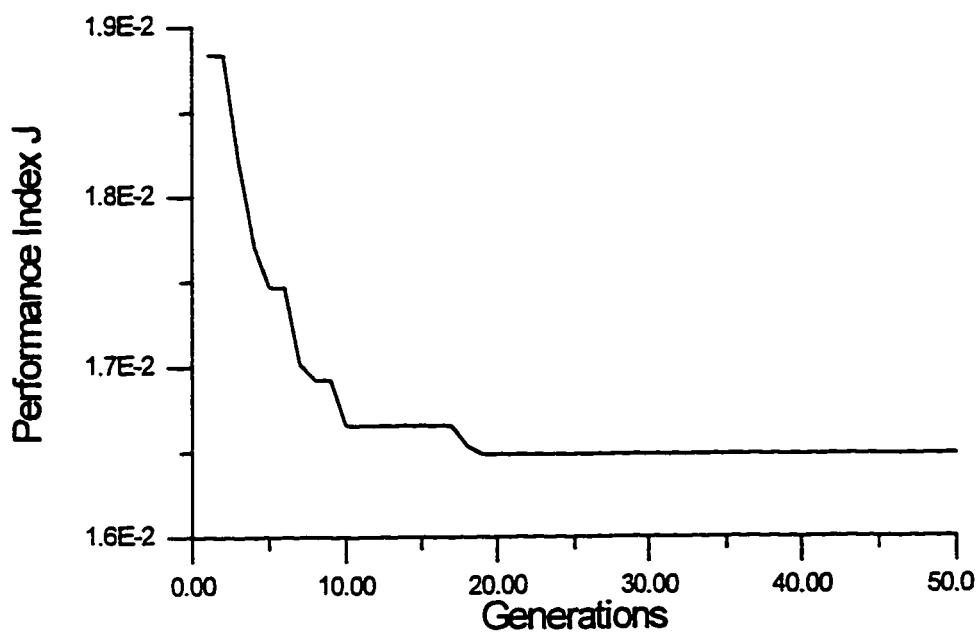
Fig. 8.19 Variations of performance index *J* for example 3

TABLE 8.4 The proposed GRBPSS parameter settings for example 3

Location	θ (rad)	D_r	U_{min} (pu)
G5	0.0803	2.3631	0.1827
G7	0.1843	10.079	0.1843
G9	0.1496	3.9378	0.1165
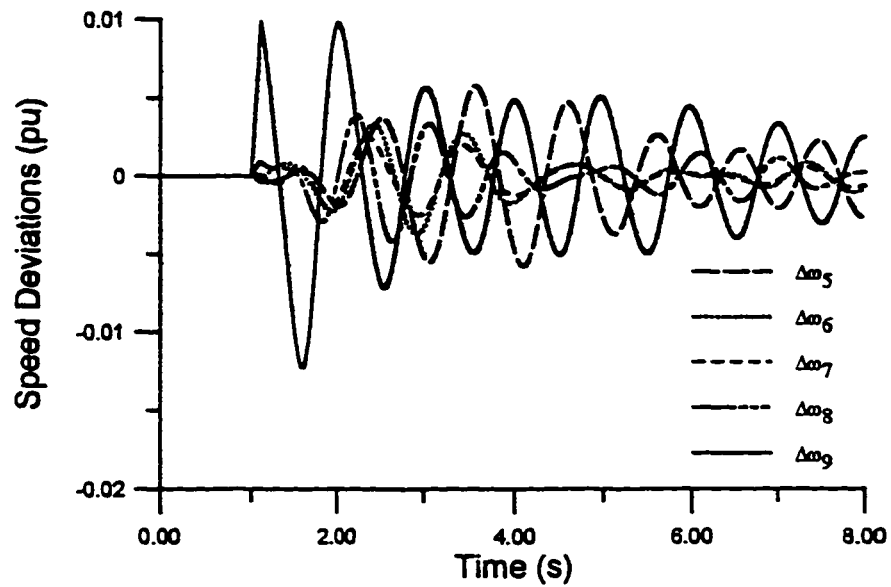
(a)
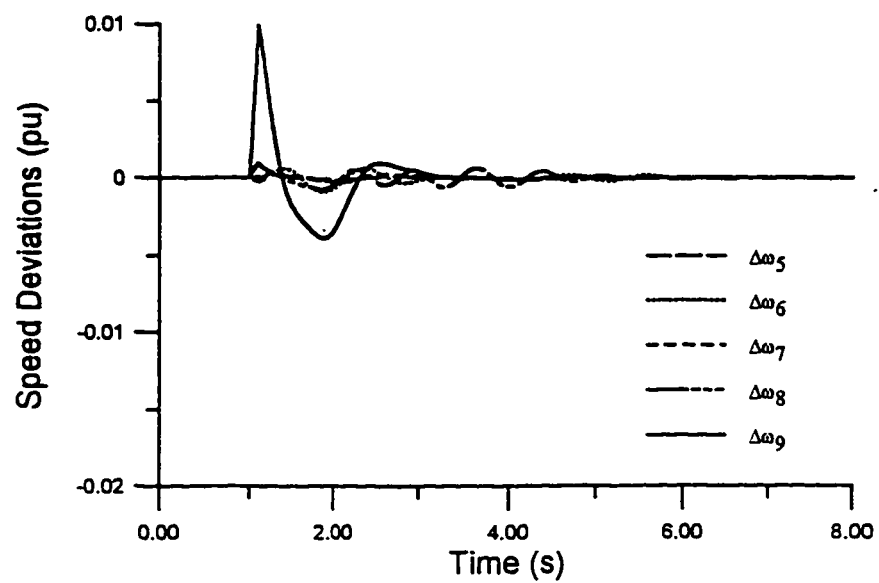
(b)

Fig 8.20 System response for disturbance (a)

(a) with CPSSs

(b) with proposed GRBPSSs
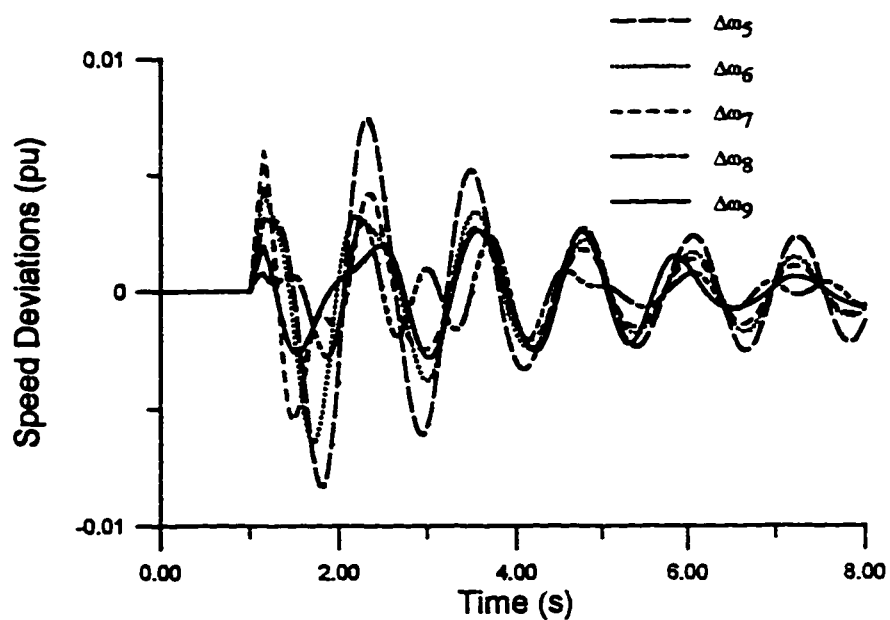
(a)
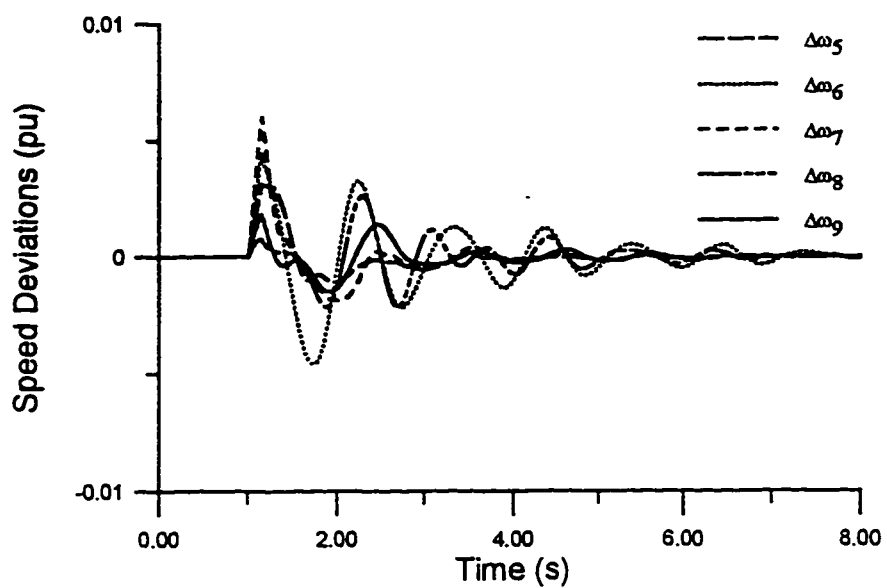
(b)

Fig 8.21 System response for disturbance (b)

(a) with CPSSs

(b) with proposed GRBPSSs
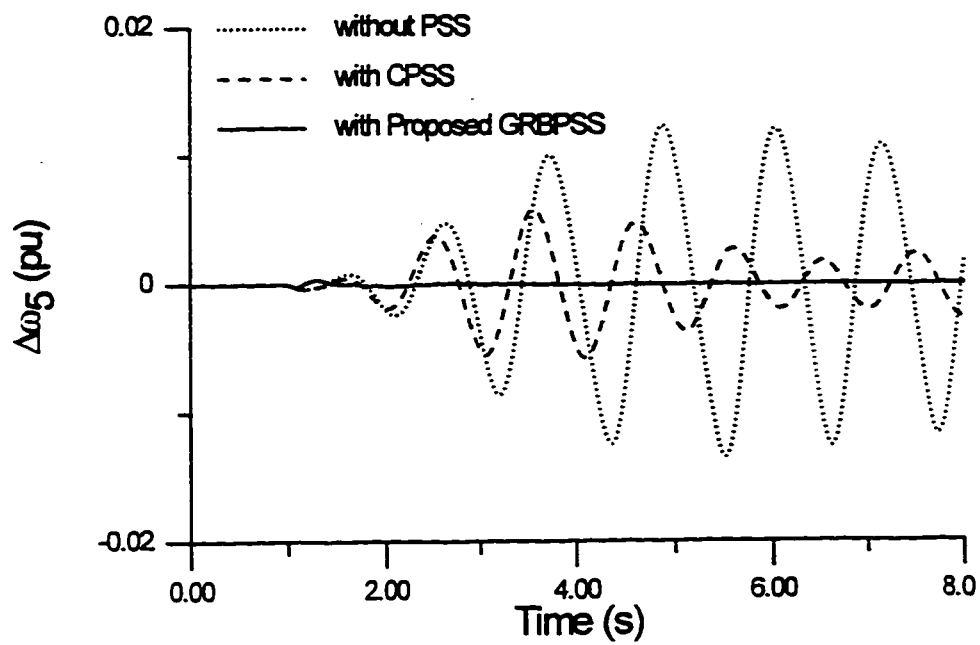
(a)
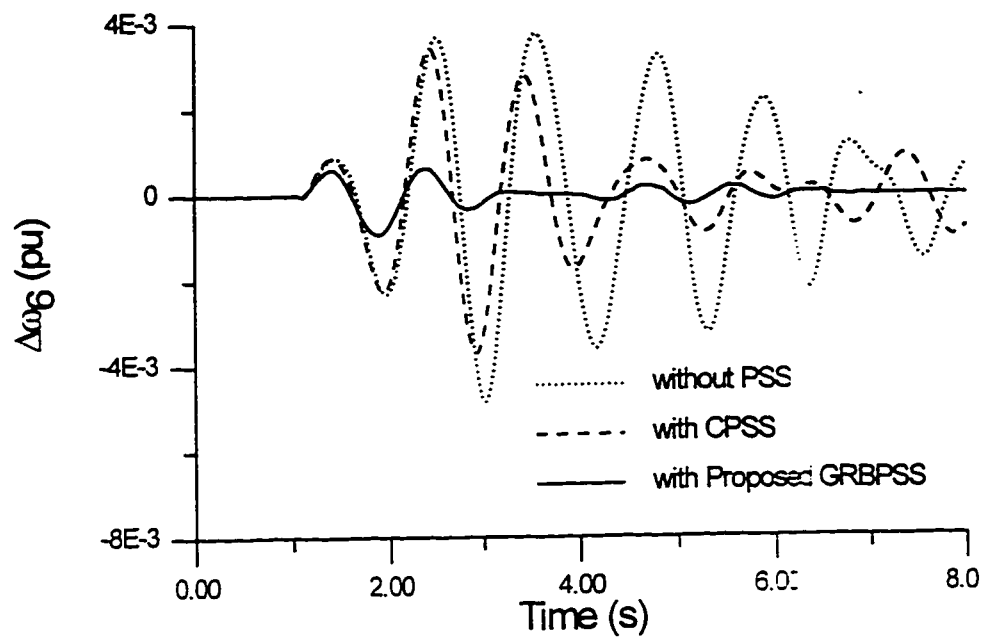
(b)
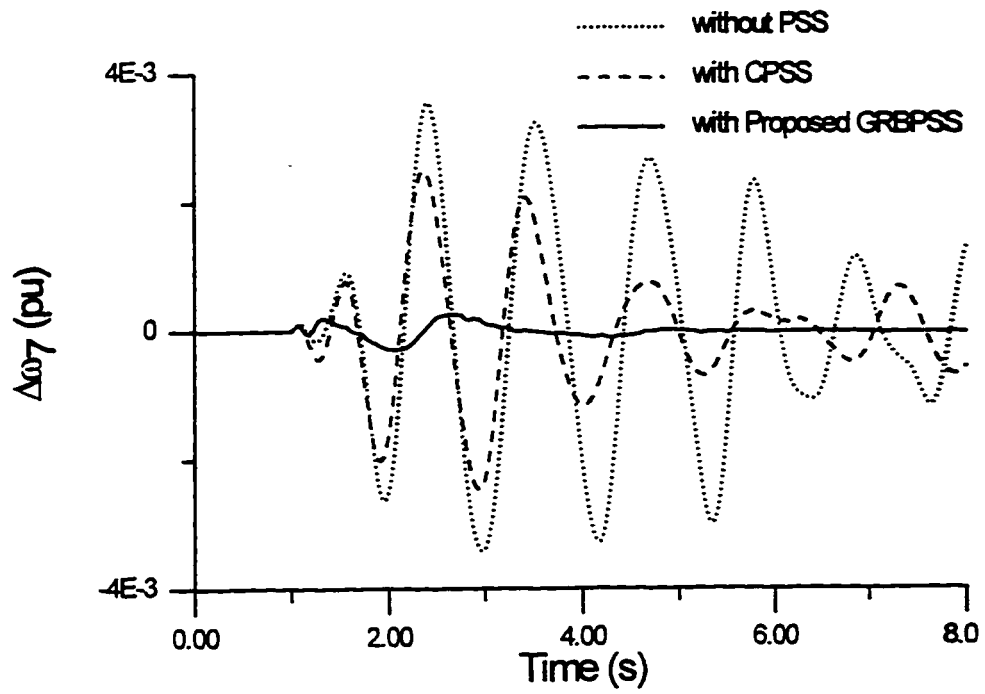
(c)
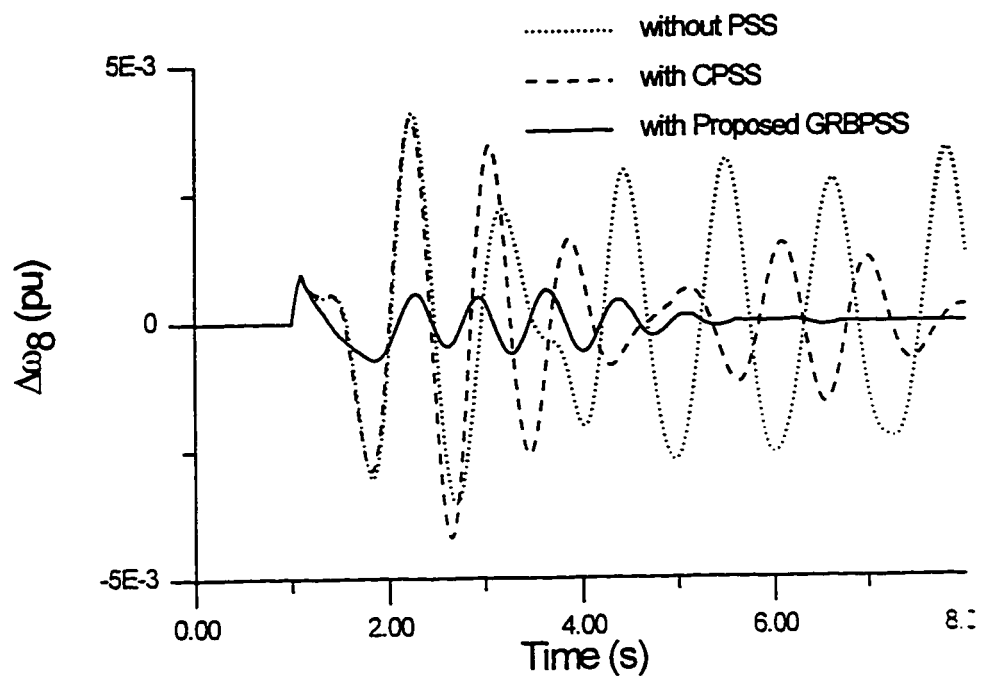
(d)
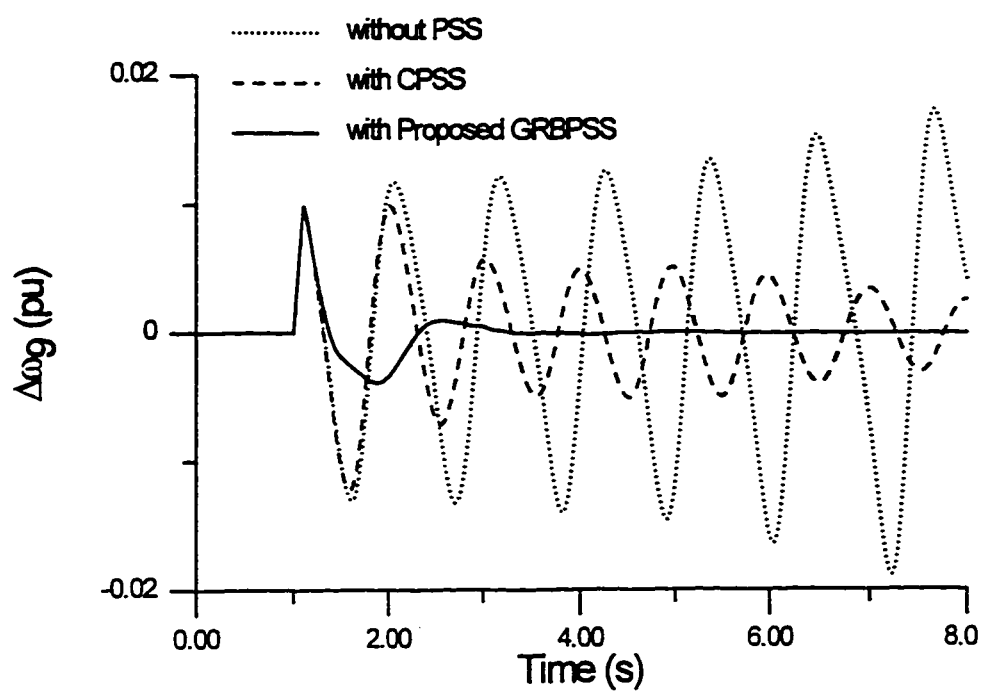
(e)

Fig. 8.22 System response for disturbance (a)

(a) G5 response

(b) G6 response

(c) G7 response

(d) G8 response
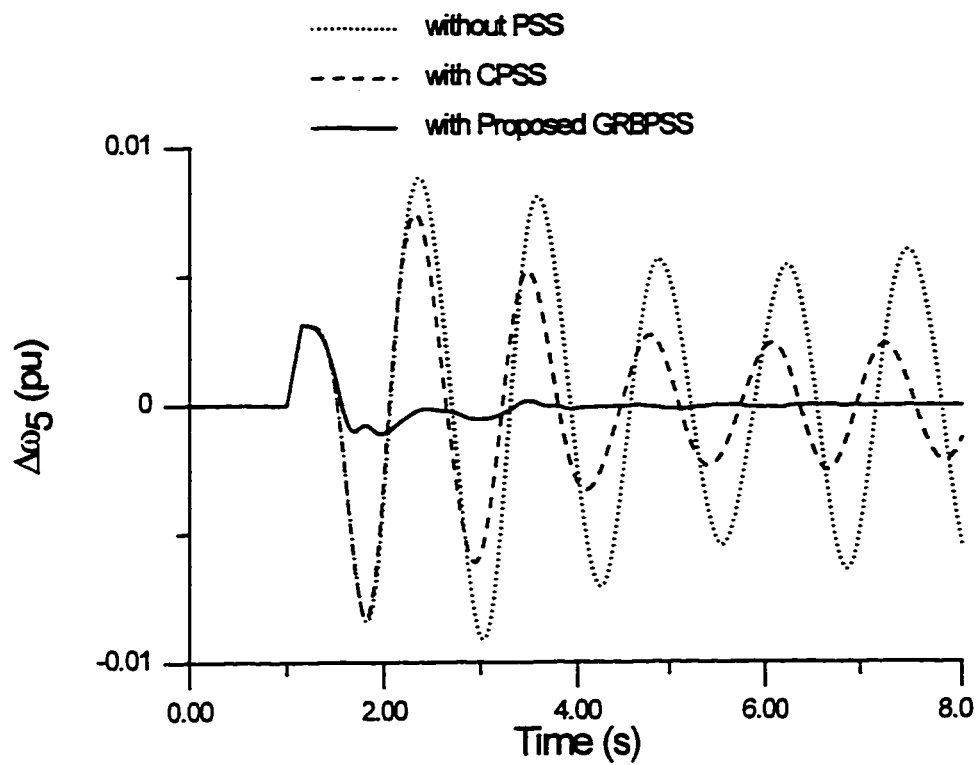
(e) G9 response

(a)
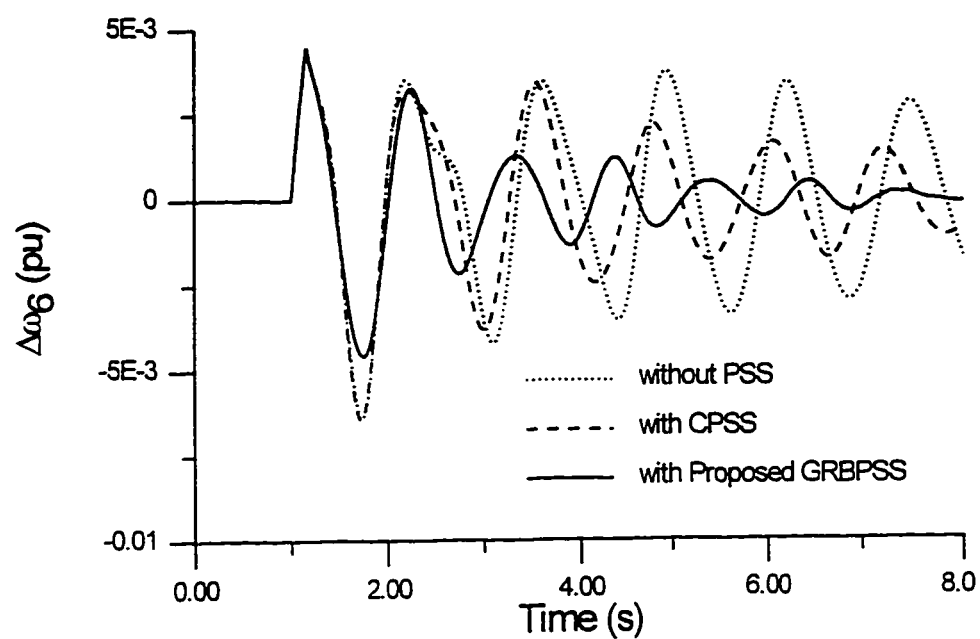
(b)
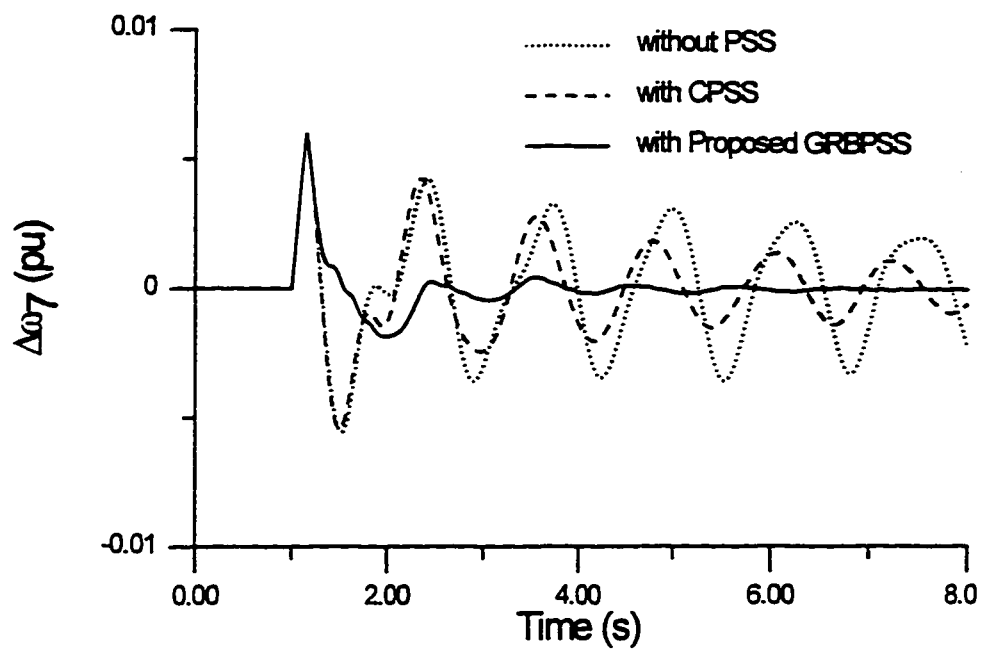
(c)
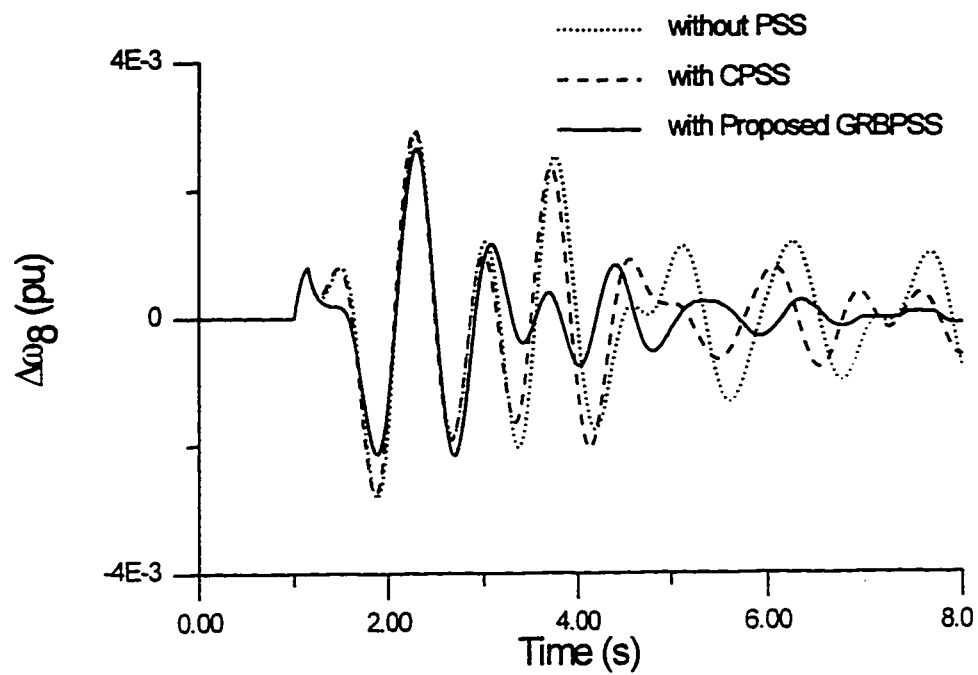
(d)
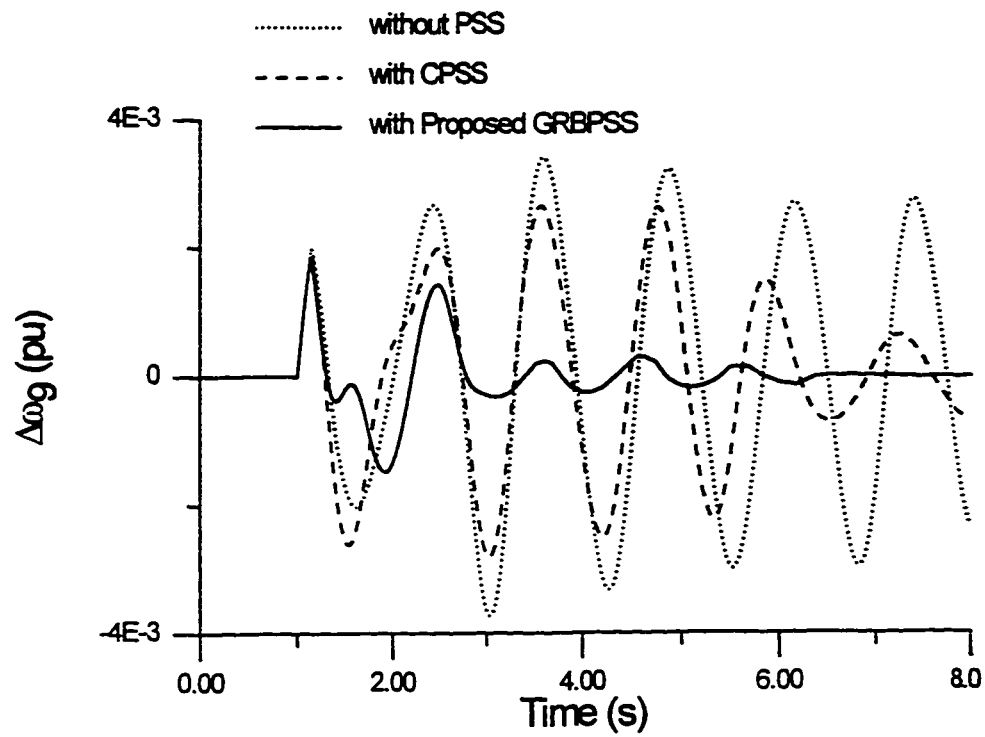
(e)

Fig. 8.23 System response for disturbance (b)

(a) G5 response

(b) G6 response

(c) G7 response

(d) G8 response

(e) G9 response

8.7 SUMMARY

This chapter presents a novel approach to hybridize the RBPSSs using GA. In this approach, GA have been used to search for optimal settings of RBPSS parameters. This overcomes the iterative and trial and error natures of the traditional RBPSS design. The proposed GRBPSS has been applied to a single machine and to two multimachine power systems. The results show that the proposed stabilizer exhibits good damping characteristics.

A natural extension to this chapter, to get still better results, is to hybridize the fuzzy logic PSSs with GA as they have the advantage of smooth transition between control rules. However, the design problems of the rule-based PSSs and fuzzy logic PSSs are similar to some extent. Incorporating GA into fuzzy logic PSSs design will be proposed in the next chapter.

CHAPTER 9

HYBRID GENETIC-BASED FUZZY LOGIC PSSs

9.1 INTRODUCTION

Recently, fuzzy logic power system stabilizers (FLPSSs) [83-95] have been proposed

and investigated. FLPSSs appear to be the most suitable stabilizers due to their lower

computation burden and robustness. Unlike the most conventional methods, an explicit

mathematical model of the system dynamics is not required to design a good FLPSS that

makes the FLPSS more suitable for on-line computer control. In addition, FLPSSs can be

easily set up and implemented using a microcomputer with A/D and D/A converters

[110-113].

Although fuzzy logic controllers showed promising results, they are subjective and

somewhat heuristic. In addition, the determination of fuzzy rules, generation of

membership functions, and the choice of scaling factors are done either iteratively, by

trial-and-error, or by human experts. There is to-date no generalized method for the

formulation of fuzzy control strategies, and design remains an ad hoc trial and error exercise. That makes the design of fuzzy logic controller a laborious and time-consuming task. To overcome such problems, the recent direction is to use GA to search for optimal settings of fuzzy logic controller parameters [114-118].

In this chapter, we propose an approach to integrate the use of GA and fuzzy logic systems in order to design the proposed hybrid genetic-based fuzzy logic power system stabilizer (GFLPSS). The proposed approach uses GA to search for optimal or near optimal settings of fuzzy logic power system stabilizer parameters. Incorporation of GA in FLPSSs design will add an intelligent dimension of these stabilizers and reduce significantly the time consumed in the design process

9.2 FUZZY LOGIC CONTROL SCHEME

As shown in Chapter 8, the supplementary stabilizing signal u is added to the excitation loop as shown in Fig. 8.1. At time t, the stabilizing signal $u(t)$ is given by

$$u(t)=U(k) \qquad kT < t < (k+1)T \qquad (9.1)$$

The value of $U(k)$ is determined at each sampling time based on fuzzy logic through the following steps:

Step 1: The speed deviation. $\Delta\omega(k)$, is measured at every sampling time. and the acceleration of the machine, $A(k)$, is calculated by

$$A(k)=[\ \Delta\omega(k) - \Delta\omega(k-1) \ ] / T \qquad (9.2)$$

Step 2: Compute the scaled acceleration, $A_s(k)$, using

$$A_s(k) = A(k)^* F_a \qquad (9.3)$$

Step 3: The generator condition is given by the point $z(k)$ in the phase plane as shown in Fig. 9.1, where

$$z(k) = (\ \Delta\omega(k)\ ,A_s(k)\ ) \qquad (9.4)$$

Step 4: From the phase plane, calculate $R(k)$ and $\theta\ (k)$ using

$$R(k) = |\ z(k)\ | \qquad (9.5)$$

and,

$$\theta\ (k) = \tan^{-1}(\ A_s(k)\ /\ \Delta\omega(k)\ ) \qquad (9.6)$$

Step 5: Determine the values of the fuzzy membership functions $N_s(\theta\ )$ and $P_s(\theta\ )$ as shown in Fig. 9.2 [84].

The membership functions $N_s(\theta\ )$ and $P_s(\theta\ )$ are defined as:

$$N_s(\theta\ )=\begin{cases} 1-\Phi(x;\theta_i,\theta_{m1},\theta_m) & \forall x \le \theta_m \\ \Phi(x;\theta_m,\theta_{m2},2\pi) & \forall x > \theta_m \end{cases} \qquad (9.7)$$

and,

$$P_s(\theta\ )=\Psi(\theta,2\pi-\theta_i,\theta_m) \qquad (9.8)$$

where

$$\Phi(x;a,b,c) = \begin{cases} 0.0 & \forall x \le a \\ 2[\dfrac{x-a}{c-a}]^2 & \forall x \in\ ]a,b\ ] \\ 1-2[\dfrac{x-c}{c-a}]^2 & \forall x \in\ ]b,c\ [\\ 1.0 & \forall x \ge c \end{cases} \qquad (9.9)$$

$$\Psi(x;b,c) = \begin{cases} \Phi(x;c-b,c-b/2,c) & \forall x \le c \\ 1-\Phi(x;c,c+b/2,c+b) & \forall x > c \end{cases} \qquad (9.10)$$

$$\theta_m = (2\pi + \theta_i) / 2 \tag{9.11}$$

$$\theta_{m1} = (\theta_i + \theta_m) / 2 \tag{9.12}$$

$$\theta_{m2} = (2\pi + \theta_m) / 2 \tag{9.13}$$

Step 6: Determine the value of the gain function $G(k)$ as shown in Fig. 9.3 [84,108].

The gain function is defined as

$$G(k) = \begin{cases} R(k) / D_r & \forall R(k) \le D_r \\ 1.0 & \forall R(k) > D_r \end{cases} \tag{9.14}$$

Step 7: Compute the stabilizing signal $U(k)$ using

$$U(k) = G(k) \, [\, N_s(\theta) - P_s(\theta) \,] \, U_{max} \tag{9.15}$$

Step 8: Increase k by 1 and return to step 1.

Step 9: Repeat until the end of simulation time.

The main tuning parameters are θ_i, F_a, and D_r. For the optimal settings of these

parameters, a quadratic performance index J_1 is considered:

$$J_1 = \sum_{i=1}^{NM} \sum_{k=1}^{L} [kT\Delta\omega_i(k)]^2 \tag{9.16}$$

In the above index, the speed deviation $\Delta\omega(k)$ is weighted by the respective time kT.

The index J_1 is selected because it reflects a small settling time, a small steady state error,

and small overshoots. The tuning parameters are adjusted so as to minimize the index J_1.

Furthermore, a non-weighted performance index J_2 is also considered for further

information and comparison purposes.

$$J_2 = \sum_{i=1}^{NM} \sum_{k=1}^{L} [\Delta\omega_i(k)]^2 \tag{9.17}$$
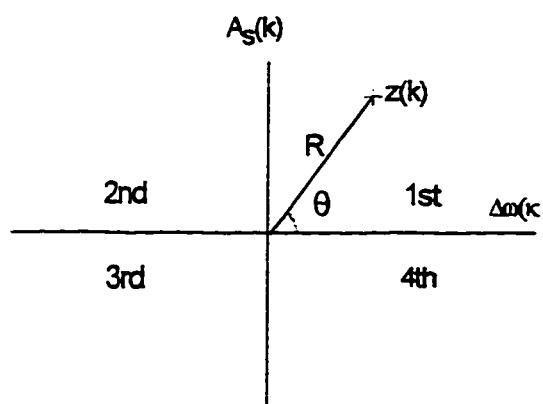
Fig. 9.1 Operating condition on the phase plane
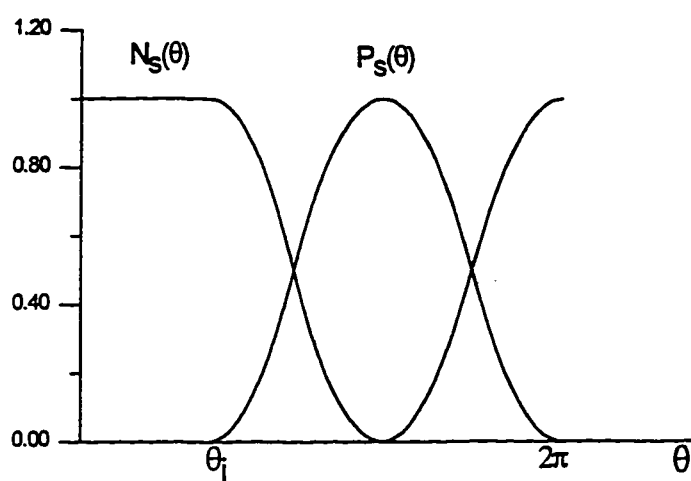
Fig. 9.2 Membership functions
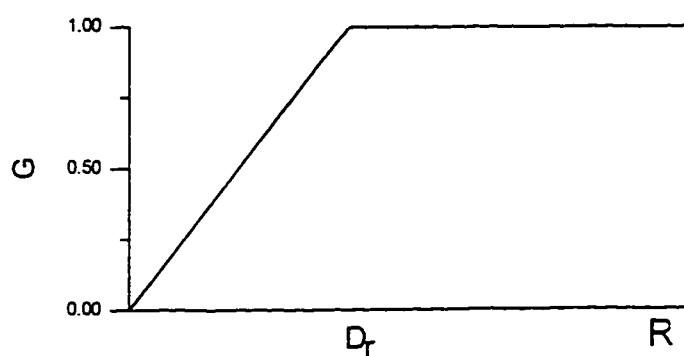
Fig. 9.3 Gain function

9.3 DESIGN OF THE PROPOSED STABILIZER

The FLPSS adjustable parameters are usually optimized to minimize the performance index J_l iteratively [84-85]. Therefore, the optimization process becomes a laborious, tedious, and time consuming task. Moreover, the interaction between parameters has not been taken into consideration. The proposed approach employs GA for optimum settings of the tuning parameters θ_i, F_a, and D_r. These parameters are optimized simultaneously. At first, the adjustable parameters are coded in a binary string and the initial population is generated randomly. The design steps of the proposed GFLPSS can be summarized in the flow chart shown in Fig. 9.4.

9.4 EXAMPLE 1: SINGLE MACHINE SYSTEM

9.4.1 TEST SYSTEM

In this study, the single machine infinite bus system shown in Fig. 8.1 is considered. The system model and parameters are given in Appendix E. The operating conditions given in Table 8.1 are used in the simulations to cover a wide range of operating conditions.
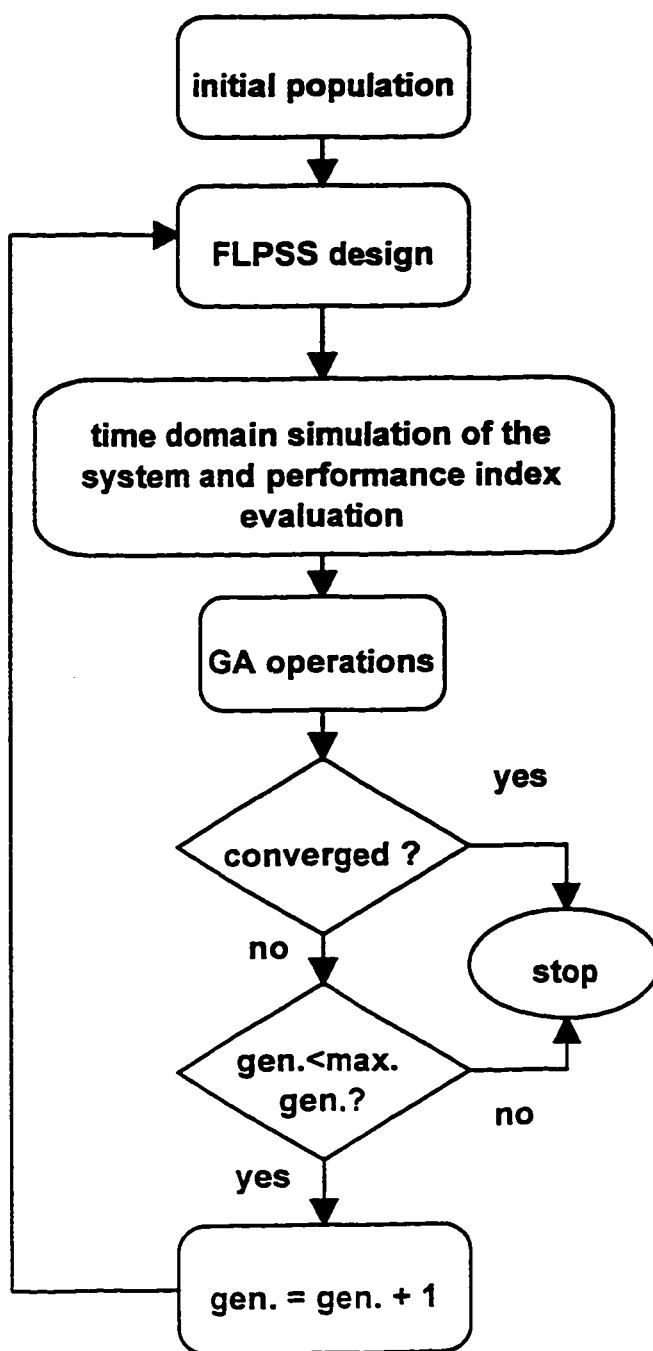
Fig. 9.4 The proposed GFLPSS computational flow chart

9.4.2 PARAMETER SETTINGS

The proposed approach has been applied to search for the optimal settings of the tuning parameters θ_i, F_{ω} and D_r. Population size, maximum number of generations, and crossover and mutation probabilities are selected based on several trials to be 30, 100, 0.75, and 0.001 respectively. The final values of the tuning parameters are given in Table 9.1. Fig. 9.5 shows the convergence rate of the performance index J with the number of generations.

9.4.3 SIMULATION RESULTS

A number of studies have been performed with the proposed GFLPSS. The performance of the proposed GFLPSS is compared to those of the FLPSS [84] and the CPSS [94] with a transfer function given in (8.14).

9.4.3.1 OPERATING CONDITION (P_I, Q_I)

The system performance with a 10% step increase in input torque is shown in Fig. 9.6. Fig. 9.7 shows the simulation results with three phase fault disturbances at the infinite bus for 0.1s. The results with a 10% pulse in reference voltage for 2s are shown in Fig. 9.8. It is obvious that, the system performance with the proposed GFLPSS is the best

in the sense that the first swing in the torque angle is significantly suppressed. This is very helpful in the improvement of the disturbance tolerance ability of the system.

9.4.3.2 OPERATING CONDITION (P_2, Q_2)

A 40% step increase in input torque and a 0.1s three phase fault at infinite bus disturbances were applied. The simulation results are shown in Figs. 9.9 and 9.10 respectively. The results show the capability of the proposed GFLPSS to damp out the oscillations and to work properly over a wide range of operating conditions.

9.4.3.3 OPERATING CONDITION (P_3, Q_3)

A 30% step increase in input torque and a 0.1s three phase fault at infinite bus disturbances were applied. The simulation results are shown in Figs. 9.11 and 9.12 respectively. It can be concluded that the proposed GFLPSS provides good damping characteristics to system oscillations.

TABLE 9.1 The proposed GFLPSS parameters settings for example 1

θ (rad)	F_a	D_r
1.9412	0.3137	4.0021
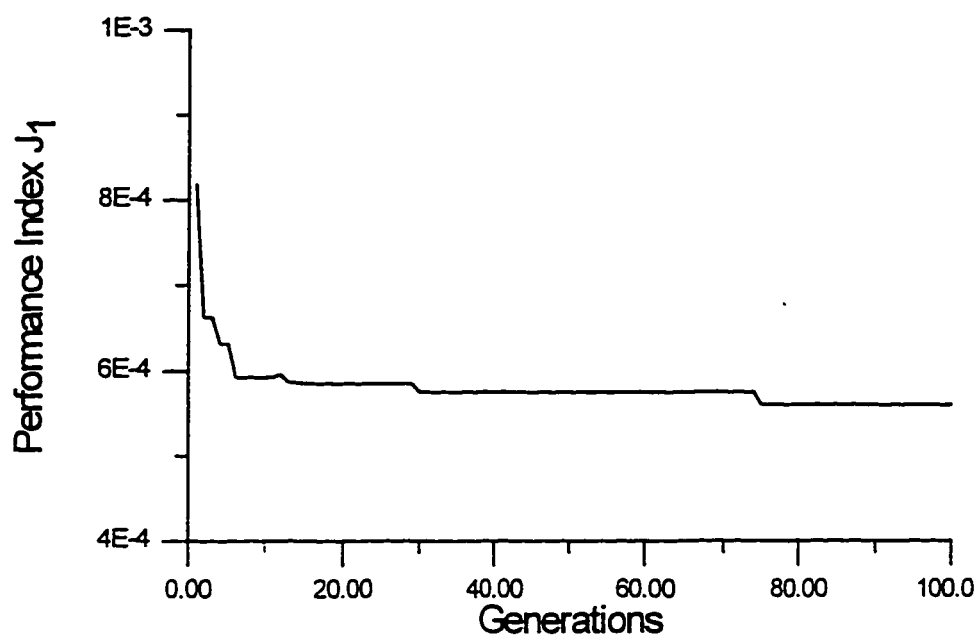
Fig. 9.5 Variations of performance index J_l for example 1
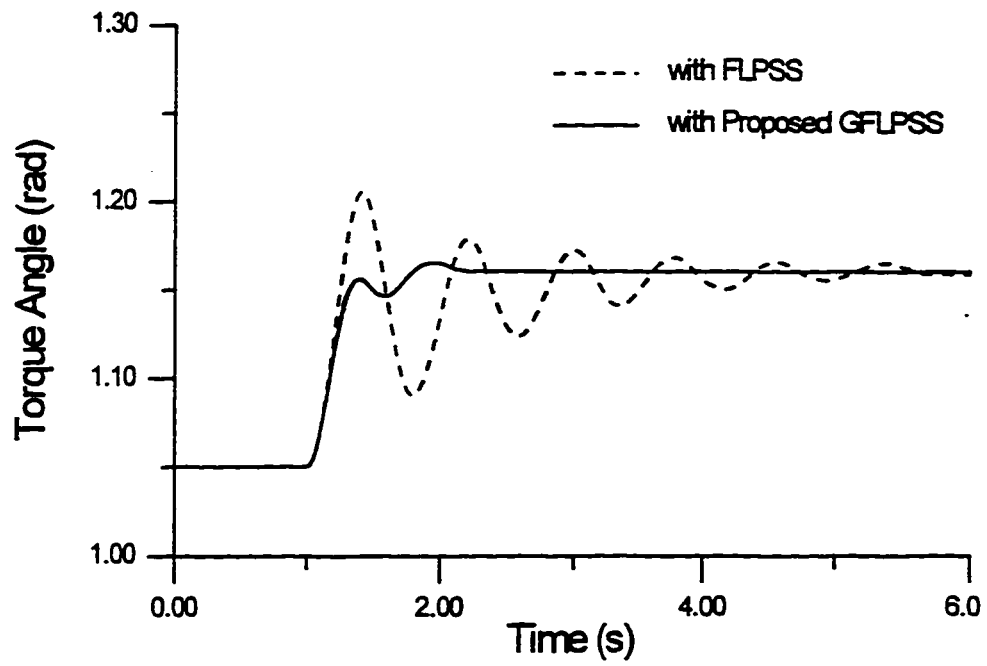
Fig. 9.6 Response to 10% step in torque for operating point (P_l, Q_l)
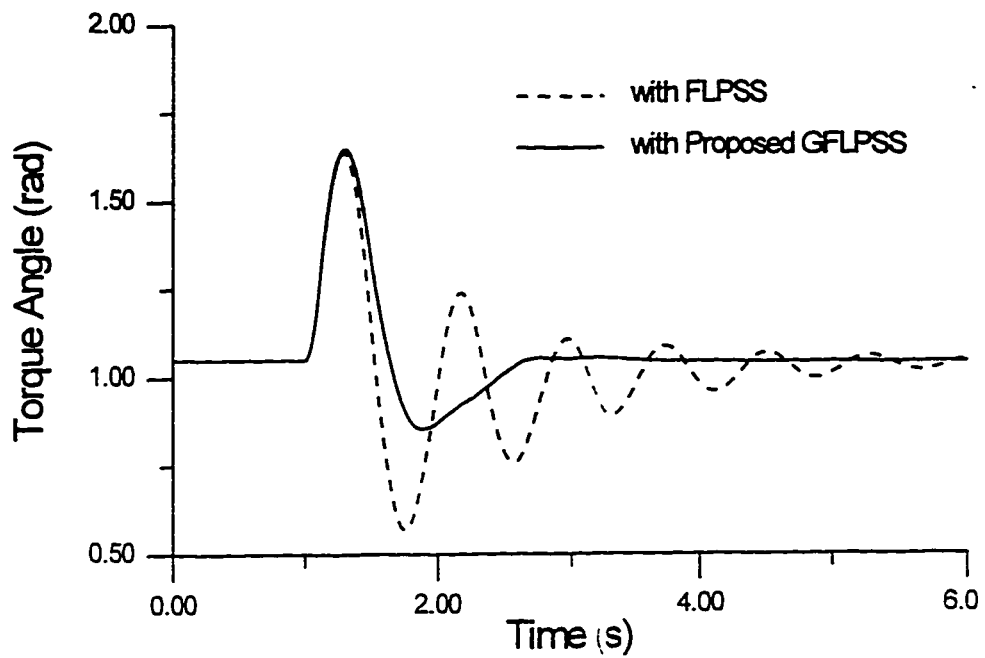
Fig. 9.7 Response to three phase fault for operating point (P_l, Q_l)
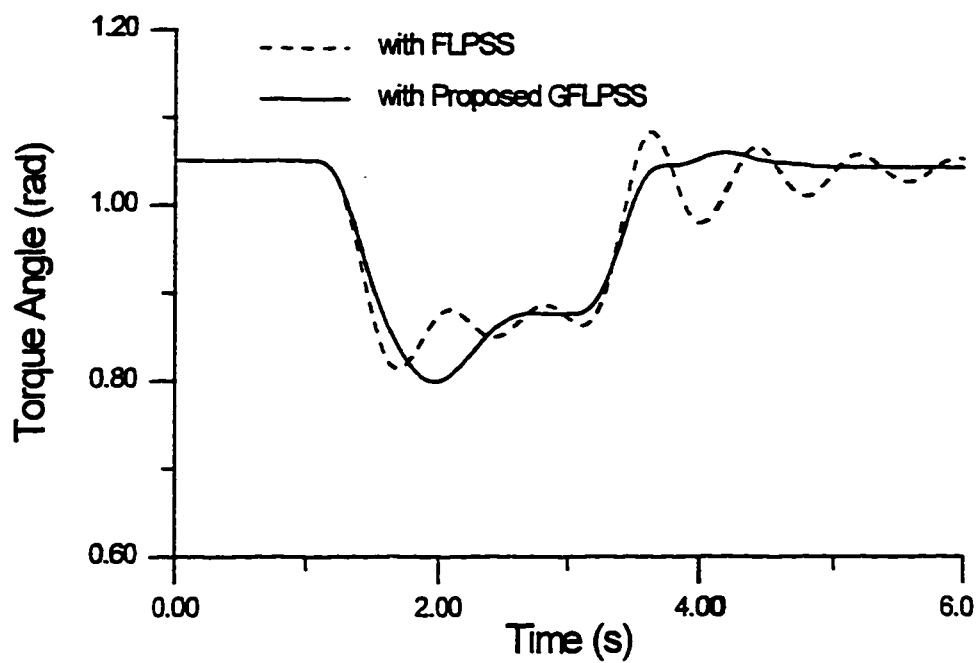
Fig. 9.8 Response to 10% pulse in reference voltage for operating point (P_1, Q_1)
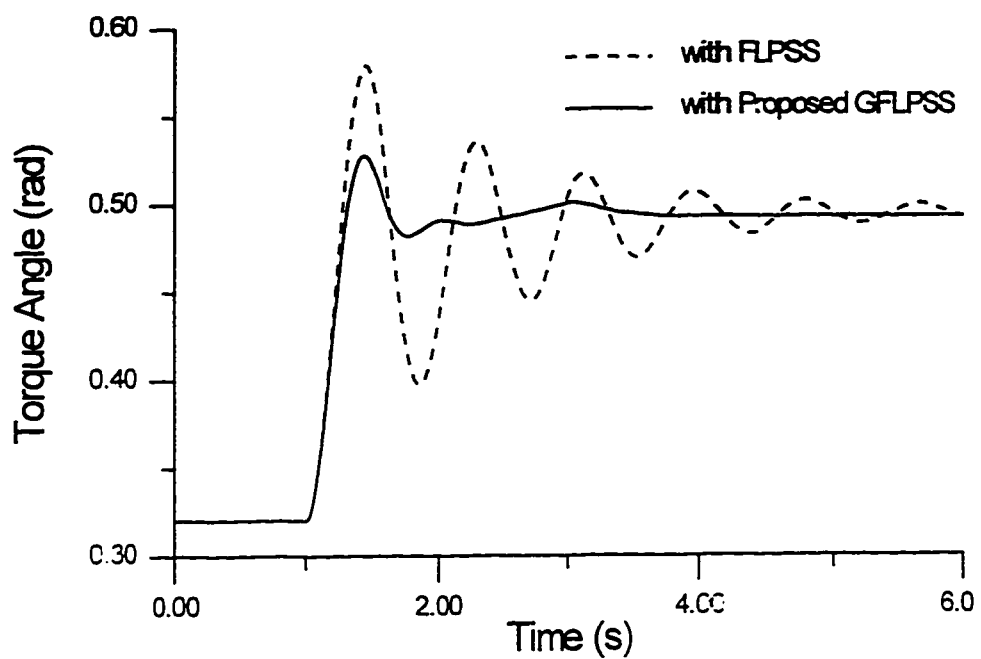
Fig. 9.9 Response to 40% step in torque for operating point (P_2, Q_2)
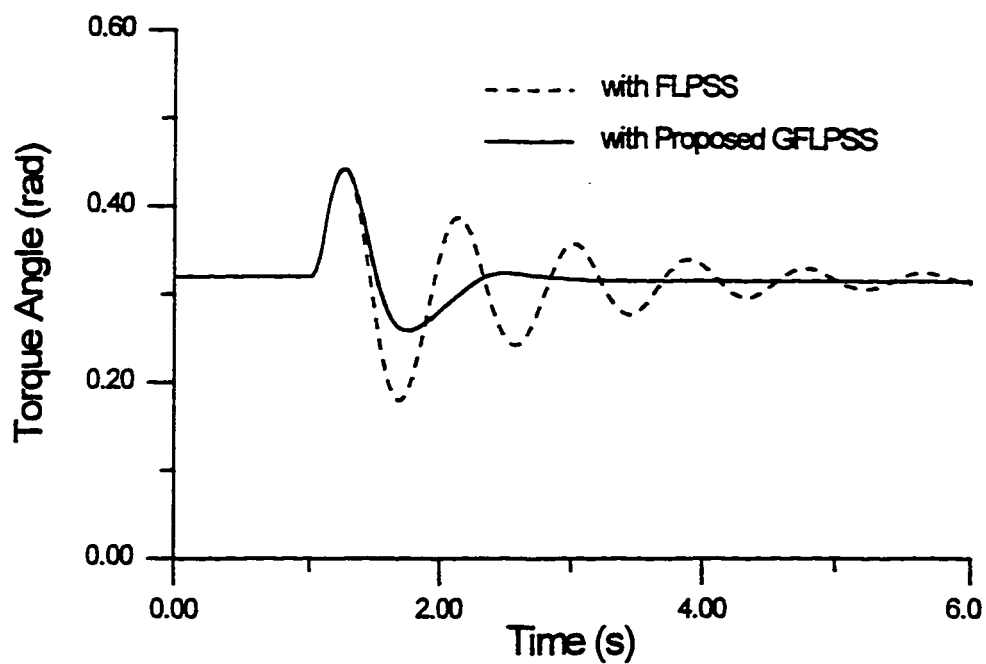
Fig. 9.10 Response to three phase fault for operating point (P_2, Q_2)
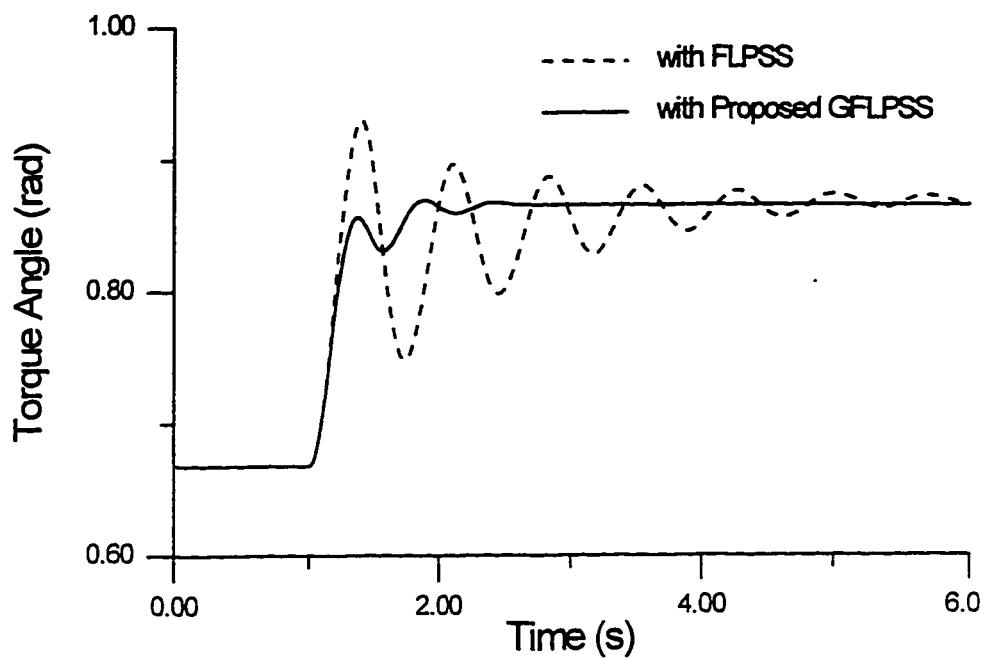
Fig. 9.11 Response to 30% step in torque for operating point (P_3, Q_3)
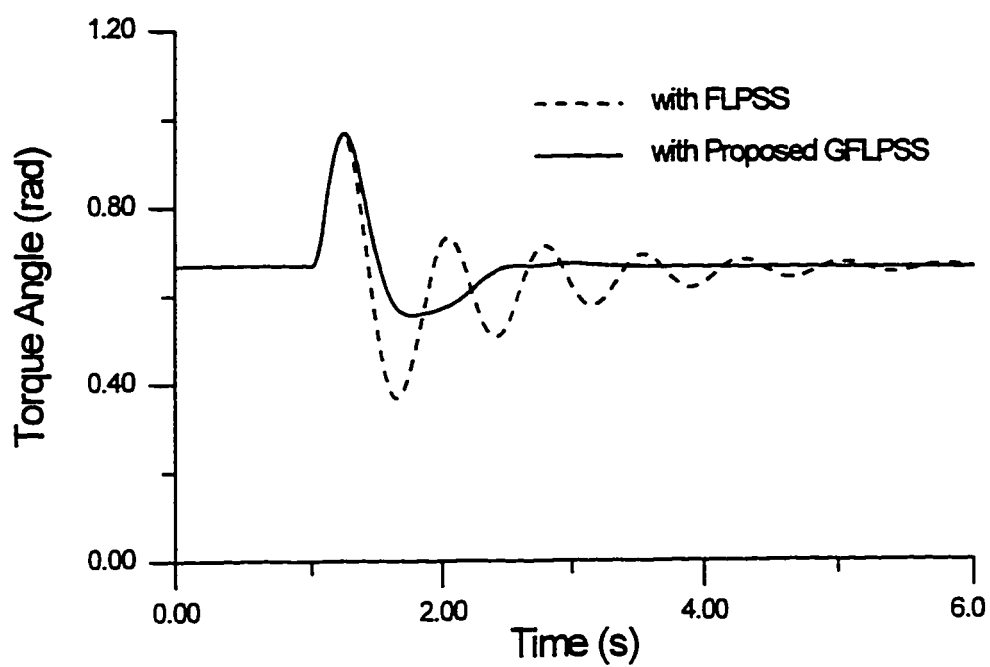
Fig. 9.12 Response to three phase fault for operating point (P_3, Q_3)

9.5 EXAMPLE 2: NEW ENGLAND SYSTEM

9.5.1 SYSTEM DESCRIPTION

In this study, the 10-machine 39-bus New England power system shown in Fig. 8.16 was considered. Details of the system data are given in Appendix F. In this study, the following disturbances are considered for the simulations:

(a) Three phase fault for 0.10s at bus 29 at the end of line 26-29.

(b) Three phase fault for 0.15s at bus 15 at the end of line 14-15.

(c) Three phase fault for 0.15s at bus 22 at the end of line 21-22.

Without PSSs, the system responses due to the above disturbances are shown in Figs. 9.13, 9.14, and 9.15 respectively. It is observed that the system damping is very poor and the system is highly oscillatory. As shown in Chapter 8, it is necessary to install three stabilizers at generators G5, G7, and G9 in order to have a good dynamic performance and damp out the electromechanical modes of oscillations. Therefore, these generators are equipped with three of the proposed GFLPSSs.
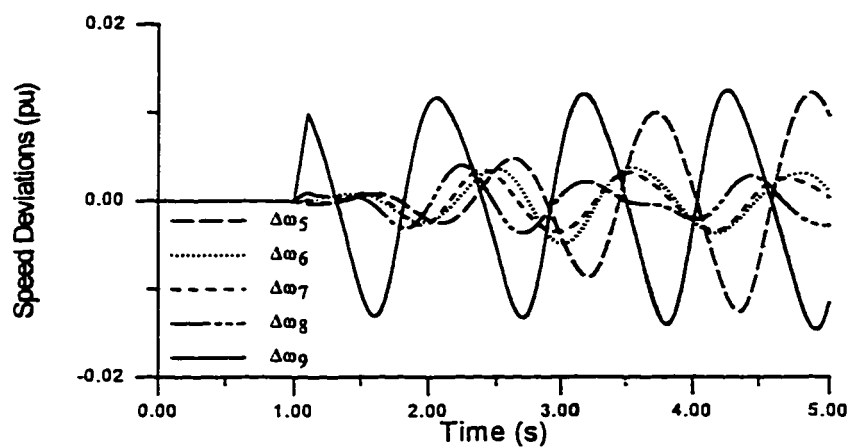
Fig 9.13 System response without PSSs for disturbance (a)
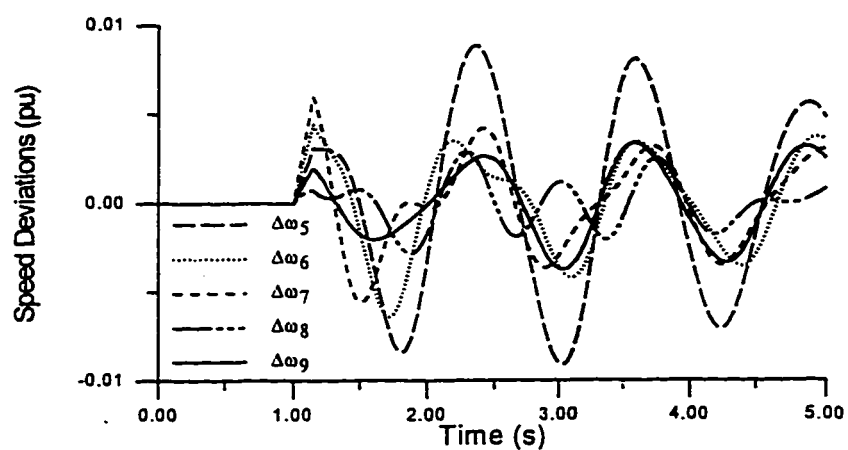
Fig 9.14 System response without PSSs for disturbance (b)
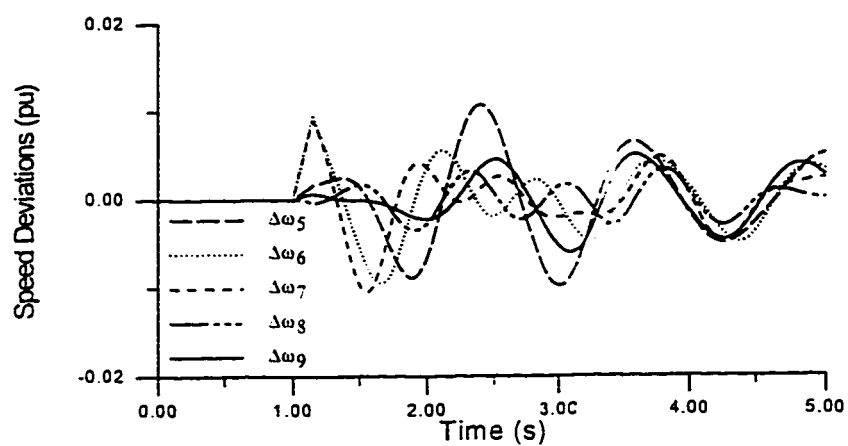
Fig 9.15 System response without PSSs for disturbance (c)

9.5.2 PARAMETER SETTINGS

The proposed approach has been applied to search for optimal settings of the proposed GFLPSSs parameters. Population size, maximum number of generations, and crossover and mutation probabilities are selected after several trials to be 30, 50, 0.75, and 0.005 respectively. The final values of the tuning parameters are given in Table 9.2. Fig. 9.16 shows the convergence rate of the performance index J_i with the number of generations.

9.5.3 SIMULATION RESULTS

To demonstrate the capability of the proposed GFLPSSs to damp out the electromechanical modes of oscillations, the system performance with the proposed GFLPSSs is compared to those with FLPSSs and CPSSs [85]. The simulation results for disturbance (a) described above is shown in Fig. 9.17. It can be seen that the dynamic behavior of the system is highly improved by applying the proposed GFLPSSs in the sense that the oscillations are damped out very quickly. However, for a better comparison. the responses of the rotor angles of generators G5 through G9 referred to G1 and the speed deviations of these generators for disturbance (a) are shown in Figs. 9.18-9.22 respectively.

TABLE 9.2 The proposed GFLPSS parameters settings for example 2

Location	θ (rad)	F_a	D_r
G5	2.4134	0.7953	17.008
G7	2.4291	0.9134	17.008
G9	2.2480	0.9528	17.165
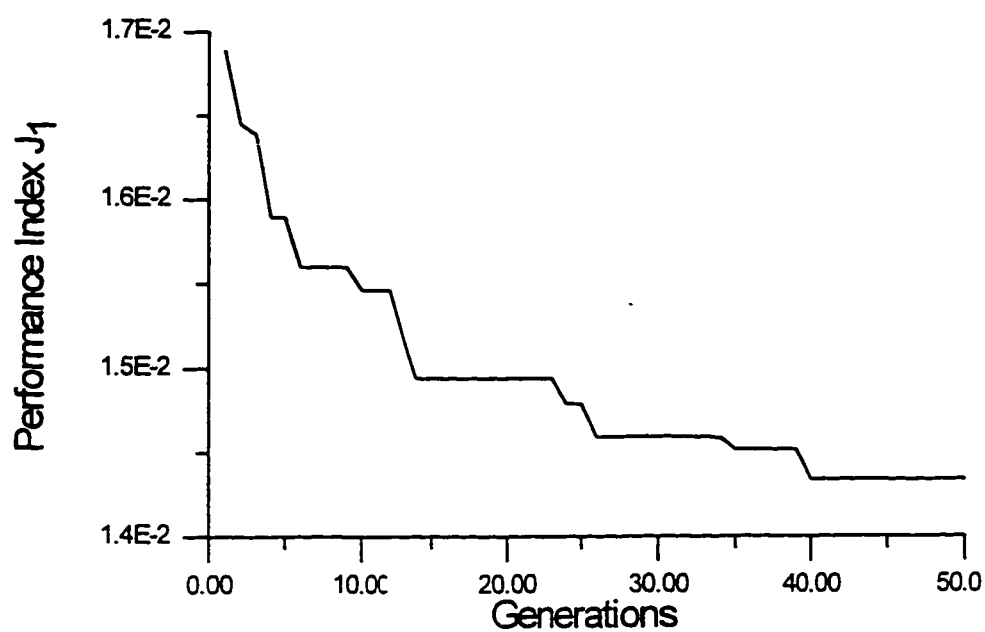
Fig. 9.16 Variations of performance index J_1 for example 2
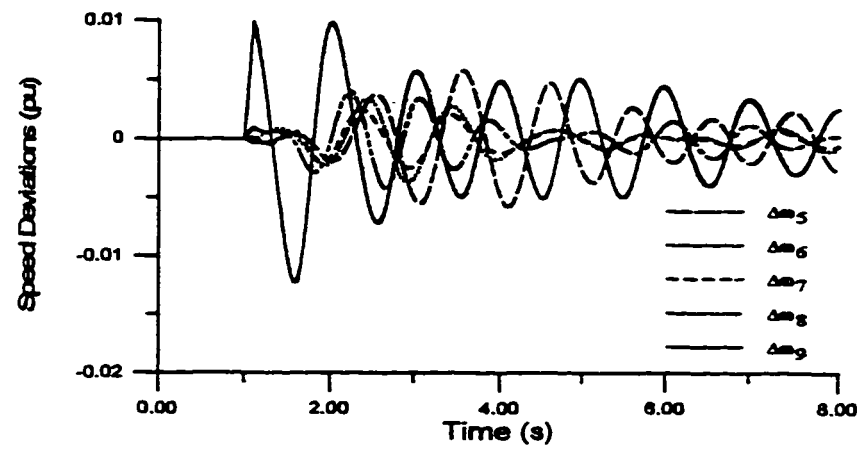
(a)
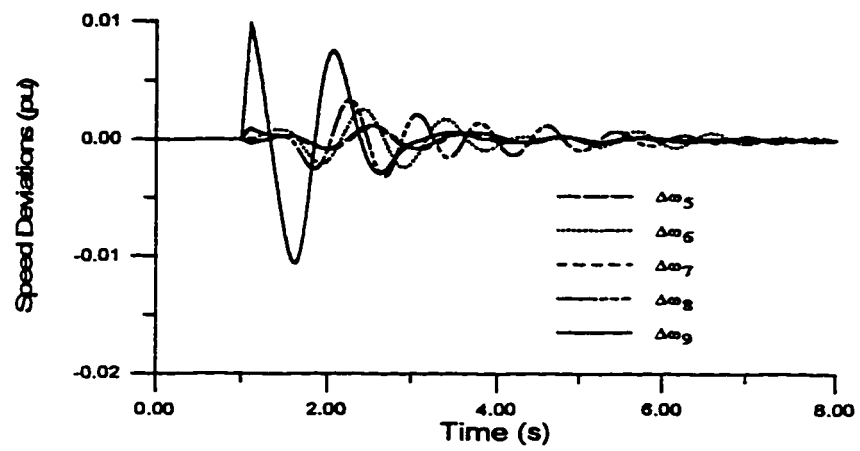
(b)
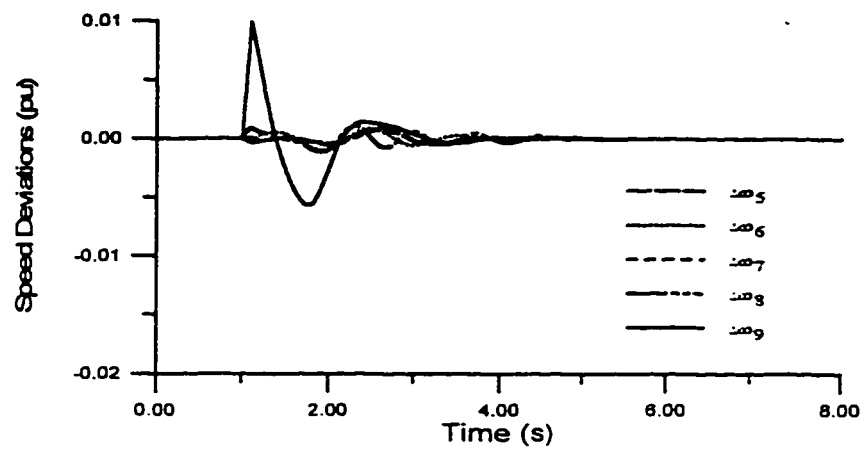
(c)

Fig 9.17 System responses for disturbance (a

(a) with CPSSs

(b) with FLPSSs

(c) with Proposed GFLPSSs
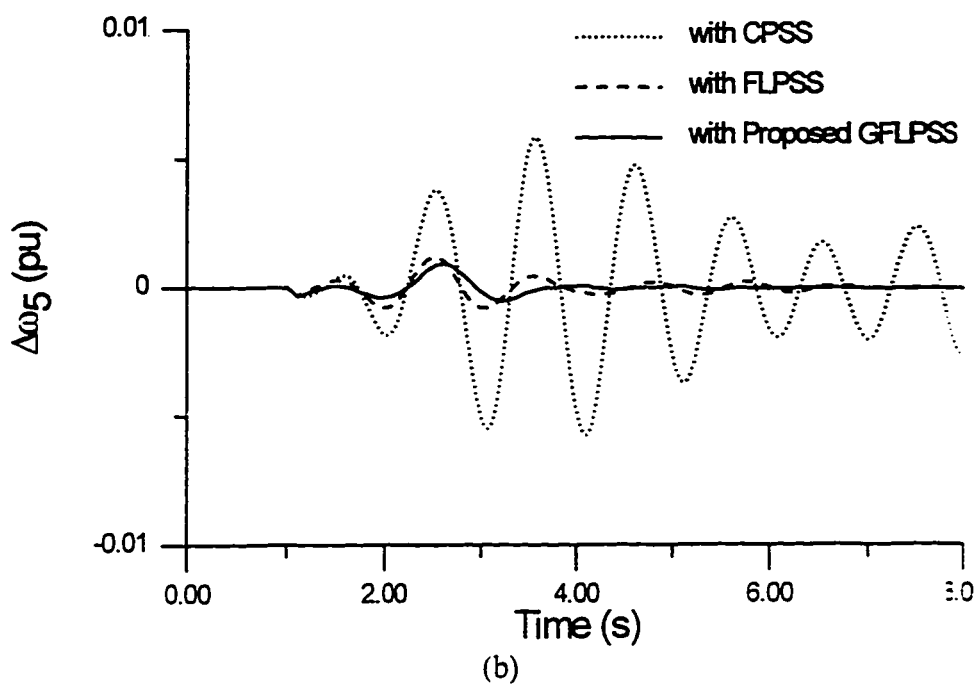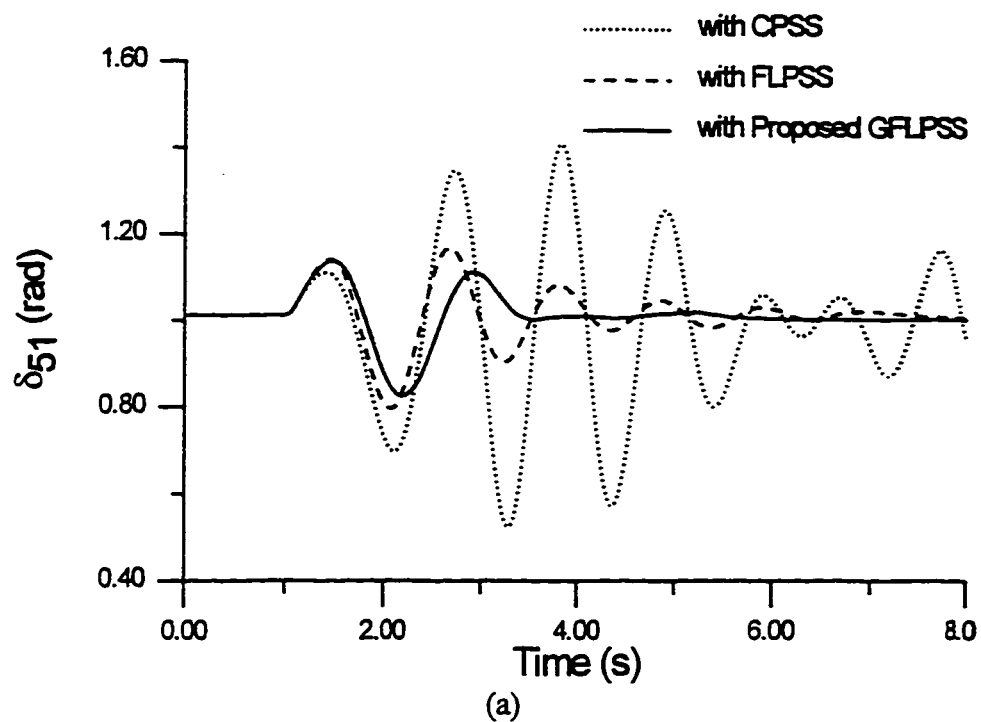
Fig 9.18 Generator G5 response for disturbance (a)
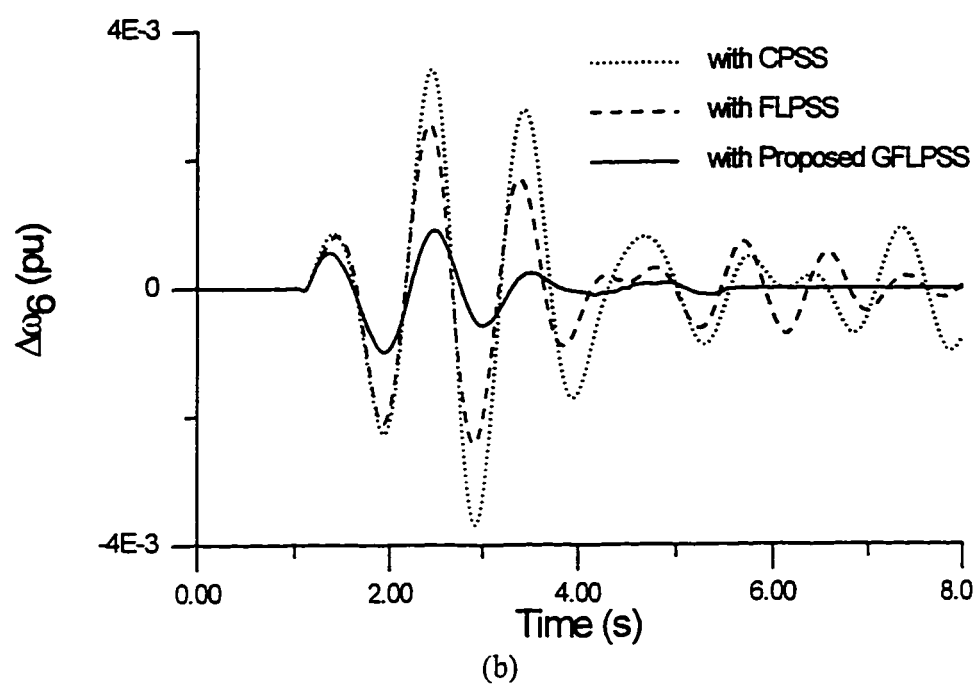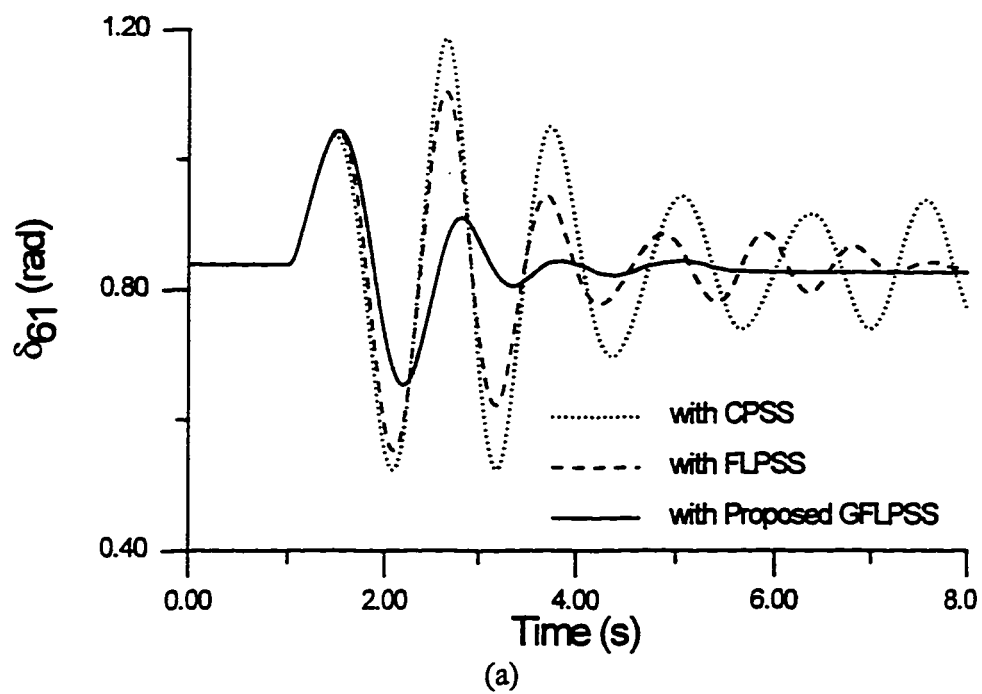
Fig 9.19 Generator G6 response for disturbance (a)
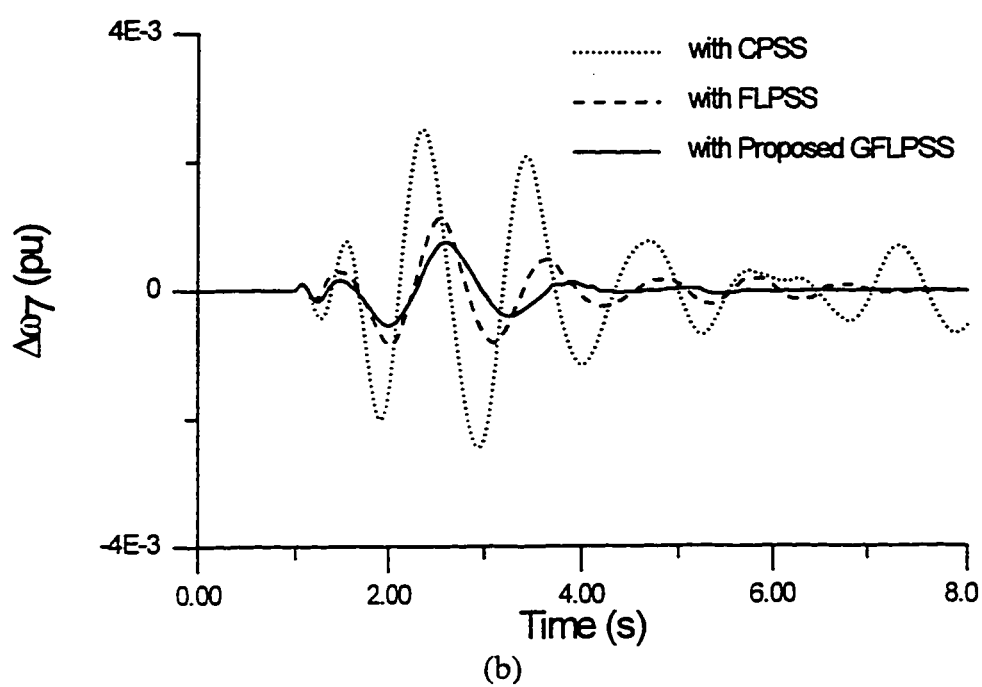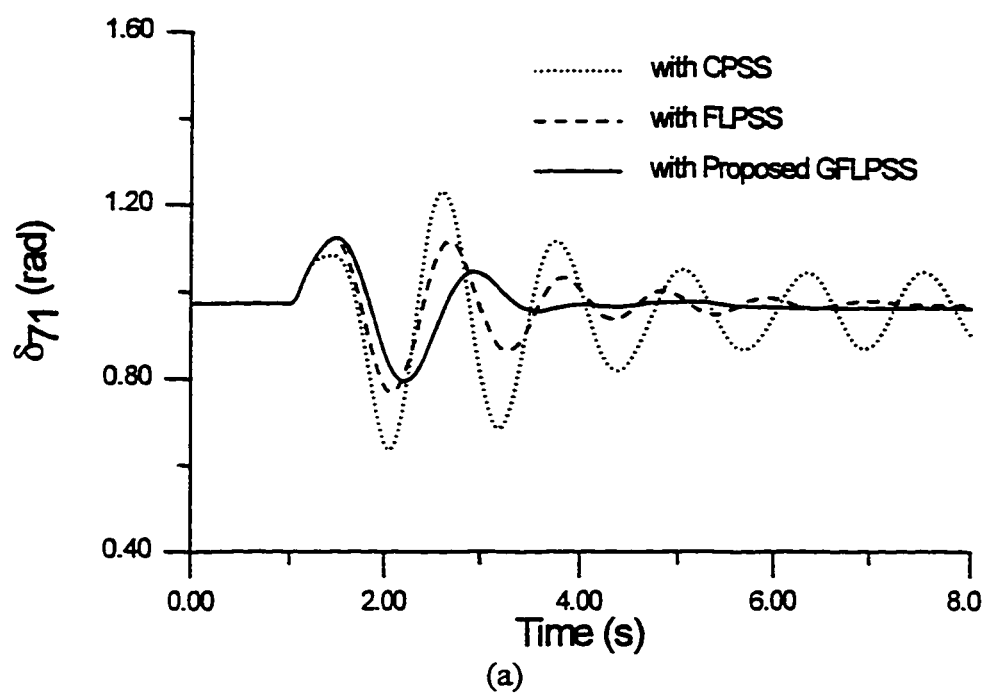
Fig 9.20 Generator G7 response for disturbance (a)
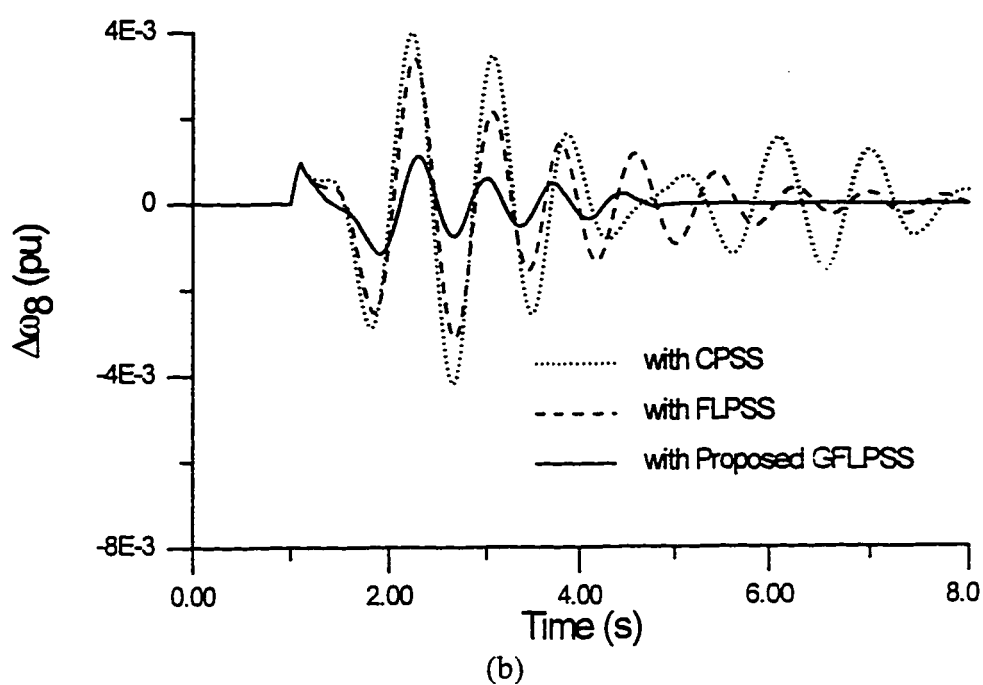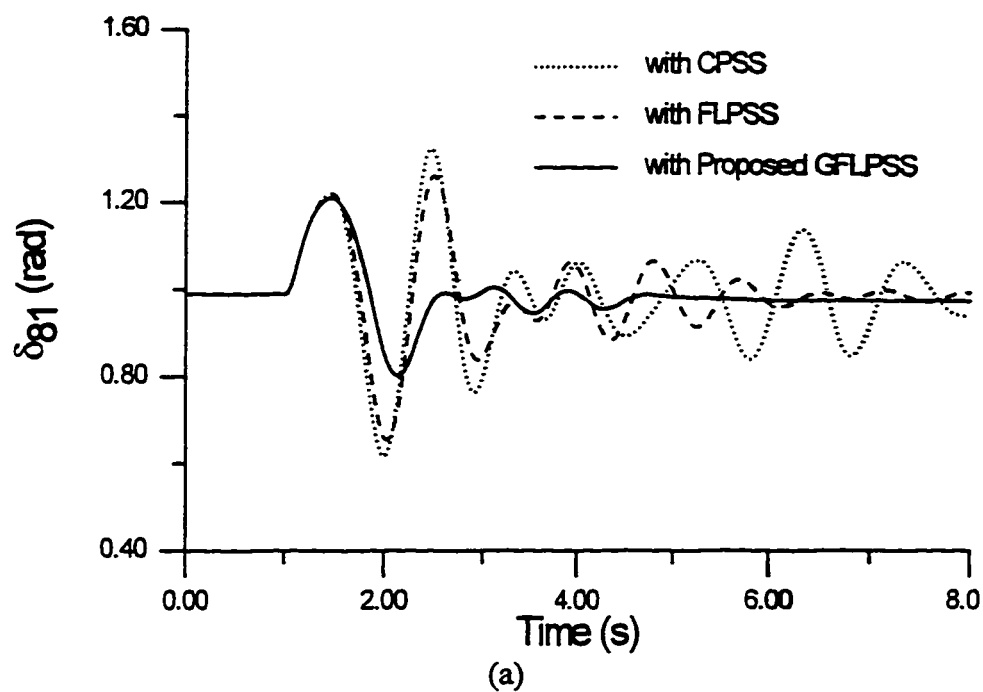
Fig 9.21 Generator G8 response for disturbance (a)
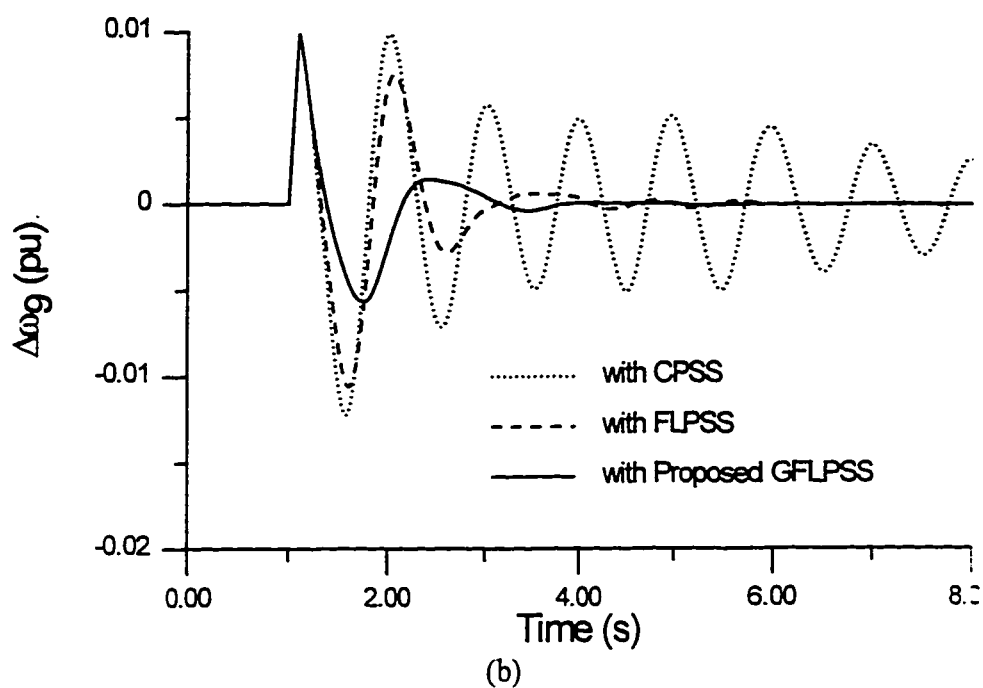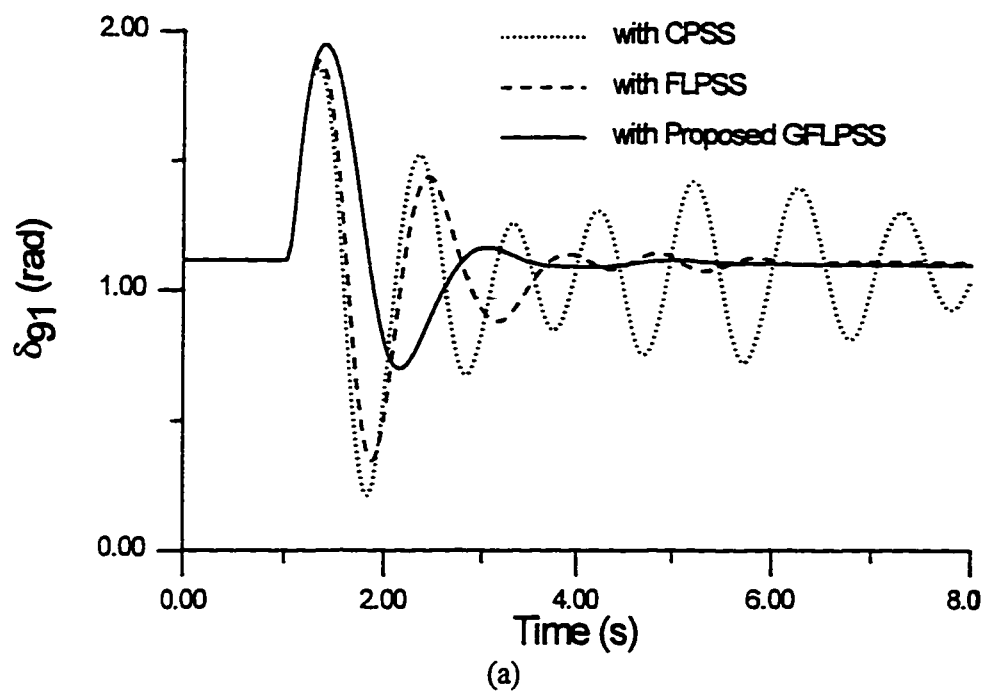
Fig 9.22 Generator G9 response for disturbance (a)

The speed deviations of generators G5 through G9 for disturbances (b) and (c) are shown in Figs. 9.23 and 9.24 respectively. It is obvious that the system performance with the proposed GFLPSSs is greatly improved and the settling times of speed deviations are much reduced. In addition, the results show the ability of the proposed GFLPSS to damp out local modes and interarea modes of oscillations as well.
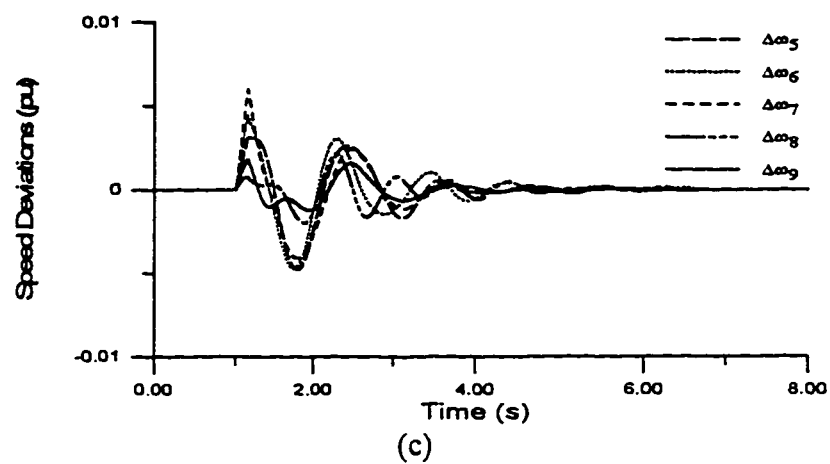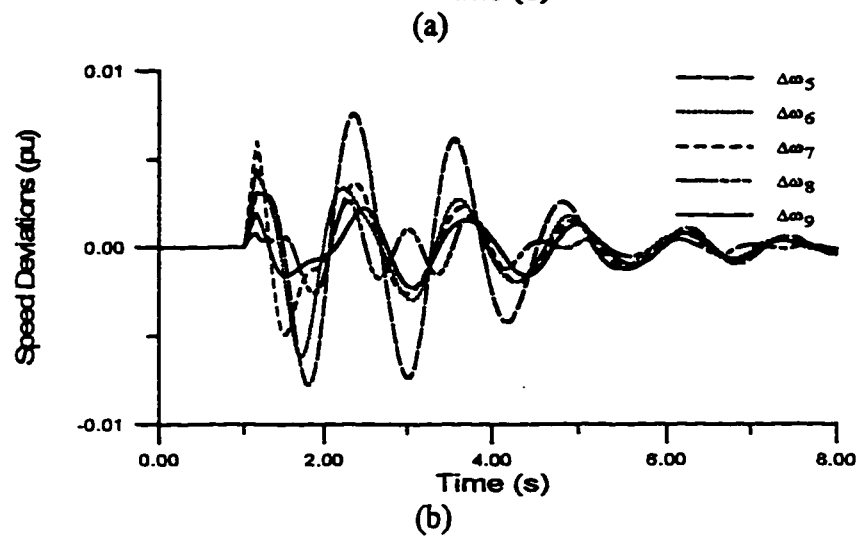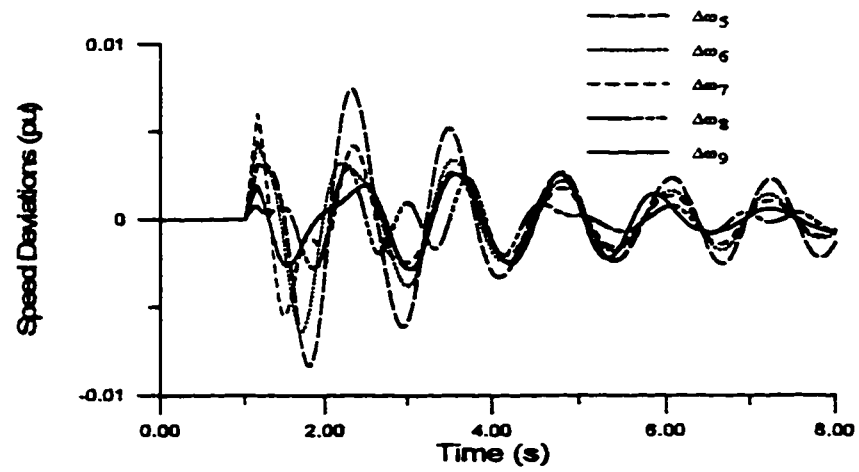
Fig 9.23 System responses for disturbance (b)

(a) with CPSSs

(b) with FLPSSs

(c) with Proposed GFLPSSs
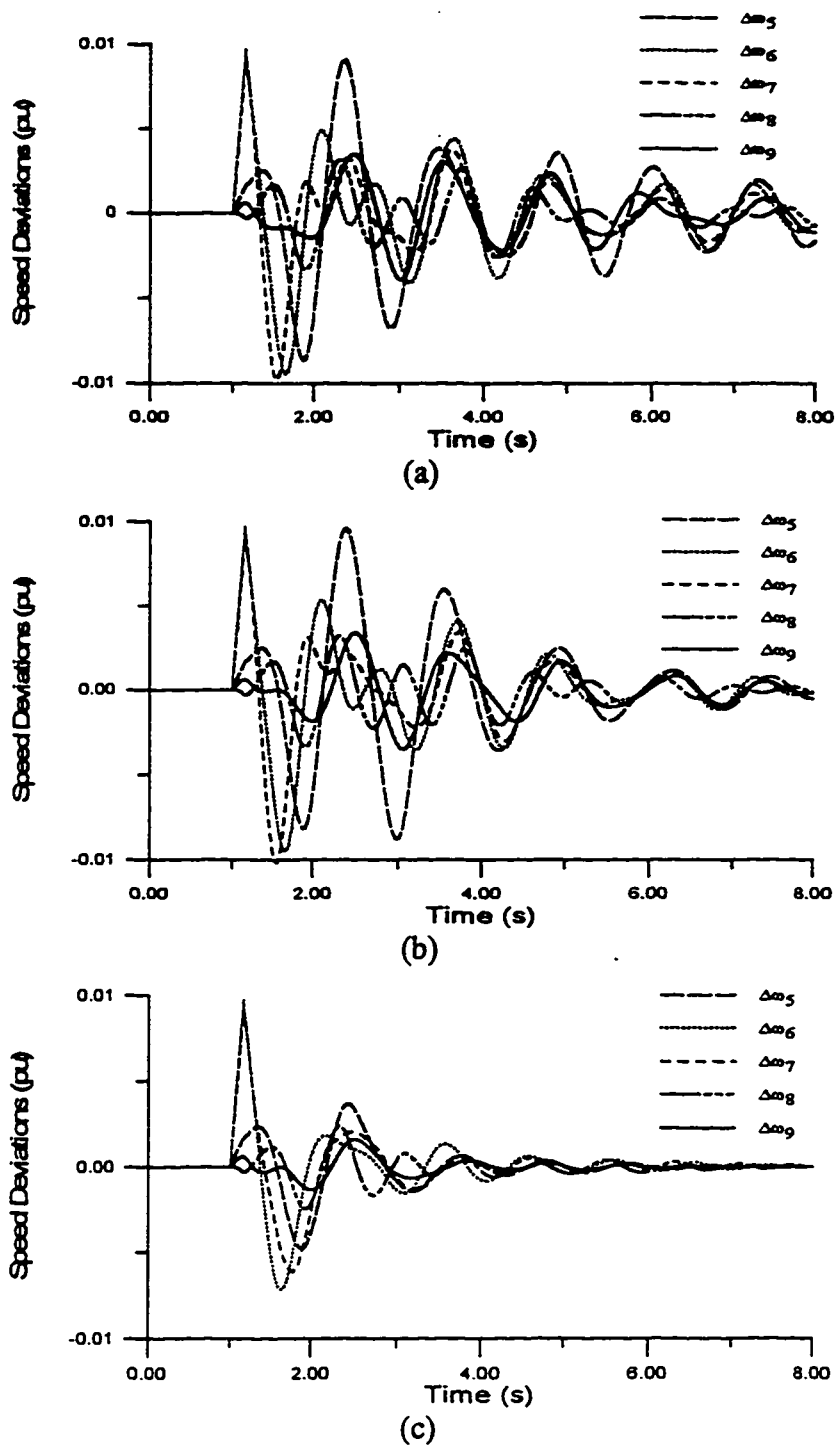
Fig 9.24 System responses for disturbance (c)

(a) with CPSSs

(b) with FLPSSs

(c) with Proposed GFLPSSs

9.6 COORDINATION BETWEEN GFLPSS AND CPSS

In most situations, the newly installed GFLPSSs will have to work together with CPSSs which already exist in a power system. In this section, system response with the proposed GFLPSSs and CPSSs working together has been also investigated. For the 10-machine 39-bus system considered in example 2, several combinations between the proposed GFLPSSs and CPSSs can be created as follows:

1. CCC
2. PCC
3. CPC
4. CCP
5. PPC
6. PCP
7. CPP
8. PPP

where C and P refer to CPSS and Proposed GFLPSS respectively. The first, second, and third letters in each combination denote the type of stabilizer installed on G5, G7, and G9 respectively.

The system responses to the disturbances (a), (b), and (c) with different combinations are shown in Figs. 9.25, 9.26, and 9.27 respectively. It can be seen that the two types of PSSs can work cooperatively. The response with the proposed GFLPSSs and CPSSs combinations is better and the oscillations are damped out much quicker than the response with only CPSSs. Generally, the system performance is improved as the number of the proposed GFLPSSs installed increases as shown in these Figs.
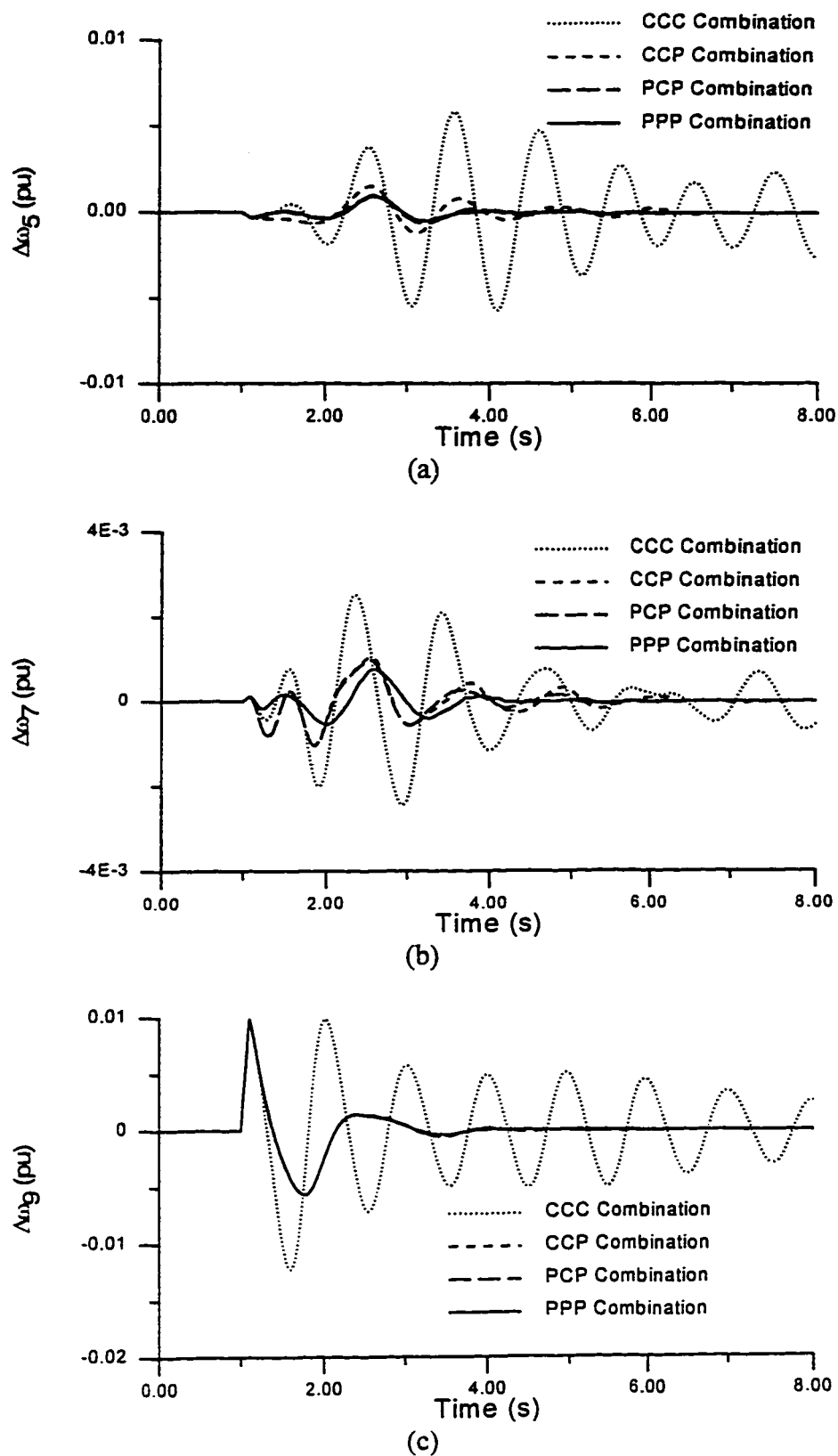
Fig. 9.25 System response with different combinations for disturbance (a)
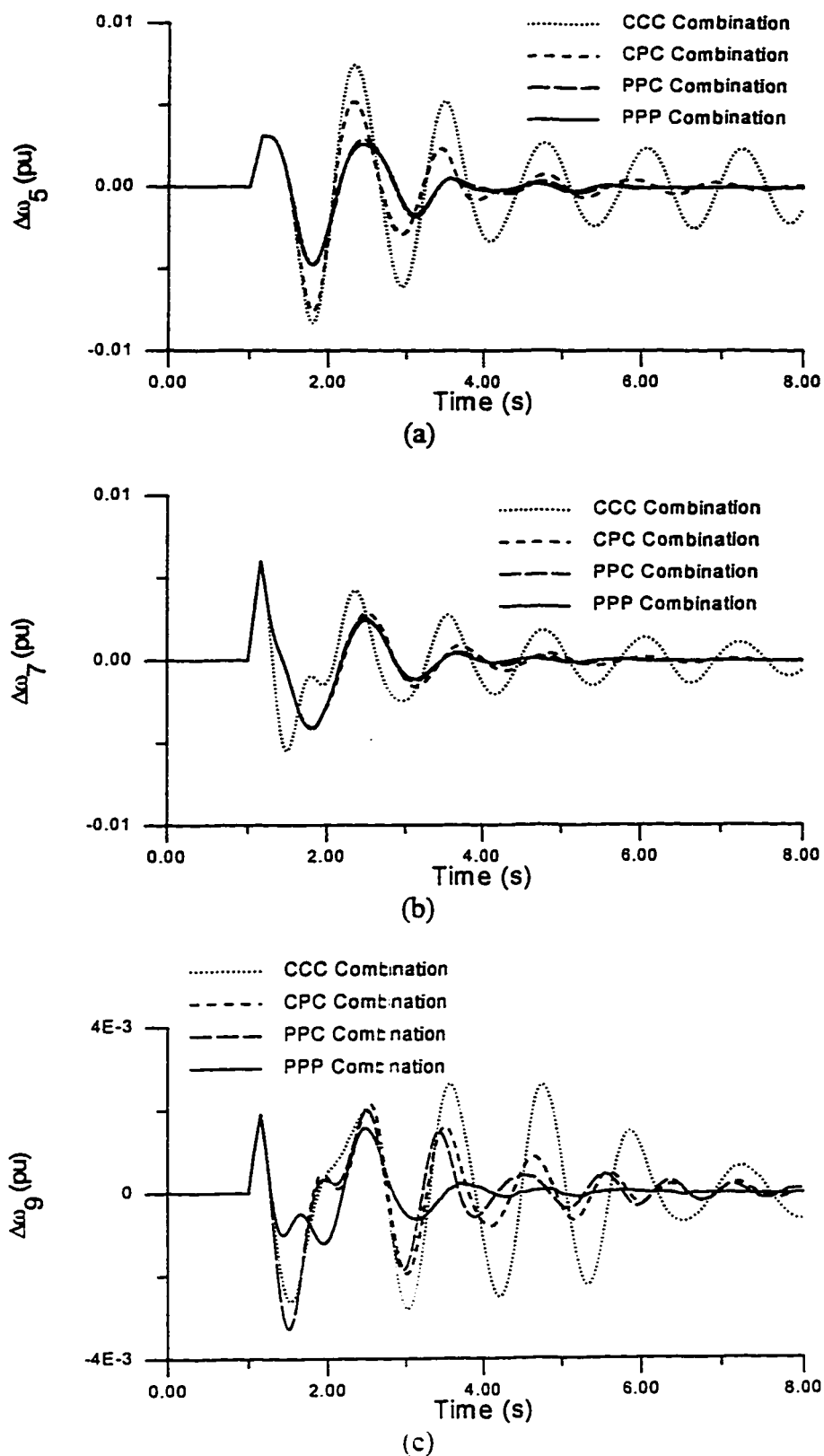
Fig. 9.26 System response with different combinations for disturbance (b)
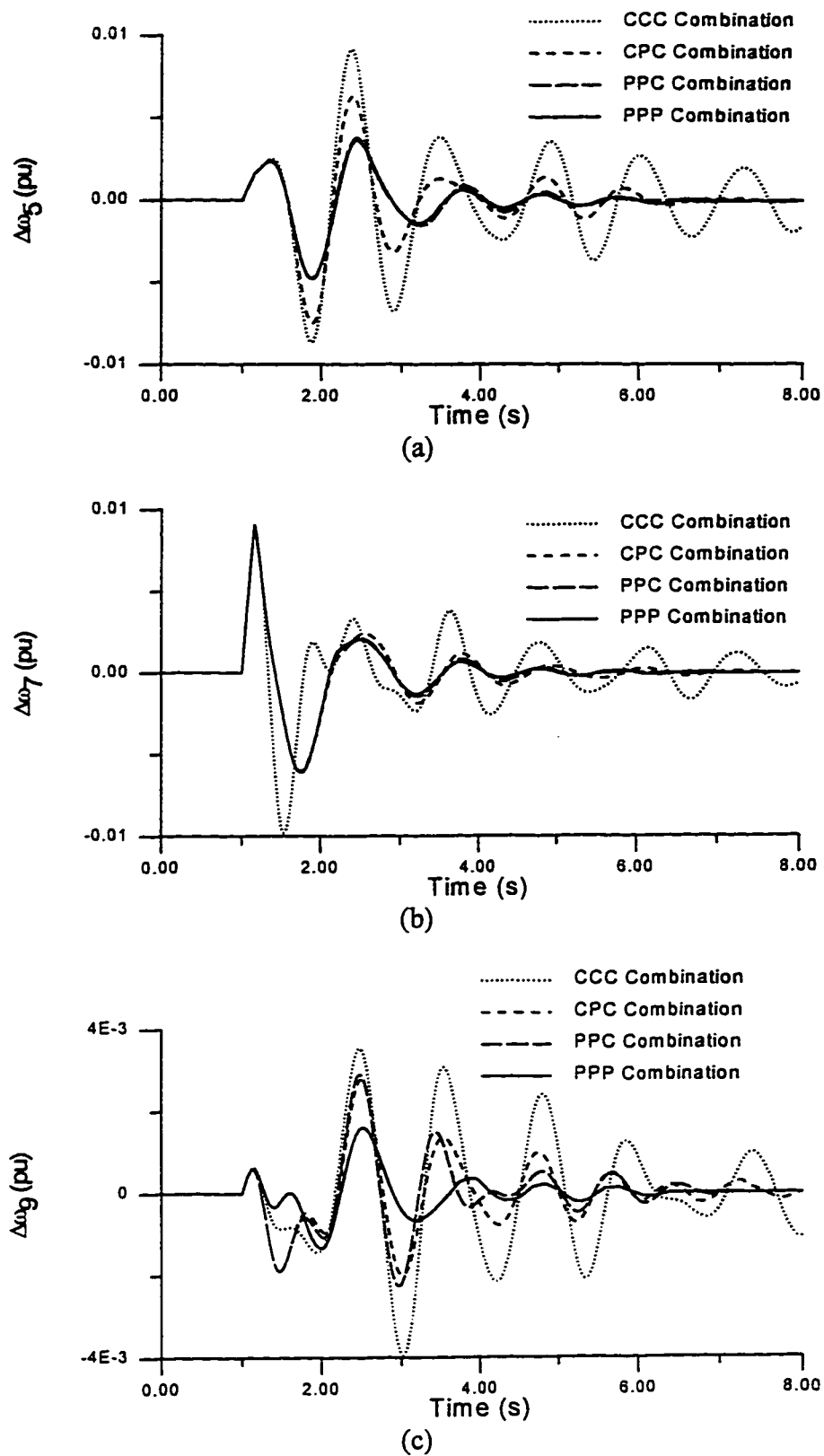
Fig. 9.27 System response with different combinations for disturbance (c)

The values of the performance indices J_1 and J_2 given in (9.15) and (9.17) for all combinations and disturbances are given in Tables 9.3, 9.4, and 9.5. It is seen that the values of the performance indices with any combination that includes any number of the proposed GFLPSSs are much reduced as compared to the cases with CPSSs. This reflects small settling times, small speed deviations, and small steady state errors. However, the values of the performance indices are reduced as the number of the proposed GFLPSSs installed increases.

9.7 SUMMARY

This chapter proposes a novel approach to hybridize the FLPSS with GA. In the proposed approach, GA are used to search for optimal parameters of FLPSS. The proposed GFLPSS has been tested in a single machine and in multimachine power systems. The coordination of the proposed GFLPSS with the CPSS has been investigated. The results show the ability of the proposed GFLPSS to damp out the local as well as the inter-area modes of oscillations. In addition, the proposed GFLPSS show its potential to work cooperatively with the CPSS.

Generally, the proposed GFLPSS shows better results than GPSS and GRBPSS proposed in chapters 7 and 8 respectively in the sense that the system with this stabilizer has better damping characteristics to different modes of oscillations.

TABLE 9.3 Values of performance indices with all combinations for disturbance (a)

Stabilizer Type and Location			Performance Index	
G5	G7	G9	J_1	J_2
without	without	without	236.401	11.7624
CPSS	CPSS	CPSS	20.3367	2.5561
GFLPSS	CPSS	CPSS	4.2198	1.2760
CPSS	GFLPSS	CPSS	4.4672	1.3101
CPSS	CPSS	GFLPSS	0.3575	0.3391
GFLPSS	GFLPSS	CPSS	3.9181	1.2290
GFLPSS	CPSS	GFLPSS	0.2465	0.3200
CPSS	GFLPSS	GFLPSS	0.2502	0.3216
GFLPSS	GFLPSS	GFLPSS	0.2045	0.3079

TABLE 9.4 Values of performance indices with all combinations for disturbance (b)

Stabilizer Type and Location			Performance Index	
G5	G7	G9	J_1	J_2
without	without	without	50.7242	4.0678
CPSS	CPSS	CPSS	14.1141	2.2615
GFLPSS	CPSS	CPSS	2.5734	1.2739
CPSS	GFLPSS	CPSS	2.0776	1.1591
CPSS	CPSS	GFLPSS	3.7721	1.4669
GFLPSS	GFLPSS	CPSS	1.2708	0.9292
GFLPSS .	CPSS	GFLPSS	1.6514	1.0919
CPSS	GFLPSS	GFLPSS	1.3959	1.0043
GFLPSS	GFLPSS	GFLPSS	0.8276	0.8017

TABLE 9.5 Values of performance indices with all combinations for disturbance (c)

Stabilizer Type and Location			Performance Index	
G5	G7	G9	J_1	J_2
without	without	without	62.6730	5.3128
CPSS	CPSS	CPSS	16.0893	2.9121
GFLPSS	CPSS	CPSS	3.7046	1.7957
CPSS	GFLPSS	CPSS	2.6404	1.4283
CPSS	CPSS	GFLPSS	5.1512	2.0475
GFLPSS	GFLPSS	CPSS	1.7177	1.1963
GFLPSS	CPSS	GFLPSS	3.0212	1.6689
CPSS	GFLPSS	GFLPSS	2.0569	1.3208
GFLPSS	GFLPSS	GFLPSS	1.4945	1.1198

CHAPTER 10

CONCLUSION

10.1 CONCLUSIONS

This dissertation has introduced several intelligent techniques and hybrid systems to power system identification, on one side, and power system stabilizer design, on the other side.

On the basis of analysis and results presented in this dissertation, the following conclusions may be drawn:

1. A novel off-line identification scheme for synchronous machines was proposed. The proposed scheme exploits the universal approximation property of radial basis function networks. Two different learning algorithms have been considered to show the potential of the proposed identifier to capture the nonlinear characteristics of synchronous machines. The proposed identifier was tested and validated under different variations in synchronous machine inputs. Moreover, a comparison between

the proposed radial basis function network identifier and backpropagation network identifier has been carried out to show the superiority of the proposed identifier.

2. A novel on-line identification scheme for synchronous machines was proposed. The proposed identifier is aimed to produce a one-step-ahead prediction of the synchronous machine outputs. A recursive learning algorithm has been developed to update the proposed identifier parameters in real-time. The proposed identifier was tested and validated under different variations in machine inputs. Fast learning capability of the proposed identifier to the nonlinear characteristics of synchronous machines has been demonstrated.

3. A novel scheme for the adaptive on-line tuning of power system stabilizer parameters using radial basis function networks was proposed. The proposed scheme is aimed to re-tune the PSS parameters based on real-time measurements of machine loading conditions. The ability of the proposed scheme to enhance power system stability has been presented.

4. A novel on-line hybrid neuro-fuzzy power system stabilizer was proposed. The proposed stabilizer incorporates the linguistic and numerical information in a uniform fashion and combines the strengths of neural networks and fuzzy logic systems. The proposed scheme uses fuzzy basis function networks to re-tune the PSS parameters based on real-time measurements of machine loading conditions. Moreover, a comparison between RBFN and FBFN based PSSs has been carried out.

5. A scheme to incorporate GA into the design of PSSs was proposed. The proposed scheme is aimed to waive the linearization step in conventional PSS design. In

addition, the coordination between the proposed stabilizer and the existing conventional stabilizers has been investigated.

6. A novel scheme for hybridizing the rule-based PSSs with GA was proposed. The proposed scheme overcomes the problems of rule-based PSS design by allowing GA to search for optimal parameters of the stabilizer.

7. A hybrid genetic-based fuzzy logic PSS was also proposed. The proposed scheme employs GA to search for optimal settings of fuzzy logic PSS parameters. The coordination of the proposed stabilizer with other existing stabilizers has been examined.

8. In case of insufficient number of training patterns, FBFN has better approximation capabilities and more robust than RBFN.

9. All the proposed schemes were tested through their applications to single machine infinite bus systems and multimachine power systems. The results of the proposed schemes were compared with those of conventional techniques reported in the literature. It has been found that the system performance is greatly improved when using the proposed schemes.

10. Upon applying the proposed schemes, it has been found that the hybrid systems such as neuro-fuzzy, genetic rule-based, and genetic-based fuzzy logic systems have better performance. This is because hybridizing two techniques combines their different strengths and overcomes their shortcomings and weaknesses.

11. All the proposed schemes are of a decentralized nature since all of them rely on local measurements. Therefore, they are easy to tune and install. In addition, the proposed

stabilizers do not require real-time parameter estimation. This makes them easy to implement on a microcomputer.

12. All computer programs used throughout this work were created personally in FORTRAN such as k-means, OLS, BP, on-line identification algorithm, GA design programs, nonlinear simulation of single machine infinite bus and multimachine power systems with several types of disturbances using the conventional as well as the proposed stabilizers.

10.2 SUGGESTION FOR FUTURE RESEARCH

For future research the following directions are recommended:

1. Application of the proposed identification schemes to load modeling and identification.

2. Investigation of the coordination of the proposed stabilizers with SVC to damp out power system oscillations.

3. Hybridizing the k-means learning algorithm and the orthogonal least squares learning algorithm for training of RBFN. This will combine the good features in both algorithms and overcome the prespecified number of centers of k-means algorithm.

4. Exploiting the capability of the GA to search for the optimal centers and widths of RBFN.

5. Extension of the proposed schemes to other types of stabilizers such as nonlinear variable structure stabilizers.

6. Exploiting the new technology of VLSI to implement the proposed schemes and test them practically on a micro-machine power system model.

7. Developing the proposed schemes to be self-organized and self-learned in real-time via interaction with the environment.

8. Examining the feasibility of applying other types of neural networks.

9. Developing strategies for on-line application of the proposed hybrid genetic based stabilizers in real-time by modifying the GA to match the on-line environment requirements.

10. Exploiting the capability of the GA to prepare the training patterns for radial basis function networks as well as fuzzy basis function networks.

Some of these topics are already under serious investigation by the author.

APPENDIX A

FLUX-LINKAGE MODEL

System Model:

$$\rho\delta = \omega_b(\omega - 1) \tag{A.1}$$

$$\rho\omega = [T_m - T_e - D(\omega - 1)]/M \tag{A.2}$$

$$\rho\psi_d = \omega_b(V_d + r_a i_d + \omega\psi_q) \tag{A.3}$$

$$\rho\psi_q = \omega_b(V_q + r_a i_q - \omega\psi_d) \tag{A.4}$$

$$\rho\psi_F = \omega_b(V_F - r_F i_F) \tag{A.5}$$

$$\rho\psi_D = \omega_b(-r_D i_D) \tag{A.6}$$

$$\rho\psi_Q = \omega_b(-r_Q i_Q) \tag{A.7}$$

$$T_e = i_q\psi_d + i_d\psi_q \tag{A.8}$$

$$V_d = V_b \sin\delta + R_T i_d - X_T i_q \tag{A.9}$$

$$V_q = V_b \cos\delta + R_T i_q + X_T i_d \tag{A.10}$$

$$V = \sqrt{V_d^2 + V_q^2} \tag{A.11}$$

$$\begin{bmatrix} \psi_d \\ \psi_F \\ \psi_D \end{bmatrix} = \begin{bmatrix} x_d & x_{md} & x_{md} \\ x_{md} & x_F & x_{md} \\ x_{md} & x_{md} & x_D \end{bmatrix} \begin{bmatrix} -i_d \\ i_F \\ i_D \end{bmatrix} \tag{A.12}$$

$$\begin{bmatrix} \psi_q \\ \psi_Q \end{bmatrix} = \begin{bmatrix} x_q & x_{mq} \\ x_{mq} & x_Q \end{bmatrix} \begin{bmatrix} -i_q \\ i_Q \end{bmatrix} \tag{A.13}$$

Parameters:

$\omega_b = 377$ rad/s;	$M = 6.5$ pu;	$x_d = 2.0$;
$x_q = 1.91$;	$x_F = 1.97$;	$x_{md} = 1.86$;
$x_{mq} = 1.77$;	$x_D = 1.94$;	$x_Q = 1.96$;
$r_F = 0.0015$;	$r_a = 0.005$;	$r_D = 0.0078$;
$r_Q = 0.0084$;	$R_T = 0.063$;	$X_T = 0.45$;
$D = 0.0$		

All resistances and reactances are in per-unit.

APPENDIX B

System Model:

$$p\delta = \omega_b(\omega - 1) \tag{B.1}$$

$$p\omega = (T_m - T_e - D(\omega - 1)) / M \tag{B.2}$$

$$pE_q' = (E_{fd} - (x_d - x_d')i_d - E_q') / T_{do}' \tag{B.3}$$

$$pE_{fd} = (K_a(V_{ref} - V + U_c) - E_{fd}) / T_a \tag{B.4}$$

$$V_d = V_b \sin\delta + R_e i_d - X_e i_q \tag{B.5}$$

$$V_q = V_b \cos\delta + R_e i_q + X_e i_d \tag{B.6}$$

$$V = \sqrt{V_d^2 + V_q^2} \tag{B.7}$$

$$T_e = E_q' i_q - (x_d' - x_q)i_d i_q \tag{B.8}$$

Parameters:

M=4.74s,	ω_b=377rad/s,	x_d=1.7,
x_q=1.64,	x_d' =0.245,	R_e=0.02,
X_e=0.4,	D=0.0,	T_{do}' =5.9,
T_a=0.05,	K_a=400,	T_2=0.1,
$-7.3pu \le E_{fd} \le 7.3pu$,	$-0.12pu \le U_c \le 0.12pu$	

All resistances and reactances are in per-unit and time constants are in seconds.

APPENDIX C

HEFFRON-PHILLIPS-DEMELLO-CONCORDIA LINEARIZED MODEL
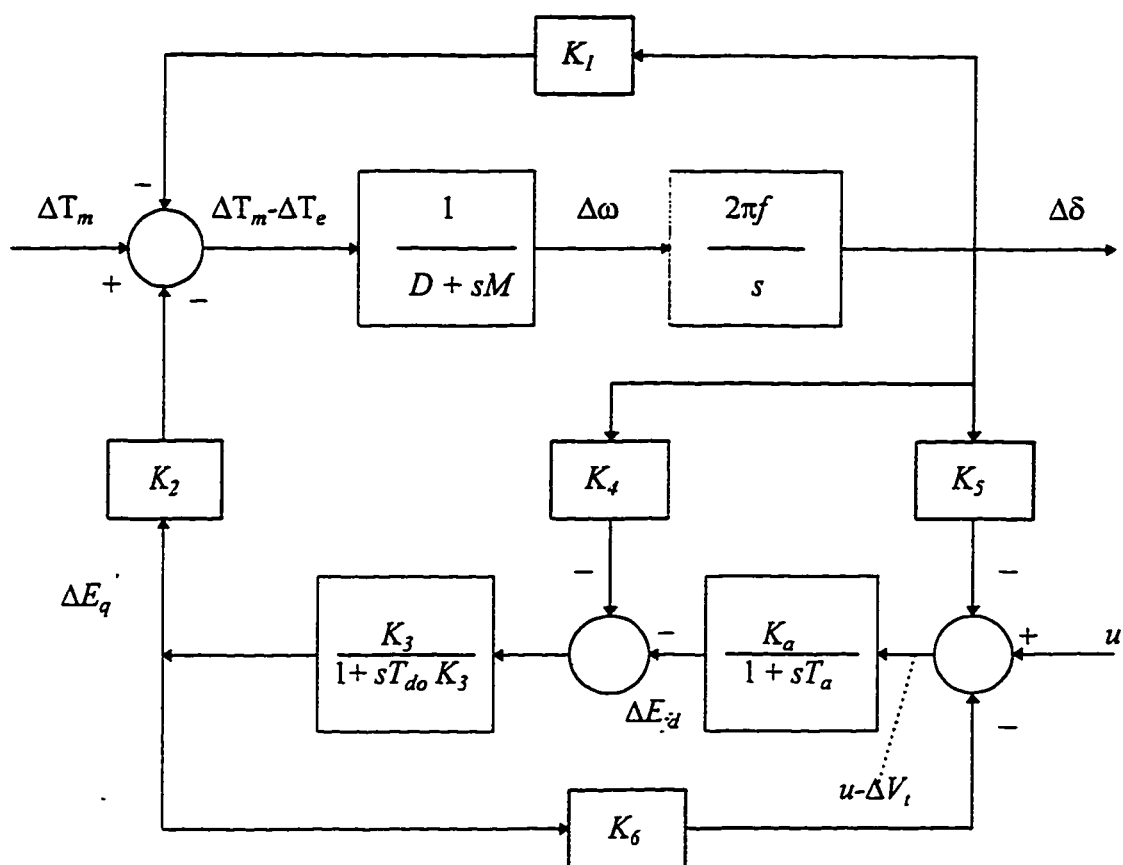
Fig. C.1 Linearized incremental model of a synchronous machine

System Model:

$$\rho[X] = [A][X] + [B][U] \qquad (C.1)$$

where;

$$[X] = [\Delta\omega \quad \Delta\delta \quad \Delta E_q^{'} \quad \Delta E_{fd}]^T \qquad (C.2)$$

$$[A] = \begin{bmatrix} 0 & -K_1/M & -K_2/M & 0 \\ \omega_b & 0 & 0 & 0 \\ 0 & -K_4/T_{do}^{'} & -1/(T_{do}^{'}K_3) & 1/T_{do}^{'} \\ 0 & -K_aK_5/T_a & -K_aK_6/T_a & -1/T_a \end{bmatrix} \qquad (C.3)$$

$$[B] = \begin{bmatrix} 0 & 0 & 0 & K_a / T_a \end{bmatrix}^T \qquad \text{(C.4)}$$

$$K_1 = F_d(x_d - x'_d)i_{q0} + F_q[E'_{q0} + (x_q - x'_d)i_{d0}] \qquad \text{(C.5)}$$

$$K_2 = Y_d(x_d - x'_d)i_{q0} + Y_q[E'_{q0} + (x_q - x'_d)i_{d0}] + i_{q0} \qquad \text{(C.6)}$$

$$K_3 = 1 / [1 + (x_d - x'_d)Y_d] \qquad \text{(C.7)}$$

$$K_4 = (x_d - x'_d)F_d \qquad \text{(C.8)}$$

$$K_5 = (-F_d x'_d V_{q0} + F_q x_q V_{d0}) / V_0 \qquad \text{(C.9)}$$

$$K_6 = (V_{q0} - Y_d x'_d V_{q0} + Y_q x_q V_{d0}) / V_0 \qquad \text{(C.10)}$$

$$F_d = V_b(-R_2 \cos\delta_0 + X_1 \sin\delta_0) / Z_e^2 \qquad \text{(C.11)}$$

$$F_q = V_b(X_2 \cos\delta_0 + R_1 \sin\delta_0) / Z_e^2 \qquad \text{(C.12)}$$

$$Y_d = (C_1 X_1 - C_2 R_2) / Z_e^2 \qquad \text{(C.13)}$$

$$Y_q = (C_1 R_1 + C_2 X_2) / Z_e^2 \qquad \text{(C.13)}$$

$$Z_e^2 = R_1 R_2 + X_1 X_2 \qquad \text{(C.14)}$$

$$R_1 = R_e - C_2 x'_d \qquad \text{(C.15)}$$

$$X_1 = X_e + C_1 x_q \qquad \text{(C.16)}$$

$$R_2 = R_e - C_2 x_q \qquad \text{(C.17)}$$

$$X_2 = X_e + C_1 x'_d \qquad \text{(C.18)}$$

$$C_1 = 1 + R_e G - X_e B \qquad \text{(C.19)}$$

$$C_2 = R_e B + X_e G \qquad \text{(C.20)}$$

Parameters:

M=4.74s,	ω_b=377rad/s,	x_d=1.7,
x_q=1.64,	x'_d=0.245,	R_e=0.02,
X_e=0.4,	D=0.0,	T'_{do}=5.9,
T_a=0.05,	K_a=400,	T_2=0.1,
G=0.0,	B=0.0,	

$$-7.3pu \le E_{fd} \le 7.3pu, \qquad -0.12pu \le U_c \le 0.12pu$$

All resistances, reactances, and admittances are in per-unit and time constants are in seconds.

APPENDIX D

THREE-MACHINE NINE-BUS POWER SYSTEM

System Model:

$$\rho \delta_i = \omega_b (\omega_i - 1) \tag{D.1}$$

$$\rho \omega_i = (T_{mi} - T_{ei} - D_i(\omega_i - 1)) / M_i \tag{D.2}$$

$$\rho E'_{qi} = (E_{fdi} - (x_{di} - x'_{di})i_{di} - E'_{qi}) / T'_{doi} \tag{D.3}$$

$$\rho E'_{di} = (-(x_{qi} - x'_{qi})i_{qi} - E'_{di}) / T'_{qoi} \tag{D.4}$$

$$\rho E_{fdi} = (K_{ai}(V_{refi} - V_i + U_{ci}) - E_{fdi}) / T_{ai} \tag{D.5}$$

$$T_{ei} = E'_{qi}i_{qi} + E'_{di}i_{di} - (x'_{qi} - x'_{di})i_{di}i_{qi} \tag{D.6}$$

Generator Data:

	G1	G2	G3
H (s)	23.6400	6.4000	3.0100
x_d	0.1460	0.8958	1.3125
x_q	0.0969	0.8645	1.2578
x'_d	0.0608	0.1198	0.1813
x'_q	0.0969	0.1969	0.2500
T'_{d0}	8.9600	6.0000	5.8900
T'_{q0}	0.0000	0.5350	0.6000
D	0.0100	0.0100	0.0100
K_a	100.00	100.00	100.00
T_a	0.0500	0.0500	0.0500

Line Data:

Line No.	From Bus	To Bus	R	X	B/2
1	1	4	0.0000	0.0576	0.0000
2	4	5	0.0100	0.0850	0.0880
3	5	7	0.0320	0.1610	0.1530
4	7	2	0.0000	0.0625	0.0000
5	7	8	0.0085	0.0720	0.0745
6	8	9	0.0119	0.1008	0.1045
7	9	3	0.0000	0.0586	0.0000
8	9	6	0.0390	0.1700	0.1790
9	6	4	0.0170	0.0920	0.0790

Bus Data:

Bus No.	Voltage		Generation		Load	
	Mag. (pu)	Ang.(deg)	P (pu)	Q (pu)	P (pu)	Q (pu)
1	1.0400	0.000	0.7160	0.2700	0.0000	0.0000
2	1.0250	9.300	1.6300	0.0670	0.0000	0.0000
3	1.0250	4.700	0.8500	-0.109	0.0000	0.0000
4	1.0260	-2.20	0.0000	0.0000	0.0000	0.0000
5	0.9960	-4.00	0.0000	0.0000	1.2500	0.5000
6	1.0130	-3.70	0.0000	0.0000	0.9000	0.3000
7	1.0260	3.700	0.0000	0.0000	0.0000	0.0000
8	1.0160	0.700	0.0000	0.0000	1.0000	0.3500
9	1.0320	2.000	0.0000	0.0000	0.0000	0.0000

APPENDIX E

System Model:

$$\rho\delta = \omega_b(\omega - 1) \tag{E.1}$$

$$\rho\omega = (T_m - T_e - D(\omega - 1)) / M \tag{E.2}$$

$$\rho E_q^{'} = (E_{fd} - (x_d - x_d^{'})i_d - E_q^{'}) / T_{do}^{'} \tag{E.3}$$

$$\rho E_{fd} = (K_a(V_{ref} - V + U_c) - E_{fd}) / T_a \tag{E.4}$$

$$V_d = V_b \sin\delta + R_e i_d - X_e i_q \tag{E.5}$$

$$V_q = V_b \cos\delta + R_e i_q + X_e i_d \tag{E.6}$$

$$V = \sqrt{V_d^2 + V_q^2} \tag{E.7}$$

$$T_e = E_q^{'} i_q - (x_d^{'} - x_q)i_d i_q \tag{E.8}$$

$$T_m = T_{m0} + \Delta T_m \tag{E.9}$$

$$\rho\Delta T_v = [-K_g(\omega - 1) - \Delta T_v] / T_g \tag{E.10}$$

$$\rho\Delta T_m = (\Delta T_v - \Delta T_m) / T_t \tag{E.11}$$

Parameters:

M=9.6s,	ω_b=377rad/s,	x_d=0.973,
x_q=0.55,	$x_d^{'}$=0.19,	R_e=0.03,
X_e=0.6,	D=0.01,	$T_{do}^{'}$=7.76,
T_a=0.1,	K_a=50,	G=0.2,
B=-0.1,	K_g=0.027,	T_g=0.1,
T_t=0.3,	$-7.0pu \le E_{fd} \le 7.0pu$,	
$-0.4pu \le U_c \le 0.4pu$,	$-0.1pu/s \le \Delta T_v \le 0.1pu/s$	

All resistances, reactances, and admittances are in per-unit and time constants are in seconds.

APPENDIX F

NEW ENGLAND POWER SYSTEM

Generator Model:

$$\rho\delta_i = \omega_b(\omega_i - 1) \tag{F.1}$$

$$\rho\omega_i = (T_{mi} - T_{ei} - D_i(\omega_i - 1)) / M_i \tag{F.2}$$

$$\rho E'_{qi} = (E_{fdi} - (x_{di} - x'_{di})i_{di} - E'_{qi}) / T'_{doi} \tag{F.3}$$

$$\rho E'_{di} = (-(x_{qi} - x'_{qi})i_{qi} - E'_{di}) / T'_{qoi} \tag{F.4}$$

$$T_{ei} = E'_{qi}i_{qi} + E'_{di}i_{di} - (x'_{qi} - x'_{di})i_{di}i_{qi} \tag{F.5}$$

Exciter Model:
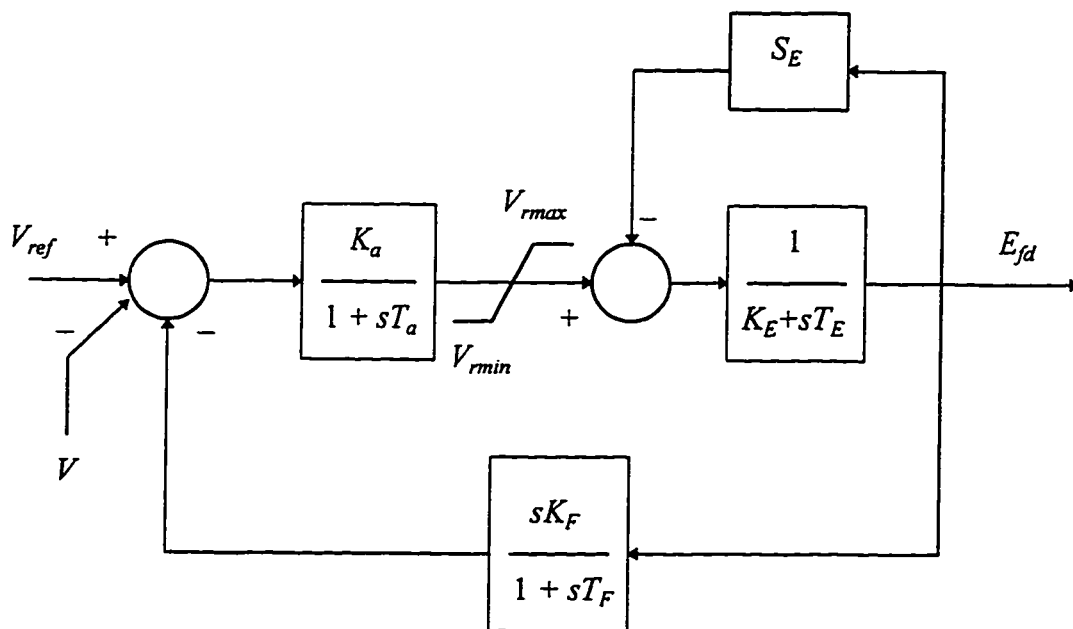
Fig. F.1 IEEE type 1 rotating excitation system model

where

$$S_E = Ae^{B.E_{fd}} \tag{F.6}$$

$$EX_2 = \frac{V_{rmax}}{K_E + C_2} \tag{F.7}$$

$$EX_1 = 0.75EX_2 \tag{F.8}$$

$$B = \ln(C_2 / C_1) / (EX_2 - EX_1) \tag{F.9}$$

$$A = C_2 / e^{B.EX_2} \tag{F.10}$$

Exciter Data:

	G1	G2	G3	G4	G5	G6	G7	G8	G9	G10
K_a	0.0	6.2	5.0	5.0	40.0	5.0	40.0	5.0	40.0	5.0
T_a	0.0	0.05	0.06	0.06	0.02	0.02	0.02	0.02	0.02	0.06
V_{rmin}	0.0	-1.0	-1.0	-1.0	-10.0	-1.0	-6.5	-1.0	-10.0	-1.0
V_{rmax}	0.0	1.0	1.0	1.0	10.0	1.0	6.5	1.0	10.0	1.0
K_E	0.0	-.633	-0.02	-.053	1.0	-.042	1.0	-.047	1.0	-.049
T_E	0.0	0.405	0.500	0.500	0.785	0.471	0.730	0.528	1.400	0.250
K_F	0.0	0.057	0.080	0.080	0.030	0.075	0.030	0.085	0.030	0.040
T_F	0.0	0.5	1.0	1.0	1.0	1.246	1.0	1.26	1.0	1.0
C_1	0.0	0.66	0.13	0.08	0.07	0.064	0.53	0.072	0.62	0.08
C_2	0.0	0.88	0.34	0.314	0.91	0.251	0.74	0.282	0.85	0.26

G1 has constant excitation.

Generator Data:

	G1	G2	G3	G4	G5	G6	G7	G8	G9	G10
H (s)	500.0	30.3	35.8	28.6	26.0	34.8	26.4	24.3	34.5	42.0
x_d	0.020	0.295	0.250	0.262	0.670	0.254	0.295	0.290	0.211	0.100
x_q	0.019	0.282	0.237	0.258	0.620	0.241	0.292	0.280	0.205	0.069
x_d'	0.006	0.070	0.053	0.044	0.132	0.050	0.049	0.057	0.057	0.031
x_q'	0.008	0.170	0.088	0.166	0.166	0.081	0.186	0.091	0.059	0.008
T_{d0}'	7.00	6.56	5.70	5.69	5.40	7.30	5.66	6.70	4.79	10.2
T_{q0}'	0.70	1.50	1.50	1.50	0.44	0.40	1.50	0.41	1.96	0.00
D	70.0	9.75	10.0	10.0	7.00	10.0	8.00	9.00	30.0	4.00

Line Data:

Line No.	From Bus	To Bus	R	X	B	Tap (%)
1	39	31	0.0035	0.0411	0.6987	0.00
2	39	1	0.0010	0.0250	0.7500	0.00
3	31	32	0.0013	0.0151	0.2572	0.00
4	31	25	0.0070	0.0086	0.1460	0.00
5	32	33	0.0013	0.0213	0.2214	0.00
6	32	18	0.0011	0.0133	0.2138	0.00
7	33	34	0.0008	0.0128	0.1342	0.00
8	33	14	0.0008	0.0129	0.1382	0.00
9	34	35	0.0002	0.0026	0.0434	0.00
10	34	37	0.0008	0.0112	0.1476	0.00
11	35	36	0.0006	0.0092	0.1130	0.00
12	35	11	0.0007	0.0082	0.1389	0.00
13	36	37	0.0004	0.0046	0.0780	0.00
14	37	38	0.0023	0.0363	0.3804	0.00

Line Data Contd

Line No.	From Bus	To Bus	R	X	B	Tap (%)
15	38	1	0.0010	0.0250	1.2000	0.00
16	30	11	0.0004	0.0043	0.0729	0.00
17	30	13	0.0004	0.0043	0.0729	0.00
18	13	14	0.0009	0.0101	0.1723	0.00
19	14	15	0.0018	0.0217	0.3660	0.00
20	15	16	0.0009	0.0094	0.1710	0.00
21	16	17	0.0007	0.0089	0.1342	0.00
22	16	19	0.0016	0.0195	0.3040	0.00
23	16	21	0.0008	0.0135	0.2548	0.00
24	16	24	0.0003	0.0059	0.0680	0.00
25	17	18	0.0007	0.0082	0.1319	0.00
26	17	27	0.0013	0.0173	0.3216	0.00
27	21	22	0.0008	0.0140	0.2565	0.00
28	22	23	0.0006	0.0096	0.1846	0.00
29	23	24	0.0022	0.0350	0.3610	0.00
30	25	26	0.0032	0.0323	0.5130	0.00
31	26	27	0.0014	0.0147	0.2396	0.00
32	26	28	0.0043	0.0474	0.7802	0.00
33	26	29	0.0057	0.0625	1.0290	0.00
34	28	29	0.0014	0.0151	0.2490	0.00
35	12	11	0.0016	0.0435	0.0000	-0.6
36	12	13	0.0016	0.0435	0.0000	0.60
37	35	2	0.0000	0.0250	0.0000	-7.0
38	30	3	0.0000	0.0200	0.0000	-7.0
39	19	4	0.0007	0.0142	0.0000	-7.0
40	20	5	0.0009	0.0180	0.0000	-0.9
41	22	6	0.0000	0.0143	0.0000	-2.5
42	23	7	0.0005	0.0272	0.0000	0.00
43	25	8	0.0006	0.0232	0.0000	-2.5
44	31	10	0.0000	0.0181	0.0000	-2.5
45	29	9	0.0008	0.0156	0.0000	-2.5
46	19	20	0.0007	0.0138	0.0000	6.00

Bus Data:

Bus No.	Voltage		Generation		Load	
	Mag. (pu)	Ang.(deg)	P (pu)	Q (pu)	P (pu)	Q (pu)
1	1.0300	0.0000	10.0000	0.8804	11.0400	2.5000
2	0.9820	10.882	5.6330	2.0541	0.0920	0.0460
3	0.9831	12.667	6.5000	2.0578	0.0000	0.0000
4	0.9972	13.178	6.3200	1.0897	0.0000	0.0000
5	1.0123	11.739	5.0800	1.6700	0.0000	0.0000
6	1.0493	15.150	6.5000	2.1115	0.0000	0.0000
7	1.0635	17.843	5.6000	1.0046	0.0000	0.0000
8	1.0278	12.318	5.4000	0.0093	0.0000	0.0000
9	1.0265	17.583	8.3000	0.2278	0.0000	0.0000
10	1.0475	6.7000	2.6040	1.4535	0.0000	0.0000
11	1.0125	3.8500	0.0000	0.0000	0.0000	0.0000
12	0.9998	3.8410	0.0000	0.0000	0.0850	0.8880
13	1.0142	3.9610	0.0000	0.0000	0.0000	0.0000
14	1.0117	2.3080	0.0000	0.0000	0.0000	0.0000
15	1.0158	1.9200	0.0000	0.0000	3.2000	1.5300
16	1.0322	3.3370	0.0000	0.0000	3.2940	0.3230
17	1.0339	2.3510	0.0000	0.0000	0.0000	0.0000
18	1.0313	1.5150	0.0000	0.0000	1.5800	0.3000
19	1.0500	7.9610	0.0000	0.0000	0.0000	0.0000
20	0.9910	6.5490	0.0000	0.0000	6.8000	1.0300
21	1.0321	5.7420	0.0000	0.0000	2.7400	1.1500
22	1.0500	10.189	0.0000	0.0000	0.0000	0.0000
23	1.0450	9.9910	0.0000	0.0000	2.4750	0.8460
24	1.0377	3.4560	0.0000	0.0000	3.0860	-0.922
25	1.0575	5.5330	0.0000	0.0000	2.2400	0.4720
26	1.0521	4.2480	0.0000	0.0000	1.3900	0.1700
27	1.0379	2.2240	0.0000	0.0000	2.8100	0.7550
28	1.0501	7.7600	0.0000	0.0000	2.0600	0.2760
29	1.0500	10.519	0.0000	0.0000	2.8350	0.2690
30	1.0170	4.6700	0.0000	0.0000	0.0000	0.0000
31	1.0490	4.1800	0.0000	0.0000	0.0000	0.0000
32	1.0304	1.2810	0.0000	0.0000	3.2200	0.0240
33	1.0038	0.4210	0.0000	0.0000	5.0000	1.8400
34	1.0051	1.5720	0.0000	0.0000	0.0000	0.0000
35	1.0074	2.2650	0.0000	0.0000	0.0000	0.0000
36	0.9967	0.0700	0.0000	0.0000	2.3380	0.8400
37	0.9958	-0.433	0.0000	0.0000	5.2200	1.7600
38	1.0281	-0.217	0.0000	0.0000	0.0000	0.0000
39	1.0475	1.5690	0.0000	0.0000	0.0000	0.0000

NOMENCLATURE

$\mathbf{x}$	neural network input vector
$\mathbf{u}$	synchronous generator input vector
$\mathbf{w}$	weight vector associated with input units
$\mathbf{v}$	weight vector associated with hidden units
$\mathbf{o}$	output vector
net	net value
$\mathbf{c}_j$	center vector of jth RBF unit
σ_j	width of jth RBF unit
μ_F	membership function
$\mathbf{y}$	time-domain simulated output vector
$\mathbf{y}_{net}$	network output vector
$\mathcal{T}_N$	set of training patterns
n	No. of inputs
m	No. of hidden units
c	No. of output units
n_n	No. of nearest neighbor centers
N	No. of training patterns
$\mathbf{t}$	target vector
$\mathbf{e}$	error vector
Γ_{xx}	auto-correlation function
Γ_{yx}	cross-correlation function
$\lambda(t)$	unit impulse function
f_s	nonlinear function expansion of lagged inputs and outputs
f_n	network approximation of f_s
n_y	lags of outputs
n_u	lags of inputs
α	learning rate
μ	forgetting factor
d	desired value
δ	torque angle
ω	angular speed
ω_b	synchronous speed
M	inertia constant
i_d , i_q	stator currents in d and q axis circuits respectively
V_d , V_q	terminal voltage in d and q axis circuits respectively
i_D, i_Q	damper circuit currents in d and q axes respectively
ψ	flux linkages
V_F, i_F	field voltage and current respectively
R_e, X_e	transmission line resistance and reactance respectively
x_d, x_q	synchronous reactances in d and q axes
x_{md}, x_{mq}	mutual reactances in d- and q-axis respectively
r_F, x_F	field winding resistance and self-reactance respectively
r_a	stator resistance
r_D, x_D	damper winding resistance and self-reactance in d-axis respectively

r_Q, x_Q	damper winding resistance and self-reactance in q-axis respectively
T_m, T_e	input mechanical and output electrical torques respectively
T_{m0}	initial value of mechanical torque
ΔT_m	deviation of mechanical torque
E_q'	q-axis component of internal voltage behind transient reactance
E_d'	d-axis component of internal voltage behind transient reactance
E_{fd}	equivalent excitation voltage
D	damping coefficient
V, V_{ref}	terminal and reference voltages respectively
V_b	infinite bus voltage
x_d'	d-axis transient reactance
T_{do}'	d-axis transient open circuit time constant
T_{qo}'	q-axis transient open circuit time constant
K_a, T_a	regulator gain and time constant respectively
U	PSS control signal
K_c	CPSS gain
T_1, T_2	CPSS time constants
T_w	washout time constant
ρ	first derivative d/dt
P	active power
Q	reactive power
K_p, K_i	proportional and integral gains of PI PSS respectively
G(s)	transfer function
M	No. of fuzzy rules
A	acceleration
A_s	scaled acceleration
z	operating point in the phase plane
U_{max}	maximum value of stabilizing signal
U_{min}	minimum value of stabilizing signal
V_{rmax}	maximum value of the regulator voltage
V_{rmin}	minimum value of the regulator voltage
G	gain function
N_s, P_s	membership functions
F_a	acceleration scaling factor
NM	No. of machines
Gi	ith generator
T	sampling period
J	performance index
G, B	local load conductance and susceptance respectively
K_g	governor gain
T_g	governor time constant
T_t	turbine time constant
ΔT_v	deviation of valve opening position
ANN	artificial neural network
APE	average percentage error
BPNN	backpropagation neural network

CPSS	conventional power system stabilizer
FBFN	fuzzy basis function network
GPSS	genetic-based power system stabilizer
GFLPSS	genetic-based fuzzy logic power system stabilizer
GRBPSS	genetic rule-based power system stabilizer
MSE	mean square error
OLS	orthogonal least squares
RBFN	radial basis function network
PI PSS	proportional integral power system stabilizer
SPE	sensitivity of power system stabilizer effect
pu	per unit
PF	power factor
VLSI	very large scale integrated circuits
A/D	analog to digital converter
D/A	digital to analog converter
SVC	static VAR compensators

REFERENCES

[1]   P. M. Anderson and A. A. Fouad, *Power System Control and Stability*, Iowa State Univ. Press, Ames, Iowa, U. S. A., 1977.

[2]   Y. N. Yu, *Electric Power System Dynamics*, Academic Press, 1983.

[3]   G. Cybenko, "Approximations by Superpositions of a Sigmoidal Function," *Mathematics of Control, Signals and Systems*, vol. 2, pp. 303-314, 1989.

[4]   K. Funahashi, "On the Approximate Realization of Continuous Mappings by Neural Networks," *Neural Networks*, vol. 2, pp. 183-192, 1989.

[5]   K. Hornik, M. Stinchcombe, and H. White, "Multilayer Feedforward Networks Are Universal Approximators," *Neural Networks*, vol. 2, pp. 359-366, 1989.

[6]   M.J.D. Powell, "Radial Basis Functions for Interpolation: a Review," *Proc. IMA Conf. on Algor. for the Approx. of Functions and Data*, (RMCS Shrivenham), 1985.

[7]   C.S. Micchelli, "Interpolation of Scattered Data: Distance matrices and Conditionally Positive Definite Functions," *Constructive Approximation*, vol. 2, pp. 11-22, 1986.

[8]   D.S. Broomhead and D. Lowe, "Multivariable Functional Interpolation and Adaptive Networks," *Complex Systems*, vol. 2, pp. 321-355, 1988.

[9]   E.J. Hartman, J.D. Keeler, and J.M. Kowalski, "Layered Neural Networks with Gaussian Hidden Units as Universal Approximations," *Neural Computations*, vol. 2, pp. 210-215, 1990.

[10]   J. Park and I.W. Sandberg, "Universal Approximations Using Radial Basis Function Networks," *Neural Computations*, vol. 3, pp. 246-257, 1991.

[11]   Y. Wong, "How Gaussian Radial Basis Functions Work," *International Joint Conference on Neural Networks*, Washington, USA, vol. II, pp. 133-138, 1991.

[12]   J.A. Leonard, M.A. Kramer, and L.H. Ungar, "A Neural Network Architecture That Computes Its Own Reliability," *Computers Chem. Eng*, vol. 16, no. 9, pp. 819-835, 1992.

[13]   L.A. Zadeh, "Fuzzy Sets," *Information and Control*, vol.8, pp. 338-353, 1965.

[14]   H.J. Zimmermann, *Fuzzy Set Theory and Its Applications*, Boston: Kluwer Academic Publishers. 1985.

[15]   J.H. Holland, *Adaptation in Natural and Artificial Systems*, Addison-Wesley, 1975.

[16]   D.E. Goldberg, *Genetic Algorithms in Search, Optimization, and Machine Learning*, Addison-Wesley, 1989.

[17]   L. Davis, *Handbook of Genetic Algorithms*, Van Nostrand Reinhold, New York, 1991.

[18]   R. Forsyth, *Expert Systems Principles and Case Studies*, New York, Chapman and Hall Computing, 1984.

[19]   G. C. Goodwin and R. L. Payne, *Dynamic System Identification: Experiment Design and Data Analysis*, Academic Press, 1977.

[20]   T. Soderstrom and P. Stocia, *System Identification*, Prentice Hall, 1989.

[21]   S. Chen and S.A. Billings, "Representation of Nonlinear Systems: The NARMAX Model ," *Int. J. Control*, vol. 49, no. 3, pp. 1013-1032, 1989.

[22]   K.S. Narendra and K. Parthasarathy, "Identification and Control of Dynamical Systems Using Neural Networks." *IEEE Trans. on Neural Networks*, vol. 1, no. 1, pp. 4-27, 1990.

[23]   Y. Chow and R.J. Thomas, "Neural Network Synchronous Machine Modeling," *IEEE Int. Symp. Circuits and Systems (ISCAS)*, pp. 495-498, 1989.

[24]   M. Djukanovic, D.J. Sobajic and Y.H. Pao, "Preliminary Results on Neural Net Based Simulation of Synchronous Machine Dynamic Response," *Electric Power System Research*, 25, pp. 159-168, 1992.

[25] V. Sagar, S. Vankayala, and N.D. Rao, "Artificial Neural Networks and Their Applications to Power Systems—a Bibliographical Survey," *Electric Power System Research*, 28, pp. 67-79, 1993.

[26] M. Gori and A. Tesi, "On the Problem of Local Minima in Backpropagation," *IEEE Trans. on Pattern Analysis and Machine Intelligence*, vol. 14, no. 1, pp. 76-85, 1992.

[27] K.S. Narendra, L.G. Kraft, L. Ungar, and S.T. Venkataraman, "Neural Networks for Identification and Control," *33 IEEE Conference on Decision and Control*, Workshop Number 6, December 12-13, 1994.

[28] S. Chen, S.A. Billings, C.F.N. Cowan, and P.M. Grant, "Practical Identification of NARMAX Models Using Radial Basis Functions," *Int. J. Control*, vol. 52, no. 6, pp. 1327-1350, 1990.

[29] S. Chen and S.A. Billings, "Neural Networks for Nonlinear Dynamic System Modelling and Identification," *Int. J. Control*, vol. 56, no. 2, pp. 319-346, 1992.

[30] F. Girosi and T. Poggio, "Networks and the Best Approximation Property," *Biological Cybernetics*, 63, pp. 169-176, 1990.

[31] R.M. Sanner and J.-J.E. Slotine, "Gaussian Networks for Direct Adaptive Control," *IEEE Trans. on Neural Networks*, vol. 3, no. 6, pp. 837-863, 1992.

[32] M.J.D. Powell, "Radial Basis Functions Approximations to Polynomials," *Proc. 12th biennial numerical Analysis Conf.*, Dundee, pp. 223-241, 1987.

[33] D. Gorinevsky, "On the Persistency of Excitation in Radial Basis Function Neural Network Identification of Nonlinear Systems," *IEEE Trans. on Neural Networks*, vol. 6, no. 5, pp. 1237-1244, 1995.

[34] J. Hertz, A. Krogh, and R.G. Palmer, *Introduction to the Theory of Neural Computation*, Addison-Wesley, Redwood City, CA, 1991.

[35] J. Moody and C. Darken, "Fast Learning in Networks of Locally-Tuned Processing Units," *Neural Computations*, vol. 1, no. 2, pp. 281-294, 1989.

[36]   S. Chen, C.F.N. Cowan, and P.M. Grant, "Orthogonal Least Squares Learning Algorithm for Radial Basis Function Networks," *IEEE Trans. on Neural Networks*, vol. 2, no. 2, pp. 302-309, 1991.

[37]   S. Chen, P.M. Grant, and C.F.N. Cowan,"Orthogonal Least Squares Algorithm for Training Multioutput Radial Basis Function Networks," *IEE Proc.* Pt. F, vol. 139, no. 6, pp. 378-384, 1992.

[38]   S. Chen, S.A. Billings, and W. Luo, "Orthogonal Least Squares Methods and Their Application to Nonlinear System Identification" *Int. J. Control.*, vol. 50, no. 5, pp. 1873-1896, 1989.

[39]   J. leantaritis and S.A. Billings, "Model Selection and Validation Methods for Nonlinear Systems," *Int. J. Control*, vol. 45,no. 1, pp. 311-341, 1987.

[40]   S.A. Billings and Q.M. Zhu, "Nonlinear Model Validation Using Correlation Tests," *Int. J. Control*, vol. 60, no. 6, pp. 1107-1120, 1994.

[41]   R.P. Lippmann, "An Introduction to Computing with Neural Nets, " *IEEE ASSP Magazine*, 4, pp. 4-22, 1987.

[42]   S. Chen, S.A. Billings, and P.M. Grant, "Recursive Hybrid Algorithm for Nonlinear System Identification Using Radial Basis Function Neural Networks," *Int. J. Control*, vol. 55, no. 5, pp. 1051-1070, 1992.

[43]   S.A. Billings and C.F. Fung, "Recurrent Radial Basis Function Networks for Adaptive Noise Cancellation," *Neural Networks*, vol. 8, no. 2, pp. 273-290. 1995.

[44]   J.M. Undrell, "Dynamic Stability Calculations for an Arbitrary Number of Interconnected Synchronous Machines," *IEEE Trans. PAS*, vol. 87, pp. 835-844, 1968.

[45]   F.P. deMello and C. Concordia, "Concepts of Synchronous Machine Stability as Affected by Excitation Control," *IEEE Trans. PAS*, vol. 88, pp. 316-329, 1969.

[46]   I. Nagy, "Block Diagrams and Torque-Angle Loop Analysis of Synchronous Machines," *IEEE Trans. PAS*, vol. 90, pp. 203-211, 1971.

[47]   Y.N. Yu and H. Moussa, "Optimal Stabilization of a Multimachine System," *IEEE Trans. PAS*, vol. 91, pp. 1174-1182, 1972.

[48] M.K. El-Sherbiny and D.M. Mehta, "Dynamic System Stability Part I - Investigation of the Effect of Different Loading and Excitation Systems," *IEEE Trans. PAS*, vol. 92, pp. 212-220, 1973.

[49] H. Moussa and Y.N. Yu, "Dynamic Interaction of Multimachine Power System and Excitation Control," *IEEE PES WM-T 74 119-4*, pp. 1150-1158, 1974.

[50] V.H. Quintana, M.A. Zohdy, and J.H. Anderson, "On the Design of Output Feedback Excitation controllers of Synchronous Machines," *IEEE Trans. PAS*, vol. 95, no. 3, pp. 954-961, 1976.

[51] F.P. De Mello and T.F. Laskowski, "Concepts of Power System Dynamic Stability," *IEEE Trans. PAS*, vol. 94, pp. 827-833, 1979.

[52] E.V. Larsen and D.A. Swann, "Applying Power System Stabilizers," *IEEE Trans. PAS*, vol. 100, no. 6, pp. 3017-3046, 1981.

[53] S. Lefebvre, "Tuning of Stabilizers in Multimachine Power Systems," *IEEE Trans. PAS*, vol. 102, no. 2, pp. 290-299, 1983.

[54] J. Kanniah, O.P. Malik, and G.S. Hope, "Excitaion Control of Synchronous Generators Using Adaptive Regulators Part I - Theory and Simulation Results," *IEEE Trans. PAS*, vol. 103, no. 5, pp. 897-903, 1984.

[55] Y.Y. Hsu and C.Y. Hsu, "Design of a Proportional-Integral Power System Stabilizer," *IEEE Trans. PWRS*, vol. 1, no. 2, pp. 46-53, 1986.

[56] Q. Lu and Y.Z. Sun, "Nonlinear Stabilizing Control of Multimachine Power Systems," *IEEE Trans. PWRS*, vol. 4, no. 1, pp. 236-241, 1989.

[57] P. Kundur, M. Klein, G.J. Rogers, and M.S. Zywno, "Application of Power System Stabilizers for Enhancement of Overall System Stability," *IEEE Trans. PWRS*, vol. 4, no. 2, pp. 614-626, 1989.

[58] E.Z. Zhou, O.P. Malik, and G.S. Hope, "Design of Stabilizer for a Multimachine Power System Based on the Sensitivity of PSS Effect," *IEEE Trans. on Energy Conversion*, vol. 7, no. 3, pp. 606-613, 1992.

[59] D. Xia and G.T. Heydt, "Self-Tuning Controller for Generator Excitation Control," *IEEE Trans. PAS*, vol. 102, pp. 1877-1885, 1983.

[60] Y.Y. Hsu and K.L. Liou, "Design of Self-Tuning PID Power System Stabilizers for Synchronous Generators," *IEEE Trans. on Energy Conversion*, vol. 2, no. 3, pp. 343-348, 1987.

[61] A. Ghandra, O.P. Malik and G.S. Hope, "A Self-Tuning Controller for the Control of Multimachine Power Systems, " *IEEE Trans. PWRS*, vol. 3. no. 3, pp. 1065-1071, 1988.

[62] A.S. Ibrahim, B.W. Hogg and M.M. Sharaf, "Self-Tuning Controllers for Turbogenerator Excitation and Governing Systems," *IEE Proc.*, vol. 136. Pt. D. no. 5, pp. 238-251, 1989.

[63] C.M. Lim and T. Hiyama, "Self-Tuning Control Scheme for Stability Enhancement of Multimachine Power Systems," *IEE Proc.*, vol. 137, no. 4, pp. 269-275, 1990.

[64] Y.Y. Hsu and C.R. Chen, "Tuning of Power System Stabilizers Using an Artificial Neural Network," *IEEE Trans. on Energy Conversion*, vol. 6, no. 4, pp. 612-619. 1991.

[65] Q.H. Wu, B.W. Hogg. and G.W. Irwin, "A Neural Network Regulator for Turbogenerators." *IEEE Trans. on Neural Networks*, vol. 3, no. 1, pp. 95-100. 1992.

[66] H. Mori, Y. Tamaru, and S. Tsuzuki, "An Artificial Neural Net Based Technique for Power System Dynamic Stability with the Kohonen Model," *IEEE Trans. on PWRS*, vol. 7, no. 2, pp. 856-864, 1992.

[67] Y. Zhang, G.P. Chen. O.P. Malik, and G.S. Hope,"An Artificial Neural Network Based Adaptive Power System Stabilizer," *IEEE Trans. on Energy Conversion*, vol. 8, no. 1. pp. 71-77. 1993.

[68] Y. Zhang, O.P. Malik, G.S. Hope, and G.P. Chen, "Application of an Inverse Input/Output Mapped ANN as a Power System Stabilizer," *IEEE Trans. on Energy Conversion*, vol. 9, no. 3, pp. 433-440, 1994.

[69] F. Beaufays, Y.L. Abdel-Magid, and B. Widrow, "Application of Neural Networks to Load-Frequency Control in Power Systems," *Neural Networks*, vol. 7, no. 1. pp. 183-194. 1994.

[70] Y.M. Park, M.S. Choi, and K.Y. Lee, "A Decentralized Control Architecture Using Multilayer Feedforward Neural Networks for Power System Stabilization," *International Conference on Intelligent Systm Application to Power systems ISAP '94*, Montpellier. France, pp. 305-311, 1994.

[71]   S.R. Chaudhry, S.A. Zaid, and N.A. Demerdash, "An Artificial Neural Network Method for the Identification of Saturated Turbogenerator Parameters Based on a Coupled Finite element/State Space Computational Algorithm," *IEEE Trans. on Energy Conversion.* vol. 10, no. 4, pp. 625-633, 1995.

[72]   Y.M. Park, S.H. Hyun, and J.H. Lee, "Power System Stabilizer Based on Inverse Dynamics Using an Artificial Neural Network," *Electrical Power and Energy Systems*, vol. 18, no. 5, pp. 297-305, 1996.

[73]   L. Guan, S. Cheng, and R. Zhou, "Artificial Neural Network Power System Stabilizer Trained with an Improved BP Algorithm," *IEE Proc. Gener, Transm. Distrib.*, vol. 143, no. 2, pp. 135-141, 1996.

[74]   K.N. Zadeh, R.C. Meyer, and G. Cauley, "Practices and New Concepts in Power System Control." *IEEE Trans. PWRS*, vol. 11, no. 1, pp. 3-10, 1996.

[75]   D.K. Ranaweera and G.G. Karady, "Active power Contingency Ranking Using a Radial Basis Function Network." *Engineering Intelligent Systems*, vol. 2, no. 3. pp. 201-206, 1994.

[76]   D.K. Ranaweera, N.F. Hubele. and A.D. Papalexopoulos, "Application of Radial Basis Function Neural Network Model for Short-Term Load Forecasting," *IEE Proc.*, vol. 142, Pt. D, no. 1, pp. 45-50, 1995.

[77]   M.A. Abido and Y.L. Abdel-Magid, "A Radial Basis Function Network Based Power System Stabilizer for a Synchronous Machine," *Fourth International Conference on Control, Automation, Robotics, and Vision ICARCV'96*, Westin Stamford, Singapore, pp. 1180-1184, 1996.

[78]   M.A. Abido and Y.L. Abdel-Magid, "Modeling of a Synchronous Machine Using Radial Basis Function Neural Networks," *International Conference, High Technology in the Power Industry IASTED*, Banff, Alberta, Canada, pp. 92-95, 1996.

[79]   M. A. Abido and Y. L. Abdel-Magid, "On-line identification of synchronous machines using radial basis function neural networks," *Accepted for Publication in IEEE Trans. on PWRS*, Feb. 1997.

[80]   Y.Y. Hsu and C.L. Chen, "Identification of Optimum Location for Stabilizer Applications Using Participation Factors," *IEE Proc.*, Pt. C, vol. 134, no. 3, pp. 238-244, 1987.

[81]   E.Z. Zhou, O.P. Malik, and G.S. Hope, "Theory and Method for Selection of Power System Stabilizer Location." *IEEE Trans. on Energy Conversion.* vol. 6. no. 1. pp. 170-176, 1991.

[82]   C.C. Lee, "Fuzzy Logic in Control Systems: Fuzzy Logic Controllers - Parts I & II," ," *IEEE Trans. syst., Man, Cybern.*, vol. 20, no. 2, pp. 404-435, 1990.

[83]   Y.Y. Hsu and C.H. Cheng, "Design of Fuzzy Power System Stabilizers for Multimachine Power Systems," *IEE Proc.*, vol. 137, Pt. C, no. 3, pp. 233-238. 1990.

[84]   M. Hassan, O.P. Malik, and G.S. Hope, "A Fuzzy Logic Based Stabilizer for a Synchronous Machine." *IEEE Trans. Energy Conversion*, vol. 6, no. 3, pp. 407-413, 1991.

[85]   T. Hiyama and T. Sameshima, "Fuzzy Logic Control Scheme for On-Line Stabilization of multimachine Power System." *Fuzzy Sets and Systems*, vol. 39. pp. 181-194, 1991.

[86]   Y.Y. Hsu and C.H. Cheng, "A Fuzzy Controller for Generator Excitation Control," *IEEE Trans. syst.. Man, Cybern.*, vol. 23, no. 2. pp. 532-539, 1993.

[87]   E. Handschin, W. Hoffmann, F. Reyer, T. Stephanblome, U. Schlucking, D. Westermann, and S.S. Ahmed, "A New Method of Excitation Control Based on Fuzzy Set Theory," *IEEE Trans. PWRS*, vol. 9, no. 1, pp. 533-539, 1994.

[88]   T. Hiyama, "Robustness of Fuzzy Logic Power System Stabilizers Applied to Multimachine Power System," *IEEE Trans. Energy Conversion*, vol. 9, no. 3, pp. 451-459, 1994.

[89]   T. Hiyama, M. Kugimiya, and H. Satoh, "Advanced PID Type Fuzzy Logic Power System Stabilizer," *IEEE Trans. Energy Conversion*, vol. 9, no. 3, pp. 514-520, 1994.

[90]   P.K. Dash and A.C. Liew, " Intelligent Supervisory Control of Power Systems," *International Conference on Intelligent System Application to Power systems ISAP'94*, Montpellier, France, pp. 329-335, 1994.

[91]   J.A. Momoh, X.W. Ma, and K. Tomsovic, "Overview and Literature Survey of Fuzzy Set Theory in Power Systems," *IEEE Trans. PWRS*, vol. 10, no. 3, pp. 1676-1690, 1995.

[92] P.K. Dash, S. Mishra. and A.C. Liew. "Design of a Fuzzy PI Controller for Power System Applications." *Journal of Intelligent and Fuzzy Systems*, vol. 3, pp. 155-163, 1995.

[93] H.A. Toliyat, J. Sadeh. and R. Ghazi. "Design of Augmented Fuzzy Logic Power System Stabilizers to Enhance Power System Stability," *IEEE Trans. Energy Conversion*, vol. 11, no. 1. pp. 97-103. 1996.

[94] Y.M. Park, U. Moon. and K.Y. Lee. "A Self-Organizing Power System Stabilizer Using Fuzzy Auto-Regressive Moving Average (FARMA) Model," *IEEE Trans. Energy Conversion*, vol. 11. no. 2. pp. 442-448, 1996.

[95] T. Hiyama, K. Miyazaki, and H. Satoh, "A Fuzzy Logic Excitation System for Stability Enhancement of Power Systems with Multimode Oscillations," *IEEE Trans. Energy Conversion*. vol. 11. no. 2, pp. 449-454, 1996.

[96] C.T. Lin and C.S. Lee. "Neural Network Based Fuzzy Logic Control and Decision System," *IEEE Trans. on Computers*. vol. 40, no. 12, pp. 1320-1336, 1991.

[97] L.X. Wang and J.M. Mendel, "Fuzzy Basis Functions, Universal Approximation, and Orthogonal Least Squares Learning," *IEEE Trans. on Neural Networks*, vol. 3, no. 5. pp. 807-814. 1992.

[98] D.A. Linkens and J. Nie. "Fuzzified RBF Network Based Learning Control: Structure and Self-Construction." *IEEE International Conference on Neural Networks IEEE-ICNN'93*. pp. 1016-1021, 1993.

[99] H.C. Chang and M.H. Wang, "Neural Network Based Self-Organizing Fuzzy Controller for Transient Stability of Multimachine Power Systems," *IEEE Trans. Energy Conversion*. vol. 10. no. 2. pp. 339-347, 1995.

[100] J.R. Jang and C.T. Sun, "Neuro-Fuzzy Modeling and Control," *Proc. of the IEEE*, vol. 83, no. 3, pp. 378-405. 1995.

[101] T.K. Yin and C.S. Lee, "Fuzzy Model Reference Adaptive Control," *IEEE Trans. syst., Man, Cybern.*, vol. 25. no. 12. pp. 1606-1615, 1995.

[102] T. Haida and Y. Akimoto. "Voltage Optimization by Using Genetic Algorithms," *Proc. of ESAP'91*, pp. 375-380, 1991.

[103] A. Bakirtzis, V. Petridis, and S. Kazarlis, "Genetic Algorithm Solution to the Economic Dispatch Problem," *IEE Proc. Gener, Transm. Distrib.*, vol. 141, no. 4, pp. 377-382, 1994.

[104] J.E. Lansberry and L. Wozniak, "Adaptive Hydrogenerator Governor Tuning with a Genetic Algorithm," *IEEE Trans. PWRS.* vol. 9, no. 1, pp. 179-183, 1994.

[105] R. Dimeo and K.Y. Lee, "Boiler-Turbine Control System Design Using a Genetic Algorithm," *IEEE Trans. on Energy Conversion,* vol. 10, no. 4, pp. 752-759, 1995.

[106] P. Ju, E. Handschin, and F. Reyer. "Genetic Algorithm Aided Controller Design with Application to SVC," *IEE Proc. Gener Transm. Distrib.,* vol. 143, no. 3, pp. 258-262, 1996.

[107] Y.L. Abdel-Magid and M.M. Dawoud, "Tuning of Power System Stabilizers Using Genetic Algorithms," *Accepted for Publication in Electric power Systems Research,* July 1996.

[108] T. Hiyama, "Application of Rule-Based Stabilizing Controller to Electrical Power System." *IEE Proc.,* vol. 136, Pt. C, no. 3, pp. 175-181, 1989.

[109] T. Hiyama, "Rule-Based Stabilizer for Multimachine Power System," *IEEE Trans. PWRS.* vol. 5, no. 2, pp. 403-411, 199).

[110] M. Hassan and O.P. Malik, "Implementation and Laboratory Test Results for a Fuzzy Logic Based Self-Tuned Power System Stabilizer," *IEEE Trans. Energy Conversion,* vol. 8, no. 2, pp. 221-228, 1993.

[111] T. Hiyama, "Real Time Control of Micro-Machine System Using Micro-Computer Based Fuzzy Logic Power System Stabilizer," *IEEE Trans. Energy Conversion.* vol. 9, no. 4, pp. 724-731, 1994

[112] K.A. El-Metwally, G.C. Hancock, and O.P. Malik, "Implementation of a Fuzzy Logic PSS Using a Micro-Controller and Experimental Test Results," *IEEE Trans. Energy Conversion,* vol. 11, no. 1, pp. 91-96, 1996.

[113] T. Hiyama, S. Oniki, and H. Nagashima. "Evaluation of Advanced Fuzzy Logic PSS on Analog Network Simulator and Actual Installation on Hydro Generators," *IEEE Trans. Energy Conversion,* vol. 11, no. 1, pp. 125-131, 1996.

[114] C.C. Karr and E.J. Gentry, "Fuzzy Control of pH Using Genetic Algorithms," *IEEE Trans. on Fuzzy Systems,* vol. 1, no. 1, pp. 46-53, 1993.

[115] M.A. Lee and H. Takgi, " Integrating Design Stages of Fuzzy Systems Using Genetic Algorithms," *IEEE International Conference on Fuzzy Systems IEEE-Fuzz'93,* pp. 612-617, 1993.

236

[116] D. Park, A. Kandel, and G. Langholz, "Genetic-Based New Fuzzy Reasonoing Models with Application to fuzzy Control," *IEEE Trans. syst., Man. Cybern.*, vol. 24, no. 1, pp. 39-47, 1994.

[117] D.A. Linkens and H.O. Nyongesa, "Genetic Algorithms for Fuzzy Control Part I: Off-Line System Development and Application," *IEE Proc. Control Theory Applications*, vol. 142, no. 3, pp. 161-176, 1995.

[118] D.A. Linkens and H.O. Nyongesa, "Genetic Algorithms for Fuzzy Control Part II: On-Line System Development and Application," *IEE Proc. Control Theory Applications*, vol. 142, no. 3, pp. 177-185, 1995.

CURRICULUM VITA

Name: Mohamed Ali Yousof Abido

Date of Birth: 1963

Place of Birth: Menoufia, Egypt

Education: Faculty of Engineering, Menoufia University, 1980-1985
                        B.Sc. (Dist. with Honor, 1/250, Electrical Engineering) 1985

                        Faculty of Engineering, Menoufia University, 1986-1989
                        M.Sc. (Electrical Engineering) 1989

                        King Fahd University of Petroleum and Minerals, 1992-1997
                        Ph.D. (Electrical Engineering) 1997

Experience: Demonstrator,
                        Faculty of Engineering, Menoufia University, 1985-1989

                        Assistant Lecturer,
                        Faculty of Engineering, Menoufia University, 1989-1992

                        Teaching and Research Assistant,
                        King Fahd University of Petroleum and Minerals, 1992-1997

Awards: Award of Excellence, Menoufia University, 1980-1985

                        Award of Excellence, Egyptian Engineering Society, 1985

                        Award of Excellence, Menoufia University, 1989

                        A Peace Fellowship in USA, 1991

Research Interests: Power system analysis, stability, and control,
                        Power system planning, and operation,
                        Optimization techniques,
                        Optimal and non-linear control,
                        System identification,
                        Artificial neural networks,
                        Fuzzy logic systems,
                        Rule-based systems,
                        Genetic algorithms,
                        Neuro-Fuzzy control,
                        Hybrid systems

Publications out of the Dissertation:

a) Journal Papers

[1] Mohammad A. Abido and Youssef L. Abdel-Magid, "On-line identification of synchronous machines using radial basis function neural networks," *Accepted for Publication in IEEE Trans. on PWRS,* Feb. 1997.

[2] M. A. Abido and Y. L. Abdel-Magid, "A genetic-based power system stabilizer," *Accepted for Publication in Electric Machines and Power Systems,* Feb. 1997.

[3] M. A. Abido and Y. L. Abdel-Magid, "Modeling of a synchronous machine using radial basis function neural networks," *Submitted to Int. J. Electrical Power & Energy Systems,* Feb. 1996.

[4] M. A. Abido and Y. L. Abdel-Magid, "Adaptive tuning of power system stabilizer using radial basis function networks," *Submitted to IEE Proc.,* Pt C, June 1996.

[5] M. A. Abido and Y. L. Abdel-Magid, "Hybrid neuro-fuzzy power system stabilizer to enhance power system stability," *Submitted to IEEE Trans. on PWRS,* June 1996.

[6] M. A. Abido and Y. L. Abdel-Magid, "Tuning of power system stabilizers using fuzzy basis function networks," *Submitted to Electric Machines and Power Systems,* Dec. 1996.

[7] M. A. Abido and Y. L. Abdel-Magid, "A fuzzy basis function network based power system stabilizer for generator excitation control," *Submitted to Electric Power Systems Research,* Dec. 1996.

b) Refereed International Conference Papers

[8] M. A. Abido and Y. L. Abdel-Magid, "Tuning of a fuzzy logic power system stabilizer using genetic algorithms," *Accepted for Presentation in 4th IEEE International Conference on Evolutionary Computation ICEC'97,* Indianapolis, USA, April 13-16, 1997.

[9] M. A. Abido and Y. L. Abdel-Magid, "On-line identification of a synchronous machine using a radial basis function network," *Accepted for Presentation in American Control Conference ACC'97*, New Mexico, USA, June 4-6, 1997.

[10] M. A. Abido and Y. L. Abdel-Magid, "Radial basis function network based power system stabilizers in multimachine power systems." *Accepted for Presentation in IEEE International Conference on Neural Networks ICNN'97*. Houston, Texas, USA, June 9-12, 1997.

[11] M. A. Abido and Y. L. Abdel-Magid, "A fuzzy basis function network based power system stabilizer for a synchronous generator," *Accepted for Presentation in Sixth IEEE International Conference on Fuzzy Systems FUZZ-IEEE'97*, Barcelona, Spain, July 1-5, 1997.

[12] M. A. Abido and Y. L. Abdel-Magid, "Hybridizing a rule-based power system stabilizer with genetic algorithms to enhance power system stability," *Submitted to International Conference on Intelligent Systems Applications to Power Systems ISAP'97*, Seoul, Korea, July 6-10, 1997.

[13] M. A. Abido and Y. L. Abdel-Magid, "A genetic-based fuzzy logic power system stabilizer for multimachine power systems," *Accepted for Presentation in IEEE International Confernce on Systems, Man, and Cybernetics SMC'97*, Orlando, Florida, USA, Oct. 12-15, 1997.

[14] M. A. Abido and Y. L. Abdel-Magid, "Modeling of a synchronous machine using radial basis function neural networks," *High Technology in the Power Industry, IASTED'96 International Conference*, June 4-8, 1996, Banff, Alberta Canada, pp. 92-95.

[15] M. A. Abido and Y. L. Abdel-Magid, "A radial basis function network based power system stabilizer for a synchronous generator," *Fourth Int. Conf. on Control, Automation, Robotics, and Vision, ICARCV'96*, Westin Stamford, Singapore, December 2-6, 1996, pp. 1180-1184.

[16] M. A. Abido and Y. L. Abdel-Magid, "Tuning of a rule-based power system stabilizer using genetic algorithms," *Accepted for Presentation in Intelligent Applications in Communication and power Systems IACPS*, Al-Ain, UAE, April 6-8, 1997.

[17] Mohammad A. Abido and Youssef L. Abdel-Magid, "Identification of synchronous machines using radial basis function neural network," *Proc. Fourth Middle East Power System Conference MEPCON'96*, January 3-5, 1996. Egypt, pp. 334-338.